Spatio-temporal distribution, physiological characterization and toxicity of the marine dinoflagellate *Ostreopsis* (Schmidt) from a temperate area, the Ebre Delta. Phylogenetic variability in comparison with a tropical area, Reunion Island

Olga Carnicer Castaño

PhD Thesis

Spatio-temporal distribution, physiological characterization and toxicity of the marine dinoflagellate *Ostreopsis* (Schmidt) from a temperate area, the Ebre Delta. Phylogenetic variability in comparison with a tropical area, Reunion Island

Olga Carnicer Castaño

Spatio-temporal distribution, physiological characterization and toxicity of the marine dinoflagellate *Ostreopsis* (Schmidt) from a temperate area, the Ebre Delta. Phylogenetic variability in comparison with a tropical area, Reunion Island

Memòria presentada per Olga Carnicer Castaño per optar al grau de doctora per la Universitat de Barcelona. Aquesta memòria ha estat realitzada dins el Programa de Doctorat en Aqüicultura sota la direcció del Dr. Jorge Diogène, i la tutela de la Dra. Isabel Navarro

Olga Carnicer Castaño
Sant Carles de la Ràpita, Setembre 2014

Director:
Dr. Jorge Diogène Fadini

Tutora:
Dra. Isabel Navarro Álvarez

"What we know is a drop,

what we don't know is an ocean."

Isaac Newton

Acknowledgments

De l' **IRTA de Sant Carles de la Ràpita**, vull agrair a tothom (administració, manteniment, tècnics, investigadors) que m'hagi ajudat en algun moment quan ho he necessitat. Vaig tenir la sort de caure a la **SMM**, on des del primer moment em van acollir com a una mes. Aquest ambient tant bo a la feina em va ajudar molt durant els primers mesos a la Ràpita quan no tenia res clar. Gràcies a **Pablo**, **Marga** i **Gemma**, que van apostar per mi i van contribuir a que aquesta tesi es dugués a terme. Però, especialment, vull agrair a **Jorge**, el meu director de tesi, per la confiança que ha dipositat en mi en tot moment durant aquesta època de crisi... per donar-me molta llibertat a l'hora d'escriure i per les correccions ràpides que m'han permès acabar dins del termini establert. També vull agrair a **Mònica**, **Laura**, **Núria**, **Vane 2** i **Esther**, perquè sempre que he necessitat alguna cosa heu estat disponibles. Gràcies al **Patró** i a **Xavi**, pels "que guapa estàs avui" a les 8 del matí que m'alegraven i em donaven forces per a la resta del dia. Al **Carles**, per la seva contribució a l'últim article, un GRÀCIES ENORME! A tota la gent que ha passat de pràctiques o màster, que m'han acompanyat en tants i tants mostrejos. Sense vosaltres no ho hagués pogut fer; **Lluís**, **Núria**, **Marteta**, **Jérôme**, **Manel**, **Idoia** i **Rosa**...Moltes gràcies! A la meva **Vane**, gràcies per la teva companyia al microscopi, fent-me les hores mes curtes! Gràcies per fer els meus mostrejos quan jo no hi era, aguantar el meu desordre al laboratori, ensenyar-me "bitxets" però sobre tot, per la teva amistat fora de la feina. **Alexis**, gràcies per ensenyar-me a córrer, aguantar els meus moments insuportables, pujar-me l'autoestima i donar-me ànims.

I also would like to say thanks to **Karl**, who, even if he is not a direct supervisor, he has guided and taught me in molecular biology when I was completely lost at the beginning. Thanks for asking me if I needed help and stop me in the corridors for a chat when I was nervous or tired.

En el piso de arriba esta mi otra pequeña familia, los becarios, en la que compartimos alegrías, frustraciones, histerismo, preocupaciones, cansancio, risas, dudas, trabajo...y un sinfín de cosas... Gracias por hacerlo todo más ameno! **Nuria**, **Elvira**, **Zohar**, **Anaïs**, **Sandra**, (**Diego** y **Mohamed** anexados). **Krunecito**, gracias por esas pelis "encefalograma plano" que tanto necesitaba. **Lucía** y **María** con las que empecé todo este camino incierto que ya se acaba. **Laia**, gràcies per estar

Content

CHAPTER 1

General Introduction

Harmful algae blooms (HAB) are natural events consisting on proliferations of microscopic algae that have occurred over the history (Hallegraeff *et al.,* 2010). These proliferations may be harmful since some of these microalgae may produce toxins that affect humans through direct exposure by skin contact or aerosols, or through indirect exposure after the accumulation of toxins in seafood (Reverté *et al.,* submitted). Of special concern for this work are outbreaks formed by the benthic dinoflagellate *Ostreopsis* (Schmidt), including several species producers of palytoxin (PLTX)-like compounds, one of the most potent marine toxins known so far, that may be accumulated in seafood (Munday, 2011). The genus is formed by nine species, though the current state of the taxonomy is controversial, partly due to the lack of genetic characterization of the original holotypes (Penna *et al.,* 2010). A re-examination of the morphological and molecular assignment of each species is reclaimed to create consensus among researchers. The first species was described in tropical areas, however, in recent years, an expansion of the genus to temperate regions worldwide has been observed (Parsons *et al.,* 2012). Of particular interest are *O.* cf. *ovata* proliferations, reported more frequently in the last decade, especially in the Mediterranean Sea, where blooms have been associated with human illness (Tubaro *et al.,* 2011) and damage to the benthic ecosystem (Tichadou *et al.,* 2010). In order to better understand *O.* cf. *ovata* adaptative dynamics and generate information applicable to future predictive models; latest studies are focused on the determination of environmental factors that trigger massive proliferations.

The aim of this thesis is, on one hand, to contribute to the improvement of the genus *Ostreopsis* taxonomy by molecular, morphological and toxicological characterization of cryptic species isolated in a tropical area and, on the other hand, to investigate, combining field and laboratory analysis, the role of environmental factors and their interaction, involved in the ecology of *O.* cf. *ovata* blooms in the NW Mediterranean Sea.

1.1. Identification and quantification of the genus *Ostreopsis*

1.1.1. Controversial status of the taxonomy

The genus *Ostreopsis* belongs to the family Ostreopsidaceae (Lindeman). The first described species, *O. siamensis* (Schmidt), was isolated in the Gulf of Siam, in Thailand at the beginning of the 20th century. It was considered as the only species for decades, no other species being reported until the late 1970s (Faust and Gulledge, 2002). Eight more species have been identified until date, based on morphological features. Fukuyo, (1981) redescribed the genus adding two new species collected in New Caledonia (French Polynesia) and Fukuyu Island (Japan), *O. ovata* and *O. lenticularis* respectively. Later on, the list was completed with the description of six new species; *O. heptagona* (Norris *et al.,* 1985); *O. mascarenensis* (Quod, 1994); *O. labens* (Faust & Morton, 1995); *O. marinus* (Faust, 1999);

O. belizeanus (Faust, 1999) and *O. caribbeanus* (Faust, 1999) (Figure 1.1). In Rhodes (2011), a possible new species is mentioned, morphologically different from the rest, *O. tholus*, identified by Morton and coworkers, but no reference has been published yet.
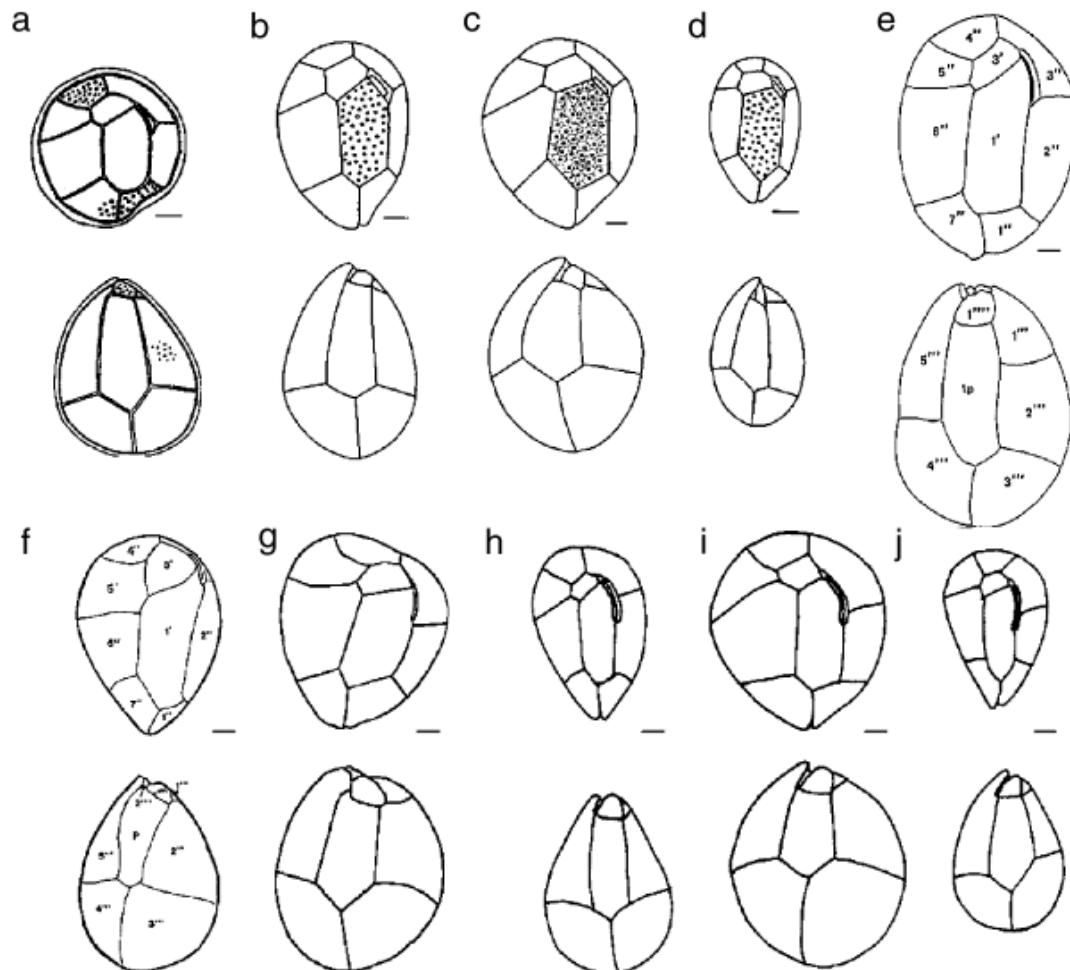
Fig. 1.1. Line drawings of the nine described *Ostreopsis* species in epithecal (upper) and hypothecal (lower) view. **a**) *O. siamensis*, after Schmidt (1901); **b–d**) *O. siamensis*, *O. lenticularis*, and *O. ovata*, respectively, after Steidinger & Tangen (1996); **e**) *O. mascarenensis*, after Quod (1994); **f**) *O. heptagona*, after Norris *et al.,* (1985); **g**) *O. labens*, redrawn from Faust and Morton (1995); **h–j**) *O. belizeanus, O. marinus*, and *O. caribbeanus*, respectively, after Faust (1999). Scale bars, 10mm. (Penna *et al.,* 2005)

1.1.1.1. Morphological aspects

The identification of *Ostreopsis* species was originally based on morphological features. Differentiation among species was established according to shape, size, ratio of dorsoventral (DV) diameter relative to anteriorposterior (AP) diameter, ratio of DV to width (W), length of the Po plates, size of the thecal pores, and shape of 1p plates of cells (references in Kang *et al.,* 2013). A debate has been presented in the scientific community since similarities in these features are shared by several species (Penna *et al.,* 2005), leading to confusion in the identification of the genus (David *et al.,* 2013). The decision of which morphological characteristics are

sufficient or not to define a species lays on taxonomist criteria. However, there are different points of view about this subject and discrepancies may occur (Fraga, 2014). Considering this problematic, and the improved DNA sequencing methods, molecular analysis are becoming a usual process as a supplementary support in algae species delimitation (Leliaert *et al.,* 2014).

In addition to these considerations, a great intra-specific variability of sizes has been observed both in field and cultured cells of this genus (Aligizaki & Nikolaidis., 2006), which further complicates the discrimination among species. In the particular case of *O.* cf. *ovata*, it has been hypothesized that small size cells could represent vegetative cells that arise from accelerated cell division or may behave as gametes (Accoroni *et al.,* 2014). Aberrant cells according to shape which appears under unfavorable conditions or towards the end of the stationary phase may constitute the precursors of the over-winter population (Bravo *et al.,* 2012). Having in mind these existing variations on cell morphology, the study of cell size variation may contribute to a better understanding of *Ostreopsis* ecology.

1.1.1.2. *Molecular characterization*

Originally holotypes of the genus *Ostreopsis,* isolated from tropical regions, were described without any corroborative genetic characterization. An unequivocal assignation to the initial morphological description is not possible at this moment, due to lack of original genetic material. For an accurate update of the taxonomy, the sequencing of strains collected from tropical areas, together with a morphological characterization, would increase the possibilities of a correct attribution to original morphotypes, and clarify some aspects of the taxonomy (Penna *et al.,* 2010). As a measure of caution, it has been suggested to name *O.* cf. *siamensis* and *O.* cf. *ovata*, both species found in the Mediterranean Sea (Penna *et al.,* 2005 and Penna *et al.,* 2010, respectively) until culture genetic material from original location is available for confirmation.

At present, there is not a standardized method to specify species through sequence data in dinoflagellates. However, the Internal Transcribed Spacer regions (ITS1 and ITS2) and 5.8S gene of the nuclear rDNA have been tested with several dinoflagellate genera for phylogenetic studies (Litaker *et al.,* 2007). Once enough sequences of *Ostreopsis* are gathered in GenBank, this would constitute a "promising tool" for detecting species in algae culture strains (Stern *et al.,* 2012).

The majority of the *Ostreopsis* spp. genetic studies provide ITS region phylogenetic trees (Pin *et al.,* 2001; Penna *et al.,* 2005; Penna *et al.,* 2010; Laza-Martínez *et al.,* 2011; Sato *et al.,* 2011; Kang *et al.,* 2013; David *et al.,* 2013). In some of these works, consistent results obtained with other genetic markers, consolidate the separation of clades. A supported distinction of two genotypes, together with a deep morphological characterization defines the species *O.* cf. *ovata* and *O.* cf. *siamensis*. A third clade is constituted by *O. lenticularis and O. labens,*

representing the most basal lineage. However, morphologically these have been described as two different species, but genetically they have been clustered together. Further analyses are needed to solve this uncertainty (Penna *et al.,* 2010). In recent years, new species have been sequenced. Of special interest is the study of Sato and coworkers (Sato *et al.,* 2011) with the identification of six new genotypes (Figure 1.2). Nevertheless, an extensive morphological description is required to identify if those genotypes match original morphotypes or, on the contrary, they represent new species not previously characterized.
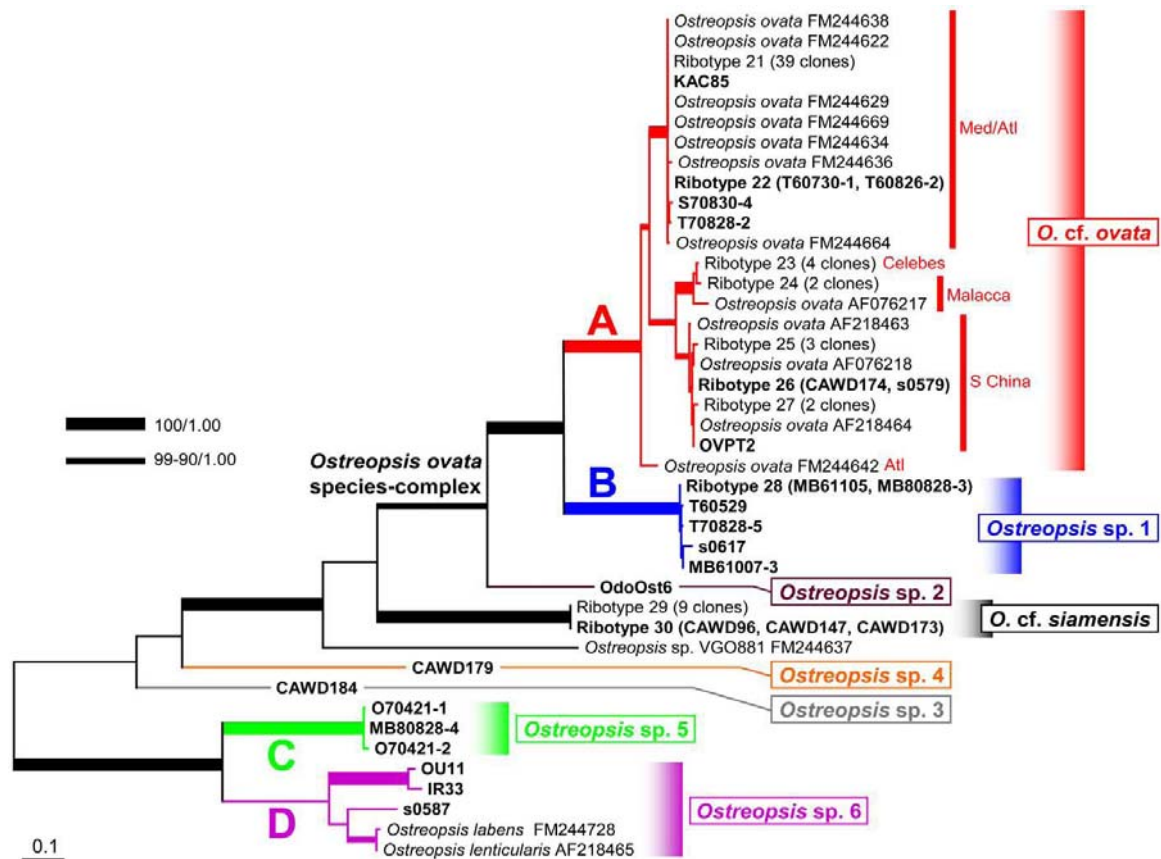
Fig. 1.2. Maximum likelihood phylogeny of *Ostreopsis* inferred from ITS sequence aligned with MAFFT. Major clades found in Japanese coast are particularly noted as clade A–D. Geographic origins of *O.* cf. *ovata* clone are indicated. Sequences of bold clone are obtained in Sato *et al.,* (2011).

Within the genus *Ostreopsis*, *O.* cf. *ovata* constitutes the species with higher amount of sequences in GenBank, and it has been clustered in three different genetic groups. Two of them are from the Indo-Pacific; one from the Malacca Strait and another from the South China Sea (Pin *et al.,* 2001). The third group corresponds to the Mediterranean-Atlantic clade (Penna *et al.,* 2010), including strains from Spain, France, Italy, Tunisia, Greece and Brazil. New sequences from following works, available in GenBank, have strengthened the three major clades, reflected in Figure 1.3. As interpreted in the work of Penna and coworkers, (Penna *et al.,* 2010), this

genetic division may be the reflection of distinct geographic provenance, separating Indo-Pacific clades and Mediterranean-Atlantic clade as a result of natural barriers such as ocean currents. However, gene flow has been observed in the former clade considering the fact that it constitutes a wide region between both coasts of the Atlantic Ocean. More recently, some strains isolated in Japanese waters were clustered in the Mediterranean-Atlantic clade (Sato *et al.,* 2011), reflecting this gene circulation, possibly due to anthropogenic activities such as transport in ballast water (Hallegraef & Bolch, 1991).
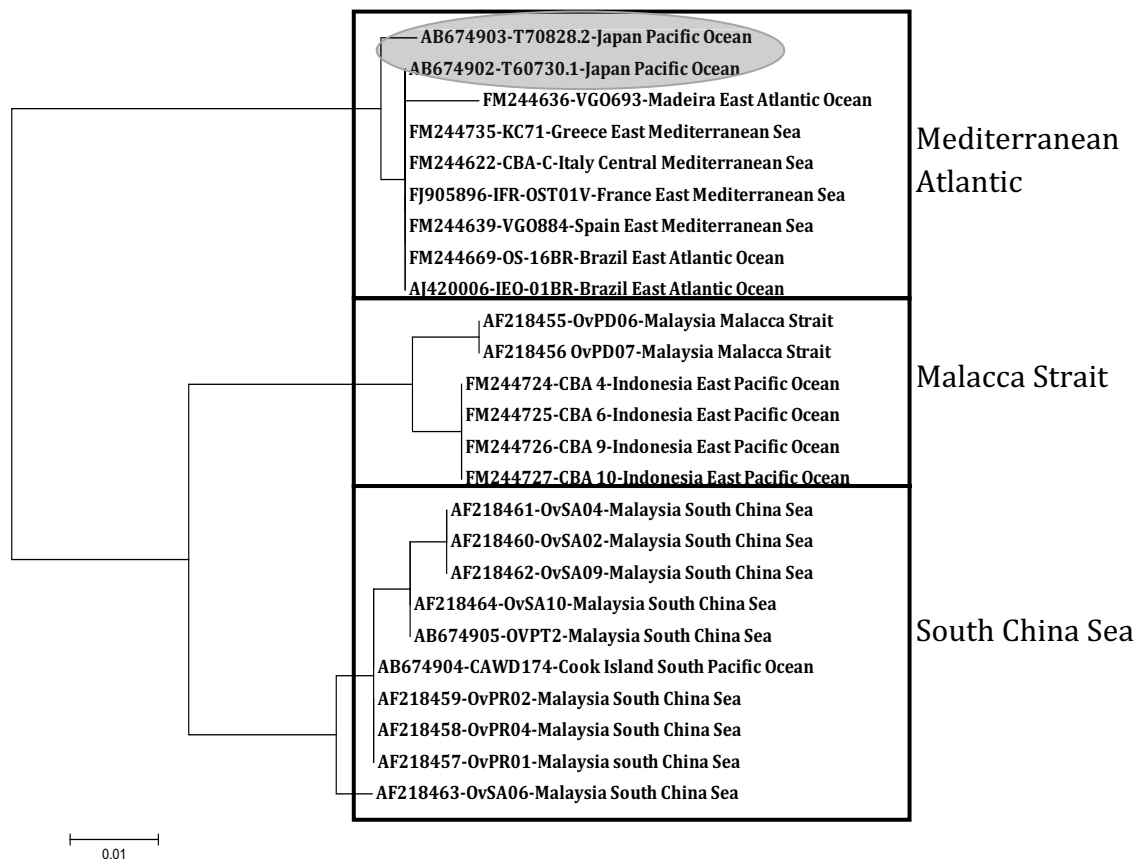
Fig. 1.3. Maximum Likelihood phylogeny of *O.* cf. *ovata* inferred from ITS sequence based on the Kimura 2-parameter model. The tree is drawn to scale, with branch lengths measured in the number of substitutions per site. The analysis involved 25 nucleotide sequences. All positions containing gaps and missing data were eliminated. There were a total of 241 positions in the final dataset. Evolutionary analyses were conducted in MEGA5.

1.1.2. Cell enumeration methodologies

Ostreopsis spp. may bloom and form a mucilaginous mat at the surface of different benthic subtracts. Recent studies have focused on *O.* cf. *ovata* ultrastructure, finding adaptations related to a benthic habitat (Honsell *et al.,* 2013; Escarlera *et al.,* 2014). The mucus excretion is suggested to be essential on their life strategy, providing a colonization mechanism (Vidyarathna & Granéli, 2011), a protection against grazers (Bravo *et al.,* 2012) or for predation (Barone *et al.,* 2007).

1.1.2.1. *Light microscopy*

When analyzing cell abundances in field and culture fixed samples, the presence of mucus that embeds the cells makes it difficult to obtain homogeneous cell suspensions, a necessity to perform an accurate cell counting under light microscopy by the Utermöhl method (Utermöhl, 1958). Different strategies have been attempted in order to reduce these aggregations. This mucilaginous net is composed by acidic polysaccharides and a high number of trichocysts (Honsell *et al.,* 2013). The addition of chemicals to the samples may neutralize negative electric charges present in cell walls and polysaccharides preventing the formation of aggregates. Two chemicals have been used in culture samples in order to perform reliable counts and obtain an accurate growth curve; sodium-ethylenediaminetetraacetic acid (Na-EDTA) (Scalco *et al.,* 2012; Pezzolesi *et al.,* 2012) and hydrochloric acid (HCl) (Guerrini *et al.,* 2010; Vanucci *et al.,* 2012b; Monti & Cecchin, 2012).

1.1.2.2. *Quantitative real time PCR (qPCR)*

Due to morphological similarities among genotypes, there is an evident difficulty to resolve species differentiation under light microscopy. Molecular methods based on genetic sequencing and quantitative real-time PCR (qPCR) have greatly improved the identification and estimation of abundance of different *Ostreopsis* species through specific primers on different matrices (Casabianca *et al.,* 2013), representing a sensitive, specific and rapid technique for marine environmental studies (Furlan *et al.,* 2013). A primary approach was attempted by Perini and co-workers (Perini *et al.,* 2011) for the detection of *O.* cf. *ovata* in samples collected on macrophytes in the Adriatic Sea, obtaining a high reproducibility and efficiency on the assay.

1.2. Distribution of the genus *Ostreopsis*

Ostreopsis spp distribution extends from tropical and sub-tropical regions to temperate areas (Figure 1.4) (Rhodes *et al.,* 2011). However, most of the species have been observed exclusively in warmer waters. The species *O.* cf. *ovata* and *O.* cf. *siamensis* are the most widespread, as they are present in temperate regions as well (Parsons *et al.,* 2012). As for the locations this thesis focuses on, the species *O. mascarenensis, O. marinus*, *O. belizeanus* and *O. caribeanus* have been observed in the coral reef ecosystem of the Mascarene Islands, in the Indian Ocean (Faust, 1999). In Reunion Island precisely, *O. lenticularis, O. siamensis* and *O. ovata* were also observed (Faust *et al.,* 1996). In Mediterranean waters, *O.* cf. *ovata* has been reported in numerous locations, with a higher frequency and abundance than *O.* cf. *siamensis* (Penna *et al.,* 2012). It is suggested that *O.* cf. *siamensis* is possibly more adapted to cooler waters taking into account that in the Atlantic coast of the Iberian Peninsula this species dominates *O.* cf. *ovata* (David *et al.,* 2013) and it has been found in Russia and the Sea of Japan (Selina & Orlova, 2010). The distribution

of both species in several areas reflects their acclimation to a wide range of environmental conditions.
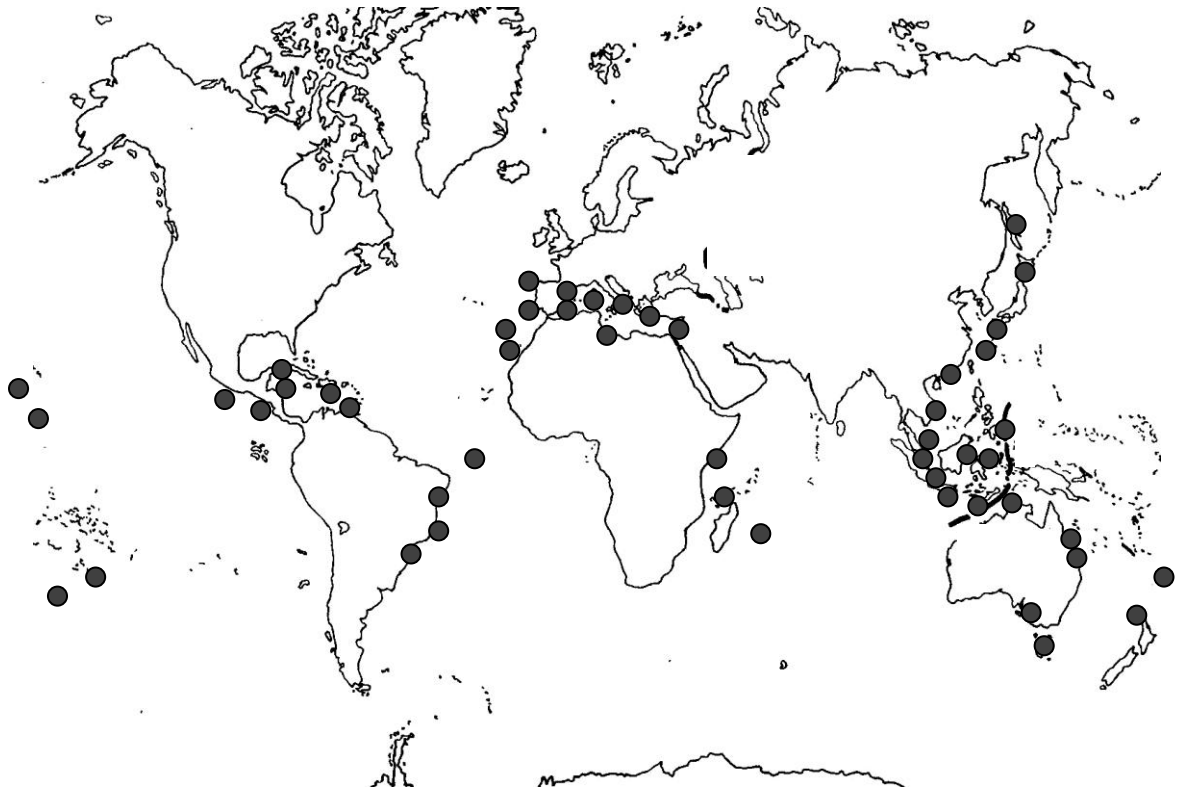
Fig. 1.4. Occurrence of the genus *Ostreopsis*.

1.3. Ecology of the genus *Ostreopsis*

1.3.1. *Effects of environmental factors*

Benthic microalgae live attached to substrates, in some cases on marine organisms such as macroalgae. Complex interactions between biotic and abiotic factors in coastal areas affect both microalgae dynamics and their substrate. When considering ecology studies, particular characteristics have to be contemplated as natural factors influencing benthic microalgae growth may differ from factors influencing planktonic microalgae which are much more documented (Fraga *et al.,* 2012).

Water temperature is considered one of the most determinant environmental factors that drives the growth of toxic benthic dinoflagellates (Pistocchi *et al.,* 2011). The presence of all *Ostreopsis* species in tropical waters shows a better adaptation to warmer waters. This hypothesis is highlighted in temperate areas, such as the Mediterranean Sea, where a marked seasonal pattern is repeated along the coast. In these waters, blooms coincide with increasing temperatures, and cells are detected only above a certain temperature threshold (Mangialajo *et al.,* 2011). However, other environmental factors, are also involved in the formation of blooms (Cohu *et al.,* 2013), and further investigation is fundamental for a correct understanding of *Ostreopsis* spp population dynamics.

1.3.2. O. cf. ovata dynamics in the Mediterranean Sea.

As mentioned above, high water temperature is crucial for *O.* cf. *ovata* growth in the Mediterranean Sea. In temperate waters, no vegetative cells are observed during the cooler months. In the spring, as water temperature rises and sunlight duration increases, *O.* cf. *ovata* cells start to be identified in water or macrophyte samples. Although there are discrepancies among different regions on the optimal temperature for outbreaks formation, blooms are likely to be formed from 22 to 30°C, as the majority of reports are found in that range (Pistocchi *et al.,* 2011). However, blooms formation does not only depend on water temperature, and these are more likely to occur in certain spots, reflecting a preference for specific sites (Cohu *et al.,* 2013). This heterogeneity may be the response to other factors and their interactions which may be determinant for the development of proliferations.

Little is known about the effects of salinity in *O.* cf. *ovata* blooms since in the environment, salinity values have little variation and the majority of observations are reported around 37 (Pistocchi *et al.,* 2011). When studying phytoplankton populations, salinity remains moderately stable all year long, but this is not the case for benthic ecosystems, highly influenced by coastal freshwater inputs. As a consequence, salinity fluctuations, especially noticeable in sites close to a river delta, may represent a limiting factor for bloom formations.

Coastal waters are influenced by anthropogenic eutrophication, intensified in the last decades due to the increase of human settlements in the coast, which leads to an enrichment of nutrient supply in benthic ecosystems. There is not a clearly relationship with nutrient load, however, it has been noticed that nutrient limitation affects *O.* cf. *ovata* growth in laboratory experiments (Vanucci *et al.,* 2012; Vidyarathna & Granéli, 2013). Results suggested a possible phosphate limitation on cell growth. However, in field observations, no links were detected between cell abundances and nutrient concentration (Vila *et al.,* 2001), or a weak negative correlation between cell abundances and nitrate concentrations has been described (Cohu & Lemée, 2011; Cohu *et al.,* 2013).

As far as hydrodynamism is concerned, it is important to study the effect of wave exposure on *O.* cf. *ovata* abundances because, being attached to the substrate, water motion may directly be implicated in cell resuspension (Fraga *et al.,* 2012), provoking blooms in the water column. Generally, toxic benthic dinoflagellates are associated with relatively "calm" waters (Shears and Ross, 2009; Richlen and Lobel, 2011). This pattern is in agreement with *O.* cf. *ovata* higher abundances found in sheltered or moderate exposed areas in studies performed in the Mediterranean Sea (Vila *et al.,* 2001; Totti *et al.,* 2010; Accoroni *et al.,* 2011) and in the temperate region of the Great Bay in Japan (Selina *et al.,* 2014). Nevertheless, taking into account the difficulty to characterize water motion, we are not sure to what extent water movement conditions are comparable in different studies.

Environmental factors influencing *O.* cf. *ovata* distribution may be those varying in relation to depth (Cohu *et al.,* 2013). Higher *O.* cf. *ovata* abundances have been observed in the first water layers (Totti *et al.,* 2010; Cohu *et al.,* 2013), suggesting that light could be the limiting factor (Accoroni *et al.,* 2012).

The fact that all these factors are likewise playing an important role on macroalgae growth, on the presence of grazers and other benthic microalgae, should be taken in consideration as these would affect indirectly *O.* cf. *ovata* abundances (Fraga *et al.,* 2012). It is difficult to evaluate separately these interactions and recognize which factor is responsible for *O.* cf. *ovata* bloom formation.

1.4. Toxicity of the genus *Ostreopsis*

1.4.1. *Palytoxin analogs*

Palytoxin (PLTX) is one of the most poisonous non-protein marine toxins (Moore & Bartolini, 1981). It was originally isolated from the soft coral *Palythoa toxica*, and thereafter in other *Palythoa* species (Moore & Scheuer, 1971; Gleibs *et al.,* 1995). Later on, other structurally related analogs have been found to be produced by species belonging to the genus *Ostreopsis* in tropical areas: ostreotoxins 1 and 3 in *O. lenticularis* (Mercado *et al.,* 1994), ostreocin D in *O. siamensis* (Usami *et al.,* 1995), and mascarenotoxins in *O. mascarenensis* (Lenoir *et al.,* 2004). Nonetheless, the most deeply studied congeners are the compounds produced by *O.* cf. *ovata*, especially from the strains in the Mediterranean Sea. The typical toxin profile is dominated by ovatoxin (OVTX)-a (Ciminiello *et al.,* 2008), representing about 60% of the total toxin content, followed by OVTX-b, OVTX-d and/or –e, OVTX-c (Ciminiello *et al.,* 2010), and putative palytoxin (pPTLX), which usually accounts for less than 1% of the total toxin content (Ciminiello *et al.,*2012). However, variation in the toxin profile with absence or changes in relative abundances of these toxins has been observed in different strains from the Mediterranean Sea, being strain-specific. A new isomer, OVTX-f, was discovered in a strain from the Adriatic Sea, representing 50% of the total toxin content and displacing OVTX-a as the major component in the profile (Ciminiello *et al.,* 2012). Additionally, in strains from Villefranche-sur-Mer (Ligurian Sea), in field samples, a higher amount of pPLTX was observed and the presence of OVTX-f was detected (Brissard *et al.,* 2014). The research group of professor Ciminiello, an international reference in the study of OVTXs by liquid chromatography analysis, has first described the toxin profile of *O.* cf. *ovata*, isolated from our sampling sites, identifying a new analog, OVTX-g (García *et al.,* submitted, ANEX). Likewise, distinct toxin profiles have been detected in different strains, belonging to the same genetic clade collected in Japan (clade A, in Figure 1.2). New isomers from OVTXs were distinguished in some isolates while in others; no toxins were found (Suzuki *et al.,* 2013).

1.4.2. Palytoxin mechanism of action

Great efforts have been made to clearly understand the mechanism of action of PLTX. At the cellular level, PLTX blocks the Na^+/K^+-ATPase pump (Hilgemann, 2003). The activity of this transmembrane protein is essential for the maintenance of the cell homeostasis, which actively transports 3 Na^+ out of the cell and 2 K^+ inside, by hydrolysing ATP under normal conditions. PLTX binds to the extracellular part of the Na^+/K^+-ATPase, inhibiting the active ion exchange by converting the pump into a permanently open ion channel, eventually causing cell lysis (Artigas *et al.,* 2003) (Figure 1.5). Moreover, an increase in the cytosolic Ca^{2+} caused by the action of a Na^+-Ca^{2+} exchange pump is observed (Shimahara *et al.,* 1990; Satoh *et al.,* 2003), also associated with cell death, apart from other secondary effects including cytoskeleton alteration, or cardiac and muscle contraction at the tissue level.
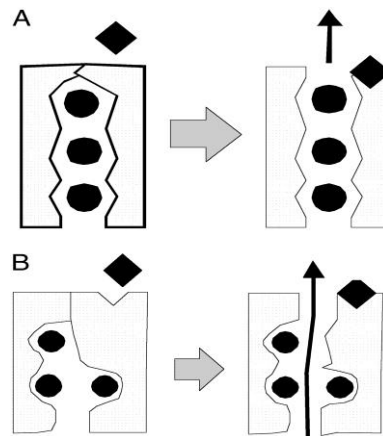
Fig 1.5. Cartoons of the permeation pathways of an ion channel (*A*) and the Na/K pump (*B*) when their gates are opened by a toxin. The ion diffusion pathway of the channel is selective, whereas that of the Na/K pump is not. (Hilgemann, 2003)

However, as for other PLTX analogues, little is known about OVTXs toxicity, which are the major components produced by *O.* cf. *ovata*. In that sense, further work needs to be intensified. Interestingly, a recent study has been performed with OVTXs purified extract coming from strains isolated in our study area, suggesting that OVTXs have the same mechanism of action and potential as PLTXs (Soliño *et al.,* in preparation-ANEX).

1.4.3. Human exposure to Palytoxins

One of the potential routes of human exposure to PLTX-like compounds is seafood consumption from organisms where PLTX-like compounds have been bioaccumulated (Deeds & Schwarts, 2010). Their presence has been detected in diverse marine organisms, such as crustaceans, fish, molluscs, gasteropods and echinoderms worldwide (Aligizaki *et al.,* 2011) (Figure 1.6). Some intoxication registered in tropical areas have been lethal (e.g. Onuma *et al.,* 1999), whereas in

temperate regions there is no record of human poisoning by PLTX in seafood (Brissard *et al.,* 2014). Nevertheless, in the latest years, several studies have confirmed the presence of PLTX-like analogs, probably produced by *O.* cf. *ovata* blooms, in seafood in the Mediterranean Sea (Aligizaki et al, 2008; Bellocci *et al.,* 2008; Amzil *et al.,* 2012; Biré *et al.,* 2013; Brissard *et al.,* 2014).

Fig. 1.6. Worldwide distribution of PLTX in seafood samples. (Aligizaki *et al.,* 2011)

Furthermore, dermal contact or inhalation of marine aerosols during *Ostreopsis* spp. blooms has become a health issue for bathers and constitute a second way of exposure (Richlen *et al.,* 2011). Several events of respiratory problems and/or skin irritation in humans, by inhalation or coetaneous contact respectively, have been recorded along the Mediterranean coast (Tubaro *et al.,* 2011). It is hypothesized that, planktonic cells are derived from re-suspended benthic cells due to wave action or vertical migration (Biré *et al.,* 2013). A successive bloom is formed in the water column deriving in aerosols, where PLTX-like compounds (Ciminiello *et al.,* 2014) and *O.* cf. *ovata* cells (Casabianca *et al.,* 2013) have been detected. Among other symptoms, the most common are flu-like manifestations including headache, mild gastrointestinal problems, and fever (Tichadou *et al.,* 2010).

1.4.4. *Toxin content variability by physico-chemical factors*

When considering toxin content in relation to physico-chemical factors, the most studied species of the genus is *O.* cf. *ovata*, especially the strains coming from the Mediterranean Sea. Laboratory experiments have been conducted in order to evaluate PLTX-like compounds content under different experimental conditions. Consistence in the results highlighted an increase in toxin content during the growth

phase (Vanucci *et al.,* 2012a-2012b; Scalco *et al.,* 2012; Pezzolesi *et al.,* 2012; Guerrini *et al.,* 2010). Regarding the influence of environmental conditions in cell toxicity, further investigation is needed to elucidate if toxin production, as secondary metabolites not fully integrated into the homeostasis of the cell, is enhanced under particular conditions (Pezzolesi *et al.,* 2014).

1.4.5. *Detection methods*

At the moment, there is no officially validated technique regarding PLTX-like compounds determination, and this depends on each laboratory and research topic. Analytical and biological methods have been implemented. As far as legislative regulation is concerned, no toxin content limits in seafood have been established in any country. In 2005 the European Union Reference Laboratory for Marine Biotoxins (EU-RLMB) set a provisional limit of 250 µg/kg of PLTX in shellfish (CRLMB, 2005). Later on, EFSA suggested to decrease the limit to 30 µg/kg of the sum of PLTXs and ostreocine-D in meat (Regulation (EC) N° 854/2004). However, these are only recommendations and not regulations.

In addition to that, there are not certified standards for PLTX analogs to be used in the detection. For that reason, assuming that molecules of the PLTX group of toxins may have the same mechanism of action (Ciminiello *et al.,* 2008), analyses are performed using PLTX standards from *Palythoa tuberculosa* and expressed as PLTX equivalents. In that sense, the purification of OVTXs standards is required to obtain reference material for a more accurate toxicological assessment (Brissard *et al.,* 2014). Moreover, attention has to be addressed to the extraction processes to evaluate the efficiency of different strategies (Riobó *et al.,* 2011).

1.4.5.1. <u>*Analytical methods*</u>

Toxin profiles of *O.* cf. *ovata* can be described accurately by Liquid Chromatography – Electro Spray Ionization – High Resolution Mass Spectrometry (LC-ESI-HRMS) (Ciminiello *et al.,* 2011). Since PLTX analogs do not have analytical standards, their identification relies on the comparison of three of their LC-ESI-HRMS characteristics with those of PLTX: a) retention time, b) consistency among the molecular formula assigned to the multiple charged ions (single, double and triple) and adducts generated by ESI, and c) elemental composition of the fragment ions from the cleavage between C-8 and C-9, highly favored in PLTX-like compounds (Ciminiello *et al.,* 2011-2012a-2012b). This strategy has been extensively applied by Ciminiello's group and others to the identification of PLTXs and analogues in samples of microalgae and seafood.

1.4.5.2. <u>*Haemolytic assay*</u>

In the early 80s, Habermann and co-workers (Habermann *et al.,* 1981a-1981b) described delayed haemolytic action of PLTX on mammal red blood cells (RBCs).

Taking as a basis this effect and a previous work with the MAb against PLTX (Bignami *et al.,* 1992), Bignami and collaborators (Bignami *et al.,* 1993) developed the first haemolytic assay for PLTX using mouse blood, considered more sensitive to the PLTX effect. As previously mentioned, to verify that haemolysis is specifically due to PLTX, the use of an antagonist was proposed. Ouabain was an appropriate antagonist when using human erythrocytes. Nevertheless, when using mouse blood, the anti-PLTX MAb seemed to be more effective (Taniyama *et al.,* 2003)*.*

Subsequent assays have derived from Bignami's test (Bignami *et al.,* 1993), just with slight modifications in the origin of RBCs and some experimental parameters (Onuma *et al.,* 1999; Taniyama *et al.,* 2003; Riobó *et al.,* 2008). Particularly interesting is the work performed by Riobó and co-workers. Taking into account that the haemolytic effect may not be linear according to the toxin dose, and in an attempt to provide a more reliable assay, these authors modelled the toxicological dynamics and kinetics of haemolysis by PLTX. The model provided optimal working conditions, indicating the necessity to operate at a moderate temperature (25 °C) and to use ouabain as an antagonist.

1.5. Aims of the thesis

The aims of the present thesis were set according to the gaps described above. Synthetically, these are the principal aims of the thesis:

- Contribute to the characterization of *Ostreopsis* species from the benthic microalgae community isolated in macrophytes in a tropical region (Reunion Island), in order to provide new insights that will lead to a better understanding in *Ostreopsis* taxonomy.

- Improve counting methodologies for *Ostreopsis* species, by reducing cell abundance estimation error by Utermöhl method through sample pre-treatment.

- Elucidate physiological effects of temperature and salinity interaction on two *O.* cf. *ovata* strains isolated in the NW Mediterranean Sea in laboratory conditions.

- Determinate the most influencing environmental factors of *Ostreopsis* spp epiphytic assemblage dynamics in a temperate region, the NW Mediterranean Sea.

1.6. References

Regulation (EC) No 854/2004 of the European Parliament and of the Council of 29 April 2004 laying down specific rules for the organisation of official controls on

products of animal origin intended for human consumption Off. J. Eur. Union, L226, pp. 83-127.

Accoroni, S., Romagnoli, T., Colombo, F., Pennesi, C., Di Camillo, C.G., Marini, M., Battocchi, C., Ciminiello, P., Dell'Aversano, C., Dello Iacovo, E., Fattorusso, E., Tartaglione, L., Penna, A., Totti, C., 2011. *Ostreopsis* cf. *ovata* bloom in the northern Adriatic Sea during summer 2009: Ecology, molecular characterization and toxin profile. Marine Pollution Bulletin 62, 2512-2519.

Accoroni, S., Romagnoli, T., Pichierri, S., Colombo, F., Totti, C., 2012. Morphometric analysis of *Ostreopsis* cf. *ovata* cells in relation to environmental conditions and bloom phases. Harmful Algae 19, 15-22.

Accoroni, S., Romagnoli, T., Pichierri, S., Totti, C., 2014. New insights on the life cycle stages of the toxic benthic dinoflagellate *Ostreopsis* cf. *ovata*. Harmful Algae 34, 7-16.

Aligizaki, K., Katikou, P., Milandri, A., Diogène, J., 2011. Occurrence of palytoxin-group toxins in seafood and future strategies to complement the present state of the art. Toxicon 57, 390-399.

Aligizaki, K., Katikou, P., Nikolaidis, G., Panou, A., 2008. First episode of shellfish contamination by palytoxin-like compounds from *Ostreopsis* species (Aegean Sea, Greece). Toxicon 51, 418-427.

Aligizaki, A and Nikolaidis, G., 2006. The presence of the potentially genera *Ostreopsis* and Coolia (Dinophyceae) in the North Aegean Sea, Greece. Harmful Algae 5, 717-730.

Amzil, Z., Sibat, M., Chomerat, N., Grossel, H., Marco-Miralles, F., Lemee, R., Nezan, E., Sechet, V., 2012. Ovatoxin-a and Palytoxin Accumulation in Seafood in Relation to *Ostreopsis* cf. *ovata* Blooms on the French Mediterranean Coast. Marine Drugs 10, 477-496.

Artigas, P., Gadsby, D.C., 2003. Na+/K+-pump ligands modulate gating of palytoxin-induced ion channels. Proceedings of the National Academy of Sciences 100, 501-505.

Barone, R., 2007. Behavioural trait of *Ostreopsis ovata* (Dinophyceae) in Mediterranean rock pools: the spider's strategy. Harmful Algae News 33: 1–3. 25.

Bellocci, M., Ronzitti, G., Milandri, A., Melchiorre, N., Grillo, C., Poletti, R., Yasumoto, T., Rossini, G.P., 2008. A cytolytic assay for the measurement of palytoxin based on a cultured monolayer cell line (vol 374, pg 48, 2008). Anal. Biochem. 381, 178-178.

Bignami, G.S., 1993. A Rapid and Sensitive Hemolysis Neutralization Assay for Palytoxin. Toxicon 31, 817-820.

Bignami, G.S., Raybould, T.J.G., Sachinvala, N.D., Grothaus, P.G., Simpson, S.B., Lazo, C.B., Byrnes, J.B., Moore, R.E., Vann, D.C., 1992. Monoclonal Antibody-Based Enzyme-Linked Immunoassays for the measurement of palytoxin in biological samples. Toxicon 30, 687-700.

Bire, R., Trotereau, S., Lemee, R., Delpont, C., Chabot, B., Aumond, Y., Krys, S., 2013. Occurrence of palytoxins in marine organisms from different trophic levels of the French Mediterranean coast harvested in 2009. Harmful Algae 28, 10-22.

Bravo, I., Vila, M., Casablanca, S., Rodriguez, F., Rial, P., Riobo, P., Penna, A., 2012. Life cycle stages of the benthic palytoxin-producing dinoflagellate *Ostreopsis* cf. *ovata* (Dinophyceae). Harmful Algae 18, 24-34.

Brissard, C., Herrenknecht, C., Sechet, V., Herve, F., Pisapia, F., Harcouet, J., Lemee, R., Chomerat, N., Hess, P., Amzil, Z., 2014. Complex Toxin Profile of French Mediterranean *Ostreopsis* cf. *ovata* Strains, Seafood Accumulation and Ovatoxins Prepurification. Marine drugs 12, 2851-2876.

Casabianca, S., Casabianca, A., Riobo, P., Franco, J.M., Vila, M., Penna, A., 2013. Quantification of the Toxic Dinoflagellate *Ostreopsis* spp. by qPCR Assay in Marine Aerosol. Environmental Science & Technology 47, 3788-3795.

Ciminiello, P., Dell'Aversano, C., Dello Iacovo, E., Fattorusso, E., Forino, M., Grauso, L., Tartaglione, L., Guerrini, F., Pezzolesi, L., Pistocchi, R., 2012a. Isolation and structure elucidation of Ovatoxin-a, the major toxin produced by *Ostreopsis ovata*. Journal of the American Chemical Society 134, 1869-1875.

Ciminiello, P., Dell'Aversano, C., Dello Iacovo, E., Fattorusso, E., Forino, M., Grauso, L., Tartaglione, L., Guerrini, F., Pistocchi, R., 2010. Complex palytoxin-like profile of *Ostreopsis ovata*. Identification of four new ovatoxins by high-resolution liquid chromatography/mass spectrometry. Rapid communications in mass spectrometry 24, 2735-2744.

Ciminiello, P., Dell'Aversano, C., Dello Iacovo, E., Fattorusso, E., Forino, M., Tartaglione, L., Battocchi, C., Crinelli, R., Carloni, E., Magnani, M., Penna, A., 2012b. Unique Toxin Profile of a Mediterranean *Ostreopsis* cf. *ovata* Strain: HR LC-MSn Characterization of Ovatoxin-f, a New Palytoxin Congener. Chemical research in toxicology 25, 1243-1252.

Ciminiello, P., Dell'Aversano, C., Dello Iacovo, E., Fattorusso, E., Forino, M., Tartaglione, L., Benedettini, G., Onorari, M., Serena, F., Battocchi, C., Casabianca, S., Penna, A., 2014. First Finding of *Ostreopsis* cf. *ovata* Toxins in Marine Aerosols. Environmental Science & Technology 48, 3532-3540.

Ciminiello, P., Dell'Aversano, C., Dello Lacovo, E., Fattorusso, E., Forino, M., Tartaglione, L., 2011. LC-MS of palytoxin and its analogues: State of the art and future perspectives. Toxicon 57, 376-389.

Ciminiello, P., Dell'Aversano, C., Fattorusso, E., Forino, M., Tartaglione, L., Grillo, C., Melchiorre, N., 2008. Putative palytoxin and its new Analogue, Ovatoxin-a, in *Ostreopsis ovata* collected along the Ligurian Coasts during the 2006 toxic outbreak. Journal of the American society for mass spectrometry 19, 111-120.

Cohu, S., Mangialajo, L., Thibaut, T., Blanfune, A., Marro, S., Lemee, R., 2013. Proliferation of the toxic dinoflagellate *Ostreopsis* cf. *ovata* in relation to depth, biotic substrate and environmental factors in the North West Mediterranean Sea. Harmful Algae 24, 32-44.

Cohu, S., Thibaut, T., Mangialajo, L., Labat, J.P., Passafiume, *O.*, Blanfune, A., Simon, N., Cottalorda, J.M., Lemee, R., 2011. Occurrence of the toxic dinoflagellate *Ostreopsis* cf. *ovata* in relation with environmental factors in Monaco (NW Mediterranean). Marine Pollution Bulletin 62, 2681-2691.

CRLMB, 2005, (Community Reference Laboratory for Marine Biotoxins) Report on toxicology working group meeting. Cesenatico, Italy.

David, H., Laza-Martinez, A., Miguel, I., Orive, E., 2013. *Ostreopsis* cf. *siamensis* and *Ostreopsis* cf. *ovata* from the Atlantic Iberian Peninsula: Morphological and phylogenetic characterization. Harmful Algae 30, 44-55.

Deeds, J.R., Schwartz, M.D., 2010. Human risk associated with palytoxin exposure. Toxicon 56, 150-162.

Escalera, L., Benvenuto, G., Scalco, E., Zingone, A., Montresor, M., 2014. Ultrastructural Features of the Benthic Dinoflagellate *Ostreopsis* cf. *ovata* (Dinophyceae). Protist 165, 260-274.

Faust, M.A., 1999. Three new Osteopsis species (Dinophyceae): *O. marinus* sp. nov., *O.* belizeanus sp. nov., and *O. caribbeanus* sp. nov. Phycologia 38, 92.

Faust, M.A., Gulledge, R.A., 2002. Identifying harmful marine dinoflagellates. Contributions from the United States National Herbarium 42, 1-144.

Faust, M.A., Morton, S.L., 1995. Morphology and Ecology of the Marine Dinoflagellate *Ostreopsis*-Labens Sp-Nov (Dinophyceae). Journal of Phycology 31, 456-463.

Faust, M.A., Morton, S.L., Quod, J.P., 1996. Further SEM study of marine dinoflagellates: The genus *Ostreopsis* (Dinophyceae). Journal of Phycology 32, 1053-1065.

Fraga, S., 2014. Caracterización taxonómica y ecología de species crípticas o pseudocrípticas de dinoflagelados nocivos. Unpublished PhD thesis. Universidade de Vig*O.*

Fraga, S., Rodriguez, F., Bravo, I., Zapata, M., Maranon, E., 2012. Review of the main ecological features affecting benthic dinoflagellate blooms. Cryptogamie Algologie 33, 171-179.

Furlan, M., Antonioli, M., Zingone, A., Sardo, A., Blason, C., Pallavicini, A., Umani, S.F., 2013. Molecular identification of *Ostreopsis* cf. *ovata* in filter feeders and putative predators. Harmful Algae 21-22, 20-29.

Gleibs, S., Mebs, D., Werding, B., 1995. Studies on the origin and distribution of palytoxin in a Caribbean coral reef. Toxicon 33, 1531-1537.

Guerrini, F., Pezzolesi, L., Feller, A., Riccardi, M., Ciminiello, P., Dell'Aversano, C., Tartaglione, L., Dello Iacovo, E., Fattorusso, E., Forino, M., Pistocchi, R., 2010. Comparative growth and toxin profile of cultured *Ostreopsis ovata* from the Tyrrhenian and Adriatic Seas. Toxicon 55, 211-220.

Habermann, E., Ahnerthilger, G., Chhatwal, G.S., Beress, L., 1981. Delayed hemolytic action of palytoxin. General characteristics. Biochimica Et Biophysica Acta 649, 481-486.

Habermann, E., Chhatwal, G.S., Hessler, H.J., 1981. Palytoxin raises the nonspecific permeability of erythrocytes in an ouabain-sensitive manner. Naunyn-Schmiedebergs Arch. Pharmacol. 317, P374-P374.

Hallegraeff, G.M., Bolch, C.J., 1991. Transport of Toxic Dinoflagellate Cysts Via Ships Ballast Water. Marine Pollution Bulletin 22, 27-30.

Hilgemann, D.W., 2003. From a pump to a pore: How palytoxin opens the gates. Proceedings of the National Academy of Sciences of the United States of America 100, 386-388.

Honsell, G., Bonifacio, A., De Bortoli, M., Penna, A., Battocchi, C., Ciminiello, P., Dell'Aversano, C., Fattorusso, E., Sosa, S., Yasumoto, T., Tubaro, A., 2013. New Insights on Cytological and Metabolic Features of *Ostreopsis* cf. *ovata* Fukuyo (Dinophyceae): A Multidisciplinary Approach. Plos One 8.

Kang, N.S., Jeong, H.J., Lee, S.Y., Lim, A.S., Lee, M.J., Kim, H.S., Yih, W., 2013. Morphology and molecular characterization of the epiphytic benthic dinoflagellate *Ostreopsis* cf. *ovata* in the temperate waters off Jeju Island, Korea. Harmful Algae 27, 98-112.

Laza-Martinez, A., Orive, E., Miguel, I., 2011. Morphological and genetic characterization of benthic dinoflagellates of the genera *Coolia*, *Ostreopsis* and Prorocentrum from the south-eastern Bay of Biscay. European Journal of Phycology 46, 45-65.

Leliaert, F., Smith, D.R., Moreau, H., Herron, M.D., Verbruggen, H., Delwiche, C.F., De Clerck, *O.*, 2014. Phylogeny and Molecular Evolution of the Green Algae. Critical Reviews in Plant Sciences 31, 1-46.

Lenoir, S., Ten-Hage, L., Turquet, J., Quod, J.P., Bernard, C., Hennion, M.C., 2004. First evidence of palytoxin analogues from an *Ostreopsis mascarenensis* (Dinophyceae) benthic bloom in Southwestern Indian Ocean. Journal of Phycology 40, 1042-1051.

Litaker, R.W., Vandersea, M.W., Kibler, S.R., Reece, K.S., Stokes, N.A., Lutzoni, F.M., Yonish, B.A., West, M.A., Black, M.N.D., Tester, P.A., 2007. Recognizing dinoflagellate species using ITS rDNA sequences. Journal of Phycology 43, 344-355.

Mangialajo, L., Bertolotto, R., Cattaneo-Vietti, R., Chiantore, M., Grillo, C., Lemee, R., Melchiorre, N., Moretto, P., Povero, P., Ruggieri, N., 2008. The toxic benthic dinoflagellate *Ostreopsis ovata*: Quantification of proliferation along the coastline of Genoa, Italy. Marine Pollution Bulletin 56, 1209-1214.

Mangialajo, L., Ganzin, N., Accoroni, S., Asnaghi, V., Blanfuné, A., Cabrini, M., Cattaneo-Vietti, R., Chavanon, F., Chiantore, M., Cohu, S., Costa, E., Fornasaro, D., Grossel, H., Marco-Miralles, F., Masó, M., Reñé, A., Rossi, A.M., Sala, M.M., Thibaut, T., Totti, C., Vila, M., Lemée, R., 2011. Trends in *Ostreopsis* proliferation along the Northern Mediterranean coasts. Toxicon In Press, Corrected Proof.

Mercado, J.A., Rivera-Rentas, A.L., Gonzalez, I., Tosteson, T.R., Molgó, J., Escalona De Motta, G., 1994. Neuro- and myo-toxicity of extracts from the benthic

dinoflagellate *Ostreopsis* lenticularis is sensitive to μ-conotoxin. Soc. Neurosci. Abstr. 20, 718, 303.717.

Monti, M., Cecchin, E., 2012. Comparative growth of three strains of *Ostreopsis ovata* at different light intensities with focus on inter-specific allelopathic interactions. Cryptogamie Algologie 33, 113-119.

Moore, R.E., Bartolini, G., 1981. Structure of palytoxin. Journal of the American Chemical Society 103, 2491-2494.

Moore, R.E., Scheuer, P.J., 1971. Palytoxin: a new marine toxin from a coelenterate. Science 172, 495-498.

Munday, R., Palytoxin toxicology: Animal studies. *Toxicon* 2011, 57, (3), 470-477.

Norris, d.r., Bomber, j.w. & Balech, e., 1985 – Benthic dinoflagellates associated with ciguatera from Florida Keys. I. *Ostreopsis* heptagona sp. nov. In: Anderson, D.M., White, A.W., Baden, D.G. (Eds.), Toxic Dinoflagellates. Elsevier, Amsterdam, 39–44.

Parsons, M.L., Aligizaki, K., Bottein, M.-Y.D., Fraga, S., Morton, S.L., Penna, A., Rhodes, L., 2012. Gambierdiscus and *Ostreopsis*: Reassessment of the state of knowledge of their taxonomy, geography, ecophysiology, and toxicology. Harmful Algae 14, 107-129.

Penna, A., Fraga, S., Battocchi, C., Casabianca, S., Giacobbe, M.G., Riobo, P., Vernesi, C., 2010. A phylogeographical study of the toxic benthic dinoflagellate genus *Ostreopsis* Schmidt. J. Biogeogr. 37, 830-841.

Penna, A., Vila, M., Fraga, S., Giacobbe, M.G., Andreoni, F., Riobo, P., Vernesi, C., 2005. Characterization of *Ostreopsis* and *Coolia* (Dinophyceae) isolates in the western Mediterranean Sea based on morphology, toxicity and internal transcribed spacer 5.8s rDNA sequences. Journal of Phycology 41, 212-225.

Perini, F., Casabianca, A., Battocchi, C., Accoroni, S., Totti, C., Penna, A., 2011. New Approach Using the Real-Time PCR Method for Estimation of the Toxic Marine Dinoflagellate *Ostreopsis* cf. *ovata* in Marine Environment. Plos One 6.

Pezzolesi, L., Guerrini, F., Ciminiello, P., Dell'Aversano, C., Dello Iacovo, E., Fattorusso, E., Forino, M., Tartaglione, L., Pistocchi, R., 2012. Influence of temperature and salinity on *Ostreopsis* cf. *ovata* growth and evaluation of toxin content through HR LC-MS and biological assays. Water Research 46, 82-92.

Pezzolesi, L., Pistocchi, R., Fratangeli, F., Dell'Aversano, C., Dello Iacovo, E., Tartaglione, L., 2014. Growth dynamics in relation to the production of the main cellular components in the toxic dinoflagellate *Ostreopsis* cf. *ovata*. Harmful Algae 36, 1-10.

Pin, L.C., Teen, L.P., Ahmad, A., Usup, G., 2001. Genetic diversity of *Ostreopsis ovata* (Dinophyceae) from Malaysia. Marine Biotechnology 3, 246-255.

Pistocchi, R., Pezzolesi, L., Guerrini, F., Vanucci, S., Dell'Aversano, C., Fattorusso, E., 2011. A review on the effects of environmental conditions on growth and toxin production of *Ostreopsis ovata*. Toxicon In Press, Corrected Proof.

Quod, J.P., Quod, J.P., 1994. *Ostreopsis-Mascarenensis* Sp-Nov (Dinophyceae), a New Toxic Dinoflagellate from Coral-Reefs in the Southwest Indian-Ocean. Cryptogamie Algologie 15, 243-251.

Reverté, L., Soliño, L., Carnicer, *O.*, Diogène, J., Campàs, M. Alternative methods for the detection of emerging marine toxins: Biosensors, biochemical and cell-based assays. Marine Drugs, submitted.

Rhodes, L., 2011. World-wide occurrence of the toxic dinoflagellate genus *Ostreopsis* Schmidt. Toxicon 57, 400-407.

Richlen, M.L., Lobel, P.S., 2011. Effects of depth, habitat, and water motion on the abundance and distribution of ciguatera dinoflagellates at Johnston Atoll, Pacific Ocean. Marine Ecology Progress Series 421, 51-66.

Riobo, P., Franco, J.M., 2011. Palytoxins: Biological and chemical determination. Toxicon 57, 368-375.

Riobo, P., Paz, B., Franco, J.M., Vazquez, J.A., Murado, M.A., 2008. Proposal for a simple and sensitive haemolytic assay for palytoxin. Toxicological dynamics, kinetics, ouabain inhibition and thermal stability. Harmful Algae 7, 415-429.

Sato, S., Nishimura, T., Uehara, K., Sakanari, H., Tawong, W., Hariganeya, N., Smith, K., Rhodes, L., Yasumoto, T., Taira, Y., Suda, S., Yamaguchi, H., Adachi, M., 2011. Phylogeography of *Ostreopsis* along West Pacific Coast, with Special Reference to a Novel Clade from Japan. PLoS ONE 6, e27983.

Satoh, E., Ishii, T., Nishimura, M., 2003. Palytoxin-induced increase in cytosolic-free Ca 2+ in mouse spleen cells. European journal of pharmacology 465, 9-13.

Scalco, E., Brunet, C., Marino, F., Rossi, R., Soprano, V., Zingone, A., Montresor, M., 2012. Growth and toxicity responses of Mediterranean *Ostreopsis* cf. *ovata* to seasonal irradiance and temperature conditions. Harmful Algae 17, 25-34.

Selina, M.S., Morozova, T.V., Vyshkvartsev, D.I., Orlova, T.Y., 2014. Seasonal dynamics and spatial distribution of epiphytic dinoflagellates in Peter the Great Bay (Sea of Japan) with special emphasis on *Ostreopsis* species. Harmful Algae 32, 1-10.

Selina, M.S., Orlova, T.Y., 2010. First occurrence of the genus *Ostreopsis* (Dinophyceae) in the Sea of Japan. Botanica Marina 53, 243-249.

Shears, N.T., Ross, P.M., 2009. Blooms of benthic dinoflagellates of the genus *Ostreopsis*; an increasing and ecologically important phenomenon on temperate reefs in New Zealand and worldwide. Harmful Algae 8, 916-925.

Shimahara, T., Molgó, J., 1990. Palytoxin enhances quantal acetylcholine release from motor nerve terminals and increases cytoplasmic calcium levels in a neuronal hybrid cell line. Life Sci Adv Pharmacol 9, 785-792.

Stern, R.F., Andersen, R.A., Jameson, I., Kuepper, F.C., Coffroth, M.-A., Vaulot, D., Le Gall, F., Veron, B., Brand, J.J., Skelton, H., Kasai, F., Lilly, E.L., Keeling, P.J., 2012. Evaluating the Ribosomal Internal Transcribed Spacer (ITS) as a Candidate Dinoflagellate Barcode Marker. Plos One 7.

Suzuki, T., Watanabe, R., Uchida, H., Matsushima, R., Nagai, H., Yasumoto, T., Yoshimatsu, T., Sato, S., Adachi, M., 2012. LC-MS/MS analysis of novel ovatoxin isomers in several *Ostreopsis* strains collected in Japan. Harmful Algae 20, 81-91.

Taniyama, S., Arakawa, *O.*, Terada, M., Nishio, S., Takatani, T., Mahmud, Y., Noguchi, T., 2003. *Ostreopsis* sp., a possible origin of palytoxin (PTX) in parrotfish Scarus ovifrons. Toxicon 42, 29-33.

Tichadou, L., Glaizal, M., Armengaud, A., Grossel, H., Lemee, R., Kantin, R., Lasalle, J.L., Drouet, G., Rambaud, L., Malfait, P., de Haro, L., 2010. Health impact of unicellular algae of the *Ostreopsis* genus blooms in the Mediterranean Sea: experience of the French Mediterranean coast surveillance network from 2006 to 2009. Clinical Toxicology 48, 839-844.

Totti, C., Accoroni, S., Cerino, F., Cucchiari, E., Romagnoli, T., 2011. *Ostreopsis ovata* bloom along the Conero Riviera (northern Adriatic Sea): Relationships with environmental conditions and substrata. Harmful Algae 9, 233-239.

Tubaro, A., Durando, P., Del Favero, G., Ansaldi, F., Icardi, G., Deeds, J.R., Sosa, S., 2011. Case definitions for human poisonings postulated to palytoxins exposure. Toxicon 57, 478-495.

Usami, M., Satake, M., Ishida, S., Inoue, A., Kan, Y., Yasumoto, T., 1995. Palytoxin analogs from the dinoflagellate *Ostreopsis siamensis*. Journal of the American Chemical Society 117, 5389-5390.

Utermöhl H., 1958. Zur Vervollkomnung der quantitativen Phytoplankton-Methodik. Mitt. int. Ver. ther. angew. Limnol 9, 1-38

Vanucci, S., Guerrini, F., Pezzolesi, L., Dell'Aversano, C., Ciminiello, P., Pistocchi, R., 2012a. Cell growth and toxins' content of *Ostreopsis* cf. *ovata* in presence and absence of associated bacteria. Cryptogamie Algologie 33, 105-112.

Vanucci, S., Pezzolesi, L., Pistocchi, R., Ciminiello, P., Dell'Aversano, C., Dello Iacovo, E., Fattorusso, E., Tartaglione, L., Guerrini, F., 2012b. Nitrogen and phosphorus limitation effects on cell growth, biovolume, and toxin production in *Ostreopsis* cf. *ovata*. Harmful Algae 15, 78-90.

Vidyarathna, N.K., Graneli, E., 2013. Physiological responses of *Ostreopsis ovata* to changes in N and P availability and temperature increase. Harmful Algae 21-22, 54-63.

Vidyarathna, N.K., Granéli, E., 2011. Influence of temperature on growth, toxicity and carbohydrate production of a Japanese *Ostreopsis ovata* strain, a toxic-bloom-forming dinoflagellate. Aquatic Microbial Ecology 65, 261-270.

Vila, M., Garces, E., Maso, M., 2001. Potentially toxic epiphytic dinoflagellate assemblages on macroalgae in the NW Mediterranean. Aquatic Microbial Ecology 26, 51-60.

CHAPTER 2

Contribution to the genus *Ostreopsis* in a tropical area, Reunion Island (Indian Ocean): molecular, morphologic and toxicity characterization

2.1. Abstract

The toxic epi-benthic dinoflagellate *Ostreopsis* is distributed worldwide in coral reef ecosystems and temperate regions. There are nine species described to date based on morphological features. Some of them have been proved to be producers of palytoxin-like compounds, representing a threat to coastal marine organisms and human health. The taxonomy of the genus is currently under revision due to morphological similarities among species. The present study aims to provide additional information on morphology, genetic data and toxin content from thirty three strains isolated in the west coast of Reunion Island, in the Indian Ocean. Two morphotypes were distinguishable, which were non overlapping in size; one small (DV=53.48±6.86 μm; W=37.72±5.64 μm) with a typical tear-drop shape and the other larger in size (DV=103.94±5.12 μm; W=85.26±6.96 μm) with a rounded shape. Phylogenetic analysis determined the presence of three genotypes. Within the small morphotype, two different species were identified, *O.* cf. *ovata* and a cryptic species not previously characterized. The larger cells constituted a genetically homogeneous clade. Nucleotide differences between this species and *Ostreopsis* sp. 5 described in Sato *et al.,* 2011, was relatively low (p<0.088) and may be the same species. Haemolytic analysis resulted in no palytoxin-like activity in any of the three species.

2.2. Introduction

The dinoflagellate *Ostreopsis* spp. grows in tropical and temperate epi-benthic microalgae communities and has been described within the benthic dinoflagellate communities in ciguatera endemic areas (Tindall *et al.,* 1984). This genus grows over a wide range, though the majority of the described species have been found in tropical waters. The nine species identified so far are based on morphological features, *O. siamensis* Schmidt 1901; *O. ovata* Fukuyo 1981; *O. lenticularis* Fukuyo 1981; *O. heptagona* Norris *et al.,* 1985; *O. mascarenensis* Quod 1994; *O.* labens Faust & Morton, 1995; *O. marinus* Faust, 1999; *O. belizeanus* Faust, 1999 and *O. caribbeanus* Faust, 1999. However, the taxonomy of the genus is under revision since different species with the same morphological characteristics show significant genetic differences. Plate pattern is very similar for all species with the exception of *O. heptagona* (Faust *et al.,* 1995). Variability in size within the same species has been observed both in field samples (e.g. Aligizaki *et al.,* 2006; Accoroni *et al.,* 2012; Carnicer *et al.,* in preparation) and in cultures (Guerrini *et al.,* 2010; Pezzolessi *et al.,* 2012; Bravo *et al.,* 2012), adding more difficulty to differentiate the species. Recent studies have implemented molecular analysis in addition to morphological description, to counteract this problem and clarify the present problematic taxonomy (Pin *et al.,* 2001; Penna *et al.,* 2005; Penna *et al.,* 2010; Laza-Martínez *et al.,* 2011; Sato *et al.,* 2011; Kang *et al.,* 2013; David *et al.,* 2013).

Proliferations of *Ostreopsis* spp. along the Mediterranean coasts during the last decade have been associated with several episodes of human intoxication (reviewed in Tubaro *et al.,* 2011). Blooms occurring in summer-fall months are produced exclusively by *O.* cf. *ovata* in most cases, or together with *O.* cf. *siamensis* in lower abundance (Mangialajo *et al.,* 2011). This fact has motivated many studies focused on these two species that have brought new insights on the ecology, toxicity and phylogeny of both species in the Mediterranean Sea. Meanwhile within these fields, the tropical taxa remained poorly studied though the number of species of *Ostreopsis* inhabiting this ecosystem is higher than in temperate areas. Recent advances have been made on the taxonomy of the dinoflagellate genus Gambierdiscus, also a benthic dinoflagellates that co-occurs with *Ostreopsis* in tropical areas and mainly responsible for ciguatera poisoning in the tropics. Indeed, phylogenetic studies have demonstrated that the genus Gambierdiscus exhibits a remarkable diversity with both endemic and cosmopolitan taxa, whereas former studies wrongly indicated *G. toxicus* to be a widespread species (Litaker *et al.,* 2010). As for *Gambierdiscus*, we consider that the genetic diversity in *Ostreopsis* may be more complex than is suggested by the current morphological descriptions and is worth describing more deeply.

More widely, molecular tools have allowed demonstrating, within benthic dinoflagellates, a larger diversity than previously reported and the descriptions of many new species and genera (Litaker *et al.,* 2007). These results should motivate a deeper investigation of the actual *Ostreopsis* taxonomy considering both the morphological and the phylogenetic relationships within the genus. For that purpose, it is important to gather sequence data of isolates from different origins and climates, which would provide valuable information necessary to perform an appropriate phylogenetic and biogeographic study of the genus. The nuclear rDNA internal transcribed spacer regions (ITS1 and ITS2) and 5.8S rRNA gene have been used in multiple phylogenetic studies (e. g. Jensen *et al.,* 1993, Hartmann *et al.,* 2001) and represent a useful element to characterize *Ostreopsis* taxonomy (Penna *et al.,* 2005). Unfortunately, there is no genetic material for the type species of the genus defined by morphology so it is not possible to assure if sequences obtained in new studies correspond to a particular species of the genus. As a cautionary measure taken after the first phylogenetic studies, the species found in the Mediterranean Sea (the most studied so far) are named *O.* cf. *siamensis* (Penna *et al.,* 2005) and *O.* cf. *ovata* (Penna *et al.,* 2010) until future confirmation. In recent years, studies have provided new sequences from cells isolated in tropical waters increasing the possibilities of matching described morphologies with genetic material. Sequences from the Pacific, the eastern Indian, the western and eastern Atlantic Oceans, have been added to the numerous sequences available from the Mediterranean Sea isolates in GenBank, contributing to a better understanding of the phylogenetic relationships. The early phylogenetic study performed in Malaysian waters by Pin

and coworkers in 2001, highlighted a subdivision within the Indo Pacific clade of *O.* cf. *ovata* and sequenced *O. lenticularis* for the first time. In a following study, (Penna *et al.,* 2005), *O.* cf. *ovata* sequences from the Mediterranean Sea and the Atlantic Ocean formed a common clade, separated from the Indo-Pacific isolates. *O. labens* was first sequenced in Penna *et al.,* 2010 and was clustered together with *O.* lenticularis, raising the issue of the need for a deep revision in the species identification. Sato *et al.,* (2011) found five clades that were not sequenced before and another very close to the sequences of *O. lenticularis* and *O. labens*, coupled within the same clade named *Ostreopsis* sp. 6. Isolates from Cuba (Moreira *et al.,* 2012) were clustered into the *O. lenticularis* clade by phylogenetic analysis as well as by morphologic features. In David *et al.,* (2013) a new sequence was published from isolates from Puerto Rico and Greece which clustered with the strain VGO881, from Canary Islands, first sequenced in Penna *et al.,* (2010). A recent *O.* cf. *ovata* isolate from Korean waters was genetically different from the reported clades (Kang *et al.,* 2013). But at that point, no sequences from the western Indian Ocean were yet available in GenBank.

Furthermore, toxin composition is an additional characteristic that may contribute to assignation of a species-specific toxin profile (Penna *et al.,* 2005). Various species belonging to the genus *Ostreopsis* have been identified as palytoxin (PLTX)-like compound producers; Ostreocin-D (Usami *et al.,* 1995) from *O. siamensis*; mascarenotoxins from *O. mascarenensis* (Lenoir *et al.,* 2004); putative PLTX and ovatoxins analogues from *O.* cf. *ovata* (Ciminiello *et al.,* 2012). Discrimination between toxic and non-toxic species has been observed in other toxic dinoflagelatte genera such as *Alexandrium* (Yoshida *et al.,* 2001) and *Gambierdiscus* (Litaker *et al.,* 2010). Therefore, a preliminary toxicity analysis would contribute to the characterization of new species identification.

The present study aims to provide additional information about genetics, morphology and toxicity of *Ostreopsis* strains collected from Reunion Island, western Indian Ocean, as a contribution to clarify the *Ostreopsis* taxonomy. Given that more attention has been focused on Mediterranean clades, these new sequences from tropical areas will enhance the diversity of sequences within Genbank, with more possibilities of finding the species originally described. Particularly, in the south-west Indian Ocean there have been reported *O. mascarenensis, O. siamensis, O. ovata, O. lenticularis, O. labens,* (Faust, 1995), and *O. marinus* (Faust, 1999). Samples from Reunion Island would thus constitute an important input of new sequences to clarify and advance the *Ostreopsis* phylogeny.

2.3. Material and Methods

2.3.1. *Sampling and cultures maintenance*

Sampling sites were located along the east coral reef coast in Reunion Island (Figure 2.1) and samples were collected weekly from September to November 2013. Different species of macroalgae were collected in each site, *Actinotrichia fragilis* (Forsskål) Børgesen, 1932*, Turbinaria conoides* (J. Agardh) Kützing 1860*, Jania* sp. (J. V. Lamouroux, 1812) and *Galaxaura* sp. (J. V. Lamouroux, 1982)*,* between 1.5 and 0.5 meters depth. Macroalgae were placed in a plastic bottle with 200 mL of 0.2 µm filtered seawater. In order to release the epiphyte community from macroalgae, bottles were intensively shaken for one minute and filtered through a 200 µm mesh so that particles were eliminated. Once in the laboratory, *Ostreopsis* cells were isolated with a glass pipette by capillary method (Hoshaw and Rosowski, 1973) under an inverted microscope (Olympus CK2). Cells were transferred to a 15-well culture microplates (FALCON) filled with autoclaved natural filtered seawater containing f/2 concentrated nutrients diluted five-fold (Guillard, 1975). Cultures were maintained at 26°C under 12:12h light:dark photoperiod. Illumination was provided by fluorescent tubes with a photon irradiance around 20-40 µmol photons m^{-2} s^{-1}. After an initial growth, cultures were inoculated in 25 cm^2 glass Erlenmeyer flasks filled with 50 mL of medium. At the end of the exponential phase, cultures were inoculated to 150 cm^2 glass Erlenmeyer flasks filled with 450 mL of acclimated medium for three weeks until extraction.
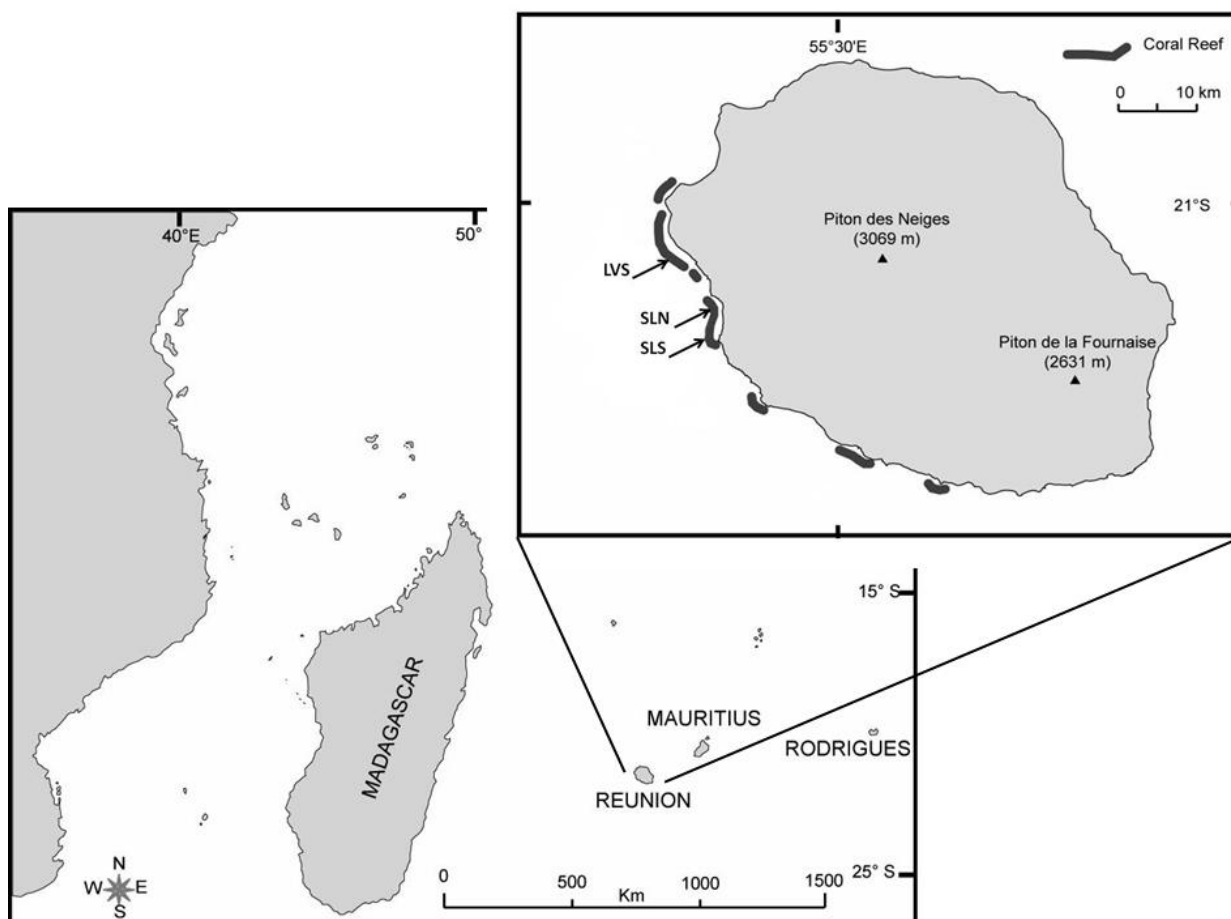
Fig 2.1. Geographic location of the studied sites in La Réunion, West Indian Ocean. Location acronyms and positions: LVS, Livingstone -21° 5' 51.3276"N; 55° 14' 17.6568" E; SLN, Saint-Leu Nord -21° 10' 52.971"N; 55° 17' 12.9516" E; SLS, Saint-Leu Sud, -21° 10' 52.971" N; 55.286931E

A total of thirty three *Ostreopsis* strains were isolated and DNA extractions were prepared. These extracts were later used for genetic characterization (see below). Of the total strain collection, twenty seven strains survived after three weeks in culture. Methanol extraction was performed for a subsequent toxin analysis.

2.3.2. Morphological characterization

Morphology was described from cells obtained in fixed field samples to avoid reporting possible deformations common in *Ostreopsis* spp. cells grown in culture. Samples, preserved with acidic lugol were analyzed under a light microscope (NIKON eclipse 80i) after staining with fluorescent Calcofluor White M2R, based on Fritz and Triemer (1985) methodology. Pictures in white light and in epifluorescence were taken using digital cameras © NIKON Digital Sight DS-5Mc and © HAMAMTSU ORCA-ER, respectively. To suppress focus problems and provide the most of morphological details, several images of each cell were taken and assembled using © Helicon Focus software.

2.3.3. Genetic characterization

The DNA extraction protocol followed Andree *et al.,* (2011). Polymerase Chain Reaction (PCR) conditions were those used in Sato *et al.,* (2011). ITS and 5.8S ribosomal RNA (rRNA) regions were obtained by using oligonucleotide primers ITSA (5'-GTAACACGGTHTCCGTAGGT-3') and ITSB (5'-AKATGCTTATRTTCAGCRGG-3'), performed in an Applied Biosytems, 2720 Thermal cycler. Resulting fragments of rRNA were evaluated by electrophoresis in agarose gel (1.5% wt/vol) stained with GelRed™ (Biotium Inc., Hayward, California, USA) and were sent to be sequenced bidirectionally (GENOSCREEN; Paris, France) using the same primers as those used in the initial amplification. Forward and reverse sequence reactions were aligned and manually edited using BioEdit, version 7.0.0 (Hall, T.A., 1999). Genetic distances were obtained by Kimura's two-parameter model (Kimura, 1980) with MEGA 5.1.

When several strains shared the same sequence, one strain was represented in the phylogenetic study. Maximum likelihood (ML) and Neighbor-joining (NJ) analyses were performed with genetic distances obtained by Kimura's two-parameter model (Kimura, 1980) or Tamura-3 parameters model (Tamura, 1992) performed with MEGA 5.1. The sequences of *Coolia monotis* VGO783, CM01 and IEO-CM7C were included as outgroups for the 5.8S-ITS ribosomal gene phylogeny (this outgroup was later discarded – see below). To estimate evolutionary divergence between ITS rDNA sequences we performed a pair-wise comparison, using Kimura, 1980 2-parameter model (Kimura, 1980), to calculate the number of base substitutions per site between sequences. Results are expressed as uncorrected genetic distance (p), 0 means no differences among sequences.

2.3.4. Toxin extraction

Twenty seven cultures of different strains were extracted for toxin evaluation after twenty-one days of growth. Cells were collected by filtration on 0.45 μm nylon filters and were stored at -80°C. For toxin extraction, 15 mL methanol/water (80:20) solution was added to filters and these were sonicated for 5 minutes in pulse mode (Touch-Screen Sonicator Ultrasonic Processor, Qsonica, LLC). The mixture was centrifuged at 600 x g for 10 minutes; the supernatant was decanted and filtered on polytetrafluoroethylene 0.45 μm membrane syringe filters. This procedure was repeated twice and filtered supernatants were pooled. The final extract was evaporated to a 25 mL methanol/water (80:20) final volume.

2.3.5. Haemolytic assay

The haemolytic test was performed following the method of Riobó *et al.,* (2008) with some modifications in reactive solution concentrations in order to perform a valid calibration curve. Palytoxin and PLTX-like analogs bind to the Na^+/K^+ pump provoking cell lysis and the heamoglobin released is quantified by a microplate Reader KC4 from BIO-TEK Instruments, Inc. (Vermont) at 405 nm absorbance. A calibration curve was done by using PLTX standard (Wako Chemicals GmbH,

Germany) with 12 concentrations from 12.5 to 1250 $pg.mL^{-1}$ adjusted to an exponential regression using SigmaPlot 9.0.

Working solution was prepared with washed sheep blood (OXOID), centrifuged (400 g, 10°C, 10 min) twice and diluted with phosphate buffered saline solution (PBS) 0.01 M, pH 7.4 (Sigma), 0.1% bovine serum albumin (BSA), 1 mM calcium chloride ($CaCl_2$ $2H_2O$) and 1 mM boric acid (H_3BO_3) to a final erythrocyte concentration of 1.5 x 10^6 $cells.mL^{-1}$. The PLTX assay specificity is verified by a blank assay with ouabain (final concentration of 2 mM). Ouabain is a glycoside that prevents PLTX binding to Na^+/K^+ pumps and thus, inhibits haemolytic activity. Toxin extractions and PLTX standard were evaporated and refilled with PBS solution to eliminate methanol and water from the extraction. Assay was performed in two non-treated 96 well microplates and samples were settled in triplicate. After 22 hours incubation at 24°C, microplates were centrifuged (200 g, 10 min), 200 μL of the supernatant was transferred to another microplate for absorbance reading. Total toxicity was expressed as PLTX equivalents per milliliter (PLTX $eq.mL^{-1}$).

2.4. Results

Description of strain isolation conditions such as location, date, macroalgae sampled, temperature and salinity are detailed in Table 2.1. *Ostreopsis* spp. abundances during sampling were very low (maximum of 200 $cell.g$ fwm^{-1}), being the small morphotype dominant.

ID	Sampling point	Date	Macroalge	Temp. (°C)	Salinity	Accession Number
P-0129	*	11/09/2013	n.d.	24.8	35.2	KM032205
P-0108	**	11/09/2013	Dead coral	nd	nd	KM032220
P-0111	SLN	18/09/2013	*Jania sp*	24	34.9	KM032198
P-0130	SLS	18/09/2013	*Turbinaria conoides*	24.6	35.4	KM032192
P-0131	SLS	18/09/2013	*Turbinaria conoides*	24.6	35.4	KM032191
P-0132	LVS	18/09/2013	*Turbinaria conoides*	25.6	35.4	KM032190
P-0106	LVS	18/09/2013	n.d.	25.6	35.4	KM032206
P-0112	SLN	25/09/2013	*Turbinaria conoides*	23.8	35	KM032207
P-0133	SLN	25/09/2013	*Turbinaria conoides*	23.8	35	KM032194
P-0134	SLN	25/09/2013	*Turbinaria conoides*	23.8	35	KM032193
P-0107	SLN	25/09/2013	*Turbinaria conoides*	23.8	35	KM032217
P-0109	SLS	25/09/2013	*Turbinaria conoides*	23.8	35	KM032218
P-0104	LVS	25/09/2013	*Turbinaria conoides*	25.6	35.4	KM032204
P-0105	LVS	25/09/2013	*Turbinaria conoides*	25.6	35.4	KM032216
P-0102	LVS	08/10/2013	*Galaxaura sp*	28.1	34.9	KM032209
P-0103	LVS	08/10/2013	*Galaxaura sp*	28.1	34.9	KM032213
P-0117	LVS	16/10/2013	*Turbinaria conoides*	26	34.5	KM032202
P-0113	SLS	16/10/2013	*Turbinaria conoides*	24.6	35	KM032202
P-0114	SLS	16/10/2013	*Turbinaria conoides*	24.6	35	KM032201
P-0115	SLS	16/10/2013	*Turbinaria conoides*	24.6	35	KM032212
P-0116	SLS	16/10/2013	*Turbinaria conoides*	24.6	35	KM032203
P-0119	SLN	29/10/2013	*Galaxaura sp*	25.3	33.2	KM032196
79.1L	SLN	29/10/2013	*Galaxaura sp*	25.3	33.2	KM032221
79.2L	SLN	29/10/2013	*Galaxaura sp*	25.3	33.2	KM032222
P-0121	SLN	29/10/2013	*Galaxaura sp*	25.3	33.2	KM032219
P-0135	SLN	29/10/2013	*Galaxaura sp*	25.3	33.2	KM032215
P-0122	SLN	29/10/2013	*Galaxaura sp*	25.3	33.2	KM032211
P-0137	LVS	29/10/2013	*Turbinaria conoides*	27.2	34.9	KM032199
P-0126	LVS	29/10/2013	*Turbinaria conoides*	27.2	34.9	KM032197
P-0127	LVS	29/10/2013	*Jania sp*	27.2	34.9	KM032214
P-0128	LVS	29/10/2013	*Jania sp*	27.2	34.9	KM032210
P-0141	SLN	05/11/2013	*Turbinaria conoides*	26.6	34.4	KM032195
P-0142	SLS	05/11/2013	*Turbinaria conoides*	27.7	34.8	KM032200

Table 2.1. Description of *Ostreopsis* strains collected in Reunion Island; location, date, macroalgae specie, temperature and salinity (nd = no data; * = 21° 11' 58.9092"N; 55° 16' 56.9706"E; ** = 21° 16' 10.2"N; 55° 19' 58.6632"E).

2.4.1. Morphological observations

Isolated cell morphology corresponded to the description of the genus *Ostreopsis*; photosynthetic, anterioposteriorly compressed and ventrally pointed cells. Plate pattern was Po, 3´, 7´´, 5´´´, 2´´´´, 1p. Two different cell morphologies were found in field samples, a group of large rounded cells and another one with a tear-drop shape and smaller size. Dorsoventral (DV) and width (W) diameters measurements from 73 cells from field samples are represented in Figure 2.2.
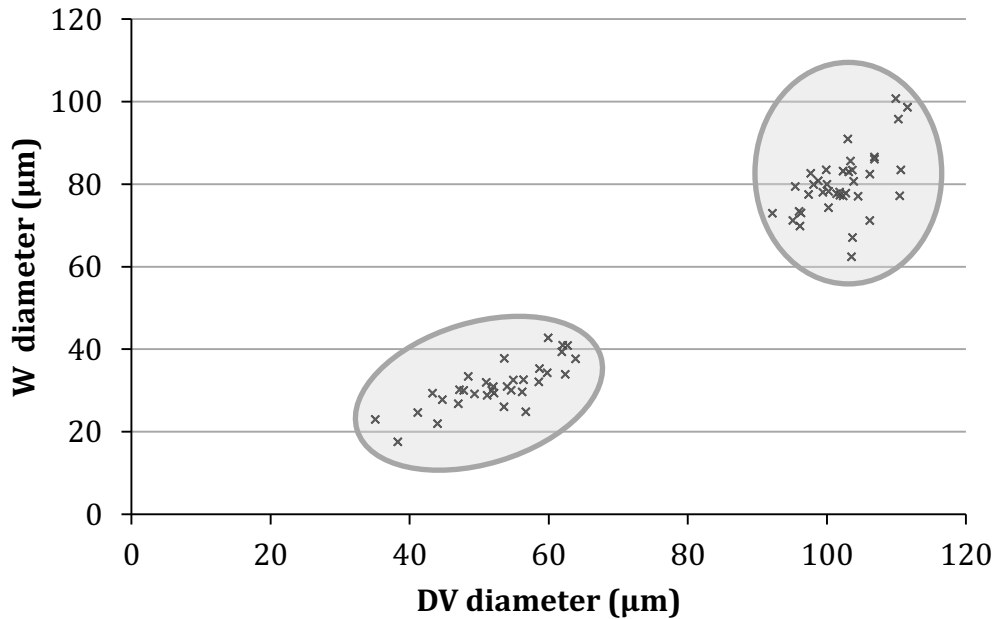
Fig 2.2. Cell size, DV and W diameters (µm) of field cells, n=73.

The large cells displayed a broad ovoid shape very similar to *O. lenticularis* but the size range (DV=103.94±5.12 µm; W=85.26±6.96 µm; n=40) fit more closely with *O. siamensis* (Faust *et al.,* 1996) and *O. marinus* (Faust, 1999). The epifluorescence microscopy revealed a plate arrangement similarly to *O. marinus* (Faust, 1999) and the presence of large pores and small pores or depressions (discernable at x600 magnification), randomly distributed on the thecal surface (Figure 2.3). This latter feature seems to coincide with the SEM observations of pres of different sizes in *O. siamensis* (Faust *et al.,* 1996). The apical pore is long and curved like in *O. siamensis* and *O. lenticularis*. Based only on the morphological features, it was not possible to clearly identify the large morphotype.
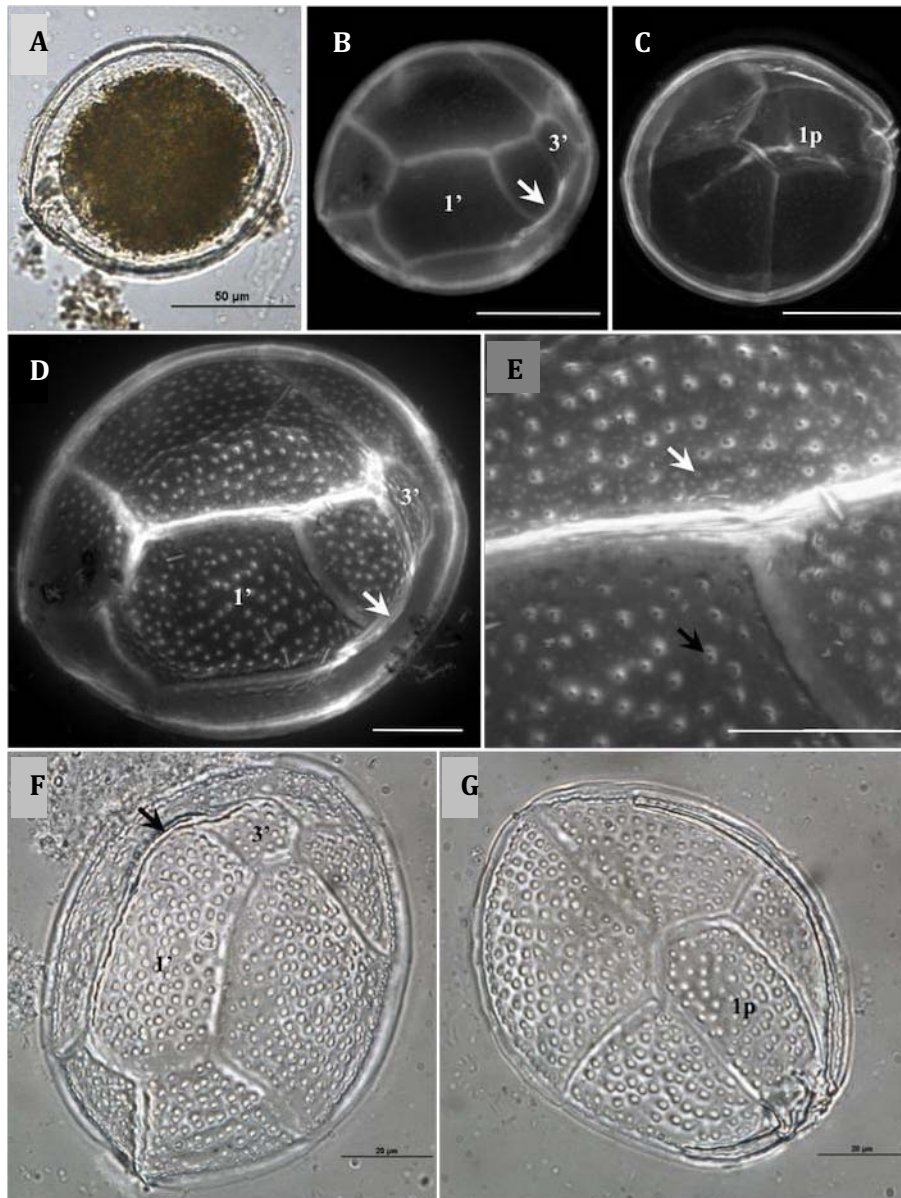
Fig 2.3. Morphology of the "Large" morphotype in field samples and in cultures. **A-D.** Shape, plate arrangement of the theca in uncultured lugol-stained cells. The apical pore position is indicated by a white arrow. **E.** Ornamentation detail on the thecal surface of an uncultured cell, showing large pores (black arrow) and smaller pores or depressions (white arrow). **F-G.** Plate arrangement in empty cells from cultured strain P-0108. The apical pore position is indicated by a black arrow. **C, G.** View of epitheca. **A-B, D-F.** View of epitheca. **A, F, G.** Bright Field microscopy images. **B-E.** Epifluorescence microscopy images with Calcofluor staining. Figs 3-5, bar scale = 50 μm. Figs 6-9, bar scale = 20 μm.

The small cells exhibited a tear-drop shape (DV=53.48±6.86 μm; W=37.72±5.64 μm; n=33). Sizes mostly coincided to those reported for *O.* cf. *ovata* (reviewed in David *et al.,* 2013). The plate pattern observed with epifluorescence also resembled the plate arrangement in *O.cf. ovata*, along with the presence of pores (discernable at x600 magnification) evenly distributed on the thecal surface and a relatively straight apical pore (Figure 2.4). But, considering the fact that plate pattern is similar to all *Ostreopsis* species except *O. heptagona*, we cannot assure the correspondence to any particular species based upon morphological description alone.
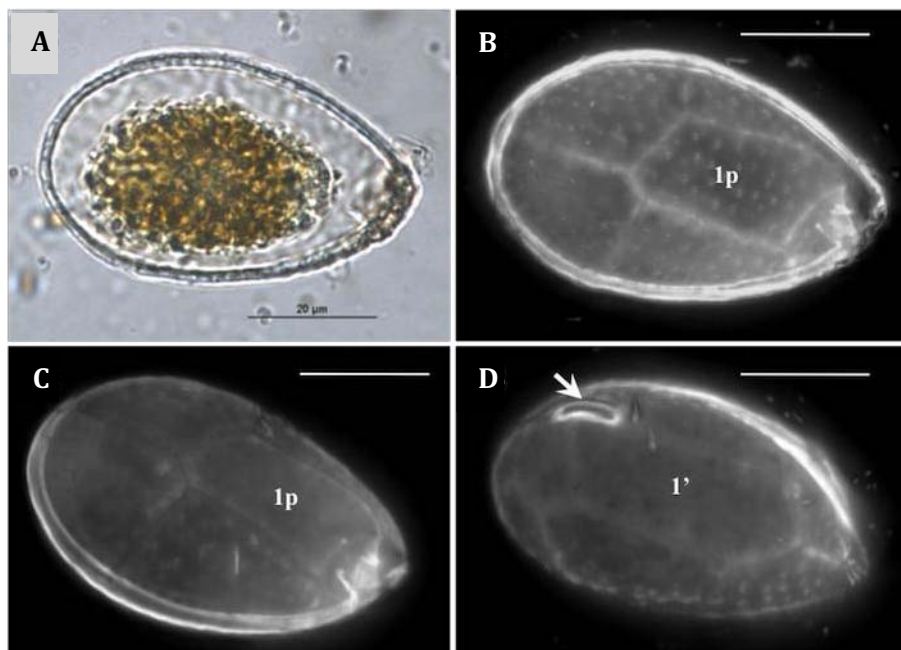
Fig. 2.4. Morphology of the "Small" morphotype identified in field samples (lugol-stained cells). **A-C.** Shape and plate arrangement of the hypotheca. **D.** Shape and plate arrangement of the epitheca. The apical pore position is indicated by a white arrow. **A.** Bright Field microscopy images. **B-D.** Epifluorescence microscopy images with Calcofluor staining. Bar scale = 20 µm.

2.4.2. ITS regions analysis

The PCR amplifications of 5.8S and ITS regions obtained from thirty six cultured samples were studied together with forty four sequences from GenBank. After alignment, the resulting data set included fragments with a final length of 279 base pairs (bp). Due to the variability in ITS regions, it was not possible to perform a correct alignment with the outgroup (*Coolia monotis*) commonly used in the phylogeny of the genus *Ostreopsis* (Penna *et al.,* 2010). The two different algorithms tested presented very similar tree topologies, differentiating the same groups of clusters; the NJ phylogenetic tree is the one represented in Figure 2.5. Utilizing the same dataset, each analysis performed using two different models (Kimura-2 parameters and Tamura-3 parameters) resulted in nearly identical cladistic differentiation. The sequences obtained in this study have been deposited in GenBank under the accession numbers show in Table 2.1.

P-0117-Reunion Island Indian Ocean
AF218457-OvPR01-Malaysia south China Sea
AF218459-OvPR02-Malaysia South China Sea
P-0128-Reunion Island Indian Ocean
61 AB674904-CAWD174-Cook Island South Pacific Ocean
AF218458-OvPR04-Malaysia South China Sea
AB674905-OVPT2-Malaysia South China Sea
95 AF218464-OvSA10-Malaysia South China Sea
62 AF218462-OvSA09-Malaysia South China Sea
AF218461-OvSA04-Malaysia South China Sea
97 AF218460-OvSA02-Malaysia South China Sea
AF218463-OvSA06-Malaysia South China Sea
88 AF218455-OvPD06-Malaysia Malacca Strait
AF218456 OvPD07-Malaysia Malacca Strait
86 FM244724-CBA 4-Indonesia East Pacific Ocean
FM244725-CBA 6-Indonesia East Pacific Ocean
95 FM244726-CBA 9-Indonesia East Pacific Ocean
FM244727-CBA 10-Indonesia East Pacific Ocean

Indo-Pacific clade

_O_. cf. _ovata_

96 AB674902-T60730.1-Japan Pacific Ocean
IRTA-SMM-11-09-Spain West Mediterranean Sea
IRTA-SMM-11-10-Spain West Mediterranean Sea
FM244735-KC71-Greece East Mediterranean Sea
FM244622-CBA-C-Italy Central Mediterranean Sea
100 FJ905896-IFR-OST01V-France East Mediterranean Sea
FM244639-VGO884-Spain East Mediterranean Sea
78 FM244669-OS-16BR-Brazil East Atlantic Ocean
AJ420006-IEO-01BR-Brazil East Atlantic Ocean
70 AB674903-T70828.2-Japan Pacific Ocean
FM244636-VGO693-Madeira East Atlantic Ocean
FM244642-VGO614-Madeira East Atlantic Ocean
100 FM244736-KC17-Greece East Mediterranean

Atlantic-Mediterranean clade

91

HE793379-OVJJ1-Jeju Island East China Sea
100 AB674911-MB61105-Japan Pacific Ocean
97 AB674909-MB61007-Japan Pacific Ocean

Ostreopsis sp 1*

74 AB674913-OdoOst6-Okinawa Isalnds-East china Sea

Ostreopsis sp 2*

AJ491333-O cf. siamensis-CSICD1-Spain West Mediterranean Sea
100 AJ491334-O cf. siamensis-CSICD7-Spain West Mediterranean Sea
AB674915-Ostreopsis cf. siamensis -CAWD96-New Zealand Pacific Ocean
AJ491335-Ostreopsis cf. siamensis-CNR-B5-Italy Central Mediterranean Sea

_O_. cf. _siamensis_

36

P-0132-Reunion Island Indian Ocean

Small morphotype

80 AB674914-CAWD184-Cook Island south Pacific Ocean

Ostreopsis sp 3*

AB674916-CAWD179- South Australia Pacific Ocean

Ostreopsis sp 2*

FM244728-VGO881-Canary Island East Atlantic Ocean
100 JX987680-Dn110EHU-Puerto Rico East Etlantic Ocean
51 JX987674-Dn84EHU-Greece East Mediterranean Sea

Ostreopsis sp 2**

99 AB674921-OU11-Okinawa Islands-East China Sea
41 AB674920-IR33-Okinawa Islands-East China Sea
94 AB674922-s0587-Okinawa Islands-East China Sea
FM244728-VGO897-Ostreopsis labens-Malaysia South China Sea
94 AF218465-Ost. lenticularis-Malaysia South China Sea

Ostreopsis sp 6*
Ostreopsis sp 1**

99 P-0108-Reunion Island Indian Ocean
100 AB674917-MB80828.4-Japan Pacific Ocean
95 AB674919-O70421.2-Japan Pacific Ocean
45 AB674918-O70421.1-Japan Pacific Ocean

Ostreopsis sp 5*

0.03

Fig 2.5. Evolutionary relationships of taxa. The evolutionary history was inferred using N-J method. The optimal tree with the sum of branch length = 2.31542155 is shown. The percentage of replicate trees in which the associated taxa clustered together in the bootstrap test (1000 replicates) are shown next to the branches. The tree is drawn to scale, with branch lengths in the same units as those of the evolutionary distances used to infer the phylogenetic tree. The evolutionary distances were computed using the Kimura 2-parameter method and are in the units of the number of base substitutions per site. The analysis involved 62 nucleotide sequences. All positions containing gaps and missing data were eliminated. There were a total of 194 positions in the final dataset.

36

Phylogenetic analysis shows ten major monophilies in accordance with other publications (Penna *et al.,* 2010; Sato *et al.,* 2011; David *et al.,* 2013). Five strains, coinciding with the group of cells with larger size reported in the morphologic analysis, P-0107; P-0108; P-0109; 79.1L and 79.2L (represented by P-0108 in Figure 2.5), were clustered very close to strains collected in Japan, in the Pacific Ocean, that were named as *Ostreopsis* sp 5 in Sato *et al.,* (2011). From the group of small cells, two different genetic clades were distinguished. Two sequences corresponding to strains P-0117 and P-0128 were classified within the species *O.* cf. *ovata*, more precisely, in the Indo-Pacific clade, together with strains from the South China Sea and the South Pacific Ocean. The rest of the sequences of the small-sized cell, a total of 26, (represented by P-0132 in Figure 2.5), shared the same sequence, representing an independent clade that diverged from *Ostreopsis* sp 3 (Sato *et al.,* 2011) collected in Cook Island, in the Pacific Ocean.

Molecular diversity among Reunion Island and GenBank ITS rDNA sequences was evaluated using a pairwise comparison of nucleotide differences (Table 2.2). *O.* cf. *ovata* isolated from Reunion Island had *p values* very low when compared with clades from the South China Sea ($p \leq 0.010$) and with strains isolated from Malacca Strait and Indonesia ($p=0.032$). Divergence was higher comparing strains from the Mediterranean clade ($p=0.07$), KC17 from the Aegean Sea and VGO614 from Madeira ($p=0.082$). The group of twenty nine isolates from Reunion Island is represented by P-0132 in Table 2, and had $p \geq 0.242$ when compared with the rest of the clades. The group of large cells that integrated five strains is represented by P-0108. Nucleotide differences were found to be low in a comparison with strains O70421.1 and O70421.2 ($p=0.065$), and MB80828.4 ($p=0.088$) from Japan.

		1	2	3	4	5	6	7	8	9	10	11	12	13	14	15	16	17	18	19	20	21	22	23	24	25	26	27	28	29	30
1	P-0117																														
2	P-0128	*0,010*																													
3	AF218459	*0,005*	*0,005*																												
4	AB674904	*0,005*	*0,005*	*0,000*																											
5	AF218460	*0,010*	*0,010*	*0,005*	*0,005*																										
6	AF218463	*0,010*	*0,010*	*0,005*	*0,005*	*0,010*																									
7	AF218455	*0,032*	*0,032*	*0,026*	*0,026*	*0,032*	*0,032*																								
8	FM244724	*0,032*	*0,032*	*0,026*	*0,026*	*0,032*	*0,032*	*0,016*																							
9	IRTA-SMM-11-09	*0,070*	*0,070*	*0,065*	*0,065*	*0,070*	*0,065*	*0,065*	*0,070*																						
10	AB674902	*0,070*	*0,070*	*0,065*	*0,065*	*0,070*	*0,065*	*0,065*	*0,070*	*0,000*																					
11	FM244736	*0,082*	*0,082*	*0,076*	*0,076*	*0,082*	*0,082*	*0,065*	*0,070*	*0,043*	*0,043*																				
12	AB674911	0,154	0,154	0,148	0,148	0,154	0,148	0,154	0,154	0,136	0,136	0,136																			
13	AB674909	0,161	0,161	0,154	0,154	0,161	0,154	0,161	0,161	0,142	0,142	0,142	*0,005*																		
14	HE793379	0,167	0,167	0,160	0,160	0,167	0,160	0,167	0,167	0,141	0,141	0,154	*0,070*	*0,065*																	
15	AB674913	0,174	0,174	0,167	0,167	0,167	0,167	0,167	0,167	0,187	0,187	0,173	0,200	0,193	0,186																
16	P-0132	0,266	0,259	0,259	0,259	0,267	0,259	0,260	0,275	0,242	0,242	0,257	0,303	0,295	0,287	0,250															
17	AB674914	0,356	0,347	0,348	0,348	0,339	0,348	0,356	0,348	0,375	0,375	0,371	0,344	0,352	0,378	0,372	0,272														
18	AJ491335	0,306	0,300	0,299	0,299	0,307	0,299	0,315	0,334	0,283	0,283	0,299	0,314	0,313	0,333	0,296	0,291	0,405													
19	AB674916	0,435	0,426	0,426	0,426	0,426	0,436	0,426	0,417	0,454	0,454	0,444	0,474	0,473	0,474	0,446	0,525	0,557	0,545												
20	FM244728	0,409	0,400	0,409	0,409	0,409	0,409	0,382	0,400	0,391	0,391	0,383	0,428	0,428	0,464	0,408	0,454	0,524	0,475	0,465											
21	JX987680	0,400	0,400	0,399	0,399	0,399	0,408	0,390	0,399	0,426	0,426	0,399	0,456	0,466	0,496	0,426	0,473	0,523	0,485	0,442	*0,105*										
22	JX987674	0,408	0,408	0,408	0,408	0,408	0,408	0,381	0,399	0,390	0,390	0,390	0,446	0,447	0,474	0,426	0,445	0,523	0,446	0,474	*0,048*	*0,059*									
23	AB674921	0,530	0,533	0,531	0,531	0,531	0,531	0,541	0,543	0,536	0,536	0,534	0,526	0,524	0,593	0,587	0,559	0,588	0,557	0,660	0,626	0,625	0,602								
24	AB674920	0,550	0,553	0,551	0,551	0,551	0,551	0,562	0,563	0,536	0,536	0,526	0,538	0,536	0,576	0,595	0,555	0,610	0,536	0,658	0,601	0,613	0,602	*0,021*							
25	AF218465	0,517	0,520	0,518	0,518	0,518	0,518	0,528	0,530	0,492	0,492	0,472	0,490	0,489	0,538	0,540	0,562	0,516	0,531	0,646	0,557	0,579	0,546	*0,106*	*0,094*						
26	FM244728	0,516	0,518	0,517	0,517	0,517	0,517	0,527	0,528	0,490	0,490	0,470	0,500	0,499	0,549	0,550	0,585	0,537	0,530	0,646	0,567	0,600	0,567	*0,124*	*0,112*	*0,016*					
27	AB674922	0,528	0,531	0,530	0,530	0,530	0,530	0,528	0,541	0,528	0,528	0,550	0,550	0,549	0,605	0,588	0,545	0,587	0,555	0,739	0,638	0,639	0,591	*0,117*	*0,142*	*0,099*	*0,111*				
28	P-0108	0,663	0,655	0,667	0,667	0,667	0,667	0,695	0,682	0,655	0,655	0,674	0,667	0,679	0,742	0,763	0,607	0,709	0,603	0,705	0,599	0,612	0,606	0,372	0,363	0,339	0,354	0,380			
29	AB674917	0,663	0,655	0,667	0,667	0,667	0,667	0,695	0,667	0,648	0,648	0,699	0,601	0,598	0,669	0,712	0,574	0,687	0,598	0,661	0,599	0,612	0,601	0,361	0,352	0,337	0,361	0,387	*0,065*		
30	AB674918	0,663	0,655	0,667	0,667	0,667	0,667	0,695	0,667	0,648	0,648	0,699	0,601	0,598	0,669	0,712	0,574	0,687	0,598	0,661	0,599	0,612	0,601	0,361	0,352	0,337	0,361	0,387	*0,065*	*0,000*	
31	AB674919	0,703	0,695	0,707	0,707	0,707	0,707	0,737	0,707	0,687	0,687	0,741	0,652	0,648	0,725	0,755	0,623	0,728	0,648	0,674	0,635	0,648	0,637	0,377	0,368	0,353	0,377	0,404	*0,088*	*0,021*	*0,021*

Table 2.2. Estimates of Evolutionary Divergence between Sequences. The number of base substitutions per site from between sequences are shown. Analyses were conducted using the Kimura 2-parameter model. The analysis involved 32 nucleotide sequences. All positions containing gaps and missing data were eliminated. There were a total of 194 positions in the final dataset.

2.4.3. Toxin analysis

In the presence of ouabain, a non-specific haemolytic activity was registered for the highest standard concentration but it did not interfere in haemolysis specific response. Haemolytic activity from Reunion Island strains analyzed was below limit detection.

2.5. Discussion

Observations from field samples, show that two morphotypes were identified based on size and shape differences. Plate pattern is much the same among species (Penna *et al.,* 2005), it was not possible to distinguish between species taking into account this criteria alone.

The large morphotype observed in our samples presented cell dimensions and an oval shaped similar to the description of *O. marinus* by Faust (1999) which actually was first described from coral debris collected in Mayotte Island, situated in SW Indian Ocean. We can thus postulate that the large cells observed in this study may correspond to *O. marinus*.

Several species of *Ostreopsis* correspond to a similar morphological description. Further, as reported in David *et al.,* (2013) for *O.* cf. *ovata* and *O.* cf. *siamensis,* some species of *Ostreopsis* may overlap in cell sizes, which renders difficulty to the taxonomic classification by morphology features. In the case of the small morphotype, no identification was possible based just on light microscopy observation, for this group of cells.

Molecular analysis is recommended to clarify ambiguity in taxonomy based upon morphology. In this regard, the ITS-5.8S rDNA sequence analysis differentiated the large and small morphotypes. Nevertheless, we still cannot be assured of the correspondence with *O. marinus* as no sequences have yet been published in Genbank for that species. In any case, sequences were closely related to *Ostreopsis* sp. 5 found in a previous phylogeographic study (Sato *et al.,* 2011). Water temperatures of locations from where our strains were isolate corresponded to a tropical climate. Interestingly, *Ostreopsis* sp. 5 was found near Japanese islands in the East China Sea, where temperatures registered were between 27 and 28°C, but was absent in the sampling performed in the same study in the north of Japan where the water was colder. Additionally, a later study regarding toxin content in Japanese strains analyzed by liquid chromatography did not detect PLTX-like compounds in *Ostreopsis* sp. 5, strain MB80828-3 (Suzuki *et al.,* 2012). In agreement to this result, Reunion Island strains of the large morphotype did not show any activity in the haemolytic test. Whether this genetic clade is *O. marinus* or not, has to be taken with caution since further research needs to be done to assure this hypothesis. Further

morphological and genetic studies, with SEM and other rDNA fragments respectively, are required to confirm this supposition.

Within the small morphotype, two phylotypes corresponding to different species were identified by phylogenetic analysis; *O.* cf. *ovata* and another morphologically indistinct species. Many studies have been performed in the characterization of *O.* cf. *ovata* worldwide. There are two well-defined clades, from the Mediterranean Sea-Atlantic Ocean and from the Indo-Pacific Ocean (Penna *et al.,* 2010). In accordance with geographical distribution, Reunion Island *O.* cf. *ovata* strains were classified within the Indo-Pacific Ocean clade. In an early study among *Ostreopsis* populations in Malaysian waters (Pin *et al.,* 2001), two genetically-distinct groups were identified within this clade; one from Malacca Straits and another from the South China Sea. Contrarily to what might have been expected from geographical distribution, being that the Malacca Strait is open to the Indian Ocean, Reunion Island strains were genetically closer to those of the South China Sea clade. It can be hypothesized that genetic exchange with the Malacca Strait population is limited since it is separated by the Malaysian Peninsula from the Pacific Ocean (Pin *et al.,* 2001) and by the Indonesian Island of Sumatra from the Indian Ocean. As a benthic organism, it is likely that genetic flow in these species may be lower than for planktonic dinoflagellates due to the substrate attachment (Penna *et al.,* 2010) or land-derived nutrient requirements (Taylor *et al.,* 2008). Consequently, more notable geographical dispersion may be reflected in the phylogeny of benthic microorganisms (Penna *et al.,* 2012). In addition to that, ocean currents and ballast water, nowadays considered the most important mechanism of spread for microalgae (Hallegraef & Boch, 1991), may contribute to the genetic dispersion.

While Mediterranean strains have largely been proven to be PLTX-like compound producers (Ciminiello *et al.,* 2012), *O.* cf. *ovata* strains analyzed in this study did not demonstrate production of PLTX-like compounds. In agreement with this result, a strain of *O.* cf. *ovata* from Japanese waters, strain s0579, (same sequence as CAWD174 in Figure 2.5 - Sato *et al.,* 2011) that belong to the same clade as the Reunion Island strains, was analyzed in Suzuki *et al.,* (2012) and no PLTX-like compounds were found. Toxin content and specific profiles may contribute to the species identification as an additional feature and may help to solve taxonomical problems. As reported in Penna *et al.,* (2010) and Parsons *et al.,* (2012), considering differences both in molecular and toxicological features, *O.* cf. *ovata* from the Mediterranean-Atlantic and Indo-Pacific clades may be classified as different species.

The other group of cells with small morphotype constituted a genetically-homogeneous clade and did not cluster with any other sequence registered in Genbank. Morphologically they may fit among any of the small-oblong shaped cells described for the genus *Ostreopsis.* It could be considered the possibility of the correspondance with *O. belizeanus* and *O. caribbeanus*, observed in the west Indean

Ocean (Faust, 1999; Rhodes, 2011). At the same time, it may represent a new species not observed previously in the field. Further investigations are needed to taxonomically characterize this phylotype.

However, it has to be considered the fact that different methodologies regarding culture maintenance and toxin extraction are performed depending on the research group. For that reason, comparison among studies has to be taken with caution. We decided to evaluate toxicity in the stationary phase where it has been observed a higher accumulation of toxin content in *O.* cf. *ovata* strains (Vanucci *et al.,* 2012a; Vanucci *et al.,* 2012b; Scalco *et al.,* 2012; Pezzolesi *et al.,* 2012; Guerrini *et al.,* 2010, Carnicer *et al.,* submitted). As for culture conditions in our laboratory, irradiance could be a limiting factor since it is much lower than average values found in tropical regions. In that contest, toxin production may be altered since cells under unfavorable conditions could use their energy in growth. Further physiological studies with these strains have to be performed in order to elucidate whether the non toxicity is due to culture conditions or it is specie-specific.

2.6. Conclusions

Our phylogenetic tree highlighted ten distinct clades and was supported by previous studies that clustered the same groups of strains together. The four species with an assigned sequence, *O.* cf. *ovata*, *O.* cf. *siamensis, O. labens* and *O. lenticularis* are clustered in the same way as reported in Penna *et al.,* 2010; Amzil *et al.,* 2012; Moreira *et al.,* 2012 and Kang *et al.,* 2013. Phylogenetic trees performed with new sequences from species not identified morphologically (Sato *et al.,* 2011; David *et al.,* 2013) are also in agreement with our results. The present study focusing on Reunion Island *Ostreospsis* strains highlights the occurrence of two morphotypes encompassing three phylotypes, one of which could constitute a new species. These results illustrate the need to reassess the controversial status of the taxonomy of the genus *Ostreopsis*. New sequences provided in this study help to define genotypes of previously described species, improve knowledge on their biogeography, and provides data for expanding the description of species within this genus. This study contributes important genetic, morphological, biogeographical and toxicological information to the description of the genus *Ostreopsis* that will clarify this problematic taxonomy.

2.7. References

Accoroni, S., Romagnoli, T., Pichierri, S., Colombo, F., Totti, C., 2012. Morphometric analysis of *Ostreopsis* cf. *ovata* cells in relation to environmental conditions and bloom phases. Harmful Algae 19, 15-22.

Aligizaki, K., Nikolaidis, G., 2006. The presence of the potentially toxic genera *Ostreopsis* and *Coolia* (Dinophyceae) in the North Aegean Sea, Greece. Harmful Algae 5, 717-730.

Amzil, Z., Sibat, M., Chomerat, N., Grossel, H., Marco-Miralles, F., Lemee, R., Nezan, E., Sechet, V., 2012. Ovatoxin-a and Palytoxin Accumulation in Seafood in Relation to *Ostreopsis* cf. *ovata* Blooms on the French Mediterranean Coast. Mar. Drugs 10, 477-496.

Andree, K.B., Fernandez-Tejedor, M., Elandaloussi, L.M., Quijano-Scheggia, S., Sampedro, N., Garces, E., Camp, J., Diogene, J., 2011. Quantitative PCR Coupled with Melt Curve Analysis for Detection of Selected Pseudo-nitzschia spp. (Bacillariophyceae) from the Northwestern Mediterranean Sea. Applied and Environmental Microbiology 77, 1651-1659.

Bravo, I., Vila, M., Casablanca, S., Rodriguez, F., Rial, P., Riobo, P., Penna, A., 2012. Life cycle stages of the benthic palytoxin-producing dinoflagellate *Ostreopsis* cf. *ovata* (Dinophyceae). Harmful Algae 18, 24-34.

Chang, F.H., Shimizu, Y., Hay, B., Stewart, R., Mackay, G., Tasker, R., 2000. Three recently recorded *Ostreopsis* spp. (Dinophyceae) in New Zealand: temporal and regional distribution in the upper North Island from 1995 to 1997. New Zealand Journal of Marine and Freshwater Research 34, 29-39.

Ciminiello, P., Dell'Aversano, C., Dello Iacovo, E., Fattorusso, E., Forino, M., Tartaglione, L., Battocchi, C., Crinelli, R., Carloni, E., Magnani, M., Penna, A., 2012. Unique Toxin Profile of a Mediterranean *Ostreopsis* cf. *ovata* Strain: HR LC-MSn Characterization of Ovatoxin-f, a New Palytoxin Congener. Chemical Research in Toxicology 25, 1243-1252.

David, H., Laza-Martinez, A., Miguel, I., Orive, E., 2013. *Ostreopsis* cf. *siamensis* and *Ostreopsis* cf. *ovata* from the Atlantic Iberian Peninsula: Morphological and phylogenetic characterization. Harmful Algae 30, 44-55.

Faust, M.A., 1995. Morphology, ecology and toxicity of benthic *Ostreopsis* species. Journal of Phycology 31, 20-20.

Faust, M.A., 1999. Three new Osteopsis species (Dinophyceae): *O. marinus* sp. nov., *O.* belizeanus sp. nov., and *O. caribbeanus* sp. nov. Phycologia 38, 92.

Faust, M.A., Morton, S.L., 1995. Morphology and Ecology of the Marine Dinoflagellate *Ostreopsis*-Labens Sp-Nov (Dinophyceae). Journal of Phycology 31, 456-463.

Fritz, L., Triemer, R.E., 1985. A Rapid Simple Technique Utilizing Calcofluor White M2r for the Visualization of Dinoflagellate Thecal Plates. Journal of Phycology 21, 662-664.

Fukuyo, Y., 1981. Taxonomical Study on Benthic Dinoflagellates Collected in Coral Reefs. Nippon Suisan Gakkaishi 47, 967-978.

Guerrini, F., Pezzolesi, L., Feller, A., Riccardi, M., Ciminiello, P., Dell'Aversano, C., Tartaglione, L., Dello Iacovo, E., Fattorusso, E., Forino, M., Pistocchi, R., 2010.

Comparative growth and toxin profile of cultured *Ostreopsis ovata* from the Tyrrhenian and Adriatic Seas. Toxicon 55, 211-220.

Guillard, R.R.L., 1975, Culture of Phyto Plankton for Feeding Marine Invertebrates. Smith, Walter L. and Matoira H. Chanley, pp. 29-60.

Hallegraeff, G.M., Bolch, C.J., 1991. Transport of Toxic Dinoflagellate Cysts Via Ships Ballast Water. Marine Pollution Bulletin 22, 27-30.

Hartmann, S., Nason, J.D., Bhattacharya, D., 2001. Extensive ribosomal DNA genic variation in the columnar cactus Lophocereus. Journal of Molecular Evolution 53, 124-134.

Hoshaw, R.W., Rosowski, J.R., 1973, Methods for Microscopic Algae. Stein, Janet R., pp. 53-67.

Jensen, P.G., 1993. Ultrastructure and phylogenetic significance of 'lattice organs' in thecostracan larvae. American Zoologist 33, 6A-6A.

Kang, N.S., Jeong, H.J., Lee, S.Y., Lim, A.S., Lee, M.J., Kim, H.S., Yih, W., 2013. Morphology and molecular characterization of the epiphytic benthic dinoflagellate *Ostreopsis* cf. *ovata* in the temperate waters off Jeju Island, Korea. Harmful Algae 27, 98-112.

Lenoir, S., Ten-Hage, L., Turquet, J., Quod, J.P., Bernard, C., Hennion, M.C., 2004. First evidence of palytoxin analogues from an *Ostreopsis mascarenensis* (Dinophyceae) benthic bloom in Southwestern Indian Ocean. Journal of Phycology 40, 1042-1051.

Litaker, R.W., Vandersea, M.W., Faust, M.A., Kibler, S.R., Nau, A.W., Holland, W.C., Chinain, M., Holmes, M.J., Tester, P.A., 2010. Global distribution of ciguatera causing dinoflagellates in the genus Gambierdiscus. Toxicon 56, 711-730.

Litaker, R.W., Vandersea, M.W., Kibler, S.R., Reece, K.S., Stokes, N.A., Lutzoni, F.M., Yonish, B.A., West, M.A., Black, M.N.D., Tester, P.A., 2007. Recognizing dinoflagellate species using ITS rDNA sequences. Journal of Phycology 43, 344-355.

Mangialajo, L., Ganzin, N., Accoroni, S., Asnaghi, V., Blanfuné, A., Cabrini, M., Cattaneo-Vietti, R., Chavanon, F., Chiantore, M., Cohu, S., Costa, E., Fornasaro, D., Grossel, H., Marco-Miralles, F., Masó, M., Reñé, A., Rossi, A.M., Sala, M.M., Thibaut, T., Totti, C., Vila, M., Lemée, R., 2011. Trends in *Ostreopsis* proliferation along the Northern Mediterranean coasts. Toxicon , 57, 408-420.

Moreira, A., Rodriguez, F., Riobo, P., Franco, J.M., Martinez, N., Chamero, D., Alonso, C., 2012. Notes on *Ostreopsis* sp from southern-central coast of Cuba. Cryptogamie Algologie 33, 217-224.

Norris, D.R., Bomber, J.W., Balech, E., 1985. Benthic dinoflagellates associated with ciguatera from Florida Keys. I. *Ostreopsis heptagona* sp. nov. In: Anderson, D.M., White, A.W., Baden, D. G. (Eds), Toxic Dinoflagellates. Elsevier, Amsterdam, 39-44.

Okolodkov, Y.B., Campos-Bautista, G., Garate-Lizarraga, I., Gonzalez-Gonzalez, J.A.G., Hoppenrath, M., Arenas, V., 2007. Seasonal changes of benthic and epiphytic

dinoflagellates in the Veracruz reef zone, Gulf of Mexic*O.* Aquatic Microbial Ecology 47, 223-237.

Parsons, M.L., Preskitt, L.B., 2007. A survey of epiphytic dinoflagellates from the coastal waters of the island of Hawai'i. Harmful Algae 6, 658-669.

Penna, A., Fraga, S., Battocchi, C., Casabianca, S., Giacobbe, M.G., Riobo, P., Vernesi, C., 2010. A phylogeographical study of the toxic benthic dinoflagellate genus *Ostreopsis* Schmidt. Journal of Biogeography 37, 830-841.

Penna, A., Fraga, S., Battocchi, C., Casabianca, S., Perini, F., Capellacci, S., Casabianca, A., Riobo, P., Giacobbe, M.G., Totti, C., Accoroni, S., Vila, M., Rene, A., Scardi, M., Aligizaki, K., Nguyen-Ngoc, L., Vernesi, C., 2012. Genetic diversity of the genus *Ostreopsis* Schmidt: phylogeographical considerations and molecular methodology applications for field detection in the Mediterranean Sea. Cryptogamie Algologie 33, 153-163.

Penna, A., Vila, M., Fraga, S., Giacobbe, M.G., Andreoni, F., Riobo, P., Vernesi, C., 2005. Characterization of *Ostreopsis* and *Coolia* (Dinophyceae) isolates in the western Mediterranean Sea based on morphology, toxicity and internal transcribed spacer 5.8s rDNA sequences. Journal of Phycology 41, 212-225.

Pezzolesi, L., Guerrini, F., Ciminiello, P., Dell'Aversano, C., Dello Iacovo, E., Fattorusso, E., Forino, M., Tartaglione, L., Pistocchi, R., 2012. Influence of temperature and salinity on *Ostreopsis* cf. *ovata* growth and evaluation of toxin content through HR LC-MS and biological assays. Water Research 46, 82-92.

Pin, L.C., Teen, L.P., Ahmad, A., Usup, G., 2001. Genetic diversity of *Ostreopsis ovata* (Dinophyceae) from Malaysia. Marine Biotechnology 3, 246-255.

Quod, J.P., Quod, J.P., 1994. *Ostreopsis-Mascarenensis* Sp-Nov (Dinophyceae), a New Toxic Dinoflagellate from Coral-Reefs in the Southwest Indian-Ocean. Cryptogamie Algologie 15, 243-251.

Riobo, P., Paz, B., Franco, J.M., Vazquez, J.A., Murado, M.A., 2008. Proposal for a simple and sensitive haemolytic assay for palytoxin Toxicological dynamics, kinetics, ouabain inhibition and thermal stability. Harmful Algae 7, 415-429.

Sato, S., Nishimura, T., Uehara, K., Sakanari, H., Tawong, W., Hariganeya, N., Smith, K., Rhodes, L., Yasumoto, T., Taira, Y., Suda, S., Yamaguchi, H., Adachi, M., 2011. Phylogeography of *Ostreopsis* along West Pacific Coast, with Special Reference to a Novel Clade from Japan. PLoS ONE 6, e27983.

Schmidt, J., 1901. Preliminary report of the botanical results of the Danish Expedition to siam (1899-1900). Pt. IV, Peridiniales. Bot. Pidsslerift. 24, 212-21.

Suzuki, T., Watanabe, R., Uchida, H., Matsushima, R., Nagai, H., Yasumoto, T., Yoshimatsu, T., Sato, S., Adachi, M., 2012. LC-MS/MS analysis of novel ovatoxin isomers in several *Ostreopsis* strains collected in Japan. Harmful Algae 20, 81-91.

Taylor, F.J.R., Hoppenrath, M., Saldarriaga, J.F., 2008. Dinoflagellate diversity and distribution. Biodiversity and Conservation 17, 407-418.

Tindall, D.R., Dickey, R.W., Carlson, R.D., Moreygaines, G., 1984. Ciguatoxigenic Dinoflagellates from the Caribbean Sea. Acs Symposium Series 262, 225-240.

Tubaro, A., Durando, P., Del Favero, G., Ansaldi, F., Icardi, G., Deeds, J.R., Sosa, S., 2011. Case Definitions for Human Poisonings Postulated to Palytoxins Exposure. Toxicon, 57, 478-495.

Usami, M., Satake, M., Ishida, S., Inoue, A., Kan, Y., Yasumoto, T., 1995. Palytoxin Analogs from the Dinoflagellate *Ostreopsis-Siamensis*. Journal of the American Chemical Society 117, 5389-5390.

Yamaguchi, H., Tanimoto, Y., Yoshimatsu, T., Sato, S., Nishimura, T., Uehara, K., Adachi, M., 2012. Culture method and growth characteristics of marine benthic dinoflagellate *Ostreopsis* spp. isolated from Japanese coastal waters. Fisheries Science 78, 993-1000.

Yoshida, T., Sako, Y., Uchida, A., 2001. Geographic differences in paralytic shellfish poisoning toxin profiles among Japanese populations of Alexandrium tamarense and A. catenella (Dinophyceae). Phycological Research 49, 13-21.

CHAPTER 3

Ostreopsis. cf. *ovata* from NW
Mediterranean Sea: Physiological
responses under different
temperature and salinity conditions

3.1. Abstract

Ostreopsis cf. *ovata* causing seasonal proliferations in the Mediterranean Sea produces putative palytoxin and ovatoxins which are considered among the most potent marine toxins. Blooms have been related with several toxic events such as respiratory problems in humans and mortality of benthic marine organisms. In the coming decades, an increase in temperature and salinity is predicted in the Mediterranean Sea as a consequence of global warming that may provoke alterations in the dynamics of marine microorganisms. In this study, we analyzed the physiological effects of water temperature and salinity, and their interaction through a multi-factorial experiment using two *O.* cf. *ovata* strains in culture that had been isolated from western Mediterranean Sea. In order to perform an accurate and reliable estimation of cell abundance, hydrochloric acid and sodium-ethylenediaminetetraacetic acid treatments were evaluated, obtaining lower counting errors with the former, especially after the stationary phase. Results of the physiological study showed that growth was inhibited at 19°C for all salinities. The highest growth rates were registered at 24°C for both strains (0.48 ± 0.05 div. day^{-1}), and a significant growth rate variability was found among salinities at 24 and 28°C. Two groups were distinguished by cell size in all high temperature conditions and a positive correlation between the amount of small cells and growth rate was found. Palytoxin-like concentration in the cultures increased with time and significant higher amount of toxin were found at 28°C in comparison with 24°C. Our results suggest that climate change may not affect intensity of blooms but their toxicity may be enhanced.

3.2. Introduction

The genus *Ostreopsis,* Schmidt (1901) is a harmful benthic marine dinoflagellate distributed widely in both subtropical and tropical marine coral reef ecosystems and temperate regions (Parsons *et al.,* 2012; Rhodes *et al.,* 2011; Pistocchi *et al.,* 2011). Nine species having very similar morphological features have been described and nowadays taxonomical identification is under revision using molecular methods to clarify controversial issues (Penna *et al.,* 2010; Sato *et al.,* 2011; Penna *et al.,* 2012). It is characterized by forming massive proliferations that reach very high concentrations in benthic subtracts such as macroalgae, rocks, or invertebrates. These blooms are associated with abundant amounts of mucilage, in which cells are embedded. This mucilaginous net is composed by acidic polysaccharides and a high number of trichocysts (Honsell *et al.,* 2013). As well, cultures maintained in the laboratory produced these aggregates that constitute an impediment to perform accurate cell abundance estimations. Previous studies have used different strategies in order to dissolve mucilage to better homogenize the samples and facilitate cell

counting. Two chemicals have been tested, sodium-ethylenediaminetetraacetic acid (Na-EDTA) (Scalco *et al.,* 2012; Pezzolesi *et al.,* 2012) and hydrochloric acid (HCl) (Guerrini *et al.,* 2010; Vanucci *et al.,* 2012b; Monti *et al.,* 2012) to counteract the interference of mucilages for cell abundance estimations. The addition of HCl liberates H^+ protons in aqueous medium that may neutralize negative electric charges present in cell walls and polysaccharides. The mechanism of action for the Na-EDTA treatment can consist in chelating Ca^{2+} and Mg^{2+} that bind polysaccharides together, and thereby disrupting the aggregation (Alldredge *et al.,* 1993).

O. cf. *ovata* has been extensively studied in the last decade regarding its morphology (Penna *et al.,* 2005; David *et al.,* 2013; Kang *et al.,* 2013), toxicity (Ciminiello *et al.,* 2006; Ciminiello *et al.,* 2008; Ciminiello *et al.,* 2011; Suzuki *et al.,* 2012; Hwang *et al.,* 2013), and distribution. It has been detected in tropical waters such as in the Atlantic Ocean, in Brazilian islands (Nascimento *et al.,* 2012b) and in the western Pacific Ocean, in the Philippine Sea and the east China Sea (Pin *et al.,* 2001; Penna *et al.,* 2010) and in temperate areas such as the east Atlantic Ocean (David *et al.,* 2013), the China Sea (Sato *et al.,* 2011; Kang *et al.,* 2013), and especially in the Mediterranean Sea (e. g. Vila *et al.,* 2001; Aligizaki *et al.,* 2006; Monti *et al.,* 2007; Mangialajo *et al.,* 2008; Totti *et al.,* 2010; Cohu *et al.,* 2011; Accoroni *et al.,* 2011; Pfakunnchen *et al.,* 2012; Ismael and Hamil, 2012). This species, with its widespread distribution, shows an adaptation to different environmental conditions that can lead to distinct physiological responses among strains from different origin. *O.* cf. *ovata* isolated from the Mediterranean and the Atlantic Sea belong to a genetic clade that presents a high degree of sequence homology (Penna *et al.,* 2010). While *O.* cf. *ovata* in tropical waters has been reported all year long (Pin *et al.,* 2001; Parsons and Preskitt, 2007; Parsons *et al.,* 2012), in the Mediterranean Sea, a seasonal pattern in bloom dynamics has been observed, coinciding with high temperatures in most cases. However, depending on the area, the threshold temperature for bloom formation varies, and correlation between temperature and *O.* cf. *ovata* outbreaks is not easy to determine, as other factors may also affect bloom dynamics (reviewed in Pistocchi *et al.,* 2011). But still, temperature ranges may or may not explain having *O.* cf. *ovata* at certain densities in a given location. Considering projections for seawater warming for the 21st century, which is expected to be more intensive in the Mediterranean Sea than in other areas (IPCC, 2013), it is necessary to intensify the efforts to understand how the growth and toxin production of *O.* cf. *ovata* is affected by high temperature regimes.

Several laboratory studies have been performed to characterize the optimal growth temperatures for *O.* cf. *ovata* strains from the Mediterranean Sea. Two experiments on Tyrrhenian strains were not consistent on the conditions where the highest growth rates were obtained: 22-26°C (Scalco *et al.,* 2012) and 26-30°C (Granéli *et al.,* 2011). Much lower optimal temperatures were found in an Adriatic strain that grew faster at 20°C in relation to higher temperatures (Pezzolesi *et al.,*

2012). From these results, differential adaptation to temperature may be expected among *O.* cf. *ovata* populations. In addition, the response of marine microalgae to warming could differ depending on other environmental factors. Coastal waters often present highly pronounced fluctuations of physicochemical factors. The interaction of these factors with temperature may have consequences in *O.* cf. *ovata* distributions. In recent studies multi-factorial experiments have combined temperature with other environmental factors. Scalco *et al.,* (2012) studied day length and irradiance, concluding that *O.* cf. *ovata* temperature and light preferences were in accordance with natural conditions in late June and September in the Mediterranean Sea. Nutrient availability was also examined by Vydiarathna and Granéli (2013) suggesting that future nutrient enrichment could enhance *O.* cf. *ovata* proliferations. In the same way, Vanucci et al., (2012b) observed a negative effect on growth rates and a reduction in cell abundances under nitrogen and phosphorus limitation. Taking into account that changes in salinity are common in coastal waters due to evaporation, rainfall and/or riverine flow fluctuations (Tanimoto *et al.*, 2013), it is very important to study the interactions of this factor with temperature to clarify the possible repercussions to microalgae physiology due to salinity changes. *O.* cf. *ovata* from Japanese coastal waters has been studied under a wide range of conditions, suggesting that high salinities and temperatures would favor its growth (Yamaguchi *et al.,* 2012b).

Morphometric changes in *O.* cf. *ovata* have been described during growth phases. Two different size classes are present in both Mediterranean waters (Penna *et al.,* 2005; Aligizaki *et al.,* 2006; Accoroni *et al.,* 2012; Bravo *et al.,* 2012; Carnicer *et al.,* in preparation) and laboratory cultures (Guerrini *et al.,* 2010; Scalco *et al.,* 2012; Vanucci *et al.,* 2012a; Vanucci *et al.,* 2012b; Pezzolesi *et al.,* 2012; Bravo *et al.,* 2012). A high abundance of small cells can be attributed to an increase in cell divisions (Silva and Faust, 1995) in accordance with favored conditions that stimulate growth (Accoroni *et al.,* 2012). A higher abundance of small cells in a population may indicate growth acceleration under certain environmental circumstances that favor a rapid proliferation.

Strains of *O.* cf. *ovata* from the Mediterranean clade produce palytoxin-like (PLTX-like) compounds, identified as putative palytoxin (pPLTX) (Ciminiello *et al.,* 2006), and 6 PLTX analogs named ovatoxins (OVTX), OVTX-a, being the major component in most cases (Ciminiello *et al.,* 2008), -b, -c, -d, -e (Ciminiello *et al.,* 2010) and -f (Ciminiello *et al.,* 2012). There is evidence of accumulation of PLTX-like compounds in seafood from the Mediterranean Sea (Aligizaki *et al.,* 2008; Aligizaki *et al.,* 2011; Amzil *et al.,* 2012; Biré *et al.,* 2013) but there is no record of human poisoning caused by consumption of contaminated seafood in this area. However, there have been many cases of human illness registered by inhalation or direct contact with cells or aerosols, as well as mass mortalities of invertebrates (reviewed in Mangialajo *et al.,* 2011). It has been observed that *O.* cf. *ovata* toxin content is

inversely correlated with growth rate (Pezzolesi *et al.,* 2012; Granéli *et al.,* 2011), suggesting that under unfavorable conditions, a higher amount of toxin is produced. Both studies differ in temperatures determined for optimal growth performance, so there is no clear pattern on the possible effects that higher water temperature could have in cell toxin content, as found by Scalco *et al.,* (2012). There is no validated methodology (either assay or analytical method) for detection of PLTX-like compounds (Riobó *et al.,* 2011), but it would be necessary to determine its presence regarding future monitoring programs in coastal waters to detect possible human intoxications or marine ecosystem damage. Riobó *et al.,* 2008 described a rapid, sensitive and reliable method based on the delayed haemolytic action produced by PLTX-like compounds on mammalian red blood cells (RBCs). The specificity of the assay lies in the inhibition of toxin haemolytic effects on RBCs in the presence of ouabain, that binds to the Na^+/K^+-ATPase pump as do PLTX-like compounds (Habermann *et al.,* 1981). Analytical methods based on liquid chromatography coupled with mass spectrometry (LC-MS) have shown great potential for investigating toxin profiles, since they allow accurate identification of known and unknown PLTX-like compounds. However, some limitations such as the lack of certified reference standards, may constrain their use as a routine method for monitoring programs (Ciminiello *et al.,* 2011). A combination of both biochemical assays, like the haemolytic assay, and instrumental analytical methods seem to be the most comprehensive strategy to assess toxicity due to PLTX-like compounds.

Studying the physiological responses of *O*. cf. *ovata* is of concern taking into consideration the potential hazard this species may represent due to the production of potent toxins. The aim of this work is on the one hand, to refine the Utermöhl method regarding sample pre-treatment for an accurate enumeration of cells of mucilage-producing microalgae like *Ostreopsis* and, on the other hand, to describe the physiological responses of *O*. cf. *ovata* strains coming from the western Mediterranean Sea that have not been studied before, under different conditions of temperature and salinity. More specifically, to determine: 1) growth performances and toxin content effects with the interaction of temperature and salinity and 2) characterization of the presence of small cells associated with growth phases and environmental conditions.

3.3. Materials and Methods

3.3.1. Ostreopsis *cf.* ovata *cultures maintenance*

Strains IRTA-SMM-11-09 and IRTA-SMM-11-10 of *O*. cf. *ovata* were isolated from macroalgae samples, *Jania rubens*, collected in the southern coast of Catalonia in August 2011 (40° 33' 15.7176" N; 0° 31' 58.242" E and 40° 50' 47.8242" N; 0° 45' 44.9532" E); both are rocky shore areas in the south and north of the Ebre Delta respectively. Cells were isolated with a glass pipette by the capillary method

(Hoshaw and Rosowski, 1973) under an inverted microscope (Leica DM-IL). After an initial growth in a 24 well microplate, stock cultures were maintained in 25 cm^2 non-treated polystyrene sterile flasks (IWAKI) filled with autoclaved sterile filtered natural seawater containing a nutrient supplement of a five-fold dilution of f/2 media (Guillard, 1975) (Sigma). Salinity was adjusted to 36 by adding autoclaved MiliQ water and re-inoculations were performed every three weeks. Cultures were maintained at a constant temperature of 24°C and illumination was provided by fluorescent tubes with a photon irradiance of 100 µmol photons m^{-2} s^{-1}under 12:12-h light:dark photoperiod, which remained constant in all experimental conditions.

3.3.2. DNA extraction, polymerase chain reaction amplification and sequencing

The DNA extraction protocol followed Andree *et al.,* (2011). Polymerase Chain Reaction (PCR) conditions were those used in Sato *et al.,* (2011). ITS and 5.8S ribosomal RNA (rRNA) gene regions were obtained by using oligonucleotide primers ITSA (5'-GTAACACGGTHTCCGTAGGT-3') and ITSB (5'-AKATGCTTATRTTCAGCRGG-3'), performed in an Eppendorf™ MasterCycler Personal Thermal Cycler. Resulting fragments of rRNA were evaluated by agarose gel electrophoresis and were sent to be sequenced bidirectionally (Sistemas Genómicos, LLC; Valencia, Spain) using the same primers as those used in the initial amplification. Forward and reverse sequence reactions were aligned and manually edited using BioEdit, version 7.0.0 (Hall, T.A., 1999). Genetic distances were obtained by Kimura's two-parameter model (Kimura, 1980) with MEGA 5.1.

3.3.3. Subsampling and cell quantification experiment

O. cf. *ovata* produces mucilaginous aggregates difficult or impossible to disrupt even after vigorous mixing. Samples of non homogeneous cultures can lead to errors in the estimation of cell abundances. We evaluated enumeration accuracy performed by the Utermöhl method (Utermöhl, 1931; Utermöhl, 1958). Two experiments with IRTA-SMM-11-10 strain were carried out in cultures grown in 600 mL, in 150 cm^2 non-treated polystyrene sterile flat bottom flasks (Nunc). Experiment 1 was performed in a late decaying phase culture (seven weeks, 4.0×10^3 cell.mL^{-1}) in May 2012 and Experiment 2 in a late stationary phase culture (four weeks, 2.5×10^3 cell.mL^{-1}) in December 2012. Six different sample volumes (0.5, 1, 3, 5, 12 and 20 mL) were taken per triplicate after vigorous shaking alterning horizontally rolling and vertical turning upside down of the sample for 100 times. Taking into consideration results of Experiment 1, samples with a volume of 0.5 and 1 mL were not used in Experiment 2. For each sample volume, two treatments were added, Na-EDTA (0.01 M final concentration) and HCl (4 mM final concentration) and then immediately fixed by adding 0.5 mL of neutral Lugol's solution per 100 mL of sample. In every case a sample without treatment was taken as a control. Each sample was settled per triplicate in counting cell chambers; 0.5 and 1 mL volume samples in a 100 µL Palmer-Maloney chamber, and the rest of the samples in a 0.5

mL Utermöhl chamber. For 20 mL volume samples an additional settlement per triplicate in 3 mL was performed in both experiments. In Experiment 2, samples with a volume of 12 mL were also settled in 3 mL. In Experiment 2 a treatment consisting of 10 seconds sonication in pulse mode with an ultrasonic processor Vibra-Cell™ (Sonics and Materials, Inc., Newton, CT, USA) was performed in all volume samples. A total of 189 settlings for Experiment 1 and 162 for Experiment 2 were analyzed. Based on Uthermöhl, 1958, the minimum number of cells counted per chamber was 100. Cell abundance per sample volume was calculated by the average from 9 settlings (3 settlings for each of the 3 samples per volume). We calculated the variability among triplicate sub-samples, calculating the difference between relative standard deviation (RSD) and Poisson distribution (λ) within the three counts. We considered high variability in enumeration when we obtained positive results which mean that the measured error was higher compared with the expected random error based on Poisson statistics (CEN, 2006).

3.3.4. *Multi-factorial experiment the effect of salinity and temperature on O. cf. ovata*

We analyzed cell growth, size and toxicity in the two *O.* cf. *ovata* strains exposed to nine different conditions, combining three temperatures (19, 24 and 28°C) and three salinities (32, 36 and 38). Acclimatization period lasted one year in temperature regulated culture rooms. Cells were grown in 50 mL culture volume in 25 cm² non-treated polystyrene sterile flashes (IWAKI).

3.3.4.1. *Cell growth*

Multi-factorial experiments were performed in triplicate, in a controlled environment chamber (IBERCEX, LTD) in 650 mL volume cultures in 150 cm² non-treated polystyrene sterile flat bottom flasks (Nunc). Experimental cultures (in triplicate for each condition) were inoculated from late exponential phase cells and initial concentration was between 100 and 150 cells mL⁻¹ for cultures at 28°C, and between 50 and 100 cells mL⁻¹ for cultures at 19°C and 24°C because cell concentration in the stock culture was lower. Cultures remained under experimental conditions for sixteen days. To determine an accurate growth curve, based on our previous experimental results, samples were taken per triplicate every 2-3 days. In the exponential phase, 5 mL volume samples were settled in 0.5 mL chamber per triplicate. In the stationary phase, samples had a volume of 10 mL and were treated with Na-EDTA at a final concentration of 0.01 M. Settling was performed in 3 mL chamber per triplicate. Cell abundance was obtained by calculating the average of three subsamples settled thrice from three cultures; twenty seven per condition and day, a total of 3888 settlings were analyzed. Average cell abundances are expressed by mean ± standard deviation (SD). The total culture volume removed from each flask at the end of the experiment due to sampling did not surpass 30% of the total

culture volume to interfere as little as possible in cell growth. Growth rate (y, div.day^{-1}) was calculated using the following equation:

$$\underline{\hspace{3cm}}$$

where N0 and N1 are cell abundances at time t0 (day 3) and t1 (day 9), coinciding with the exponential phase. We did not include growth from the two first days considering the latency phase. For the 19°C treatments, t0 was day 9 and t1 was day 16 according to the growth pattern.

3.3.4.2. *Cell size*

We selected one culture for each condition and strain to measure cell size. A minimum of 40 cells were analyzed every 2-3 days along the growth curve. Dorso-ventral (DV) and width (W) diameters were measured using an image capture system (Analysis) with a Olympus DP70 camera connected to a Nikon Eclipse TE2000-S inverted microscope at 400x magnification. Cell dimensions were expressed by mean ± SD.

3.3.4.3. *Toxicity*

Toxin content was analyzed for 24 and 28°C temperature conditions. Three cultures of both *O.* cf. *ovata* strains were grown in parallel under the same multi-factorial conditions. Cultures were grown in 200 mL non-treated polystyrene sterile flasks (Thermo) inoculated from the same initial acclimatized stock culture as for the multi-factorial experimental cultures. Cells were collected at the late exponential phase (12 days), stationary phase (21 days) and during decaying phase (28 days). Samples of 10 mL were taken and settled per triplicate in 3 mL Utermöhl chambers. Samples from stationary and decaying phase were treated with Na-EDTA before fixation.

3.3.4.3.1. *Toxin extraction*

Cells were collected by filtration on 0.45 μm nylon filters and stored at -80°C. For toxin extraction, 5 mL methanol/water (80:20) solution was added to filters and these were sonicated for 35 minutes in pulse mode. The mixture was centrifuged at 2000 g for 10 minutes; the supernatant was decanted and filtered using 0.45 μm polytetrafluoroethylene membrane syringe filters. This procedure was repeated tree times and filtered supernatants were pooled. The final extract was evaporated and made up to a final volume of 10 mL.

3.3.4.3.2. *Haemolytic assay*

Haemolytic test of *O.* cf. *ovata* strains was analyzed following the method of Riobó et al, (2008) with slight modifications regarding concentration of reagents in order to adjust the working range and calibration curve. Heamoglobin released in presence of PLTX-like compounds after cell lysis, is quantified by a microplate

Reader KC4 from BIO-TEK Instruments, Inc. (Vermont) at 405 nm absorbance. A calibration curve was done by using PLTX standard (Wako Chemicals GmbH, Germany) with 12 concentrations from 12.5 to 1250 $pg.mL^{-1}$ adjusted to an exponential regression using SigmaPlot 9.0. The percentage of haemolysis (%H) obtained was referenced to toxin concentration.

Working solution was prepared with washed sheep blood (OXOID), centrifuged (4000 g, 10°C, 10 min) twice and diluted with phosphate buffered saline solution (PBS) 0.01 M, pH 7.4 (Sigma), 0.1% bovine serum albumin (BSA), 1 mM calcium chloride ($CaCl_2$ $2H_2O$) and 1 mM boric acid (H_3BO_3) to a final concentration of 1.5 x 10^6 $cells.mL^{-1}$. The assay for PLTX specificity was verified by a blank assay with ouabain (2 mM final concentration). Toxin extracts and PLTX standard were evaporated and refilled with PBS solution to eliminate methanol and water from the extraction. The assay was performed in two non-treated 96 well microplates and samples were analyzed in triplicate. After 22 hours incubation at 24°C, microplates were centrifuged (416 g, 10 min), 200 µL of the supernatant was transferred to another microplate for absorbance reading. Total toxicity was expressed as palytoxin equivalents per milliliter of culture (pg PLTX $eq.mL^{-1}$) related to the extracted volume.

3.3.4.3.3. *Toxin profile analysis by liquid chromatography–high resolution mass spectrometry (LC-HRMS).*

From the extracts used in the haemolytic assay to quantify toxin content, we selected those collected in the decaying phase (28 days) to analyze their toxin profile by liquid chromatography – electrospray ionization – high resolution mass spectrometry (LC-ESI-HRMS) in both strains. The analyses were performed on a hybrid linear ion trap LTQ Orbitrap XL Fourier transform mass spectrometer (FTMS) equipped with an ESI ION MAX™ source (Thermo Fisher, San José, USA) coupled to an Agilent 1100 LC binary system (Palo Alto, CA, USA). Organic solvents (HPLC grade quality) and glacial acetic acid used in the LC-MS analysis were purchased from Carlo Erba (Milan, Italy), The analytical method was previously described in Ciminiello *et al.,* 2010. A 3µm Gemini C18 column (150×2.00 mm; Phenomenex, Torrance, CA, USA) was eluted at 0.2 mL/min with water (eluent A) and 95% acetonitrile/water (eluent B), both containing 30 mM acetic acid (control conditions). A gradient elution (20–50% B over 20 min, 50–80% B over 10 min, 80–100% B in 1 min, and hold 5 min) was used. Injection volume was 5 µl.

Palytoxin standard was dissolved in methanol/water (1:1, vol/vol) to a concentration of 1µg.mL^{-1}. Strain OOAN0601 from the Adriatic Sea (Pezzolesi *et al.,* 2012) was used as reference to check for retention times and ionization behavior of OVTX-a to -e.

HR full MS experiments (positive ionization) were acquired in the range of *m/z* 700-1400. The following source settings were used: spray voltage = 4.8 (Source

Voltage (kV): 4.80); capillary temperature = 290 °C; capillary voltage = 50 V; sheath gas flow = 32 and auxiliary gas flow = 4 (arbitrary units); tube lens voltage = 130 V. Resolving power was set at 60,000 (FWHM at 400 m/z).

Calculation of elemental formulae was performed on the mono-isotopic peak of the most intense bi-charged ($[M+2H-H_2O]^{2+}$) and tri-charged ($[M+H+Ca]^{3+}$) ions, and the isotopic patter of each ion cluster was taken into consideration for identification purposes. The tuning, control, data acquisition and data analysis were done with Xcalibur® software v2.0.7.

4.3.5. Data analysis

Variation in cell abundance estimations among treatments, temperature and salinity effects on specific growth rates and cell DV diameter, as well as PLTX eq content in different growth phases were statistically studied by the analysis of variance (ANOVA). Results are reported as follow: F(degrees of freedom) =F-value, MSE= mean-square error, p-value). For significant differences ($p<0.05$), a multiple comparison Tukey's HSD test was performed. Pearson's correlation test was computed to assess the relationship between growth rate and cell DV diameter. To perform statistical analysis we used the software package IBM SPSS Statistics.

3.4. Results

3.4.1. Molecular Phylogeny

The *Ostreopsis* strains IRTA-SMM-11-09 and IRTA-SMM-11-10 were were phylogenetically analysed based on ITS and 5.8S regions of the rRNA genes. A phylogenetic analysis was performed and demonstrated both strains group within the species *O.* cf. *ovata,* being part of the Mediterranean and West Atlantic clade.

3.4.2. Subsampling method

Mucilaginous matrix was present in both experiments. Post-hoc Tukey's HSD test showed that an underestimation in the number of cells (1.81±0.76 x 10^6 cells mL^{-1}) was significant ($p<0.001$) when counting was performed in 0.5 and 1 mL volume samples compared to the average cell abundance calculated with the other sample volumes (4.57±0.66x10^6 cells mL^{-1}). For control and HCl treated samples we obtained high variation in cell counting within triplicates of settling enumerations, seven out of fifteen had negative results in the difference between RSD and λ (Table 3.1).The average of subsample triplicates for 0.5 mL settling volume was negative for sample volumes 3, 5 and 20 mL. In samples treated with Na-EDTA, negative results for settling triplicates were less abundant, and only two out of fifteen were negative. In Experiment 2, the culture contained 2.52±0.34x10^6 cells mL^{-1}, and 162 settlements were performed for cell counting. Cell enumeration was more accurate for all treatments and control; five out of fifty four replicates were negative in total

(Table 3.1). Broken cells were found in sonicated samples, thus we decided not to include these results for cell abundance estimations in our analyses.

	Settlement volume (mL)	Subsample volume (mL)	Control				HCl treatment				Na-EDTA treatment			
			Average	triplicates			Average	triplicates			Average	triplicates		
Exp 1	0,5	3	*-3,3*	-2,8	-0,1	-6,0	**-6,5**	0,8	3,6	**-9,8**	*1,4*	3,2	6,4	**-0,9**
	0,5	5	*-2,1*	1,9	1,3	**-4,2**	*-3,3*	**-1,8**	2,2	**-7,3**	*-2,1*	0,9	5,6	4,9
	0,5	20	*-6,5*	5,3	**-7,8**	**-4,2**	*-0,1*	**-0,6**	**-6,3**	**-2,8**	*0,9*	3,2	8,2	5,9
	3	12	*1,6*	9,0	6,8	0,3	*-0,2*	6,8	**-2,5**	1,4	*2,4*	2,5	5,8	**-1,0**
	3	20	*3,6*	5,9	-0,2	2,0	*4,8*	0,4	9,5	6,5	*4,2*	9,5	2,5	6,0
Exp 2	0,5	3	*9*	10,5	6,9	12,2	*9,6*	13,0	12,0	11,6	*4,5*	11,2	8,6	12,2
	0,5	5	*5,2*	3,3	11,6	3,4	*3,2*	**-5,1**	8,9	13,5	*4*	2,2	6,1	8,3
	0,5	12	*-0,2*	7,7	0,0	-1,5	*7,1*	**-0,2**	10,6	12,2	*0*	4,2	9,4	5,7
	0,5	20	*-0,9*	2,4	9,4	9,6	*4,2*	9,0	8,6	9,8	*7,6*	15,4	2,0	8,2
	3	12	*0,8*	2,0	2,3	-4,7	*2,5*	6,1	2,6	2,3	*0,6*	7,3	4,2	1,5
	3	20	*3,2*	5,6	4,0	7,9	*3,4*	3,7	0,0	6,0	*3,6*	6,8	**-1,1**	6,1

Table 3.1. Results obtained from the difference between the relative standard deviation (RSD) and Poisson distribution (λ) of three settlement countings. Bold values indicate negative results, thus not an acceptable enumeration estimation by the Utermöhl method.

Abundance cell estimation in Experiment 1 was significantly different considering sample volume ($F(4)=9.4$ MSE=2.19 x 10^{12}; $p<0.001$), settling volume ($F(1)=19.3$ MSE=4.51 x 10^{12}; $p<0.001$), and treatment ($F(2)=11.4$ MSE=2.68 x 10^{12}; $p<0.001$). For Experiment 2, abundance cell estimation was significantly different for sample volume ($F(3)=5.3$ MSE=5.31x10^{11}; $p<0.01$) and settlement volume ($F(1)=11.7$ MSE=1.16x10^{12}; $p<0.001$) but not according to treatment.

3.4.3. Cell growth, cell abundances and growth rate

Cell growth was observed for all multi-factorial experimental conditions. At 24 and 28°C, a typical growth curve was obtained with differentiation between exponential and stationary phases as early as the seventh day. At 19°C, this trend was not observed, and stationary phase was not achieved (Figure 3.1).
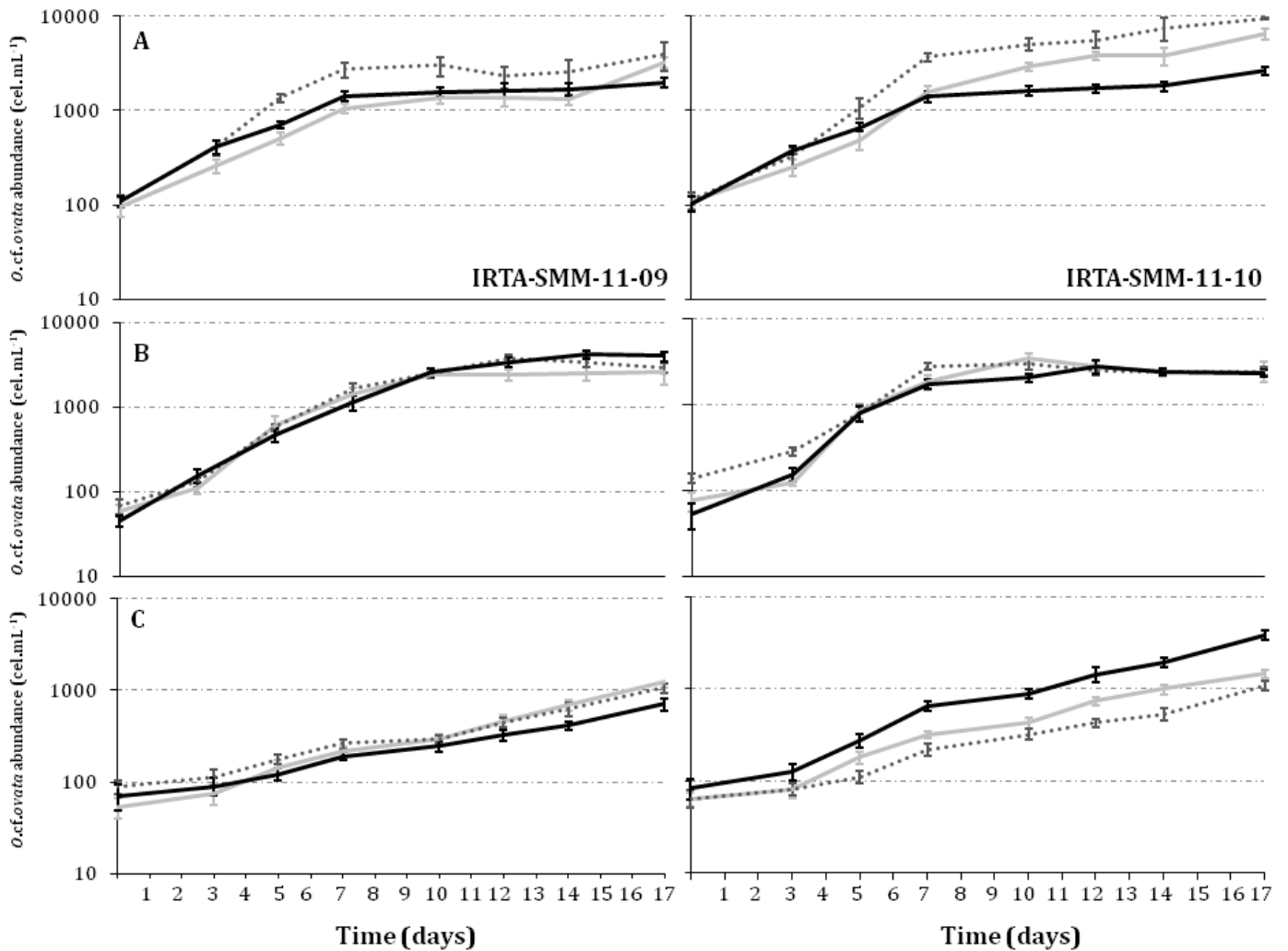
Fig. 3.1. Growth curves of *O.* cf. *ovata* strains IRTA-SMM-11-09 and IRTA-SMM-11-10 grown at nine different conditions of temperature (A. 19°C; B. 24°C; C. 28°C) and salinity (black, 38; grey, 36; dotted line, 32) during sixteen days. Error bars represent two standard deviation, n=9.

Maximal cell abundances at the end of the experiment were $9.48 \pm 2.20 \times 10^3$ cells mL^{-1} (28°C; salinity 36) and $3.97 \pm 0.55 \times 10^3$ cells mL^{-1} (24°C, salinity 38) for IRTA-SMM-11-10 and IRTA-SMM-11-09 respectively. The lowest maximal cell abundances were found at 19°C; $0.71 \pm 0.11 \times 10^3$ cells mL^{-1} for IRTA-SMM-11-10 at salinity 38. Maximal growth rates in replicates were 0.61 ± 0.05 div.day^{-1} for IRTA-SMM-11-10 (28°C, salinity 36) and 0.51 ± 0.01 div.day^{-1} for IRTA-SMM-11-09 (24°C, salinity 32). However, on average, growth rate was significantly higher at 24°C (0.48 ± 0.05 div. day^{-1}) than at 28°C (0.42 ± 0.11 div. day^{-1}) ($p<0.05$, Tukey test). Salinity significantly influenced growth rates at 24 and 28 °C ($F(2)=85.7$; $MSE=0.041$; $p<0.001$). At 24°C, there was not a clear pattern regarding differences in growth rate among salinities in both strains, whereas at 28°C, the highest growth rates were found at salinity 36, significantly different from salinity 38 for both strains (Tukey test; $p<0.005$), and from salinity 32 for IRTA-SMM-11-09. (Tukey test; $p<0.005$). The lowest growth rate was registered at 19°C (0.17 ± 0.02 div.day^{-1}) and little variability

was obtained for growth rates among salinities and strains, being significantly different from to the rest of temperatures (Tukey test, $p < 0.001$) (Figure 3.2).
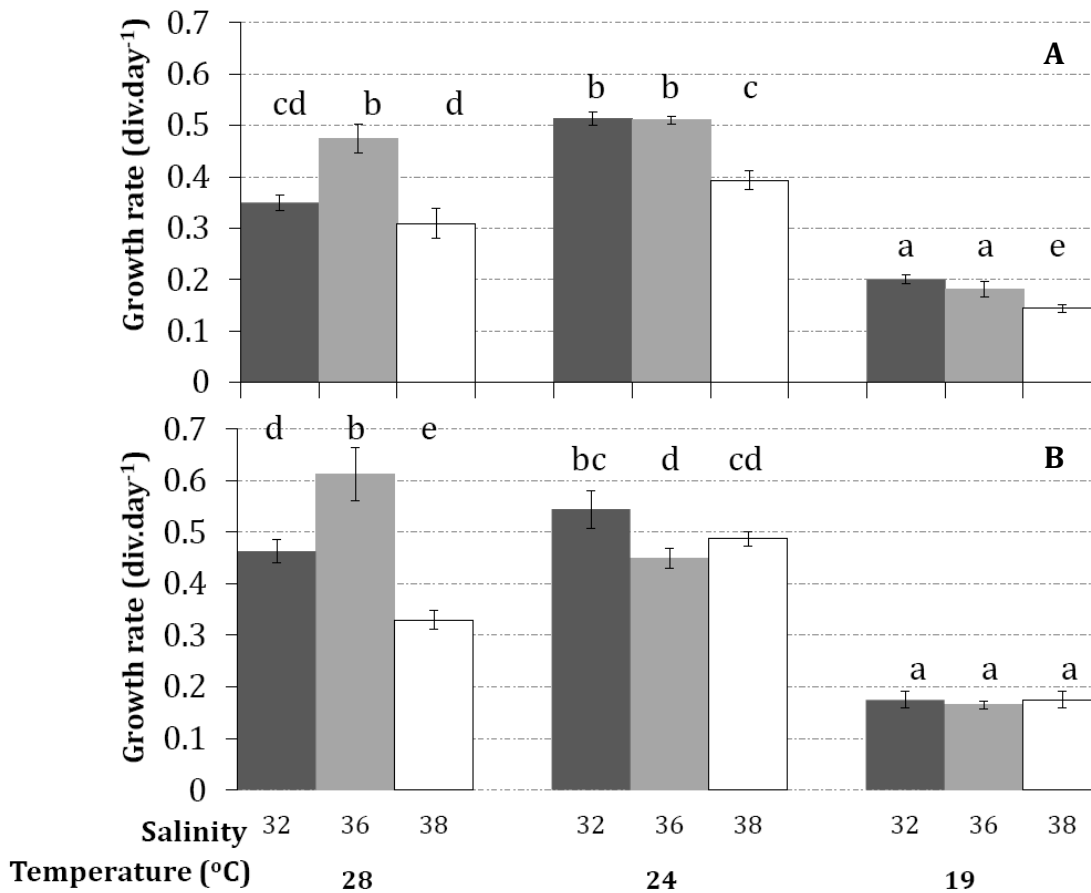
Fig. 3.2. Growth rate (div.day^{-1}) of *O.* cf. *ovata* strains IRTA-SMM-11-09 (A) and IRTA-SMM-11-10 (B) grown at nine different conditions of temperature and salinity during sixteen days. Error bars represent two standard deviation, n=3

3.4.4. Cell size

Presence of cysts and aberrant cell shapes were observed at 19°C in all growth phases (Figure 3.3a) and therefore it was difficult to recognize cell shapes to perform correct measurements. Consequently we decided not to include cells measurements from 19°C cultures in the cell size analysis. Average cell size was 38.40 ±9.03 in DV and 29.61±8.38 in W (n=3863). A variability of cell dimensions was found in all experimental conditions that ranged from 14.34 to 62.03 μm for the DV diameter, and from 14.27 to 44.73 μm for the W diameter, both found at 24°C, salinity 36 in IRTA-SMM-11-09. We observed that cultured cells were rounded (Figure 3.3b) rather than tear-drop shaped *O.* cf. *ovata,* as found in field samples (Figure 3.3c).
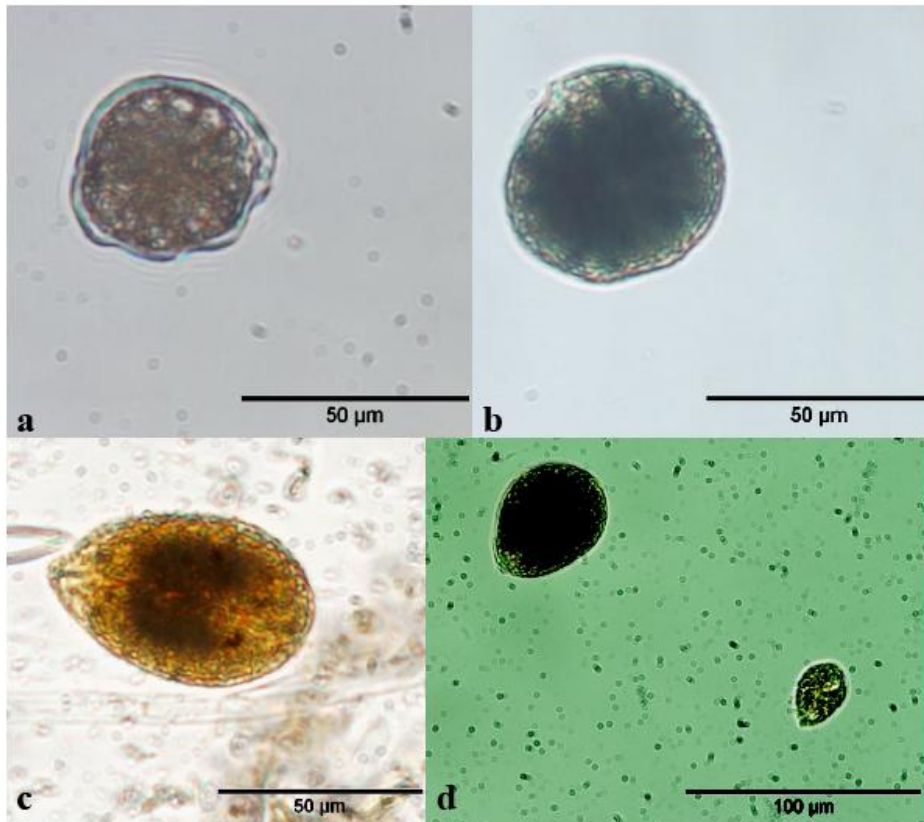
Fig 3.3. a. Morphology of *O.* cf. *ovata*. **a**. Aberrant cell from IRTA-SMM-11-09 in exponential phase at 19°C salinity 36 culture; **b**. Cell with wide W diameter from IRTA-SMM-11-09 in stationary phase at 24°C, salinity 36 culture; **c**. Field *O.* cf. *ovata* cell from 40°50' 47.8242" N; 0°45' 44.9532" E in August 2013; **d**.. Example of large and small cells from IRTA-SMM-11-10 in exponential phase at 28°C, salinity 38 culture.

In addition, a difficulty can arise from the position of the cell in the counting chamber. It is sometimes difficult to determine whether cells are in a planar orientation which may lead to false cell dimensions being obtained. We chose the DV diameter as a representative feature to study cell dimensions. Based on a DV diameter/frequency distribution histogram dividing DV diameter every 1 μm (Figure 3.4), two different sizes of cells were distinguished, a group of small cells (DV≤35 μm; *DV mean*=28.64 ± 3.78 μm; *W mean*= 21.20 ± 3.99 μm; n=1474) and another composed by large cells (DV>35 μm; *DV mean*=44.43 ± 5.29 μm; *W mean*=34.81±5.77 μm; n=2389) (Figure 3.3d).
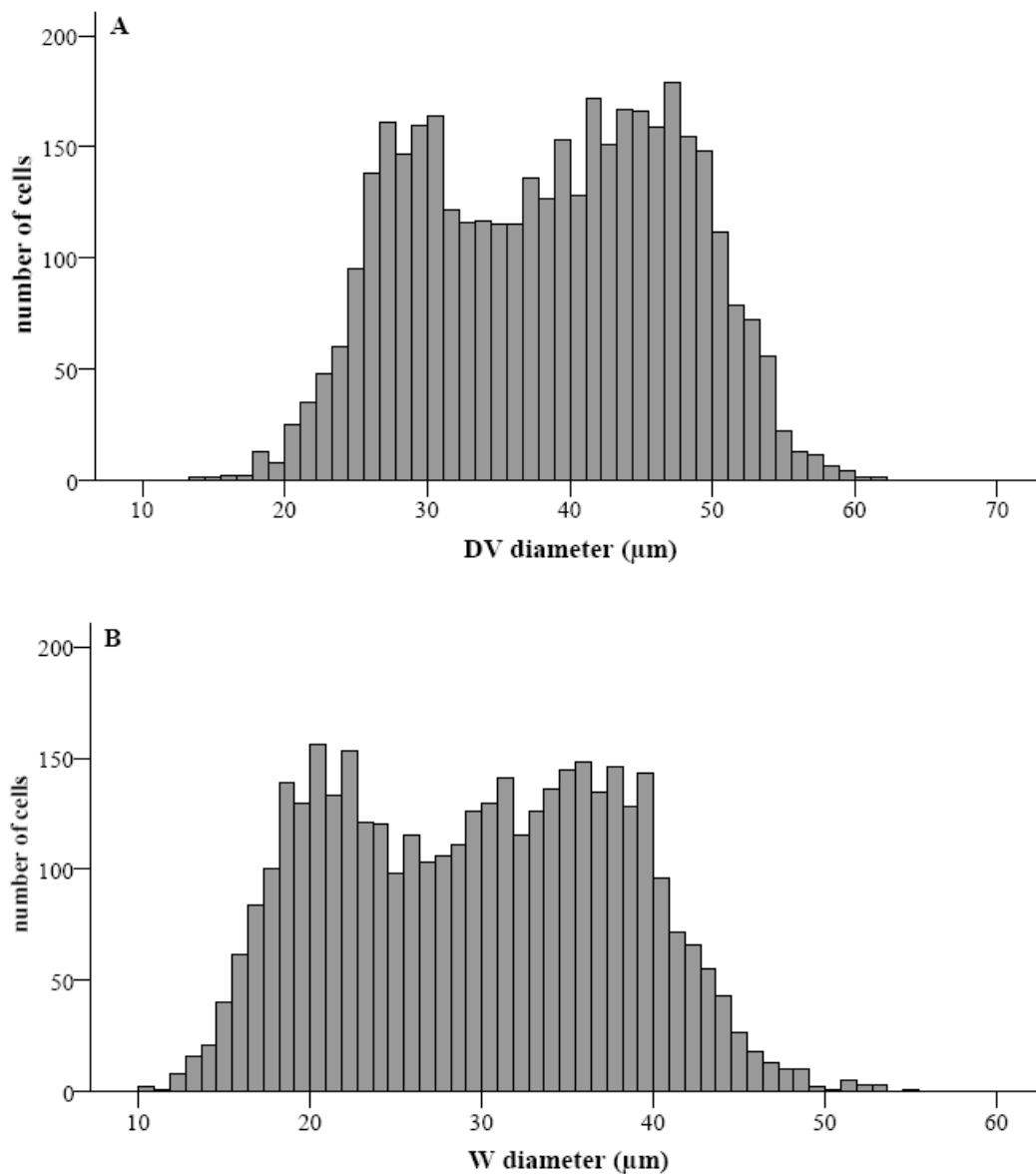
Fig 3.4. Size variability of *O.* cf. *ovata* for cultures at 24 and 28°C (n=3863). Histogram every 1 μm in **A.** dorsoventral (DV) diameter and **B.** width (W) diameter for all condition at 24 and 28°C for both strains.

An increase in the number of small cells during the exponential phase was observed, more evident at 24°C (Figure 3.5). This observation is more visible if the first day of sampling is not considered, as we should take into account that cell size corresponds to a character of the cells from a late exponential phase stock culture that was used as a source of inoculums. Small cells are more abundant when growth rate is higher. The smallest average DV diameter was found for IRTA-SMM-11-10 at 28°C, salinity 36 (31.61 ± 6.02 μm) that corresponds with the highest growth rate. The DV diameter was negatively correlated (r= -0.785; n=12; p<0.01) with growth rate.
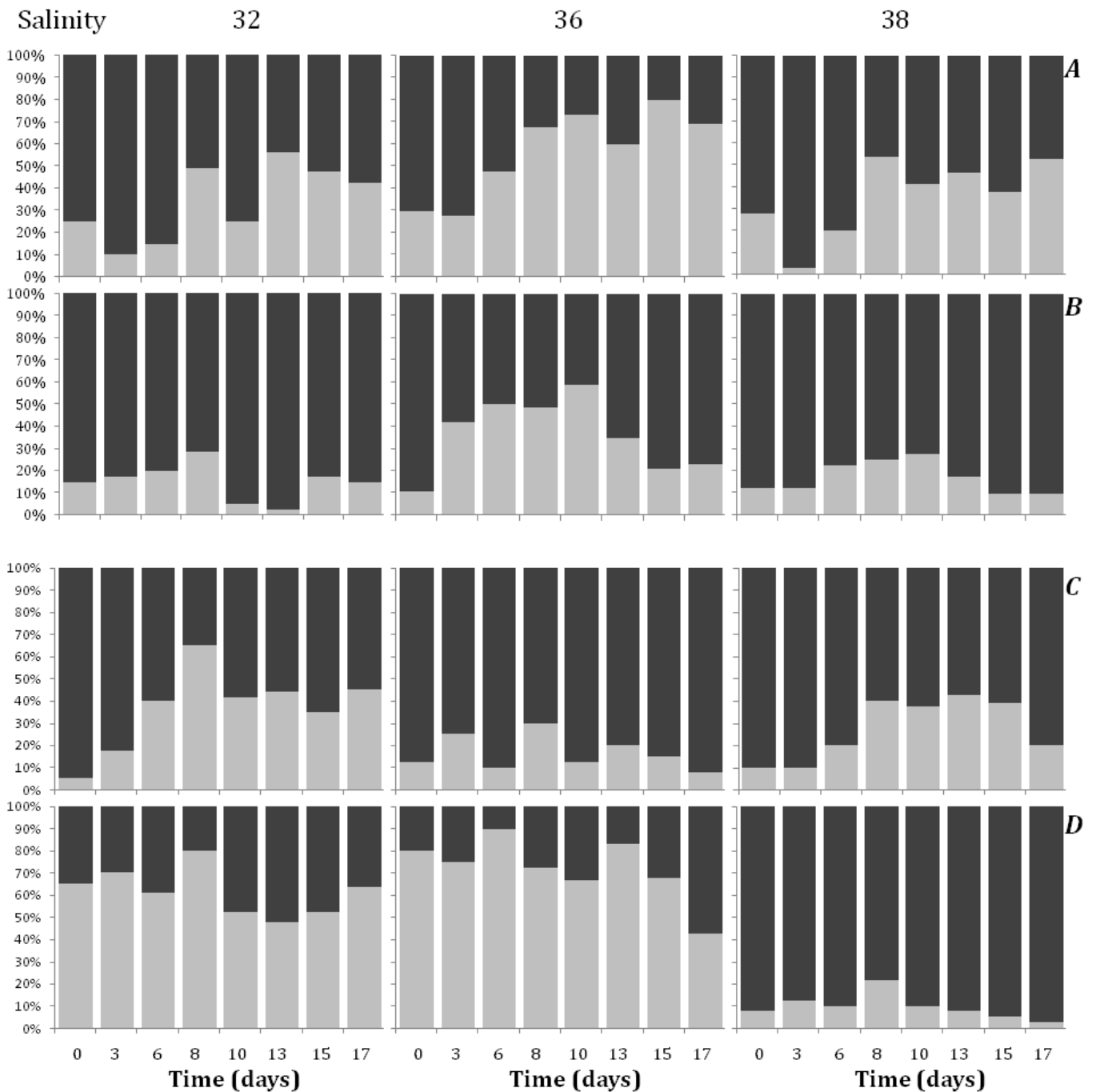
Fig 3.5. Percentage of number of small cells, DV≤35 µm, (bright grey) and big cells, DV>35µm (dark grey) during growth phases for IRTA-SMM-11-09 at 24°C (**A**) and 28°C (**B**) and IRTA-SMM-11-09 at 24°C (**C**) and 28°C (**D**) .

Significant differences regarding the average DV diameter were found for different conditions temperature ($F(2)=66.5$; $MSE=3695.21$; $p<0.001$), salinity ($F(2)=45.2$; $MSE=2511.1$; $p<0.001$) and the interaction of both ($F(4)=80.1$; $MSE=4454.7$; $p<0.001$).

3.4.5. Cell toxicity and toxin profile

Toxin concentration was quantified for samples at 24 and 28°C as they had typical growth trends and marked differentiation between exponential and stationary phases. In addition, *O.* cf. *ovata* in the field is not observed at 19°C in the area where these were isolated, thus blooms at this temperatures do not occur. Using the haemolytic test, we calculated PLTX-like concentration between $\%H_{20}$ and $\%H_{60}$ obtained in the calibration curve, according to the equation: $y = 0.0153e^{0.064x}$ ($R^2 = 0.96$), see Figure 3.6. In the presence of ouabain, a non-specific haemolytic activity was registered for the highest standard concentration but it was lower than $\%H_7$ and did not interfere in the haemolysis specific response.
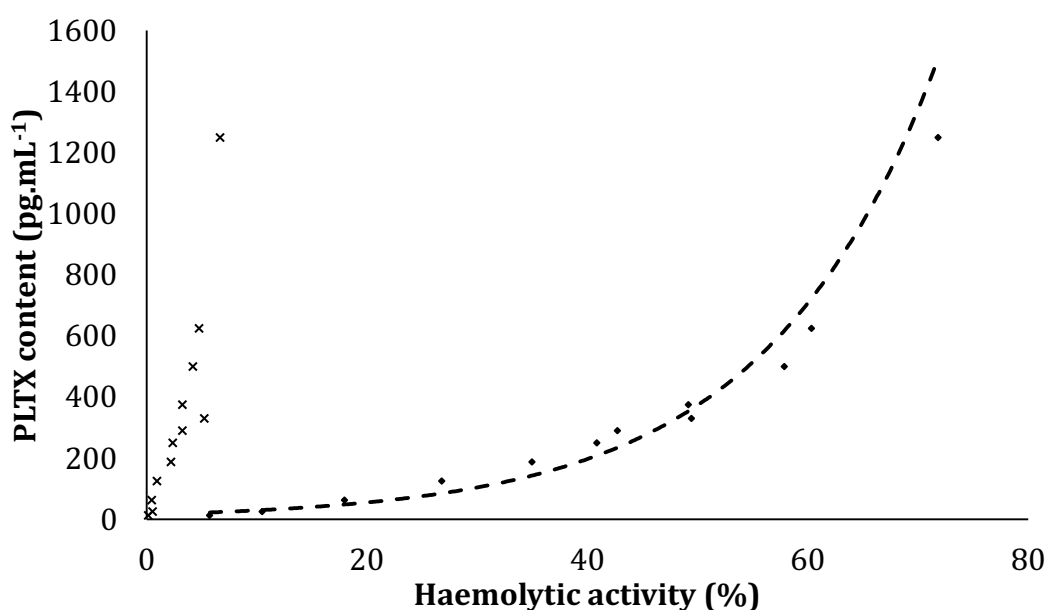
Fig. 3.6. Haemolytic assay exponential calibration curve without ouabain (dotted line) and with ouabain (crosses).

Haemolytic activity was registered in all analyzed samples. PLTX-like concentration increased significantly ($F(2) = 48.52$; $MSE = 2.49$; $p < 0.001$) with time for both strains and for all conditions with the exception of IRTA-SMM-11-09 at 28°C, salinity 38 (Figure 3.7). Significant differences in average toxin concentration were found among temperatures ($F(1) = 19.88$; $MSE = 1.68$; $p < 0.001$) finding higher values at 28°C (0.54 ± 0.37 pg PLTX eq. mL^{-1}) than at 24°C (0.28 ± 0.20 pg PLTX eq. mL-1). PLTX-like concentrations ranged from 0.06 ± 0.01 pg PLTX eq. mL^{-1} (late exponential phase, 24°C, salinity 32, IRTA-SMM-11-10) to 1.03 ± 0.12 pg PLTX eq.mL^{-1} (decaying phase; 28°C, salinity 38, IRTA-SMM-11-09).
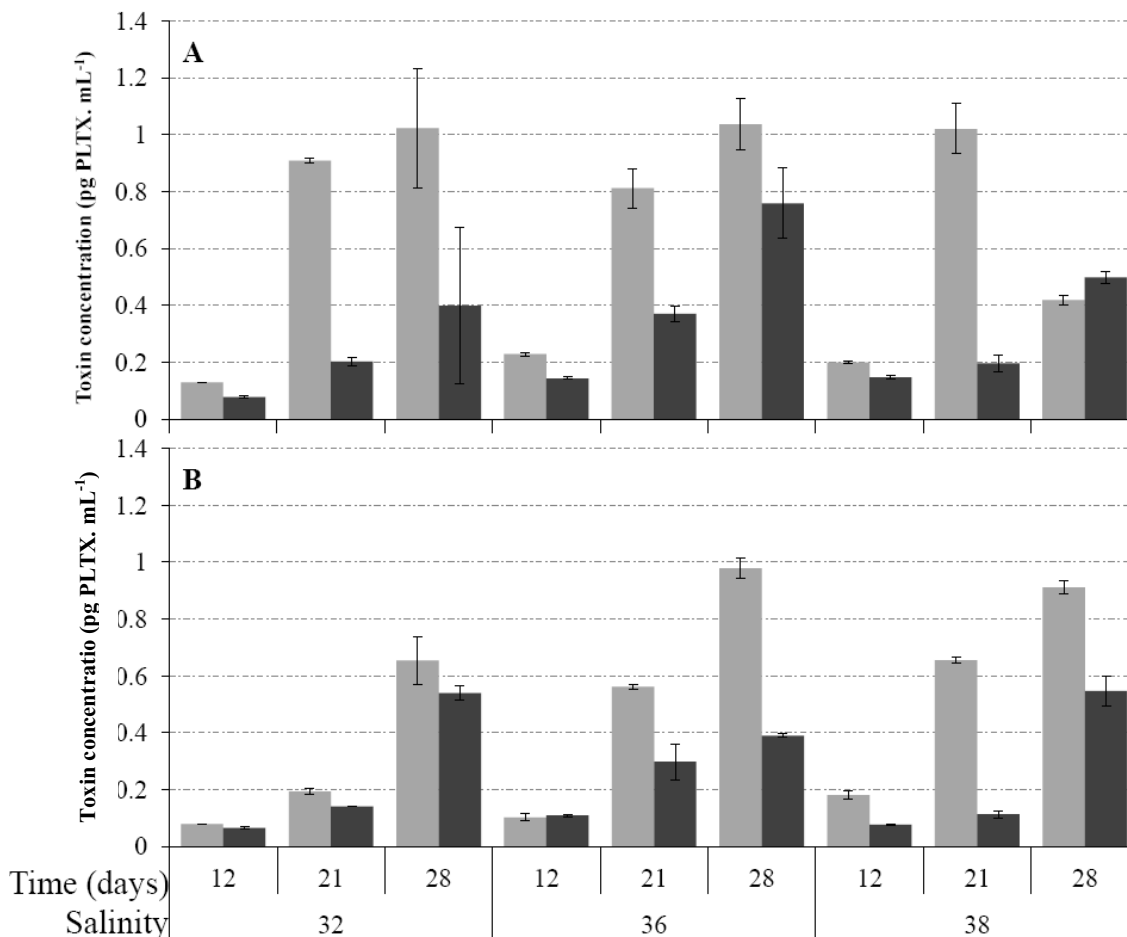
Fig. 3.7. PLTX-like content (pg PLTX eq.mL^{-1}) of *O.* cf. *ovata* IRTA-SMM-11-09 (A) and IRTA-SMM-11-10 (B) strains grown under different conditions of temperature (28°C bright grey; 24°C dark grey) and salinity estimated with haemolytic assay. Error bars represent two standard deviation from the average of three wells result from haemolytic assay.

The study of the toxin profile of the cultures harvested in the decaying phase revealed that pPLTX and OVTX-a, -b, -c and –d&-e were present in all the extracts; their relative abundance was practically the same in both the *O.* cf. *ovata* strains (IRTA-SMM-11-09 and IRTA-SMM-11-10) and did not vary depending on either temperature or salinity (Figure 3.8). OVTX-a always represented almost 60% of the total toxin content, and pPLTX was the minor toxin component, accounting for less than 1% of the total PLTX-like compounds in the extracts. Ovatoxin-b accounted for 30% of the total toxin content, while OVTX-c represented 4%. Ovatoxins-d and –e are isomers and could not be fully separated by chromatographic means, thus their quantitation was made as a sum of both compounds, which accounted for about 9%.
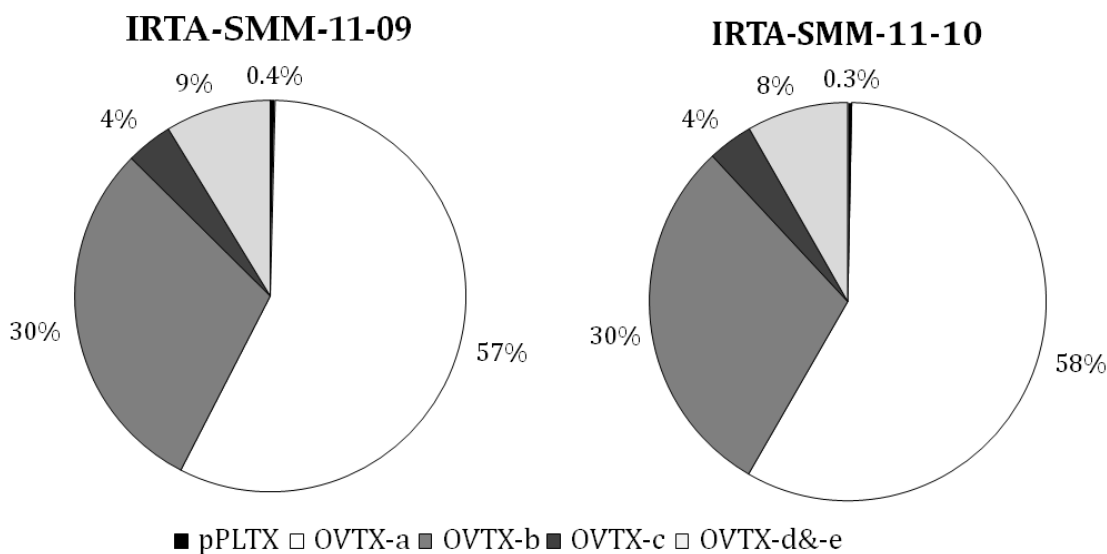
Fig. 3.8. Relative abundance (in percentage) of the palytoxin-like compounds produced by two strains of *Ostreopsis cf. ovata* in the post-exponential growth phase. Average of six cultures (n=6) under two temperatures (24°C and 28°C) and three salinities (32, 36, 38). Temperature and salinity did not have any effect on the toxin profile. pPLTX = putative palytoxin; OVTX-a = ovatoxin-a; OVTX-b = ovatoxin-b; OVTX-c = ovatoxin-c; OVTX-d&-e = sum of ovatoxin-d and ovatxin-e (these last two compounds did not achieve complete chromatographic separation).

The identification of pPLTX and OVTX-a to -e in the extract was supported by the comparison of retention times and full HRMS spectra with those obtained under the same experimental conditions for a reference sample of *O.* cf. *ovata* from the Adriatic Sea previously characterized (Pezzolesi *et al.,* 2012); ionization behavior of individual toxins, isotopic patterns, and elemental formulae assigned to mono-isotopic ion peaks in full MS spectra were consistent with those reported for OVTXs and pPLTX by Ciminiello *et al.,* 2010 (Table 3.2).

	pPLTX RT=8.6-8.9 min		OVTX-a RT=11.2-11.7 min		OVTX-b RT=10.56-10.95		OVTX-c RT=9.11-9.46		OVTX-d&e RT=9.77-10.35	
	$[M+H+Ca]^{3+}$ $C_{129}H_{224}O_{54}N_3Ca$ RDB 19.5	$[M+2H-H_2O]^{2+}$ $C_{129}H_{223}O_{53}N_3$ RDB 20	$[M+H+Ca]^{3+}$ $C_{129}H_{224}O_{52}N_3Ca$ RDB 19.5	$[M+2H-H_2O]^{2+}$ $C_{129}H_{223}O_{51}N_3$ RDB 20	$[M+H+Ca]^{3+}$ $C_{131}H_{228}O_{53}N_3Ca$ RDB 19.5	$[M+2H-H_2O]^{2+}$ $C_{131}H_{227}O_{52}N_3$ RDB 20	$[M+H+Ca]^{3+}$ $C_{131}H_{228}O_{54}N_3Ca$ RDB 19.5	$[M+2H-H_2O]^{2+}$ $C_{131}H_{227}O_{53}N_3$ RDB 20	$[M+H+Ca]^{3+}$ $C_{129}H_{224}O_{53}N_3Ca$ RDB 19.5	$[M+2H-H_2O]^{2+}$ $C_{129}H_{223}O_{52}N_3$ RDB 20
	m/z found Δ (ppm)	m/z found Δ (ppm)	m/z found Δ (ppm)	m/z found Δ (ppm)	m/z found Δ (ppm)	m/z found Δ (ppm)	m/z found Δ (ppm)	m/z found Δ (ppm)	m/z found Δ (ppm)	m/z found Δ (ppm)
IRTA-SMM-11-09										
Tª 24 Salinity 32	906.4831	Not found	895.8197	1315.2479	910.4953	1337.2612	915.8269	1345.2581	901.1510	1323.2451
	0.32		0.23	0.74	0.37	0.92	0.37	0.46	-0.18	0.56
Tª 24 Salinity 36	906.4837	Not found	895.8197	1315.2474	910.4953	1337.2690	915.8269	1345.2582	901.1513	1323.2452
	1.04		0.199	0.38	0.45	0.61	0.42	0.59	0.13	0.69
Tª 24 Salinity 38	906.4826	Not found	895.8197	1315.2479	910.4952	1337.2608	915.8266	1345.2584	901.1517	1323.2452
	-0.21		0.26	0.77	0.29	0.63	0.04	0.74	0.01	0.63
Tª 28 Salinity 32	906.4826	1331.2426	895.8204	1315.2485	910.4954	1337.2612	915.8269	1345.2567	901.1516	1323.245
	-0.26	0.61	0.96	1.21	0.61	0.92	0.33	-0.53	0.46	0.88
Tª 28 Salinity 36	906.4829	Not found	895.8198	1315.2478	910.4950	1337.2611	915.8273	1345.2593	901.1516	1323.2456
	0.17		0.30	0.71	0.42	0.86	0.83	1.34	0.52	0.97
Tª 28 Salinity 38	906.4823	Not found	895.8194	1315.2473	910.4951	1337.2610	915.8268	1345.2577	901.1508	1323.2444
	-0.51		-0.16	0.35	0.21	0.72	0.24	0.22	-0.41	0.07
IRTA-SMM-11-10										
Tª 24 Salinity 32	906.4831	Not found	895.8196	1315.2474	910.4950	1337.2603	915.8268	1345.2571	901.1515	1323.2452
	0.26		0.12	0.56	0.04	0.35	0.23	-0.35	0.31	0.89
Tª 24 Salinity 36	906.4823	Not found	895.8198	1315.2479	910.4952	1337.2605	915.8268	1345.2579	901.1513	1323.2446
	-0.51		0.28	0.99	0.23	0.52	0.23	0.49	0.14	0.31
Tª 24 Salinity 38	906.4834	Not found	895.8197	1315.2475	910.4953	1337.2610	915.8267	1345.2594	901.1510	1323.2446
	0.57		0.15	0.59	0.35	0.100	0.18	1.98	-0.14	0.23
Tª 28 Salinity 32	906.4830	1331.2423	895.8195	1315.2472	910.4950	1337.2604	915.8268	1345.2581	901.1509	1323.2445
	0.24	0.60	-0.03	0.33	0.08	0.38	0.27	0.67	-0.26	0.19
Tª 28 Salinity 36	906.4826	Not found	895.4871	1315.2481	910.4950	1337.2607	915.8263	1345.2572	901.1510	1323.2451
	-0.20		0.29	1.20	0.10	0.75	-0.21	-0.22	-0.12	0.74
Tª 28 Salinity 38	906.4824	Not found	895.8192	1315.2468	910.4947	1337.2601	915.8264	1345.2590	901.1510	1323.2447
	-0.44		-0.33	-0.05	-0.21	0.16	-0.18	1.55	-0.14	0.39

Table 3.2. HRMS data of putative palytoxin (pPLTX), and ovatoxins –a to –e (OVTX-a, -b, -c, -d&-e) obtained from full MS spectra in the mass range m/z 700-1400 on a LTQ Orbitrap XL® (Resolution 60,000 FWHM). Retention times (RT), molecular formulae and relative double bonds equivalents (RDB) of the mono-isotopic peak of the most intense bi-charged ($[M+2H-H_2O]^{2+}$) and tri-charged ($[M+H+Ca]^{3+}$) ions in the full MS spectra of the samples of the *multi-factorial* experiment (temperatures 24 and 28°C; salinity 32, 36 and 36) with two strains of *Ostreopsis* cf. *ovata* (IRTA-SMM-11-09 and IRTA-SMM-11-10) collected in the post-exponential phase. Found *m/z* related to those ions and mass error (in ppm) associated with the molecular formulae are provided.

3.5. Discussion

3.5.1. *Counting methodology*

During *Ostreopsis* blooms in Mediterranean coasts, a brownish mucilage covering different substrates such as macrophytes and rocks, has been observed (e.g. Vila *et al.,* 2001; Totti *et al.,* 2010; Aligizaki *et al.,* 2006; Mangialajo *et al.,* 2008). This mucilage plays an important role on epi-benthic microalgae ecology, providing attachment to the substrate (Vidyaranthna and Granéli, 2013), working as a micropredation mechanism that traps small organisms (Barone, 2007), or as a protective coat (Bravo *et al.,* 2012). This mucilage is composed of acid polysaccharides and trichocysts sticking together (Honsell *et al.,* 2013). The formation of cell aggregates embedded in mucilage impedes the accurate estimations of cell abundance. Some studies have employed different strategies adding HCl or Na-EDTA to samples in order to obtain more accurate cell abundance estimations in their growth curves. Guerrini *et al* (2010) and Pezzolesi *et al* (2012) performed batch cultures inoculated with the same initial cell concentrations from a stock culture. Every 2-3 days two cultures were treated with HCl for counting and discarded afterwards. Scalco *et al.,* (2012), followed a similar methodology adding a solution of Na-EDTA. Vanucci *et al* (2012b) and Monti *et al* (2012) added solutions of HCl and Na-EDTA respectively to samples taken from the same culture every 2-3 days. Treatments with HCl and Na-EDTA can minimize ionic interactions produced in the mucilage that could help to disaggregate cells in culture (Allgredge *et al.,* 1993). In order to evaluate this fact, we compared cell enumeration variability obtained in samples treated with HCl or Na-EDTA. We decided to analyze sampling strategy considering the fact that inoculations from the same stock culture may contain cell aggregates that can lead to a different initial cell concentration among parallel cultures. In our study, we included sample and settling volumes as supplementary factors involved in accuracy of cell abundance estimations. Sample and settling volumes vary among studies; in some studies 1 mL (Scalco *et al.,* 2012; Monti *et al.,* 2012), or 5 mL (Nascimento *et al.,* 2012a), were used but both were settled in a 1 mL chamber, while in others 50-250 mL were used (Vanucci *et al* 2012b) with no specification in settlement volume. In the experiment performed in the decaying phase, cell enumeration from 0.5 and 1 mL sample volumes was significantly lower than in other volumes. This result may be due to the large cell size of *O.* cf. *ovata* for a Palmer-Maloney chamber. Another reason may be that cells stuck to the inside walls of the pipette tip during pipetting for settlement while in bigger chambers settling is done directly, and this reduces cell losses. Less error was obtained in counting performed in 3 mL chambers for both treatments and control, showing that bigger settling volumes, and thus bigger sample volumes, are more suitable to estimate *O.* cf. *ovata* cell concentration. Cell abundance estimation in Na-EDTA treated samples was more accurate than in control and HCl treated samples,

suggesting a better aggregate disruption with Na-EDTA. In Experiment 2, less error was registered in all cases meaning that in cultures where cell concentration is lower, no need of treatment is required to obtain better cell abundance estimation.

Otherways of determining *O.* cf. *ovata* growth curves have to be cited. Granéli *et al* (2011) performed cultures in 8 mL Petri dishes and cell enumeration was done directly in alive cells. Chlorophyll a (Chll. a) content has been used recently (Vyatathna and Granéli, 2011; Vyatathna and Granéli, 2013; Tanimoto *et al.,* 2013; Yamaguchi *et al.,* 2012b) and constitutes a rapid and simple method for cell abundance estimation. Yamaguchi *et al* (2012a) found a significantly correlation with chlorophyll a fluorescence measurements and cell abundances in different *Ostreopsis* spp strains. Nevertheless, fluorescence techniques have to be considered carefully when performing growth rate curves as advised by Raven and Beardall (2006), and Kruskopf and Flynn (2006), because of changes in fluorescence per cell under different nutrient condition and/or daily cycle.

From our results, we suggest to use no treatment in samples obtained during the exponential phase as cell aggregates are less abundant. Addition of Na-EDTA to samples is recommended starting at stationary phase when mucilage production is high.

3.5.2. Growth under different temperature and salinity conditions

We performed a multi-factorial experiment combining different water temperatures (19, 24, 28°C), and salinities (32, 36, 38) and measured responses in growth, cell size and toxicity in two *O.* cf. *ovata* strains isolated from the western Mediterranean Sea, for which their physiology had not been studied before. Both strains presented growth in all experimental conditions, although at 19°C growth rate was significantly lower. This is in agreement with other laboratory studies where *O.* cf. *ovata* from Mediterranean clade (Pezzolesi *et al.,* 2012) and from Japan (Yamaguchi *et al* 2012b) grew in a wide range of temperatures and salinities. Presence of *O.* cf. *ovata* has been reported by other authors in different regions of the world presenting a wide spectrum of water temperature and salinity conditions (Pistocchi *et al.,* 2011 and references herein). This growth tolerance could explain why *O.* cf. *ovata* is capable of inhabiting both tropical and temperate areas and can be adapt to highly variable environments in coastal waters (Tanimoto *et al.,* 2013).

Growth curves obtained at 24 and 28°C followed the same pattern as other *O.* cf. *ovata* strains from the Mediterranean Sea (Pezzolesi *et al.,* 2012; Guerrini *et al.,* 2010; Vanucci *et al.,* 2012a; Vanucci *et al* 2012b), characterized by a rapid exponential phase during the first week.

Water temperature is considered the most important factor that affects growth of benthic dinoflagellates (Pistocchi *et al.,* 2011; Mangialajo *et al.,* 2011; Parsons *et al.,* 2012). Different optimal temperatures for the growth of *O.* cf. *ovata* from the

Mediterranean Sea have been proposed from laboratory studies. Adriatic strains have presented high growth performance at 30°C, with a growth rate of 0.74±0.1 div.day^{-1}(Granéli *et al.,* 2011), while Tyrrhenian strains have shown optimal temperature of growth at 20°C, 0.49 div.day^{-1}(Pezzolesi *et al.,* 2012). However, Scalco *et al.,* (2012) studied strains from both Seas under the same conditions without finding differences in their optimal growth temperatures that ranged between 22 and 26°C, with growth rates higher than 0.6 div.day^{-1}for both temperatures. Slightly lower maximal growth rates were registered in our experiment (0.61±0.05 div. day^{-1}), but optimal temperature conditions were within a similar range (24-28 °C), finding higher average growth rates at 24 °C, than at 28°C. The lowest growth rates in *O.* cf. *ovata* have been observed in Nascimento *et al.,* (2012a), from a Brazilian strain grown at 24°C, (0.22 div. day^{-1}). By contrast, in a *O.* cf. *ovata* strain from Japan, Vidyarathna et Granéli, (2011) and Yamaguchi *et al.,* (2012) found growth rates higher than those found in Mediterranean strains, 1.03±0.03 day^{-1} between 25 and 30°C. Those results are in agreement with field temperatures where cells were isolated, reflecting that populations from diverse environments may present different optimal temperatures for growth. Nevertheless, those data have to be analyzed with caution taking into account possible differences on cell culture characteristics and counting methodology used in each study. Culture volume, recipient material, initial cell concentration, acclimation period and medium components, among others, can affect growth performances (Andersen, 2005).

Influence of salinity on cell growth in *O.* cf. *ovata* is not as well studied and conclusions about its effects are not as robust (Pistocchi *et al.,* 2011; Parsons *et al.,* 2012). Blooms of *O.* cf. *ovata* in Mediterranean waters occur normally between June and November when salinity values are higher than 37 on average. This is in agreement with results found in Pezolessi *et al.,* 2011 where maximal growth rates were obtained at salinities between 36 and 40. In addition, there is no presence of cells in waters under direct influence of rivers (Pistocchi *et al.,* 2011), indicating that this species does not grow in areas where salinity drops below 20 (Yamaguchi *et al.,* 2012b). We observed that our strains were tolerant to salinities between 32 and 38 but different growth performances were observed depending on temperature. Tanimoto *et al.,* (2013) provided the first evidence for significant effects of temperature, salinity and their interaction on the growth of two *Ostreopsis* sp strains. In our multi-factorial experiment, where cells were acclimated for one year to experimental conditions, we found that salinity variations affected significantly growth rate. At 24 °C there was not a clear pattern, while at 28°C, growth rate was higher at salinity 36 than at salinity 38, and 32. In accordance with references cited above, temperature would be the predominant environmental factor that influences bloom formation. However, from our laboratory results, we hypothesized that an exposure to higher temperatures and salinities, possible scenario according to climate change predictions in the Mediterranean Sea (IPCC, 2013), the role of

salinity could be crucial. We suggest that such an occurrence may not enhance *O*. cf. *ovata* bloom formation due to the interaction with higher salinities. Nevertheless, the response of marine communities to warming is difficult to predict as many environmental factors are involved and are not possible to control in a laboratory setting. Experimental results obtained in our multi-factorial study cannot be directly extrapolated to future natural conditions.

3.5.3. Cell size

Cells in culture had a more rounded morphology and were smaller than field cells from the area where they had been isolated as reported in other studies (Aligizaki et al, 2006; Accoroni et al, 2012; Nascimento et al 2012a; Laza-Martinez et al, 2011; David et at, 2013). A relevant heterogeneity in *O*. cf. *ovata* morphology has been observed, distinguishing two different cell types not overlapping in size. This representative diversity of *O*. cf. *ovata* population morphology has been detected both in field samples (Penna *et al.,* 2005; Aligizaki *et al.,* 2006; Accoroni *et al.,* 2012; Bravo *et al.,* 2012; Nascimento *et al.,* 2012b; David *et al.,* 2013; Carnicer et al, in preparation) and in cultures (Guerrini *et al.,* 2010; Scalco *et al.,* 2012; Vanucci *et al.,* 2012a; Vanucci *et al.,* 2012b; Pezzolesi *et al.,* 2012; Bravo *et al.,* 2012). Silva and Faust (1995), hypothesized that small cells, could be either gametes or vegetative cells that perform rapid divisions resulting in a rapid increase of cell populations. Nevertheless, Bravo et al (2012), questioned the explanation of small cells being gametes as they identified gametes from all sizes. Accoroni *et al.,* (2012) suggested that cell size could be related with bloom phases. In Scalco *et al.,* (2012), small cells with DV diameters below 20 μm were considered small while we defined small cells for DV diameters down to 35 μm. A significant positive correlation between the percentage of large cells and growth rate was found in the former study, but as cell size ranges were determined differently, an overlap in cell size with our study could have been produced and comparisons may not be consistent. In our study, at 24 and 28°C, in general, the number of small cells increased from early to late exponential phase. High amounts of small cells during the exponential growth phase are significantly correlated with high growth rates. This is in agreement with the approach that small cells can act as vegetative cells that rapidly divide. In our experiments, at 19°C, the majority of cells were morphologically deformed from the beginning of the growth curve while at 24 and 28°C, the percentage of anomalous cells increased with time. This is in accordance with results in Scalco *et al.,* (2012), where it was observed the presence of cells of different sizes at 22, 26 and 30°C but not at 18°C where the percentage of anomalous cells increased. The appearance of these cells has been attributed with non optimal conditions of growth (Bravo *et al.,* 2012) and more specifically at the end of stationary phase (Aligizaki *et al.,* 2008; Guerrini *et al.,* 2010, Accoroni *et al.,* 2012). A possible additional explanation is the genes responsible for cell size, or their protein products may be temperature sensitive in some way, but such an explanation requires deep investigations.

Seasonal variations of *O.* cf. *ovata* have been reported by numerous field observations in Mediterranean waters (reviewed in Pistocchi *et al.,* 2011), populations not being observed from around late fall to early summer. Since aberrant cells with granulated cytoplasm can constitute the precursors of cyst formation described as described previously, these forms could represent the overwinter populations (Bravo *et al.,* 2012).

3.5.4. Toxicity

Under all tested conditions, the estimation of PLTX-like compounds per cell increased from late exponential phase to decaying phase. These results are in agreement with other studies on toxin content of *O.* cf. *ovata* strains from the Mediterranean area (Vanucci *et al.,* 2012a; Vanucci *et al.,* 2012b; Scalco *et al.,* 2012; Pezzolesi *et al.,* 2012; Guerrini *et al.,* 2010) and from Japan (Granéli et al, 2011; Vidyarathna and Granéli, 2011; Vidyarathna and Granéli, 2013). A similar response has been observed also in other phytoplankton species (Bates, 1998; Grzebyk, *et al.,* 2003) and it has been related to the fact that toxins are secondary metabolites that probably accumulate in cells after growth. The only exception was found in *Ostreopsis* cf. *ovata* strains from Brazilian waters that belong to the same Mediterranean/Atlantic clade, which did not follow this trend in toxin content progress over time (Nascimento *et al.,* 2012a).

Taking into account cells variability, we calculated total toxin concentration to avoid cell toxin differences regarding cell size or growing phase (Pezzolesi et al., 2014). A negative correlation between PLTX-like content and growth of *O.* cf. *ovata* has been described under unfavorable conditions regarding temperature (Pezzolesi *et al.,* 2012; Granéli *et al.,* 2011), and nutrient concentrations (Vannucci *et al.,* 2012a; Vydyaranthna *&* Granéli., 2011). Nevertheless, it is still not clear to what extent environmental factors are involved in toxin production. Our PLTX-like concentration study was focused on tolerable temperature growth conditions which limited the range of temperatures tested, and no correlation between toxin content and growth in our strains was observed. However, higher toxin concentrations were found at 28ºC than at 24ºC, reflecting the possibility that in warmer waters, toxicity could be enhanced.

Toxin profiles of the two analyzed *O.* cf. *ovata* strains (IRTA-SMM-11-09 and IRTA-SMM-11-10) were almost identical, and relative abundance of individual toxins was not affected by temperature and/or salinity: OVTX-a dominated the profile (about 60%, Fig. 7), and OVTX-b, -c and –d&-e represented around 40% of total toxin content. Putative PLTX was the least abundant compound in all the analyzed samples and accounted for less than 1%. Such a toxin profile is similar to that reported for most of the Mediterranean strains reported so far (Ciminiello *et al.,* 2010; Pezzolesi *et al.,* 2012; Scalco *et al.,* 2012; Vanucci *et al.,* 2012a; Accoroni *et al.,* 2011; Sechet *et al.,* 2012), in which OVTX-a is the major toxin produced. In both the

O. cf. *ovata* strains that were analyzed, OVTX-f was not detected; this PLTX-like compound represented the major component (50% of the total toxin content) of an Adriatic strain producing all the ovatoxins described so far, including OVTX-a (23%), OVTX-b (17%), OVTX-c (2.4%), OVTX-d+e (6.7%) and pPLTX (0.3%) (Ciminiello *et al.,* 2012). *O.* cf. *ovata* from other geographical origins have different toxin compositions as well. Brazilian strains had approximately the same amount of OVTX-a and -b (Nascimento *et al.,* 2012a). In several Japanese strains, new OVTX isomers were identified (Suzuki *et al.,* 2012), as well as Ostreol A was structurally elucidated in strains isolated from Jeju Island in Korea (Hwang *et al.,* 2013). Differences in toxin profile occurred not only among species but also among strains belonging to the same genetic clade. This physiological feature represents an additional factor that contributes to the characterization of *O.* cf. *ovata* geographical distribution (Penna *et al.,* 2005).

According to the haemolytic assay, total toxicity reached its maximum at the decaying phase for both strains and all conditions (except for one single case, IRTA-SMM-11-09 at temperature 28°C and salinity 38). Therefore, we selected these samples to obtain the best accuracy in the toxin profile analysis (García-Altares et al. 2014, in preparation).

3.6. Conclusions

In our experiment we found that big sample and settlement volumes seem to improve accuracy in cell abundance estimations, as well as the addition of Na-EDTA to samples to help disrupt aggregates in *O.* cf. *ovata* cultures*,* and thus, obtain a higher homogeneity. Different strategies to calculate the number of cells in cultures have been reported in different studies. This fact can lead to errors when comparing growth rates or toxin content per cell. A similar methodology for estimation of cell abundance and culturing may help to obtain more reliable conclusions between comparisons among different strain studies performed around the world.

It was demonstrated *O.* cf. *ovata* from the north western Mediterranean Sea is tolerant to a wide range of temperatures and salinities, in agreement with other strains which could explain the colonization of widely different climates and regions. The optimal growth temperatures for strains could differ depending on the environmental conditions of their origin. Highest growth rates were found at 24°C, coinciding with average temperature in field. The variation among salinity is significant at 24 and 28 °C reflected in a growth inhibition at salinities 32 and 38 at 28°C. Variation in salinity values may act as a limiting factor in high temperature conditions such as is predicted for the coming years.

Small cells may be a result of an acceleration of cell division, as we found a correlation between growth rate and an increase in the amount of this group of cells. The question whether these cells act as gametes or vegetative cells is still unsolved.

An increase of toxin content with time was observed throughout the growth phases, and toxicity of the cultures was higher at 28 ºC than at 24 ºC, indicating a possible toxin enhancement with temperature. Toxin profiles did not change with different conditions of temperature, or salinity, and it was similar to the majority found in the Mediterranean clade, representing a characteristic feature of this clade.

From our results, a simultaneous increase on sea water temperature and salinity, as predicted in global warming projections for the Mediterranean may not result in higher intensity of *O.* cf. *ovata* bloom formations, though it might enhance their toxicity.

3.7. References

Accoroni, S., Romagnoli, T., Colombo, F., Pennesi, C., Di Camillo, C.G., Marini, M., Battocchi, C., Ciminiello, P., Dell'Aversano, C., Dello Iacovo, E., Fattorusso, E., Tartaglione, L., Penna, A., Totti, C., 2011. *Ostreopsis* cf. *ovata* bloom in the northern Adriatic Sea during summer 2009: Ecology, molecular characterization and toxin profile. Marine Pollution Bulletin 62(11), 2512-2519.

Accoroni, S., Romagnoli, T., Pichierri, S., Colombo, F., Totti, C., 2012. Morphometric analysis of *Ostreopsis* cf. *ovata* cells in relation to environmental conditions and bloom phases. Harmful Algae 19, 15-22.

Aligizaki, K., Katikou, P., Milandri, A., Diogène, J., 2011. Occurrence of palytoxin-group toxins in seafood and future strategies to complement the present state of the art. Toxicon 57(3), 390-399.

Aligizaki, K., Katikou, P., Nikolaidis, G., Panou, A., 2008. First episode of shellfish contamination by palytoxin-like compounds from *Ostreopsis* species (Aegean Sea, Greece). Toxicon 51(3), 418-427.

Aligizaki, K., Nikolaidis, G., 2006. The presence of the potentially toxic genera *Ostreopsis* and Coolia (Dinophyceae) in the North Aegean Sea, Greece. Harmful Algae 5(6), 717-730.

Alldredge, A.L., Passow, U., Logan, B.E., 1993. The Abundance and Significance of a Class of Large, Transparent Organic Particles in the Ocean. Deep-Sea Research Part I-Oceanographic Research Papers 40(6), 1131-1140.

Amzil, Z., Sibat, M., Chomerat, N., Grossel, H., Marco-Miralles, F., Lemee, R., Nezan, E., Sechet, V., 2012. Ovatoxin-a and Palytoxin Accumulation in Seafood in Relation to *Ostreopsis* cf. *ovata* Blooms on the French Mediterranean Coast. Marine Drugs 10(2), 477-496.

Andersen, R.A., 2005. Algal Culturing Techniques. Elsevier/Academic Press.

Andree, K.B., Fernandez-Tejedor, M., Elandaloussi, L.M., Quijano-Scheggia, S., Sampedro, N., Garces, E., Camp, J., Diogene, J., 2011. Quantitative PCR Coupled with Melt Curve Analysis for Detection of Selected Pseudo-nitzschia spp. (Bacillariophyceae) from the Northwestern Mediterranean Sea. Applied and Environmental Microbiology 77(5), 1651-1659.

Bates, S. S. 1998. Ecophysiology and metabolism of ASP toxin production. In D. M. Anderson, A. D. Cembella and G. M. Hallegraeff [eds.], Physiological ecology of harmful algal blooms. Springer-Verlag. 405–426

Barone, R., 2007. Behavioural trait of *Ostreopsis ovata* (Dinophyceae) in Mediterranean rock pools: the spider's strategy. Harmful Algae News 33, 1–3.

Biré, R., Trotereau, S., Lemee, R., Delpont, C., Chabot, B., Aumond, Y., Krys, S., 2013. Occurrence of palytoxins in marine organisms from different trophic levels of the French Mediterranean coast harvested in 2009. Harmful Algae 28, 10-22.

Bravo, I., Vila, M., Casablanca, S., Rodriguez, F., Rial, P., Riobo, P., Penna, A., 2012. Life cycle stages of the benthic palytoxin-producing dinoflagellate *Ostreopsis* cf. *ovata* (Dinophyceae). Harmful Algae 18, 24-34.

Ciminiello, P., Dell'Aversano, C., Dello Iacovo, E., Fattorusso, E., Forino, M., Tartaglione, L., Battocchi, C., Crinelli, R., Carloni, E., Magnani, M., Penna, A., 2012. Unique Toxin Profile of a Mediterranean *Ostreopsis* cf. *ovata* Strain: HR LC-MSn Characterization of Ovatoxin-f, a New Palytoxin Congener. Chemical Research in Toxicology 25(6), 1243-1252.

Ciminiello, P., Dell'Aversano, C., Dello Lacovo, E., Fattorusso, E., Forino, M., Tartaglione, L., 2011. LC-MS of palytoxin and its analogues: State of the art and future perspectives. Toxicon 57(3), 376-389.

Ciminiello, P., Dell'Aversano,C., Dello Iacovo, E., Fatturosso, E., Forino, M., Grauso, L., Targlione, L., Guerrini, F., Pistocchi, R., 2010. Complex palytoxin-like profile of *Ostreopsis ovata*. Identification of four new ovatoxins by high-resolution liquid chromatography/mass spectrometry. Rapid Communication in Mass Spectrometry 24, 2735-2744.

Ciminiello, P., Dell'Aversano, C., Fattorusso, E., Forino, M., Tartaglione, L., Grillo, C., Melchiorre, N., 2008. Putative palytoxin and its new analogue, ovatoxin-a, in *Ostreopsis ovata* collected along the Ligurian coasts during the 2006 toxic outbreak. Journal of the American Society for Mass Spectrometry 19(1), 111-120.

Ciminiello, P., Dell'Aversano, C., Fattorusso, E., Forino, M., Magno, G.S., Tartaglione, L., Grillo, C., Melchiorre, N., 2006. The Genoa 2005 outbreak. Determination of putative palytoxin in Mediterranean *Ostreopsis ovata* by a new liquid chromatography tandem mass spectrometry method. Analytical Chemistry 78(17), 6153-6159.

Cohu, S., Thibaut, T., Mangialajo, L., Labat, J.P., Passafiume, O., Blanfune, A., Simon, N., Cottalorda, J.M., Lemee, R., 2011. Occurrence of the toxic dinoflagellate *Ostreopsis* cf. *ovata* in relation with environmental factors in Monaco (NW Mediterranean). Marine Pollution Bulletin 62(12), 2681-2691.

David, H., Laza-Martinez, A., Miguel, I., Orive, E., 2013. *Ostreopsis* cf. siamensis and *Ostreopsis* cf. *ovata* from the Atlantic Iberian Peninsula: Morphological and phylogenetic characterization. Harmful Algae 30, 44-55.

Granéli, E., Vidyarathna, N.K., Funari, E., Cumaranatunga, P.R.T., Scenati, R., 2011. Can increases in temperature stimulate blooms of the toxic benthic dinoflagellate *Ostreopsis ovata*? Harmful Algae 10(2), 165-172.

Grzebyk, D., Bechemin, C., Ward, C.J., Verite, C., Codd, G.A., Maestrini, S.Y., 2003. Effects of salinity and two coastal waters on the growth and toxin content of the dinoflagellate Alexandrium minutum. Journal of Plankton Research 25(10), 1185-1199.

Guerrini, F., Pezzolesi, L., Feller, A., Riccardi, M., Ciminiello, P., Dell'Aversano, C., Tartaglione, L., Dello Iacovo, E., Fattorusso, E., Forino, M., Pistocchi, R., 2010. Comparative growth and toxin profile of cultured *Ostreopsis ovata* from the Tyrrhenian and Adriatic Seas. Toxicon 55(2-3), 211-220.

Guillard, R.R.L., 1975. Culture of Phyto Plankton for Feeding Marine Invertebrates, Smith, Walter L. and Matoira H. Chanley, pp. 29-60.

Habermann, E., Ahnerthilger, G., Chhatwal, G.S., Beress, L., 1981. Delayed Hemolytic Action of Palytoxin General-Characteristics. Biochimica Et Biophysica Acta 649(2), 481-486.

Hall T, A., 1999. BioEdit, a user friendly biological sequence alignment editor and analysis program for Windows 95/98/NT. Nucleic Acids Symposium Series 41, 95-98.

Hallegraeff, G.M., 1988. Plankton: Microscopic World. E.J. Brill/Robert Brown.

Honsell, G., Bonifacio, A., De Bortoli, M., Penna, A., Battocchi, C., Ciminiello, P., Dell'Aversano, C., Fattorusso, E., Sosa, S., Yasumoto, T., Tubaro, A., 2013. New Insights on Cytological and Metabolic Features of *Ostreopsis* cf. *ovata* Fukuyo (Dinophyceae): A Multidisciplinary Approach. Plos One 8(2).

Hoshaw, R.W., Rosowski, J.R., 1973. Methods for Microscopic Algae, Stein, Janet R., pp. 53-67.

Hwang, B.S., Yoon, E.Y., Kim, H.S., Yih, W., Park, J.Y., Jeong, H.J., Rho, J.-R., 2013. Ostreol A: A new cytotoxic compound isolated from the epiphytic dinollagellate *Ostreopsis* cf. *ovata* from the coastal waters of Jeju Island, Korea. Bioorganic & Medicinal Chemistry Letters 23(10), 3023-3027.

IPCC, 2013. Climate Change 2013: The Physical Science Basis. Retrieved from http://www.buildingclimatesolutions.org/view/article/524b2c2f0cf264abcd86106 a.

Ismael, A., Halim, Y., 2012. Potentially harmful *Ostreopsis* spp. in the coastal waters of Alexandria - Egypt. Mediterranean Marine Science 13(2), 208-212.

Kang, N.S., Jeong, H.J., Lee, S.Y., Lim, A.S., Lee, M.J., Kim, H.S., Yih, W., 2013. Morphology and molecular characterization of the epiphytic benthic dinoflagellate *Ostreopsis* cf. *ovata* in the temperate waters off Jeju Island, Korea. Harmful Algae 27, 98-112.

Kimura, M. 1980., A simple method for estimating evolutionary rates of base substitutions through comparative studies of nucleotide sequences. Journal of Molecular Evolution 16, 111-120

Kruskopf, M., Flynn, K.J., 2006. Chlorophyll content and fluorescence responses cannot be used to gauge reliably phytoplankton biomass, nutrient status or growth rate. New Phytologist 169(3), 525-536.

Laza-Martinez, A., Orive, E., Miguel, I., 2011. Morphological and genetic characterization of benthic dinoflagellates of the genera Coolia, *Ostreopsis* and Prorocentrum from the south-eastern Bay of Biscay. European Journal of Phycology 46(1), 45-65.

Mangialajo, L., Ganzin, N., Accoroni, S., Asnaghi, V., Blanfuné, A., Cabrini, M., Cattaneo-Vietti, R., Chavanon, F., Chiantore, M., Cohu, S., Costa, E., Fornasaro, D., Grossel, H., Marco-Miralles, F., Masó, M., Reñé, A., Rossi, A.M., Sala, M.M., Thibaut, T., Totti, C., Vila, M., Lemée, R., 2011. Trends in *Ostreopsis* proliferation along the Northern Mediterranean coasts. Toxicon 57(3), 408-420.

Mangialajo, L., Bertolotto, R., Cattaneo-Vietti, R., Chiantore, M., Grillo, C., Lemee, R., Melchiorre, N., Moretto, P., Povero, P., Ruggieri, N., 2008. The toxic benthic dinoflagellate *Ostreopsis ovata*: Quantification of proliferation along the coastline of Genoa, Italy. Marine Pollution Bulletin 56(6), 1209-1214.

Monti, M., Cecchin, E., 2012. Comparative growth of three strains of *Ostreopsis ovata* at different light intensities with focus on inter-specific allelopathic interactions. Cryptogamie Algologie 33(2), 113-119.

Monti, M., Minocci, M., Beran, A., Ivesa, L., 2007. First record of *Ostreopsis* cfr. *ovata* on macroalgae in the Northern Adriatic Sea. Marine Pollution Bulletin 54(5), 598-601.

Nascimento, S.M., Corrêa, E.V., Menezes, M.n., Varela, D., Paredes, J., Morris, S., 2012a. Growth and toxin profile of *Ostreopsis* cf. *ovata* (Dinophyta) from Rio de Janeiro, Brazil. Harmful Algae 13, 1-9.

Nascimento, S.M., Franca, J.V., Goncalves, J.E.A., Ferreira, C.E.L., 2012b. *Ostreopsis* cf. *ovata* (Dinophyta) bloom in an equatorial island of the Atlantic Ocean. Marine Pollution Bulletin 64(5), 1074-1078.

Parsons, M.L., Aligizaki, K., Bottein, M.-Y.D., Fraga, S., Morton, S.L., Penna, A., Rhodes, L., 2012. Gambierdiscus and *Ostreopsis*: Reassessment of the state of knowledge of their taxonomy, geography, ecophysiology, and toxicology. Harmful Algae 14(0), 107-129.

Parsons, M.L., Preskitt, L.B., 2007. A survey of epiphytic dinoflagellates from the coastal waters of the island of Hawai'i. Harmful Algae 6(5), 658-669.

Penna, A., Fraga, S., Battocchi, C., Casabianca, S., Perini, F., Capellacci, S., Casabianca, A., Riobo, P., Giacobbe, M.G., Totti, C., Accoroni, S., Vila, M., Rene, A., Scardi, M., Aligizaki, K., Nguyen-Ngoc, L., Vernesi, C., 2012. Genetic diversity of the genus *Ostreopsis* Schmidt: phylogeographical considerations and molecular

methodology applications for field detection in the Mediterranean Sea. Cryptogamie Algologie 33(2), 153-163.

Penna, A., Fraga, S., Battocchi, C., Casabianca, S., Giacobbe, M.G., Riobo, P., Vernesi, C., 2010. A phylogeographical study of the toxic benthic dinoflagellate genus *Ostreopsis* Schmidt. Journal of Biogeography 37(5), 830-841.

Pezzolesi, L., Pistocchi, R., Fratangeli, F., Dell'Aversano, C., Dello Iacovo, E., Tartaglione, L., 2014. Growth dynamics in relation to the production of the main cellular components in the toxic dinoflagellate *Ostreopsis*. cf. *ovata.* Harmful Algae (36), 1-10.

Pezzolesi, L., Guerrini, F., Ciminiello, P., Dell'Aversano, C., Dello Iacovo, E., Fattorusso, E., Forino, M., Tartaglione, L., Pistocchi, R., 2012. Influence of temperature and salinity on *Ostreopsis* cf. *ovata* growth and evaluation of toxin content through HR LC-MS and biological assays. Water Research 46(1), 82-92.

Penna, A., Vila, M., Fraga, S., Giacobbe, M.G., Andreoni, F., Riobo, P., Vernesi, C., 2005. Characterization of *Ostreopsis* and Coolia (Dinophyceae) isolates in the western Mediterranean Sea based on morphology, toxicity and internal transcribed spacer 5.8s rDNA sequences. Journal of Phycology 41(1), 212-225.

Pfannkuchen, M., Godrijan, J., Pfannkuchen, D.M., Ivesa, L., Kruzic, P., Ciminiello, P., Dell'Aversano, C., Dello Iacovo, E., Fattorusso, E., Forino, M., Tartaglione, L., Godrijan, M., 2012. Toxin-Producing *Ostreopsis* cf. *ovata* are Likely to Bloom Undetected along Coastal Areas. Environmental Science & Technology 46(10), 5574-5582.

Pin, L.C., Teen, L.P., Ahmad, A., Usup, G., 2001. Genetic diversity of *Ostreopsis ovata* (Dinophyceae) from Malaysia. Marine Biotechnology 3(3), 246-255.

Pistocchi, R., Pezzolesi, L., Guerrini, F., Vanucci, S., Dell'Aversano, C., Fattorusso, E., 2011. A review on the effects of environmental conditions on growth and toxin production of *Ostreopsis ovata*. Toxicon 57(3), 421-428.

Raven, J.A., Beardall, J., 2006. Chlorophyll fluorescence and ecophysiology: seeing red? New Phytologist 169(3), 449-451.

Rhodes, L.L., Smith, K.F., Munday, R., Selwood, A.I., McNabb, P.S., Holland, P.T., Bottein, M.-Y., 2011. Toxic dinoflagellates (Dinophyceae) from Rarotonga, Cook Islands. Toxicon 56(5), 751-758.

Riobó, P., Franco, J.M., 2011. Palytoxins: Biological and chemical determination. Toxicon 57(3), 368-375.

Riobó, P., Paz, B., Franco, J.M., Vazquez, J.A., Murado, M.A., 2008. Proposal for a simple and sensitive haemolytic assay for palytoxin Toxicological dynamics, kinetics, ouabain inhibition and thermal stability. Harmful Algae 7(4), 415-429.

Sato, S., Nishimura, T., Uehara, K., Sakanari, H., Tawong, W., Hariganeya, N., Smith, K., Rhodes, L., Yasumoto, T., Taira, Y., Suda, S., Yamaguchi, H., Adachi, M., 2011. Phylogeography of *Ostreopsis* along West Pacific Coast, with Special Reference to a Novel Clade from Japan. Plos One 6(12).

Scalco, E., Brunet, C., Marino, F., Rossi, R., Soprano, V., Zingone, A., Montresor, M., 2012. Growth and toxicity responses of Mediterranean *Ostreopsis* cf. *ovata* to seasonal irradiance and temperature conditions. Harmful Algae 17, 25-34.

Schmidt, I., 1901. Flora of Koh Chang, contributions to the knowledge of the vegetation in the Gulf of Siam Peridinales. Botanisk Tidkrift 24, 25-34.

Silva, E.S., Faust, M.A., 1995. Small-Cells in the Life-History of Dinoflagellates (Dinophyceae) - a Review. Phycologia 34(5), 396-408.

Suzuki, T., Watanabe, R., Uchida, H., Matsushima, R., Nagai, H., Yasumoto, T., Yoshimatsu, T., Sato, S., Adachi, M., 2012. LC-MS/MS analysis of novel ovatoxin isomers in several *Ostreopsis* strains collected in Japan. Harmful Algae 20, 81-91.

Tanimoto, Y., Yamaguchi, H., Yoshimatsu, T., Sato, S., Adachi, M., 2013. Effects of temperature, salinity and their interaction on growth of toxic *Ostreopsis* sp 1 and *Ostreopsis* sp 6 (Dinophyceae) isolated from Japanese coastal waters. Fisheries Science 79(2), 285-291.

Totti, C., Accoroni, S., Cerino, F., Cucchiari, E., Romagnoli, T., 2011. *Ostreopsis ovata* bloom along the Conero Riviera (northern Adriatic Sea): Relationships with environmental conditions and substrata. Harmful Algae 9(2), 233-239.

Utermöhl H., 1958. Zur Vervollkomnung der quantitativen Phytoplankton-Methodik. Mitteilungen. Internationale Vereiningung fuer Theoretische und Angewandte Limnologie 9, 1-38.

Utermöhl. H., 1931. Neue Wege in der quantitativen Erfassung des Planktons (mit besonderer Berücksichtigung des Ultraplanktons). Verhandlungen der Internationalen Vereinigung für Theoretische und Angewandte Limnologie 5, 567-596.

Vanucci, S., Guerrini, F., Pezzolesi, L., Dell'Aversano, C., Ciminiello, P., Pistocchi, R., 2012a. Cell growth and toxins' content of *Ostreopsis* cf. *ovata* in presence and absence of associated bacteria. Cryptogamie Algologie 33(2), 105-112.

Vanucci, S., Pezzolesi, L., Pistocchi, R., Ciminiello, P., Dell'Aversano, C., Dello Iacovo, E., Fattorusso, E., Tartaglione, L., Guerrini, F., 2012b. Nitrogen and phosphorus limitation effects on cell growth, biovolume, and toxin production in *Ostreopsis* cf. *ovata*. Harmful Algae 15, 78-90.

Vidyarathna, N.K., Graneli, E., 2013. Physiological responses of *Ostreopsis ovata* to changes in N and P availability and temperature increase. Harmful Algae 21-22, 54-63.

Vidyarathna, N.K., Granéli, E., 2011. Influence of temperature on growth, toxicity and carbohydrate production of a Japanese *Ostreopsis ovata* strain, a toxic-bloom-forming dinoflagellate. Aquatic Microbial Ecology 65(3), 261-270.

Vila, M., Garces, E., Maso, M., 2001. Potentially toxic epiphytic dinoflagellate assemblages on macroalgae in the NW Mediterranean. Aquatic Microbial Ecology 26(1), 51-60.

Yamaguchi, H., Tanimoto, Y., Yoshimatsu, T., Sato, S., Nishimura, T., Uehara, K., Adachi, M., 2012a. Culture method and growth characteristics of marine benthic

dinoflagellate *Ostreopsis* spp. isolated from Japanese coastal waters. Fisheries Science 78(5), 993-1000.

Yamaguchi, H., Yoshimatsu, T., Tanimoto, Y., Sato, S., Nishimura, T., Uehara, K., Adachi, M., 2012b. Effects of temperature, salinity and their interaction on growth of the benthic dinoflagellate *Ostreopsis* cf. *ovata* (Dinophyceae) from Japanese coastal waters. Phycological Research 60(4), 297-304.

CHAPTER 4

Ostreopsis cf. *ovata* dynamics in the NW Mediterranean Sea in relation to biotic and abiotic factors

4.1. Abstract

An expansion of the distribution of *Ostreopsis* cf. *ovata*, a dinoflagellate which produces palytoxin-like compounds, has been reported in recent years. Economical and social interests are affected by blooms which are responsible for respiratory and skin problems in humans and may cause damage to marine organisms. In order to identify the most influential environmental factors that trigger proliferations of *O.* cf. *ovata* in the adjacent shallow rocky coast area of the Ebro Delta, NW Mediterranean Sea, a three-year survey on the epi-benthic microalgae community on the macrophyte *Jania rubens* was performed. Small-size diatoms were more abundant than dinoflagellates; *O.* cf. *ovata* was identified as the only species present from the genus. Temperature, salinity and wind speed had a strong impact on defining the ecological niche of benthic microalgae. Freshwater and groundwater fluxes were more pronounced in southern than in northern sites, possibly derived in a distinct *O.* cf. *ovata* spatial distribution; with highest abundances and bloom frequency in the north. Weak negative correlations between the abundance of *O.* cf. *ovata* and nitrate and silicate concentrations and positive correlation with salinity was observed. The temporal pattern of *O.* cf. *ovata* dynamics from mid-July to early-November is probably due to the fact that this species is observed only above a certain temperature threshold. Epiphytic *O.* cf. *ovata* cells were smaller in the northern site than in the south, coinciding with higher abundance, and this could be an indicator of favorable conditions as a result of an increase in cell division. Toxicity in planktonic cells was negatively correlated with cell abundance in water column; achieving maximum concentrations of 25 pg PLTX eq·cell^{-1}.

4.2. Introduction

An increase in the frequency, intensity and dispersion of Harmful Algal Blooms (HABs), has been reported in recent decades (Hallegraeff, 2010). Of special concern are the epibenthic dinoflagellates from tropical regions present in ciguatera endemic areas (Tindall *et al.,* 1989). Among them, two species from the genus *Ostreopsis*; *O.* cf. *ovata* (Fukuyo) and *O.* cf. *siamensis* (Schmidt), are widely distributed in temperate areas (Rhodes *et al.,* 2011) such as the north of the Mediterranean Sea, where periodic toxic outbreaks have been described in recent years along expansive areas of the coast (Mangialajo *et al.,* 2011). Economical and social interests are affected due to the presence of these two species are a cause of respiratory and skin problems in humans (Tubaro *et al.,* 2011); mortalities in marine organisms (Simoni *et al.,* 2003; Totti *et al.,* 2010) have also been associated with their proliferations. The morphological features of these two species, shape, size and plate pattern, are very similar and this makes them very difficult to be distinguished by light microscopy (Penna *et al.,* 2005). In order to assess this problematic circumstance recent studies have coupled molecular analysis with microalgae surveys to perform

a more accurate identification (Parsons *et al.,* 2012). In the north Mediterranean Sea, one of the best studied areas for *Ostreopsis* spp., genetic studies have been conducted in field samples in order to characterize species composition during *Ostreopsis* spp. blooms. In the Ligurian and Adriatic Seas, as well as in the Gulf of Lion, *O.* cf. *ovata* has been detected as the only genotype, while along the north coast of Catalonia (Mangialajo *et al.,* 2011), and in Pesaro, in the Adriatic Sea (Battocchi *et al.,* 2010), this species has been identified together with *O.* cf. *siamensis* but the latter being in lower abundance. Recent studies have developed molecular methods through real-time PCR (qPCR) that allow to detect and quantify *Ostreopsis* spp. in water samples (Perini *et al.,* 2011; Hariganeya *et al.,* 2013), mussels (Furlan *et al.,* 2013) and marine aerosols (Casabianca *et al.,* 2013). Thus, the support of alternative molecular methods would allow the unequivocal characterization of the *Ostreopsis* community. The importance of this discrimination lies on the distinct toxicological profile of each species. *O.* cf. *ovata* strains from different areas of the Mediterranean Sea have been identified as PLTX-like analogue producers (Ciminiello *et al.,* 2012; Pfannkuchen *et al.,* 2012; Brissard *et al.,* 2014; Carnicer *et al.,* submitted), while, *O.* cf. *siamensis* has been described as not toxic (Ciminiello *et al.,* 2013).

Global change, reflected amongst other symptoms in global warming and increasing eutrophication of coastal waters during the last century, is deteriorating coastal marine ecosystems (Waycott *et al.,* 2009). Their effect on benthic microalgae dynamics could differ since it has been suggested that warming may have complex synergistic effects with other environmental factors (Reise *et al.,* 2008). Understanding theses dynamics has become a challenge as natural parameters influencing *O.* cf. *ovata* blooms are still ambiguous, to a certain extent, due to scarce field studies (Pistocchi *et al.,* 2011) and controversial results obtained in experimental settings. Among the most important physic-chemical parameters that may determine benthic microalgae distribution, are water temperature, salinity, hydrodynamics, nutrient concentrations, type of substrate, light, presence of grazers and competition (Fraga *et al.,* 2012).

A considerable number of studies in the Mediterranean Sea pointed out that seawater temperature is the major factor that drives *O.* cf. *ovata* growth (Pistocchi *et al.,* 2011) taking into account that in most locations its presence is limited to summer and fall (Aligizaki & Nikolaidi, 2006; Totti *et al.,* 2010; Mangialajo *et al.,* 2008; Cohu *et al.,* 2013). David *et al.,* (2012) proposed that it is actually the duration of a certain temperature threshold that could exert more influence on *Ostreopsis* sp. growth. In any case, different optimal growth temperature ranges in laboratory experiments (e.g. Granéli *et al.,* 2011 and Pezolessi *et al.,* 2012) and disparity in temperatures that lead to the onset of bloom in different areas (Pistocchi *et al.,* 2011) raise the issue of the role of temperature during the proliferation period. Salinity has been suggested to interact with high temperature values in experimental conditions, increasing (Yamaguchi *et al.,* 2012) or decreasing (Carnicer

et al., submitted) growth rate. As far as hydrodynamism is concerned, due to the difficulty of quantification, the number of studies in the Mediterranean Sea is scarce. It is likely though that *O.* cf. *ovata* has a preference for moderate wave exposure (Vila *et al.,* 2001a; Cohu *et al.,* 2013). Although Accoroni *et al.,* (2011), found higher *O.* cf. *ovata* abundances in sheltered areas, further investigation should be conducted to confirm this habitat preference. Due to the scarce available data a direct relationship of *Ostreopsis* spp. distribution with nutrient loading cannot be made. Laboratory studies revealed a negative effect in *O.* cf. *ovata* growth under N-limited cultures (Vannucci *et al.,* 2012b; Vidyarathna & Granéli., 2013), whereas no pattern (Vila *et al.,* 2011a; Accoroni *et al.,* 2011; Cohu *et al.,* 2011), or slightly negative correlation of *O.* cf. *ovata* growth with nitrates was observed in field studies (Cohu *et al.,* 2013). There are no references about predation on *O.* cf. *ovata* but it is expected that benthic organisms that feed on macrophytes may alter microalgae population (Fraga *et al.,* 2012). The presence of associated bacteria was also investigated not finding any influence neither in growth or toxin content of *O.* cf. *ovata* cells (Vanucci *et al.,* 2012a).

An additional factor to take into account would be the relation with other microalgae present in the epiphytic community as competition may exist for substrate colonization, light or nutrients (Legrand *et al.,* 2003). A similar benthic microalgae community has been observed in different areas and substrates along the Mediterranean coast and is composed of diatoms that usually dominate dinoflagellates (Totti *et al.,* 2007); with the most frequent species in this group being *O.* cf. *ovata*, *Prorocentrum lima*, and *Coolia monotis* depending on the time of the year. In field observations, Cohu & Lemée, (2012) suggested that competition among them could be the reflection of environmental parameters involving in vertical distribution, among these parameters light being dominant. Monti & Cecchin, (2012) found a weak allelophatic effect between *P. minimum*, *C. monotis* and *Coscinodiscus granii* in laboratory experiments under different light intensities. The definition of ecological niches in the epi-benthic microalgae community could guide us to precisely define which factors have more weight in the spatial and temporal distribution of *O.* cf. *ovata* (Cohu *et al.,* 2013).

The response of microalgae to environmentally unfavorable conditions may be reflected in physiological and biochemical adaptations such as variation in surface area to volume ratio, mixotrophy, allelopathy or production of toxins, among others (Legrand *et al.,* 2003). Thus, it is important to consider alterations on microalgae cells in the study of their dynamics, especially in the case of toxic dinoflagellates whose responses may have an impact on humans and benthic ecosystems. Little is known about the influences on the morphometry of cells in field observations. In Accoroni *et al.,* (2011), higher amount of larger cells were found in exposed areas, resulting in unfavorable growth, suggesting that small cells contribute to a rapid growth by active division. This result is in agreement with laboratory findings under

nutrient-limited conditions where the amount of small cells was more abundant in favorable growth conditions (Vanucci *et al.,* 2012b; Vydyarathna & Granéli, 2013). Variability in cell size has been commonly observed in the field (Penna *et al.,* 2005; Aligizaki & Nikolaidis 2006; Accoroni *et al.,* 2012) and culture populations (Guerrini *et al.,* 2010; Scalco *et al.,* 2012; Vanucci *et al.,* 2012a; Vanucci *et al.,* 2012b; Pezzolesi *et al.,* 2012; Bravo *et al.,* 2012; Carnicer *et al.,* submitted). Different morphotypes in *O.* cf *ovata* have been described by Accoroni *et al.,* (2014) including small cells whose role are still under discussion; they were described as gametes or vegetative cells. Two kinds of dark motile cysts have been characterized as well, and were still capable of germination after five months storage in culture media. Toxicity of *O.* cf *ovata* has been studied in Mediterranean strains under stress conditions to assess its' relation with environmental factors and growth. Higher toxin content was detected under growth conditions unfavorable in regards to temperature (Pezzolesi *et al.,* 2012; Granéli *et al.,* 2011), and nutrient concentrations (Vannucci *et al.,* 2012a; Vydyaranthna & Granéli., 2011).

Our sampling location covers the two coastal areas adjacent to the Ebre Delta (north and south), the most important shellfish harvesting area in Catalonia (Vila *et al.,* 2001b). The Ebre Delta includes two bays, Fangar at the north and Alfacs at the south of the Ebre river mouth, where discharge channels from rice fields in the Ebre Delta drain nutrient-rich freshwater into the bays. Additionally variations in groundwater influx throughout the year have to be considered. Therefore, these coastal areas present special peculiarities interesting for the study of microalgae distribution since multiple factors vary in a relatively small spatial scale. This study has been designed to describe the biotic and abiotic factors influencing *O.* cf. *ovata* blooms and gain information for the future development of predictive models. Particularly, we address our study to i) Identification of *Ostreopsis* species present in the area. ii) Determination of the ecological niche of epi-benthic microalgae associated with *O.* cf. *ovata*, iii) Characterization of the role of temperature, salinity and hydrodynamics, as well as identification of the effects of nutrient inputs, influencing microalgae assemblages, during the period of blooms iv) Evaluation of the physiological effects of these factors on morphology and toxicity.

4.3. Materials and Methods

4.3.1. Sampling sites and methodology

The study was carried out in the northern and southern coastal waters adjacent of the Ebre Delta (NW Mediterranean, in Catalonia, Spain). A total of 8 sampling sites were distributed between 15 km north of Fangar Bay and 15 km south of Alfacs Bay. In the north and the south, distance between sites ranged from 1.5 to 4 km (Figure 4.1). Sampling sites were characterized by shallow depths and rocky substrate where macroalgae grow.
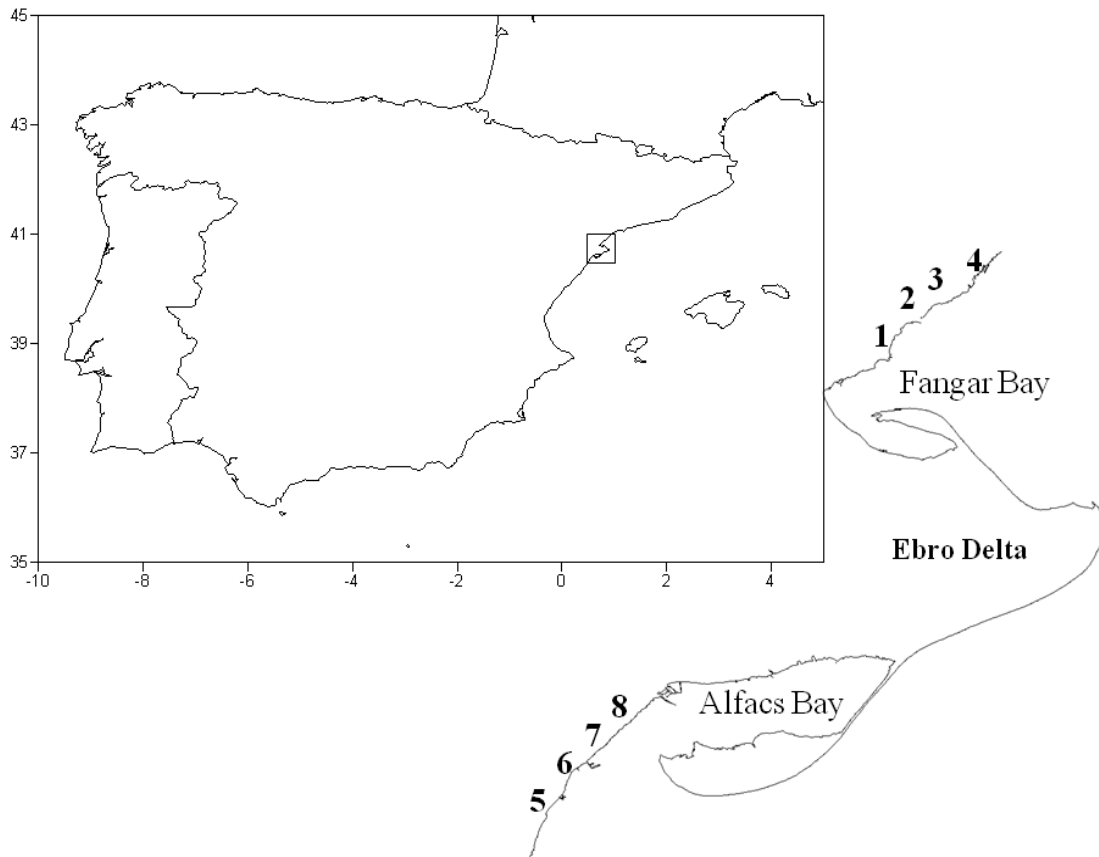
Fig. 4.1. Sampling sites.

The epiphytic microalgae community was quantified on two species of macroalgae (*Jania rubens* and *Corallina elongata* when not available) collected approximately at 0.5 meter depth. Sampling was performed from August 2011 to October 2013; the frequency was weekly during the months when *O.* cf. *ovata* bloom formation is more likely, biweekly during two months before and after this period and monthly the rest of the year. A total of 423 samples were analyzed for identification and enumeration of microalgae during the experimental period. Macroalgae were placed delicately in a plastic bottle containing 200 mL of filtered seawater. In order to release the epiphyte community from macroalgae, bottles were intensively shaken for one minute and water was filtered through a 200 μm mesh to eliminate larger particles and organisms constituting the "epiphytic sample". Half of the resulting water was fixed with 3% Lugol's solution for cell counting and, from July to September 2012 and July to October 2013, for DNA extraction. Additionally, previous to the collection of macroalgae, a sample of the adjacent water column was taken for different purposes; 100 mL were fixed with 3% Lugol's solution to evaluate abundance of *Ostreopsis* planktonic cells; 15 mL were stored at -20°C for nutrient analysis; and 1 liter was filtered for chlorophyll a (Chl a) quantification. Another 2 liters of the adjacent water column were sampled for analysis of content of PLTX-like compounds during *O.* cf. *ovata* blooms in sites 3 and 6. Surface

temperature, salinity and dissolved oxygen were measured *in situ* using a portable multi-sensor probe, CTD (YSI 556 MPS).

4.3.2. *Molecular analysis and Quantitative PCR (qPCR)*

A total of 133 DNA extractions were performed from the "epiphytic sample" following the protocol of Andree *et al.,* (2011). Samples were 100 fold diluted to improve reproducibility among replicates. Two analyses were performed for each sample on an ABI 7300 in 20 µL volume, using two species-specific primers from *O.* cf. *ovata* and *O.* cf. *siamensis* designed in the 5.8S rDNA-ITS regions (Battocchi *et al.,* 2010). Amplification detection and melt curve analysis were performed in duplicate in final reaction volume of 20 µL that contained 10 µL of SYBR Green (2X) and primers (final concentration 0.5 µM) and 2 µL of 1:100 diluted field sample extracts. The qPCR conditions included 45 cycles following a standard three-step protocol of 94°C for 20 s followed by primer annealing at 54°C for 30 s and extension at 72°C for 30 s. The thermal profile for melt curve determination began with incubation of 1 min at 60°C with a gradual increase in temperature (1°C/15s) to 95°C, during which time, changes in fluorescence were monitored.

A previous analysis with strains IRTA-SMM-11-10 *O.* cf. *ovata* and VGO978 *O.* cf. *siamensis* DNA were used to optimize and demonstrate the specificity of each primer set.

4.3.3. *Microalgae abundance estimation*

For cell abundance estimation enumeration, fixed water samples were settled in Utermöhl chambers (Utermöhl, 1958). Planktonic samples were settled in 50 mL for 24 hours and "epiphytic samples" in 3 mL chamber for 3 hours. Counting was performed under an inverted microscope (Leica DM-IL). The entire bottom of the chamber was scanned at 100 x magnification to enumerate the larger organisms, and one/two transects or five/ten fields at 200-400 x magnification were examined to count the small and more abundant organisms. The epiphytic microalgae community was described at the genus level for diatoms of the genera *Grammatophora* (Ehrenberg), *Pleurosigma* (Smith)*, Coscinodiscus* (Ehrenberg), and *Licmophora* (Agardh). The rest of diatom genera were counted collectively. Enumeration of dinoflagellates was focused on potential toxic species; *O.* cf*. ovata*, *Coolia monotis* (Meunier), *Prorocentrum lima* (Ehrenberg), and *Amphidinium* sp. (Claperède & Lachmann).

Water column cell estimation was directed to *O.* cf. *ovata* exclusively. Cell abundance was expressed as number of individual cells per gram of fresh weight of macrophyte (cell.g fwm^{-1}) for "epiphyte samples" and cells per liter (cell.L^{-1}) for planktonic samples.

4.3.4. Chorophyll-a, nutrient analysis

One liter of water column was filtered on Whatman GF/F filters and kept at -80°C until Chl a analysis, minimum 24 hours. Filters were placed in acetone 90% for 6-10 hours, following the protocol of Jeffrey and Humphrey, (1975). Absorbance was measured with Shimadzu UV240 spectophotometer for samples until October 2011 and with Triligy ™ Laboratory fluorometer (Turner Desings) until the end of the sampling.

Seawater nutrients were analyzed during the presence of *O.* cf. *ovata* in the epiphyte community, a total of 268 samples. Nitrate, nitrite, phosphate and silicate analyses were performed following the protocol of Grasshoff, (1999), and ammonia according to Kérouel and Aminot, (2008). Samples were sent to CEAB-CSIC (Centre d'Estudis Avançats del Mediterrani, Blanes, Spain) for these analyses.

4.3.5. Meteorological data

Climate data were kindly provided by the Catalonian Meteorological Service (meteocat). The stations belong to the network of automatic meteorological stations (XEMA), integrated in the meteorological equipment of the Catalonian Government (Xemec). They are located in Alcanar (40° 32' 15.4314" N; 0° 29' 53.4732"W) for the southern sites and in el Perelló (40° 52' 29.0202"N; 0° 42' 56.1636"W) for the northern sites. These data include climatic variables related to mean day temperature, precipitation (mm rainfall. day^{-1} average accumulation), and wind speed (m. s^{-1}) collected at 10 meters height in el Perelló station and at 2 meters height at Alcanar station. Data are the average of mean daily values of one week. Correction of rugosity was applied for Alcanar station through the following equation:

$$—$$

where v_n is wind speed (m. s^{-1}) at n meters, and *p* is Hellman index, 0.14 in our case (flat lands).

4.3.6. Cell size of Ostreopsis cf. ovata

Dorso-ventral (DV) and width (W) diameters of *O.* cf. *ovata* cells from epiphytic and planktonic samples from sites 3 and 6 were measured using an image capture system (MCID™ Analysis) with an Olympus DP70 camera connected to a Nikon Eclipse TE2000-S inverted microscope at 400x magnification. A minimum of 40 cells were measured in each sample. Cell dimensions were expressed by mean ± Standard Deviation (SD). A total of 2306 epiphytic and 524 planktonic cells were measured.

4.3.7. Toxin extraction and Haemolytic assay

Toxin content of the water column was analyzed from 2 liter samples. Cells were collected by filtration on 0.45 μm nylon filters and stored at -80°C. For toxin extraction, 5 mL methanol/water (80:20) solution was added to filters and these were sonicated for 20 minutes in pulse mode. The mixture was centrifuged at 600 x g for 10 minutes; the supernatant was decanted and filtered using 0.45 μm polytetrafluoroethylene membrane syringe filters. This procedure was repeated twice and filtered supernatants were pooled. The final extract was evaporated and made up to a final volume of 10 mL.

Haemolytic activity of *O.* cf. *ovata* strains was analyzed following the method of Riobó *et al.,* (2008) with slight modifications regarding concentration of reagents in order to adjust the working range and the calibration curve. Haemoglobin released in presence of PLTX-like compounds after cell lysis, was quantified using a microplate Reader KC4 from BIO-TEK Instruments, Inc. (Vermont) at 405 nm absorbance. A calibration curve was prepared using PLTX standard (Wako Chemicals GmbH, Germany) with 12 concentrations from 12.5 to 1250 pg·mL^{-1} adjusted to an exponential regression using SigmaPlot 9.0. Working solution was prepared with washed sheep blood (OXOID), centrifuged twice (400 x g, 10°C, 10 min) and diluted with phosphate buffered saline solution (PBS) 0.01 M, pH 7.4 (Sigma), 0.1% bovine serum albumin (BSA), 1 mM calcium chloride (CaCl$_2$ 2H$_2$O) and 1 mM boric acid (H$_3$BO$_3$) to a final concentration of 1.5 x 10^6 cells·mL^{-1}. The assay for PLTX specificity was verified by a blank assay with ouabain (2 mM final concentration). Microalgae extracts, from two liters of the water column, and PLTX standard were evaporated and refilled with PBS solution to eliminate methanol and water from the extraction. The assay was performed in two non-treated 96 well microplates and samples were analyzed in triplicate. After 22 hours incubation at 24°C, microplates were centrifuged (416 x g, 10 min), 200 μL of the supernatant was transferred to another microplate for absorbance reading. Total toxicity was expressed as palytoxin equivalents per cell (pg PLTX eq·cell^{-1}) related to the number of cells contained in the culture.

4.3.8. Data analysis

Variations in nutrients concentration were statistically studied by the analysis of variance (ANOVA). Results are reported as follow: *F*(degrees of freedom) =*F*-value, *MSE*= mean-square error, *p*-value. For significant differences (*p*<0.05), a multiple comparison Tukey's HSD test was performed. Spearman correlation test was computed to assess the relationship between physic-chemical factors and PLTX-like compounds with *O.* cf. *ovata* cell abundances. Statistic analyses were done with IBM SPSS Statistics software package.

A principal component analysis (PCA), using R v2.8.1 (R Development Core Team 2005), based on physic-chemical factors: temperature, salinity, irradiance,

dissolved oxigen, Chl a, wind speed and direction, was performed to summarize in a reduced number of dimensions the environmental conditions of the ecosystem studied. To characterize the environmental occupancy of each species, we carried out an Outlying Mean Index analysis (OMI) (Doledec *et al.,* 2000) based on the PCA analysis done with the environmental variables. This multivariate technique determines the ecological niche by calculating the distance between the average habitat conditions used by a particular species and the average habitat conditions of a sampling area. The statistically significance of the marginality of each species was tested by a random permutation test with 10 000 permutations. The frequency of random permutations with values greater than the observed marginality was used as an estimated probability of rejecting the null hypothesis that the environmental gradient does not constrain species distribution.We transformed the species abundances into $\log_{10}(x+1)$ to reduce the effect of dominant species.

4.4. Results

4.4.1. *Effects of environmental variables*

Coastal seawater of the area adjacent to the Ebre Delta is influenced by direct groundwater and freshwater inputs from the river, part of which is used in rice fields and managed according to agricultural practices. Due to the significant addition of freshwater into this coastal ecosystem, our study sites represent a very interesting area to study microalgae population dynamics. The first three axes of the PCA explained 66.27% of the variability (PCA1: 33.9, PCA2: 17.8, and PCA3: 14.5). First axis segregates water samples with higher temperatures and most irradiated in summer months from those with higher winds from the north direction in winter months. Positive values of PCA2 are related with higher salinities, while negative values were associated with higher Chl a and dissolved oxygen values. This situation highlights a gradient of freshwater influence in which the higher Chlorophyll a concentration is influenced from freshwater (Figure 4.2). Finally, PCA3 axis segregates waters with higher Chl a concentration from those with higher oxygen content.
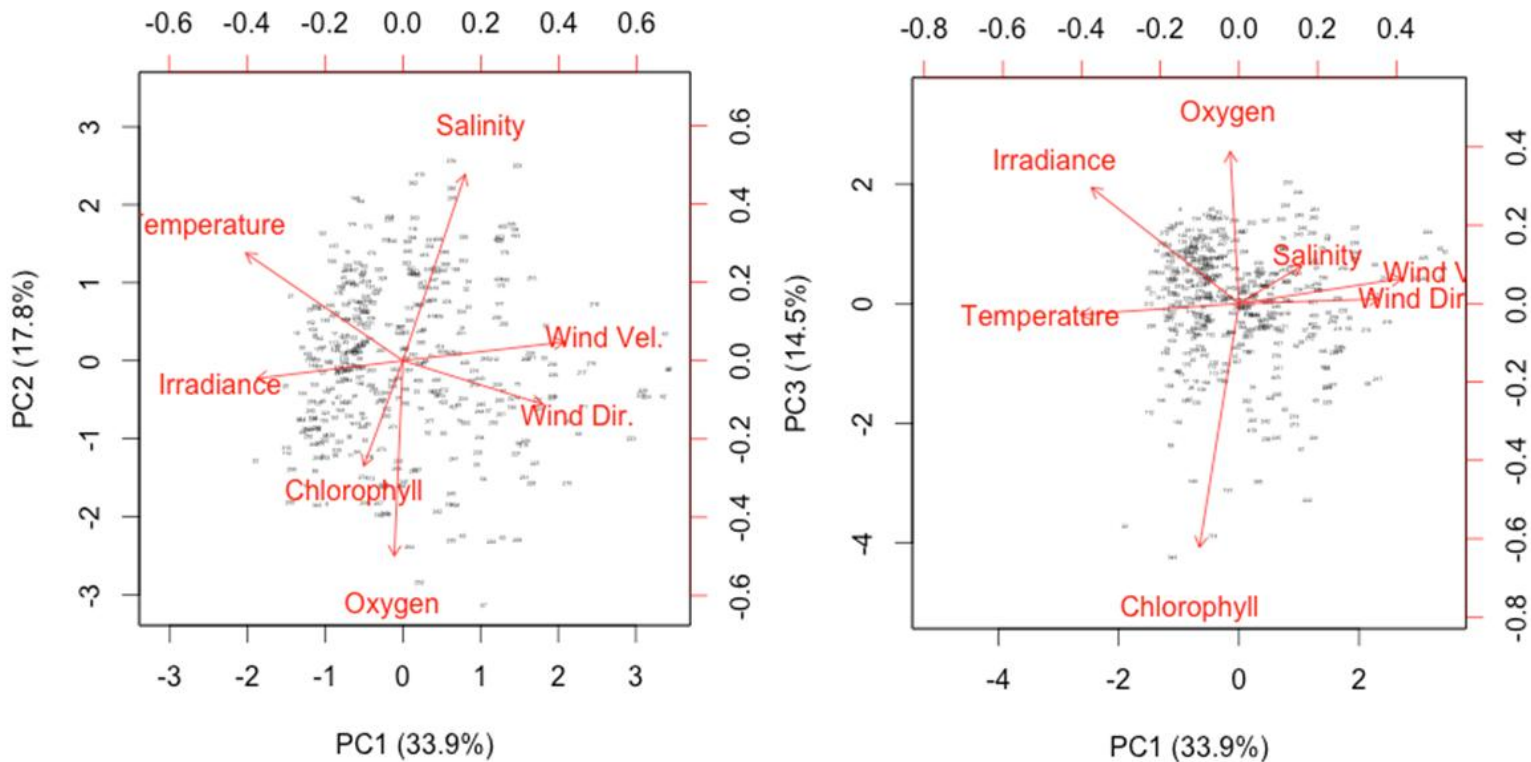
Fig. 4.2. OMI PCA of environmental parameters: Temperature, Salinity, Wind speed (Wind Vel) and direction (Wind Dir), Chlorophyll a, dissolved oxygen, Irradiance). Axis 1 = 33.9%, Axis 2 = 17.8%, Axis 3 = 14.5% of total variance

4.4.2. Meteorological and physical factors

We studied wind speed as an indicator of wave exposure influencing, among other parameters, water hydrodynamism. We found significantly ($F(1)$ =548.24, MSE= 1257.03, p<0.001) higher wind speed in the north (mean=2.43±1.82 m.s^{-1}) compared with the south (mean=1.00±0.47 m.s^{-1}).

No differences were found either for Chl a (max= 7.31; min=0; mean=0.84±0.98 µg.L^{-1}), dissolved oxygen (max=133; min=51.8; mean=89.87 ± 10.81) or irradiance in a regional and temporal scale. Seawater temperature followed a marked seasonal pattern; values ranged from 7.59 to 28.77°C. Differences in salinity were significant between the north (36.96±1.88) and the south (34.15±2.77) ($F(1)$ =149.56, MSE= 831.8, p<0.001), ranging from 23.03 to 39.35. Lower salinities were found in sites closer to the Delta. Site 8 registered the lowest values (31.19±2.06), different from all the other sampling sites (Tukey test).

4.4.3. Nutrients

In order to understand more deeply the interactions between environmental factors that trigger *O.* cf. *ovata* blooms, we analyzed seawater nutrients in 2011 from August to October and in 2012 and 2013, from July to October, coinciding with the presence of *O.* cf. *ovata* in the epiphytic community. We performed a PCA analysis with these data (Figure 4.3). The first two axis explained 68.7% of the variability (PCA1: 41.2% and PCA2: 27.5%). Nitrate and silicate were found together and nitrite was associated with phosphate.This analysis reflects a spatial separation between north and south regarding nutrient concentrations, as it has been found for salinity.
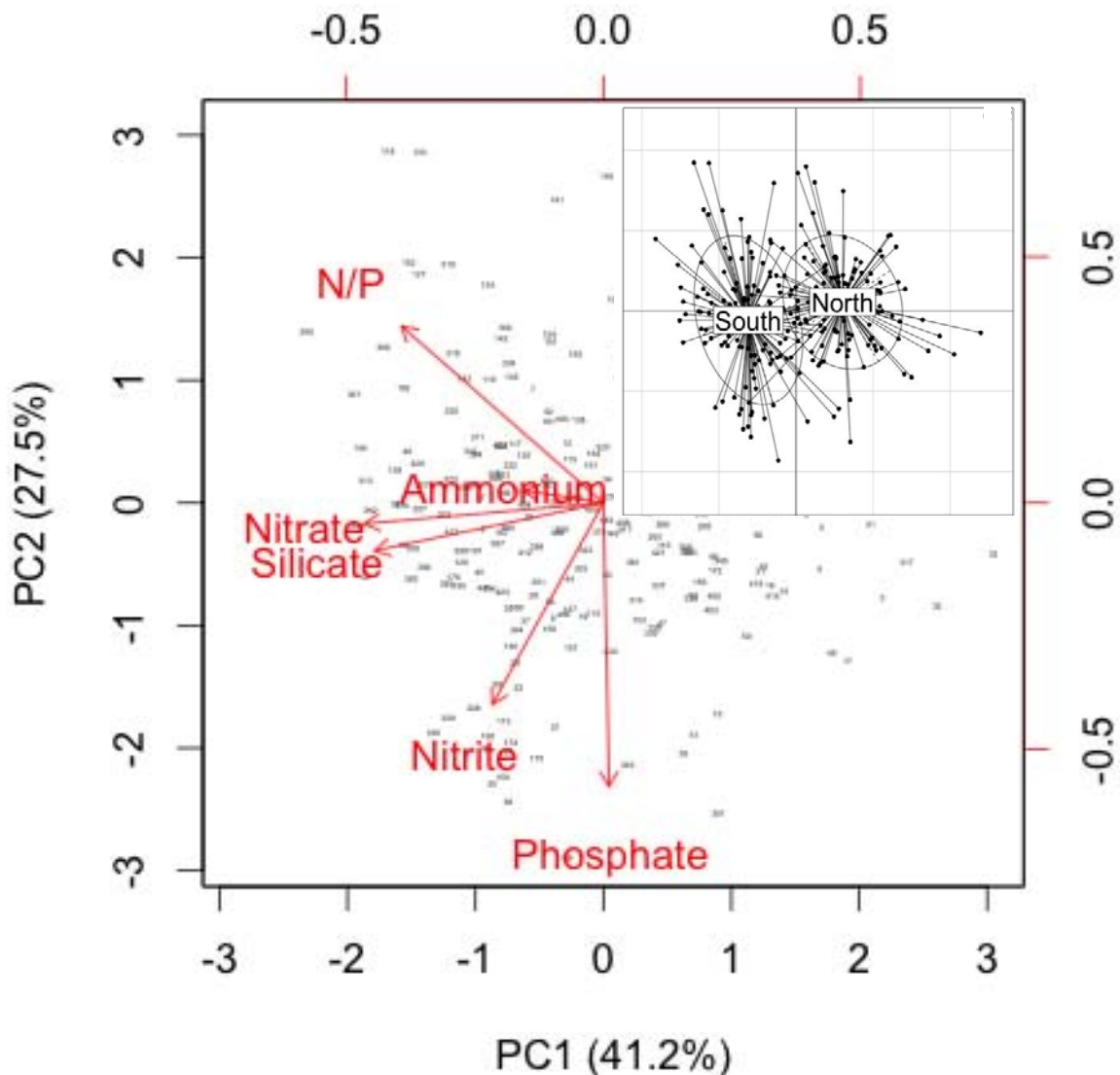
Fig. 4.3. Principal component analysis based on nutrient concentration (nitrate; nitrite; phosphate; ammonia; silicate, N:P ratio).

More precisely, there was significant enrichment of a nitrate ($F(7) = 50.14$, $MSE= 1549.74$, $p<0.001$) and silicate ($F(7) = 61.38$, $MSE= 943.45$, $p<0.001$) in the southern sampling sites ($NO_3^- = 12.54 \pm 9.13$ µmol l^{-1}; $Si = 10.25 \pm 6.93$) in comparison with the northern sites ($NO_3^- = 1.36 \pm 0.92$ µmol l^{-1}; $Si = 2.40 \pm 1.86$). For phosphates, nitrites, ammonia and N:P ratio, no significant differences were found among sites (mean values: $PO_3^{4-} = 0.21 \pm 0.28$; $NH_3^+ = 3.78 \pm 3.80$; $NO_2^- = 0.18 \pm 0.12$). Values are represented in Figure 4.4, together with Chloroplyll a and dissolved oxygen. Salinity, nitrate and silicate concentrations and salinity values during the three years in sampling sites are represented in Figure 4.5.
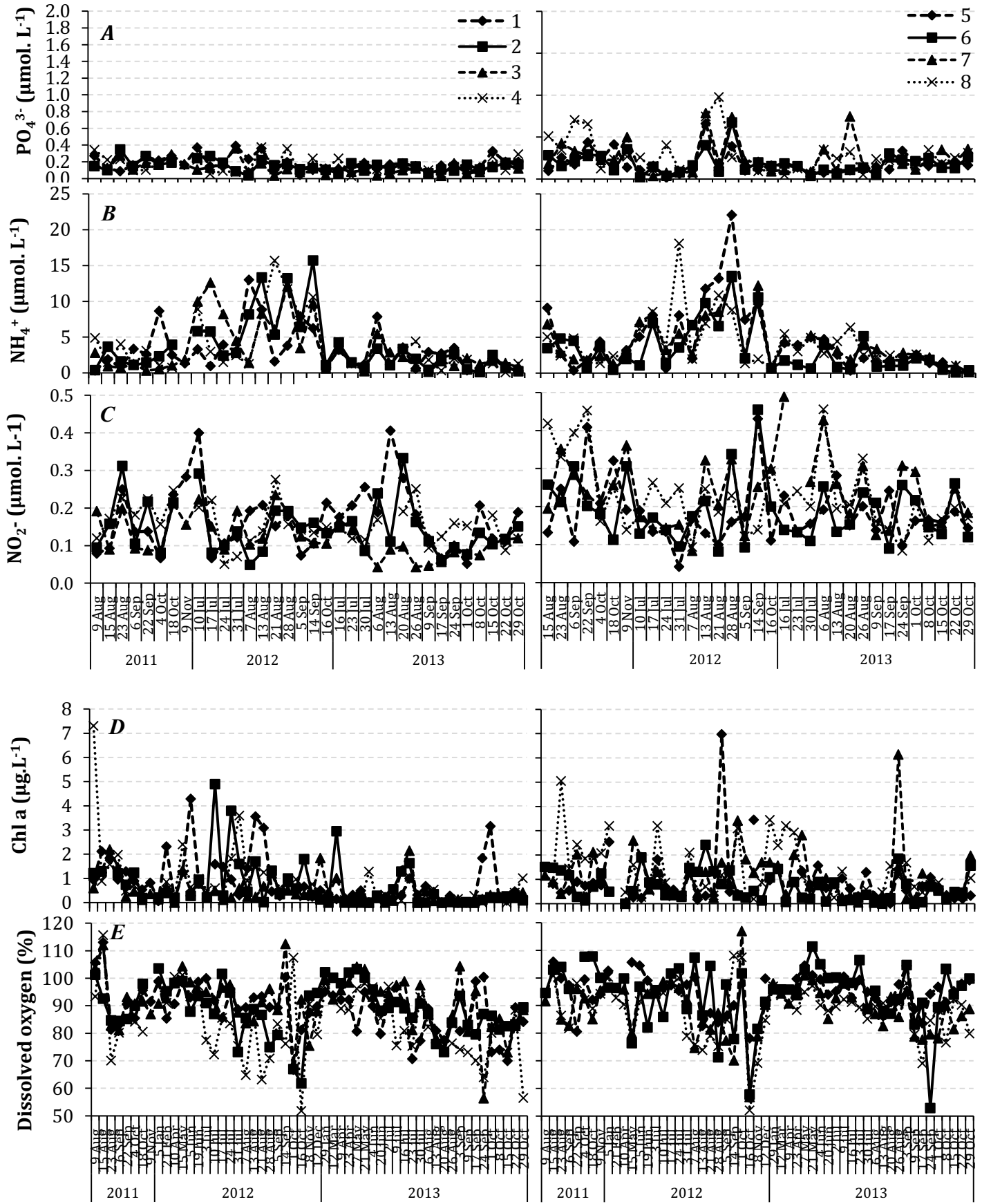
Fig. 4.4. Temporal variation of **A.** Phosphates; **B.** Ammonia; **C.** Nitrites; **D.** Chlorophyll a; and **E.** Dissolved oxygen. Left: northern sites and Right: southern sites.
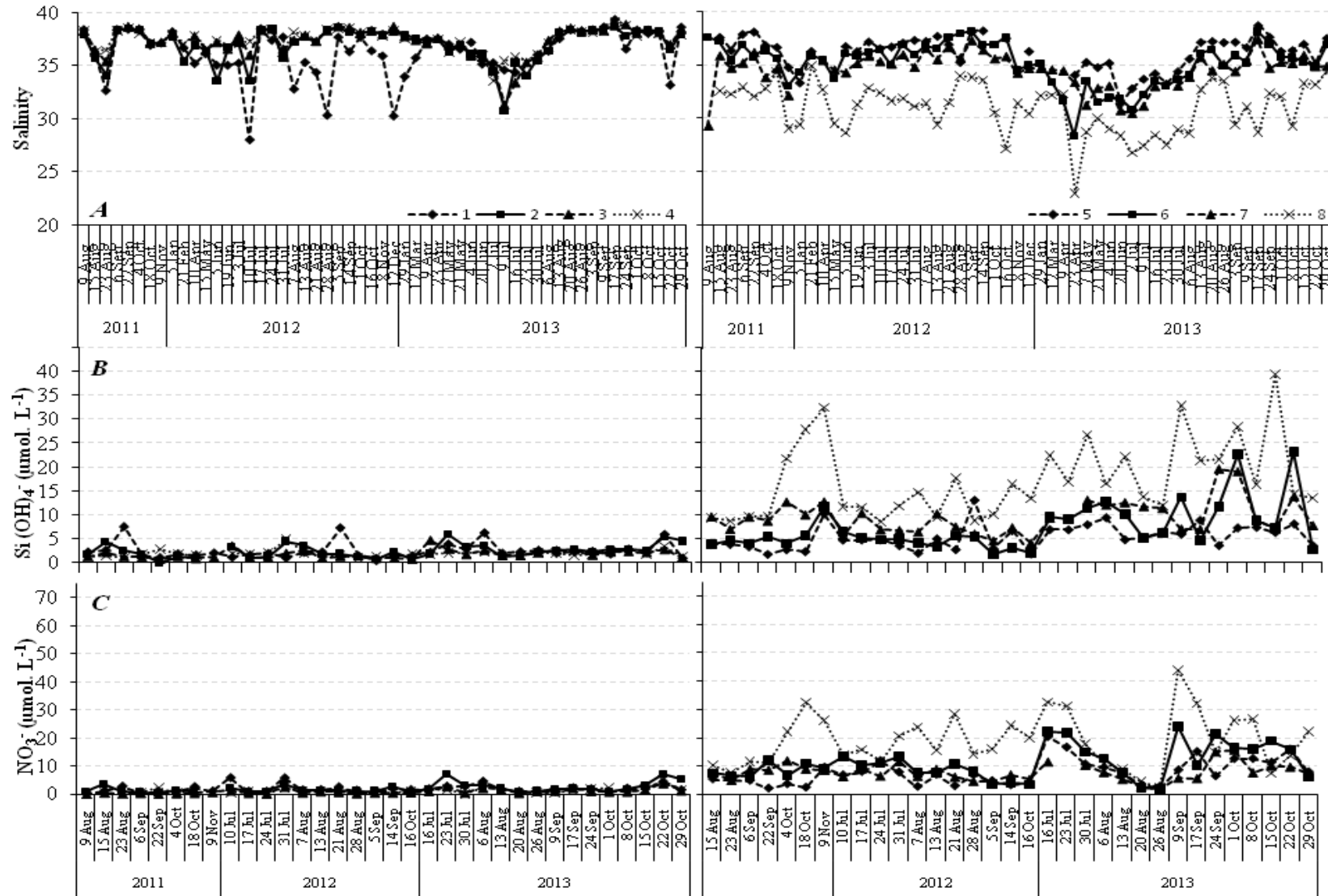
Fig. 4.5. Temporal variation of **A**. salinity, **B**. silicates, **C**. nitrates in sampling sites. Left: northern sites and Right: southern sites.

4.4.4. *Epiphytic community*

4.4.4.1. <u>Ostreopsis *characterization in field samples by DNA analysis*</u>

High specificity for this method was obtained as no amplification of the non-target species was observed with the two species-specific primers tested in *O.* cf. *ovata* IRTA-SMM-11-10 and *O.* cf. *siamensis* VGO978 cultures. Genomic amplification did not occur in samples were *Ostreopsis* was absent, verified by microscopy enumeration. No amplification was observed using *O.* cf. *siamensis* primers in any field samples and only *O.* cf. *ovata* DNA was detected in field samples.

4.4.4.2. <u>*Microscope evaluation of the epiphytic microalgae community*</u>

The pennate diatoms assemblage was the most abundant in all sampling sites, largely comprised by small-sized species from the order Naviculales. This group of microalgae continually dominated the epiphytic community for all sites and seasons followed by *Licmophora* sp. and *Coscinodiscus* sp. Dinoflagellates represented a very low percentage, less than 5% on average of the total epiphytic microalgae assemblage, but increased up to 43% on average, during *O.* cf*. ovata* blooms. From a regional point of view, the northern sites had significantly (F(1)= 12.89 *MSE*= 137.43; p<0.001) higher dinoflagellate average abundance (14.29±6.52%) in the epiphytic community compared to the southern sites (8.20±2.41%). Figures 4.6 and 4.7 represents sites 3 and 4 epiphytic microalgae abundances respectively.
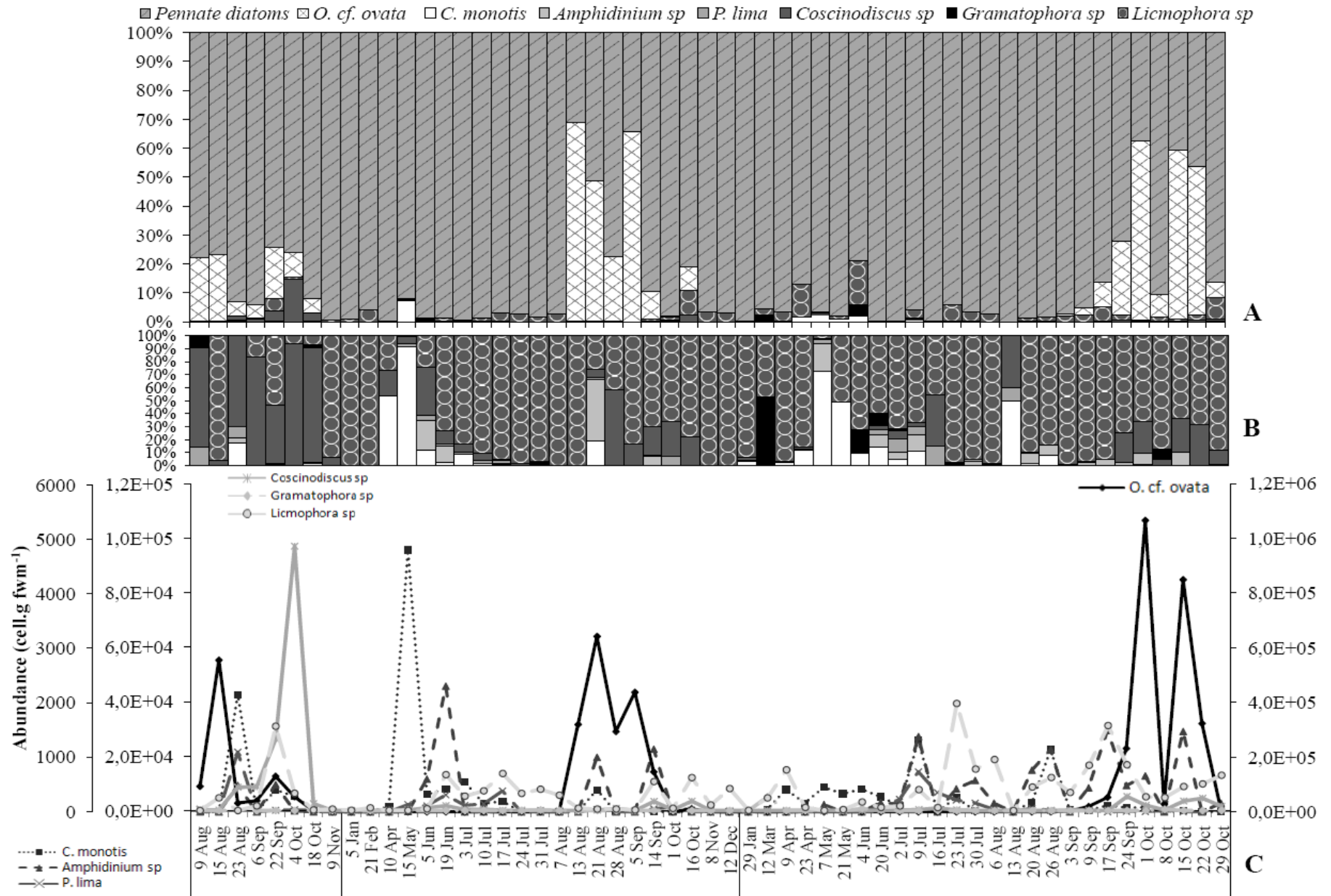
Fig. 4.6. Site 3 epiphyte community description for every sampling day **A**. Abundance percentage of microalgae in epiphytic field samples during experimental monitoring **B**. Abundance percentage without pennate diatoms and *O*. cf. *ovata*. **C**. Cell abundance per gram of fresh weight macrophyte.
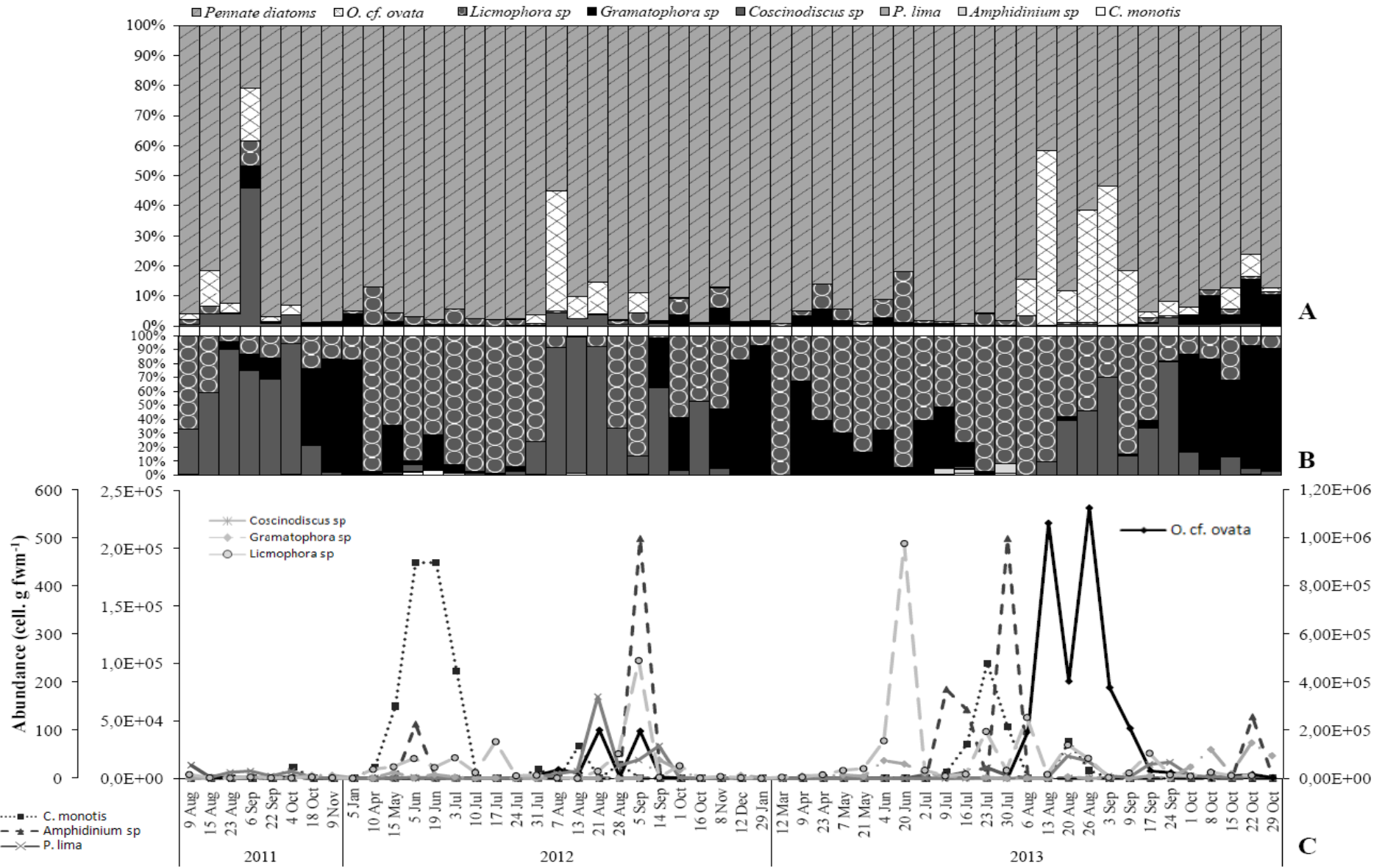
Fig. 4.7. Site 6 epiphyte community description for every sampling day **A**. Abundance percentage of microalgae in epiphytic field samples during experimental monitoring **B**. Abundance percentage without pennate diatoms and *O*. cf. *ovata*. **C**. Cell abundance per gram of fresh weight macrophyte.

4.4.4.3. *Ecological niche of the epiphytic microalgae community*

According to the environmental parameters PCA analysis in Figure 4.2, microalgae species and assemblage distribution is reflected in Figure 4.6, *O.* cf. *ovata* is the most affected by high temperature values, followed by *P. lima*, and *Coscinodiscus* sp. Other groups of species seem to be more influenced by salinity; *Amphidinium* sp. and *C. monotis* more abundant at higher salinity values, contrarily to *Grammatophora* sp. with preference for lower salinities. The pennate diatom assemblage and *Licmophora* sp. show less influence by climatological and bio-physical seawater conditions.
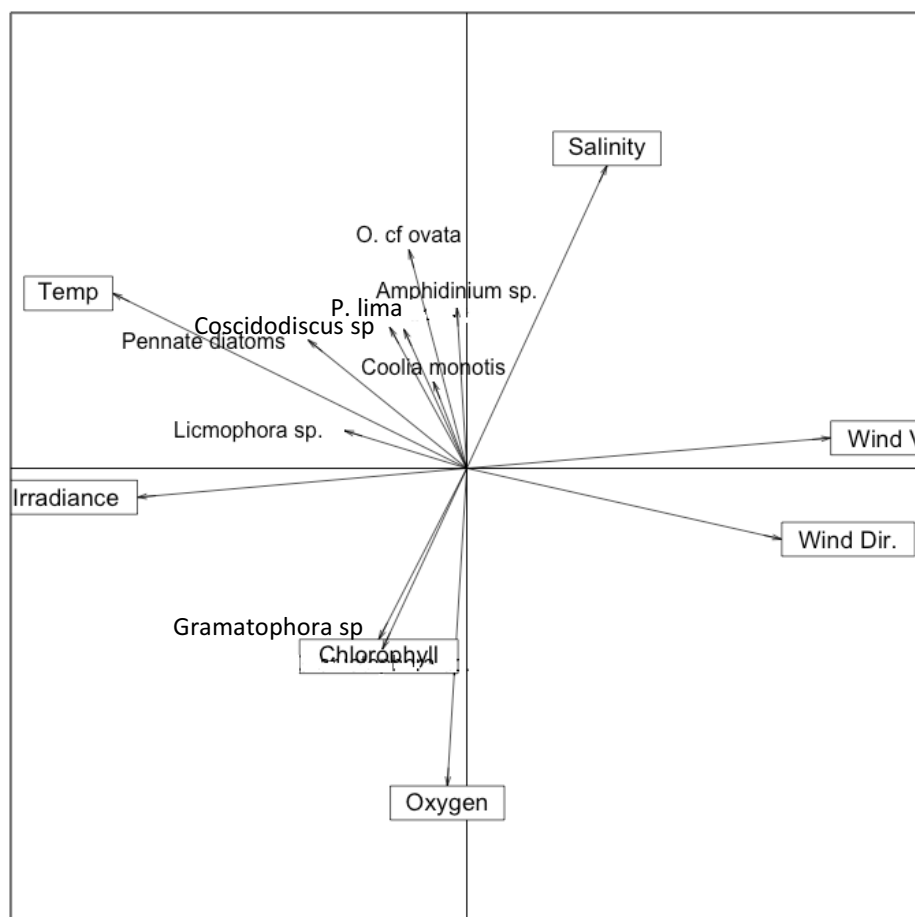
Fig. 4.6. Microalgae species and assemblage distribution in the PCA (axis 1 = 0.76%, axis 2 = 0.18% of total marginality); Temp = Temperature; Wind V = wind speed; Wind Dir = Wind Direction.

The different species or groups of species studied showed a significant marginality suggesting a considerable influence of the selected environmental variables on species distribution. However, all the species had a high residual tolerance (Table 1). This fact suggests that, although their distribution in the study area is significantly correlated with the environmental variables used, there are

other factors that also affect species distribution. Results reflect different patterns of specialization and niche breadth within the epiphytic microalgae community. Mainly pennate diatoms and *Licmophora* sp are generalists, showed by a very low values of marginality and a wider niche breadth (tolerance); in the other hand, *O.* cf. *ovata* and *Amphidinium* sp are specialized species, with the higher values of marginality and a narrow niche breadth (tolerance) of the epiphytic microalgae community studied.

	Inertia	OMI	Tol	OMI(%)	Tol(%)	Rtol(%)	Num
O. cf. *ovata*	5.9	0.56	0.43	9.5	7.3	83.2	0
Coolia monotis	6.78	0.15	0.60	2.3	8.8	88.9	0
Amphidinium sp	5.28	0.47	0.81	8.9	15.5	75.7	0
Prorocentrum lima	5.93	0.37	0.65	6.3	10.9	82.8	0
Coscinodiscus sp	6.36	0.18	0.91	2.9	14.3	82.8	0
Grammatophora sp	6.07	0.36	0.91	6	14.9	79.1	0
Licmophora sp	6.48	0.37	1.56	0.3	24.1	75.6	0
Pennate diatoms	6.82	0.01	1.67	0.1	24.4	75.6	0

Table 4.1. Niche parameters of microalgae benthic community; Inertia = total variability; OMI= Outlying Mean Index; Tol = species tolerance; Rtol = residual tolerance; Num = number of random permutations (out of 10000).

4.4.5. O. cf. ovata abundances

4.4.5.1. *Temporal distribution*

We considered a bloom of *O.* cf. *ovata* when abundances were above 5 x 10^4 cell. g fwm^{-1}, taking into account abundances found in our sampling sites and other Mediterranean areas. A repeated marked temporal trend was observed every year, coinciding with warm temperatures; growing in summer and not being detected during late fall and winter (minimum temperature where *O.* cf. *ovata* cells were observed was 16.31°C, the 8th November 2012 in site 4) (Figure 4.7)*.*
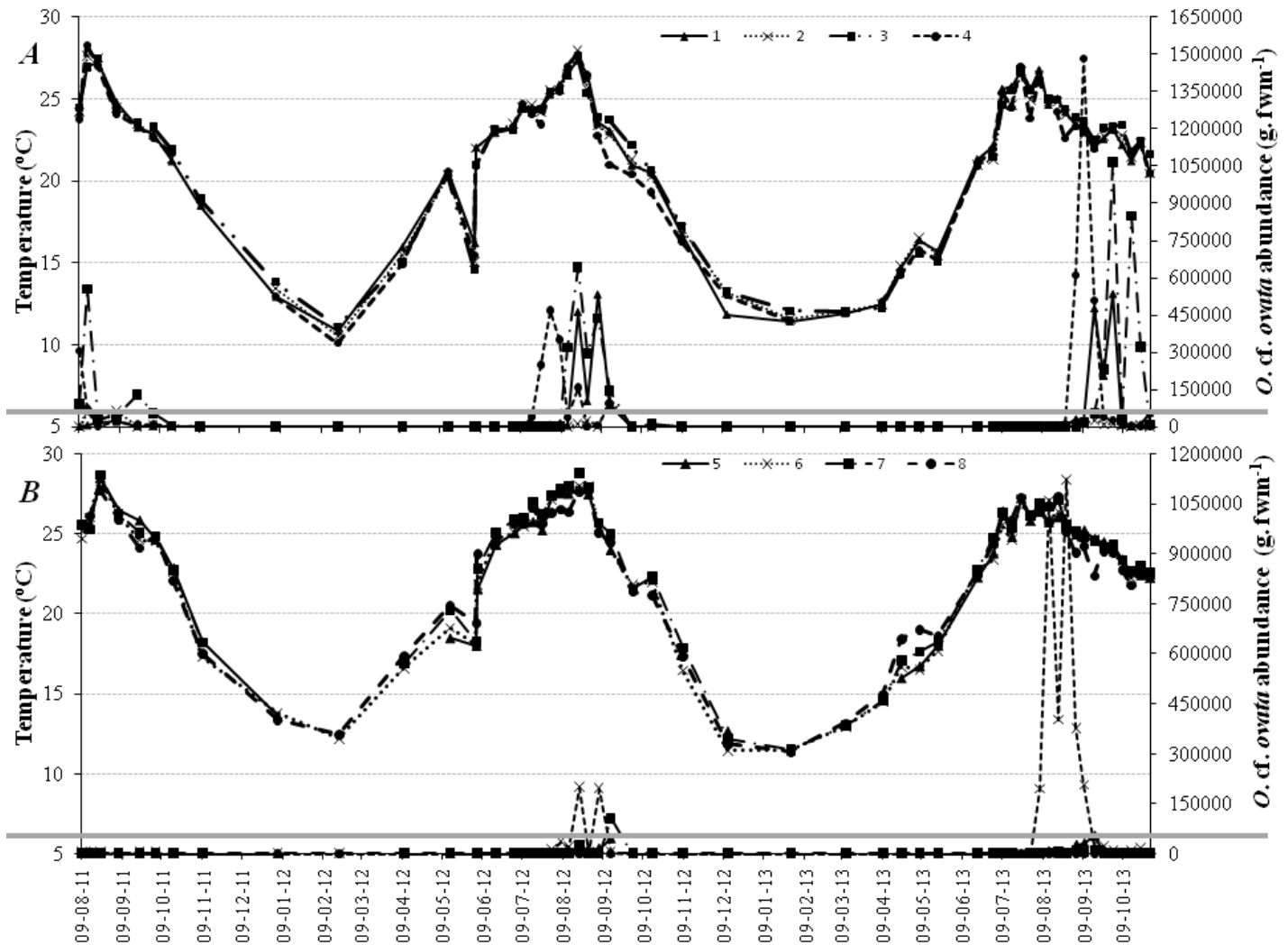
Fig. 4.7. Temporal variation of temperature and epiphytic cell abundance in **A**. northern sites and **B**. southern sites. Grey line represents 5 x 10^4 cell. g fwm^{-1} (considered as a bloom).

In a preliminary survey that preceded the present study, carried out in the same area (data not shown) from June to the beginning of July 2011 no *O.* cf. *ovata* cells were observed. Sometime between this period and the 2nd of August, *O.* cf. *ovata* started growing in sampling sites, forming a small proliferation in the north two weeks later. In 2012, the first cells were observed the 3rd July in the south and the 10th July in north, and formed blooms from mid-august to mid-September. Interestingly, in 2013 a bloom of *Gonyaulax fragilis* occurred at the end of July along the Catalonia coast, but did not reach the southern sites. *O.* cf. *ovata* did not grow until the 10th of August in the north, whereas the 16th July, *O.* cf. *ovata* was already observed in site 6. Blooms in the south occurred as in the previous years, in mid-August, but in the north, *O.* cf. *ovata* bloomed later, in mid-September. Cells were observed until the end of October/early November in the majority of sampling sites for the three years. This seasonality was repeated the three years, coinciding in most cases with a decrease of water temperature (Figure 4.6). Average temperature

104

during blooms was 24.49±1.96 with maximum of 28.28°C in site 4 the 15th August 2011 and minimum 20.48°C in site 1 the 29th November 2013.

4.4.5.2. Regional distribution

The number of blooms during the three years was more than 3 fold higher in the northern sites than in the southern sites. A total of 35 blooms occurred in the north (8 in site 1; 3 in site 2; 14 in site 3 and 10 in site 4). In the south, just 10 blooms were registered, 8 of them corresponding to site 6 and none in site 8. Average abundances were significantly higher in northern sites ($F(1)$=6.5 MSE=1.51 x 10^{11}; $p<0.05$) when compared to the southern sites.

Heterogeneity in bloom formation was observed among sites of each area. In the north, highest abundances were detected in site 4, (maximum = 1.48 x 10^6 cell·g fwm^{-1}) whereas in site 2, *O.* cf. *ovata* abundance was more than tenfold lower, 0.11 x 10^6 cell·g fwm^{-1}. In the southern sites, *O.* cf. *ovata* highest densities occurred in site 6 (maximum 1.12 x 10^6 cell·g fwm^{-1} the 26th August 2013), that were significantly different ($F(3)$= 5.13 MSE= 6.5x10^{10}; $p<0.01$) from the rest of southern sites where highest abundances were tenfold lower, 0.1 x 10^6 cell.g fwm^{-1} on average, being especially low in site 8 (above 4.8 x 10^3 cell.g fwm^{-1}).

4.4.5.3. Relation with environmental factors

We analyzed the influence of nutrient content; salinity and temperature during the presence of *O.* cf. *ovata* in macrophyte samples. Significant negative correlation was found between all nutrient concentrations and *O.* cf. *ovata* abundances (Spearman test) except for phosphates. Nitrate and silicate had the highest significant negative correlation (R^2 = -0.315; R^2 = -0.305 respectively; $p<0.001$), although its low value indicates a weak influence. Salinity had the highest impact (R^2 = 0.451; $p<0.001$) thought it cannot be considered very strong. The lowest salinity registered for a bloom was 30.34 with an abundance of 1.02 x 10^5 cell. g fwm^{-1} in site 1. Temperature, which ranged from 17.28 to 28.77°C during this period, had no significant correlation with *O.* cf. *ovata* concentrations.

4.4.6. O. cf. ovata physiological responses

4.4.6.1. Morphometric analysis

A wide range of sizes was observed in epiphytic cells, from 21.24 to 76.95 μm for DV diameter with a mean value of 54.50±6.80 μm, and from 15.57 to 50.99 μm for W diameter with a mean value of 33.05 ± 5.51 μm. A significant difference in DV diameters ($F(1)$= 95.61 MSE= 4.25x10^3 $p<0.001$) and W ($F(1)$= 178.88 MSE= 5.03x10^3; $p<0.001$) of *O.* cf. *ovata* epiphyte cells was found between site 3 (DV: 53.09±7.06 μm; W: 31.51±5.33 μm) and site 6 (DV: 55.81±6.28; W: 34.47±5.29). Cells from the water column ranged from 32.49 to 76.49 for DV diameter and from

15.4 to 49.59 for W diameter. As it happens for epiphytic cells, W diameter in cells from the water column was significantly higher ($F(1)= 19.41$ $MSE= 4460.1$ $p<0.001$) in site 6 (33.99 ± 4.87 µm) than in site 3 (32.57 ± 4.87 µm), however, DV diameter did not show differences (site 3: 55.05 ± 7.04 µm; site 6: 55.55 ± 5.97 µm). Sizes between epiphytic and planktonic cells were similar.

We divided the blooms into three phases as in Accoroni *et al.* (2012). An initial growth phase (phase I; 645 cells measured) followed by the proliferation bloom phase (Phase II; 657 cells measured), and a decline phase at the end (Phase III; 1004 cells measured). Identification of different phases was based on cell abundances and time (Figure 4.8). We observed a significant increase in cell size from the beginning to the end of the bloom in both sites (site 3, DV: $F(2)= 7.34$ $MSE= 362.49$ $p<0.01$; W: $F(2)= 19.34$ $MSE= 531.04$ $p<0.001$; site 6, DV: $F(2)= 11.9$ $MSE= 461.23$ $p<0.001$; W: $F(2)= 21.99$ $MSE= 593.55$ $p<0.001$). Tukey test results indicated a significant difference in DV diameter between the initial phase and the other two while for the W diameter there was a significant increase after the proliferation phase.
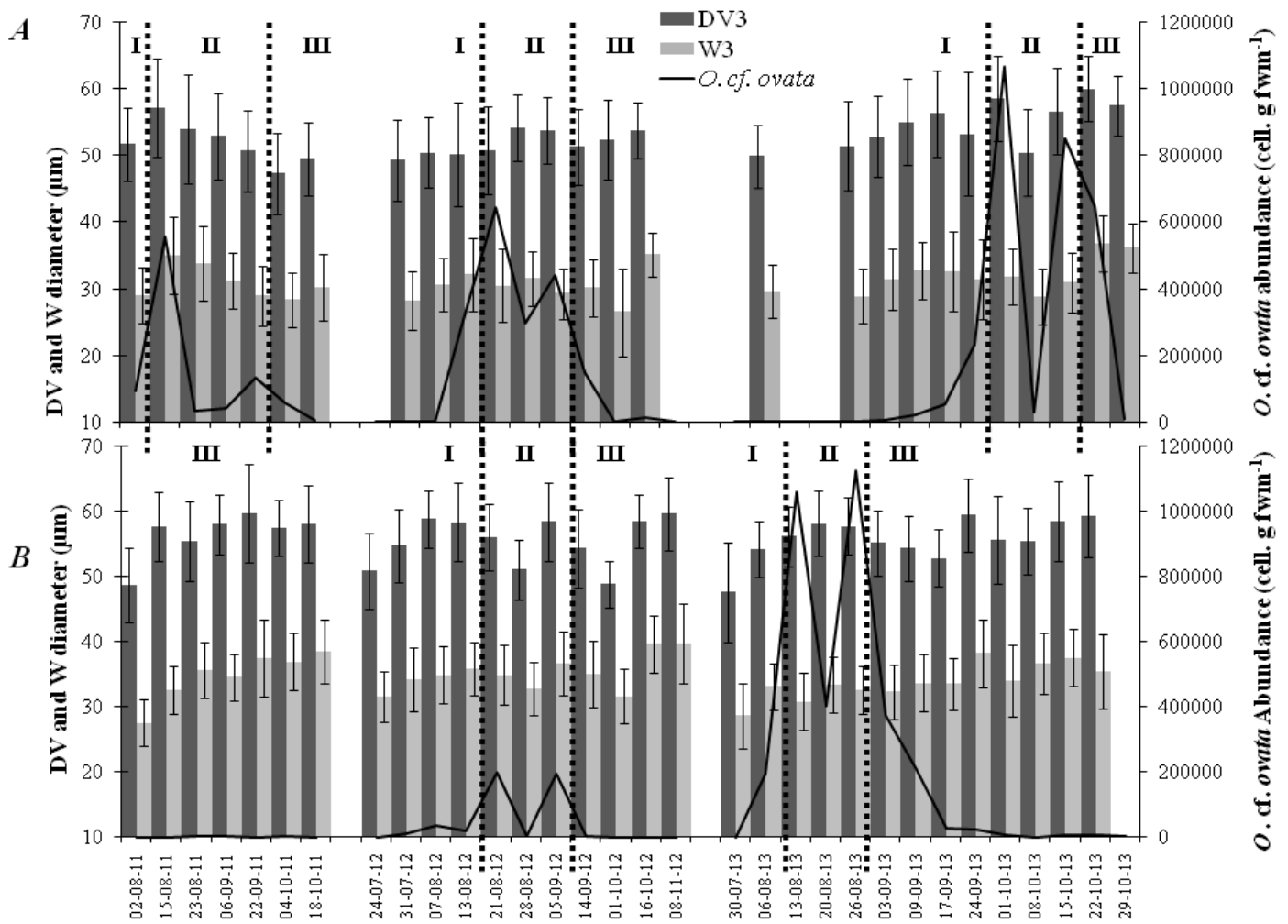
Fig. 4.8. *O.* cf. *ovata* abundances and cell dimensions (DV and W diameters) during the three phases considered in the bloom (I, II, III) in **A**. site 3 and **B**. site 6. Error bars represent two standard deviation from the average of measured cells.

4.4.6.2. *Toxin content in planktonic cells according to cell abundances in water column in sites 3 and 6.*

Ostreopsis cf. *ovata* abundances in the water column achieved higher concentrations in site 6 with maximum densities of 4.5×10^4 and 5.3×10^4 cell. L^{-1} in 2012 and 2013 respectively. A positive correlation (Spearman test) was found between planktonic and epiphytic cells ($R^2=0.86$; *p*<0.001), especially visible during the bloom in 2013 in site 6 (Figure 4.9).
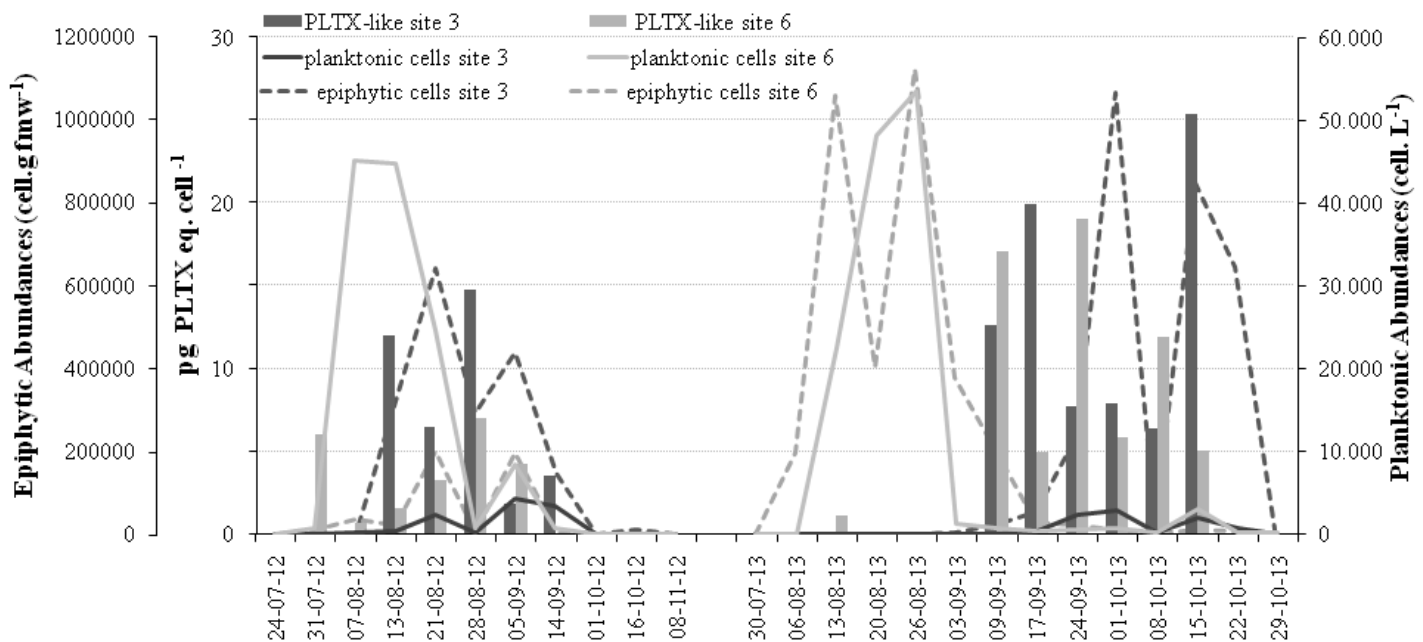
Fig. 4.9. PLTX-like content (pg PLTX eq.cell^{-1}) in *O.* cf. *ovata* from the water column in sites 3 and 6 and planktonic (cell. L^{-1}) and epiphytic cell abundances (cell. g fwm^{-1}) in both sites.

Haemolytic activity from water column samples was evaluated when haemolytic values ranged between $\%H_{15}$ and $\%H_{55}$ obtained in the calibration curve, according to the equation: $y= 0.00932e^{0.0778x}$ ($R^2= 0.98$). In the presence of ouabain, a non-specific haemolytic activity was registered for the highest standard concentration but it was lower than $\%H_5$ and did not interfere in the haemolysis specific response.

PLTX-like compounds content in *O.* cf. *ovata* planktonic cells ranged from very low (less than 1 pg PLTX eq·cell^{-1}) to 25 pg PLTX eq·cell^{-1}. A negative correlation (Spearman test) was observed between PLTX-like content and planktonic cell abundance ($R^2 = -0.55$; *p*<0.01).

4.5. Discussion

4.5.1. *O.* cf. *ovata* associated epiphytic community

There are only two *Ostreopsis* species, from the nine described so far, that have been detected in the Mediterranean Sea (Battocchi *et al.,* 2010); *O.* cf. *ovata,* a PLTX-like compounds producer (Ciminiello *et al.,* 2012), and *O.* cf. *siamensis*, a non toxic species (Ciminiello *et al.,* 2013). *O.* cf. *ovata* seems to be the most predominant species in the Mediterranean Sea compared to the scarce distribution of *O.* cf. *siamensis* (Penna *et al.,* 2010). As morphological features are very similar, molecular

108

methods have been developed in order to ascertain species identification (Perini *et al.,* 2011). Blooms of *Ostreopsis* have been associated with human intoxications and with damage to benthic communities (Tubaro *et al.,* 2011; Tachidou *et al.,* 2010), most probably attributed to *O.* cf. *ovata*. Due to the sensitivity of qPCR it should be possible to detect unequivocally the species present in the water, especially before blooms, and therefore prevent potential human intoxications (Penna *&* Luca, 2013).

Observations in coastal microphytobenthos communities in different substrata in the Mediterranean Sea indicate that diatoms dominate over dinoflagellates in the composition of microalgae (Totti *et al.,* 2010; Mounir *et al.,* 2013). The same community structure has been found in all our samples, with ubiquitous small-sized diatoms representing the major proportion. On the basis of the results of OMI analysis, pennate diatoms would be described as generalists, which are species that grow in a widely range of environmental conditions. Nonetheless, a higher amount of diatoms was observed in the southern area, while dinoflagellates were more abundant in northern sites. The association of *O.* cf. *ovata* with *C. monotis* and *P. lima* has been reported among the epiphytic communities in shallow waters in the Mediterranean Sea (Vila *et al.,* 2001a; Aligizaki & Nikolaidis., 2006), with *O.* cf. *ovata* generally being the most abundant. From our results, we observe that these three species comprise a group of specialists, since they have narrow niche breadth compare with the rest of microalgae.

It has been suggested that, when different dinoflagellate species compete for an ecological niche the most important environmental factors are those varying according to depth (Cohu & Lemée, 2012), such as substrate or light, interfering with *O.* cf. *ovata* proliferations (Aligizaki & Nikolaidis, 2006). Apparently, coexistence with other species does not interfere in *O.* cf. *ovata* blooms as supported by laboratory experiments where only a weak allelopathy has been found among dinoflagellate species (Monti & Cecchin, 2012). Interestingly, during our research, a bloom of *Gonyaulax fragilis* produced high amounts of mucus that remained attached to the macrophytes for several days in the northern sites. This circumstance may be the reason why *O.* cf. *ovata* growth was delayed in this area that particular year. In addition to that, other biotic factors have to be considered such as the life cycle of the host macroalgae, light, grazing pressure or adjacent surface cover (Fraga *et al.,* 2012) that may interfere with benthic microalgae dynamics. The relationships with other microalgae species needs further investigation in order to elucidate their possible contribution to the formation of massive proliferations. Environmental factors and *O.* cf. *ovata* bloom dynamics.

4.5.1.1. *Hydrodynamism*

Hydrodynamics is a major factor influencing benthic dinoflagellate abundances (Totti *et al.,* 2010), mainly during the bloom proliferation phase when the highest densities are reached. Due to the difficulty to describe or quantify wave exposure,

based on wind speed, or to subjective descriptions of hydrodynamic conditions, it is difficult to compare results from different studies. It has been suggested that *Ostreopsis* in temperate areas might have preference for "moderate" wave exposure in relation to "quiet" waters (Vila *et al.,* 2001a; Shears *&* Ross, 2009; Parsons *et al.,* 2012; Selina *et al.,* 2014). Our results are in agreement with this hypothesis, as we found higher abundances in the north, where wind (an indicator of wave exposure) was strongest. A consensus among scientists regarding the methodology to measure or classify hydrodynamism would contribute to more accuracy of any conclusions.

4.5.1.2. *Temperature*

Seawater temperature is the most determinant factor concerning toxic benthic dinoflagellate dynamics (Pistocchi *et al.,* 2011). A temporal distribution was observed in the epiphytic microalgae community in all our sampling sites. *O.* cf. *ovata* proliferation in summer-autumn in different areas of the north of the Mediterranean Sea has been well characterized (Mangialajo *et al.,* 2011). This seasonal pattern may be partly explained by the variation of seawater temperature in temperate climates (Cohu *et al.,* 2013). Besides, blooms have been detected once the seawater temperature starts to decrease in the Mediterranean Sea (reviewed in Pistocchi *et al.,* 2011), and in a recent study in temperate waters in Japan (Selina *et al.,* 2014). The same pattern is observed in our samplings, raising the hypothesis that it is the length of warm period and not the maximal temperatures reached that determine the presence and abundance of *O.* cf. *ovata* on macrophytes (David *et al.,* 2012). Given the fact that *O.* cf. *ovata* had been originally associated to sub-tropical and tropical waters (Rhodes, 2011), preference to warm conditions is expected. This is in agreement with our OMI analysis that highlighted the different optimal conditions and tolerances to certain environmental factors from the species and group of species studied. *O.* cf. *ovata* shows a more restricted ecological niche, probably due to the fact that its presence in macrophytes is exclusively limited above a certain temperature threshold (Mangialajo *et al.,* 2011). Nevertheless, contrasting conclusions have been reported regarding the role of temperature in *O.* cf. *ovata* growth in the Mediterranean Sea. Results from laboratory studies performed in strains from distinct locations, suggest a possible adaptation to different optimal temperatures depending on strain origin. This is reflected as well in field observations of populations in the areas of bloom origin where the ranges of temperature are the same as those used in the laboratory (Pezzolesi *et al.,* 2012). However, recent studies have found *O.* cf. *ovata* in higher latitudes where seawater is cooler (Selina & Orlova, 2010; Laza-Martinez *et al.,* 2011), which may imply an adaptation and consequent colonization of new habitats.

An important issue worth of discussing is the reappearance, year after year, of *O.* cf. *ovata* after several months during which it is not detected in the ecosystem. It will be important to better understand the fate of *O.* cf. *ovata* cells with the arrival of fall

and the decrease in water temperature. It could be explained by resistance forms, that may facilitate the re-colonization of macrophytes, may be involved or maybe, advective processes in the spring determine their reappearance.

4.5.1.3.   *Salinity*

It is not evident to what extent seawater salinity may affect *O.* cf. *ovata* growth (Pistocchi *et al.,* 2011), though a response to salinity in interaction with temperature has been reported in other *Ostreopsis* species (Tanimoto *et al.,* 2013) and particularly in *O.* cf. *ovata* (Yamaguchi *et al.,* 2012; Carnicer *et al.,* submitted). An interesting observation from this study is that sampling locations are close to a river delta where salinity can reach low values. Interestingly, site 8 registered lower salinities and higher amount of nutrients corresponding to the site where lowest abundances of *O.* cf. *ovata* were recorded and no blooms were formed. Outbreaks were registered in the rest of sampling sites, where salinity was in agreement with other field values observed in the Mediterranean Sea, where blooms occurred when salinity was between 35 and 38 (Pistocchi *et al.,* 2011). Although community responses obtained in laboratory conditions are not directly extrapolated to natural environments, in an experiment conducted with strains of *O.* cf. *ovata* isolated in our sampling area (Carnicer *et al.,* submitted), a decrease in growth rate was observed at high temperatures (28°C) and at high salinity (38), contrary to the positive correlation between *O.* cf. *ovata* abundances and salinity observed during bloom periods in this study. Taking into account that laboratory strains were acclimated for a year and that the bloom season is shorter, it may be hypothesized that the exposure to longer periods of higher temperature and salinity could affect in a different way *O.* cf. *ovata* growth. In a climate change scenario in the Mediterranean Sea, where an increase of salinity and temperature is expected (IPCC, 2013), these new conditions may influence *O.* cf. *ovata* dynamics. It is however very difficult to predict those changes, as many other factors that could potentially enhance or decrease blooms formation would vary at the same time as a consequence of global change.

4.5.1.4.   *Nutrients*

To establish the relationship between nutrient loading and algal proliferation is complicated due to interactions with other factors alter the assimilation of nutrients by microalgae (Anderson *et al.,* 2002). Freshwater inputs in coastal waters contribute to decrease salinity and increase nutrient concentrations; in this study increases were more pronounced in nitrates and silicates. It is thus practically impossible to discern whether microalgae responses are due to one fact or the other. Sampling points in the south are closer to Alfacs Bay than the northern points are to Fangar Bay. In addition, Alfacs Bay is much larger than Fangar Bay resulting in higher freshwater inputs. In addition to that, Salat *et al.,* (2002) have observed an anticyclonic circulation in the south of the Delta, where continental water remains

trapped, and may contribute to an accumulation of low salinity and increased nutrient concentration. The sum of these factors could explain differences in seawater parameters in both areas.

Laboratory studies have shown that nutrient limitation decreases *O.*cf. *ovata* growth, an effect that is more accentuated under N-limitation (Vannucci *et al.,* 2012; Vidyarathna & Granéli, 2013; Accoroni *et al.,* 2014). There are not many *in situ* studies about the relationship between nutrients and *O.* cf. *ovata* blooms. We observed a weak negative correlation with nitrate and silicate concentration in agreement with results obtained by Cohu & Lemée (2011) and Cohu *et al.,* (2013), whereas Vila *et al.,* (2001) and Accoroni *et al.,* (2011) did not find such a relationship.

In any case, blooms were observed in both areas, in the north and the south, showing a heterogeneity and patchy spatial distribution already described in other studies (Cohu *et al.,* 2011). This behavior may be the response to the interaction of multiple environmental factors at a small regional scale which may increase the difficulty to understand the ecological features of *O.* cf. *ovata* dynamics.

4.5.2. *O. cf. ovata physiological responses*

4.5.2.1. <u>*Morphometric analysis*</u>

Two cell sizes have been defined for *O.* cf. *ovata* in laboratory cultures and field samples, being the latter larger on average from the ones growing in the laboratory (Scalco *et al.,* 2012; David *et al.,* 2013). Our results reflected that *O.* cf. *ovata* population in site 6 (south) was larger than in site 3 (north). Physiological experiments have been addressed to examine variability in cell size under different controlled conditions. No particular pattern of cell size has been found with temperature and salinity (Pezzolessi *et al.,* 2012; Carnicer *et al.,* submitted) or with irradiance (Scalco *et al.,* 2012). A higher cell size of *O.* cf. *ovata* in culture was observed with the presence of bacteria (Vanucci *et al.,* 2012) and at low nutrient concentrations (Vanucci *et al.,* 2012; Vydyarathna & Granéli, 2013). These studies suggested that under stress conditions, an increase in cell volume is caused by the inhibition of cell division provoked by disruptions in metabolic adjustments. Field observations in Accoroni *et al.,* (2012) corroborate this fact as larger DV diameters were found in areas that represented unfavorable growth conditions. In advantageous circumstances, cells undergo an intense division in which small cells are more abundant (Carnicer *et al.,* submitted) and this is reflected in the average population size. This is in accordance with our observations in site 3, where cell size average was smaller, and blooms more frequent than in site 6, located in the south where freshwater inputs may affect *O.* cf. *ovata* proliferations.

4.5.2.2.   *Toxicity*

There are contradictory results about the effect of physico-chemical parameters in *O.* cf. *ovata* toxin content. Experiments performed under controlled conditions have been reported in recent years. Scalco *et al.,* (2012) did not find any clear pattern under different irradiance conditions. Using strains of *O.* cf. *ovata* from the Adriatic Sea nutrient deficient cultures produced lower toxicity (Vannucci *et al.,* 2012b), contrary to Tyrrhenian strains for which N deficiency significantly increased cell toxicity (Vydyaranthna & Granéli., 2013). These differences may be attributed to distinct physiological adaptations from the area of origin, as well as distinct experimental methodologies either related with microalgae culture or toxin analyses performance. Regarding temperature effects, it has been found that higher toxin production occurs under non-optimal temperature growth conditions (although no conformity in temperature ranges) (Granéli *et al.,* 2010; Pezzolessi *et al.,* 2012; Vydiarathna & Granéli, 2011). Carnicer *et al.* (submitted) hypothesized that high temperature may accelerate toxin gene transcription independently of optimal growth temperature. However, little is known about cell toxicity in field; a decrease in toxin content with increasing depth was found in Villefranche-sur-Mer (Ligurian Sea), attributed possibly to a decrease in the irradiance (Brissard *et al.,* 2014). On the other hand, consensus seems to be achieved regarding the increase in toxin content during the stationary phase of growth when compared to the exponential phase (references above).

We focused our toxicity analyses in planktonic cells, as probably cells in the water column resuspended as marine aerosols (Tichadou *et al.,* 2010) are responsible for respiratory and systemic syndromes by contact or inhalation in humans (Tubaro *et al.,* 2011). In our study, toxic content per cell was lower when *O.* cf. *ovata* abundance was higher. We can hypothesize that during an intensive bloom, cells metabolism is focused on growth, and toxin production may not particularly be intensified. In addition, when cells are actively dividing within a population, a high proportion of cells are recently divided cells, smaller in size, and these may on average contain less metabolites in their cytoplasm than larger cells, possibly explaining a decrease in toxin content per cell. It is thus possible that cells during blooms may have lower toxin content per cell, but still, due to higher cell densities, the toxin load of the bloom may result harmful.

4.6. Conclusions

The present study confirmed, through real-time qPCR, the presence of a single genotype, *O.* cf. *ovata*, and the absence of *O.* cf. *siamensis* in our sampling area. It is recommended that monitoring programs and scientific studies include molecular analysis of the benthic microalgae community prior to the blooms, as an additional specific tool to identify potential risk to humans and marine ecosystems.

The study of the relationship between environmental factors and *O.* cf. *ovata* dynamics in temperate regions is still uncertain, considering the limited number of field studies and contradictory experimental results. Our findings highlight that temperature is the most important parameter affecting *O.* cf. *ovata* distribution, defining a restricted ecological niche and a clear seasonal pattern. However, the interaction with other environmental factors is what certainly determines the formation of blooms, considering the spatial heterogeneity of outbreaks occurring in our sampling sites.

Among the parameters studied, wave exposure (studied through wind speed) and salinity seem to have a strong impact on *O.* cf. *ovata* abundance. Hydrodynamism plays an important role on bloom formation; in our study, *O.* cf. *ovata* blooms were more numerous where wind speed was on average higher. Salinity positively correlated with cell abundance during the months of bloom presence, drawing the attention to the relative impact of this factor, not clearly emphasized in the literature. Regarding nutrient concentrations, a weakly negative interaction was observed for nitrate and silicate loads during the same period.

Morphometric and toxicological evaluation were also taken into consideration in our study as environmental factors also influence cell physiology. Cells were smaller in the north where, on average, more abundance of *O.* cf. *ovata* was observed, indicating possible favorable conditions for cell division, attributed probably to lower freshwater inputs. However blooms occurred in both sites with a similar magnitude, but with lower frequency in the south.

Planktonic *O.* cf. *ovata* PLTX-like toxin content was detected coinciding lower concentrations with higher abundances, probably due to cells growth phase. However, being in high densities, it constitutes a potential risk to people in contact.

The development of future predictive models for *O.* cf. *ovata* abundances is necessary to understand its ecology and facilitate management actions to protect human health and the environment. Given the complexity and difficulty of field work we would encourage researchers to intensify their effort to harmonize methods and strategies to obtain more reliable results. An adaptation to coastal benthic ecosystems is crucial as the majority of models are designed for planktonic species.

4.7. References

Accoroni, S., Romagnoli, T., Pichierri, S., Totti, C., 2014. New insights on the life cycle stages of the toxic benthic dinoflagellate *Ostreopsis* cf. *ovata*. Harmful Algae 34, 7-16.

Accoroni, S., Romagnoli, T., Pichierri, S., Colombo, F., Totti, C., 2012. Morphometric analysis of *Ostreopsis* cf. *ovata* cells in relation to environmental conditions and bloom phases. Harmful Algae 19, 15-22.

Accoroni, S., Romagnoli, T., Colombo, F., Pennesi, C., Di Camillo, C.G., Marini, M., Battocchi, C., Ciminiello, P., Dell'Aversano, C., Dello Iacovo, E., Fattorusso, E., Tartaglione, L., Penna, A., Totti, C., 2011. *Ostreopsis* cf. *ovata* bloom in the northern Adriatic Sea during summer 2009: Ecology, molecular characterization and toxin profile. Marine Pollution Bulletin 62, 2512-2519.

Aligizaki, K., Nikolaidis, G., 2006. The presence of the potentially toxic genera *Ostreopsis* and Coolia (Dinophyceae) in the North Aegean Sea, Greece. Harmful Algae 5, 717-730.

Anderson, D.M., Glibert, P.M., Burkholder, J.M., 2002. Harmful algal blooms and eutrophication: Nutrient sources, composition, and consequences. Estuaries 25, 704-726.

Andree, K.B., Fernandez-Tejedor, M., Elandaloussi, L.M., Quijano-Scheggia, S., Sampedro, N., Garces, E., Camp, J., Diogene, J., 2011. Quantitative PCR Coupled with Melt Curve Analysis for Detection of Selected Pseudo-nitzschia spp. (Bacillariophyceae) from the Northwestern Mediterranean Sea. Applied and Environmental Microbiology 77, 1651-1659.

Armi, Z., Turki, S., Trabelsi, E., Ben Maiz, N., 2010. First recorded proliferation of Coolia monotis (Meunier, 1919) in the North Lake of Tunis (Tunisia) correlation with environmental factors. Environmental Monitoring and Assessment 164, 423-433.

Battocchi, C., Totti, C., Vila, M., Maso, M., Capellacci, S., Accoroni, S., Rene, A., Scardi, M., Penna, A., 2010. Monitoring toxic microalgae *Ostreopsis* (dinoflagellate) species in coastal waters of the Mediterranean Sea using molecular PCR-based assay combined with light microscopy. Marine Pollution Bulletin 60, 1074-1084.

Bravo, I., Vila, M., Casablanca, S., Rodriguez, F., Rial, P., Riobo, P., Penna, A., 2012. Life cycle stages of the benthic palytoxin-producing dinoflagellate *Ostreopsis* cf. *ovata* (Dinophyceae). Harmful Algae 18, 24-34.

Brissard, C., Herrenknecht, C., Sechet, V., Herve, F., Pisapia, F., Harcouet, J., Lemee, R., Chomerat, N., Hess, P., Amzil, Z., 2014. Complex Toxin Profile of French Mediterranean *Ostreopsis* cf. *ovata* Strains, Seafood Accumulation and Ovatoxins Prepurification. Marine drugs 12, 2851-2876.

Casabianca, S., Casabianca, A., Riobo, P., Franco, J.M., Vila, M., Penna, A., 2013. Quantification of the Toxic Dinoflagellate *Ostreopsis* spp. by qPCR Assay in Marine Aerosol. Environmental Science & Technology 47, 3788-3795.

Ciminiello, P., Dell'Aversano, C., Dello Iacovo, E., Fattorusso, E., Forino, M., Tartaglione, L., Yasumoto, T., Battocchi, C., Giacobbe, M., Amorim, A., Penna, A., 2013. Investigation of toxin profile of Mediterranean and Atlantic strains of *Ostreopsis* cf. siamensis (Dinophyceae) by liquid chromatography-high resolution mass spectrometry. Harmful Algae 23, 19-27.

Ciminiello, P., Dell'Aversano, C., Dello Iacovo, E., Fattorusso, E., Forino, M., Tartaglione, L., Battocchi, C., Crinelli, R., Carloni, E., Magnani, M., Penna, A., 2012.

Unique Toxin Profile of a Mediterranean *Ostreopsis* cf. *ovata* Strain: HR LC-MSn Characterization of Ovatoxin-f, a New Palytoxin Congener. Chemical Research in Toxicology 25, 1243-1252.

Cohu, S., Mangialajo, L., Thibaut, T., Blanfune, A., Marro, S., Lemee, R., 2013. Proliferation of the toxic dinoflagellate *Ostreopsis* cf. *ovata* in relation to depth, biotic substrate and environmental factors in the North West Mediterranean Sea. Harmful Algae 24, 32-44.

Cohu, S., Lemee, R., 2012. Vertical distribution of the toxic epibenthic dinoflagellates *Ostreopsis* cf. *ovata, Prorocentrum lima* and *Coolia monotis* in the NW Mediterranean Sea. Cahiers De Biologie Marine 53, 373-380.

Cohu, S., Thibaut, T., Mangialajo, L., Labat, J.P., Passafiume, *O.*, Blanfuné, A., Simon, N., Cottalorda, J.M., Lemée, R., 2011. Occurrence of the toxic dinoflagellate *Ostreopsis* cf. *ovata* in relation with environmental factors in Monaco (NW Mediterranean). Marine Pollution Bulletin 62, 2681–2691.

Cruzado, A., Velasquez, Z., Perez, M.D., Bahamon, N., Grimaldo, N.S., Ridolfi, F., 2002. Nutrient fluxes from the Ebre River and subsequent across-shelf dispersion. Continental Shelf Research 22, 349-360.

David, H., Ganzedo, U., Laza-Martinez, A., Orive, E., 2012. Relationships between the presence of *Ostreopsis* (Dinophyceae) in the Atlantic coast of the Iberian Peninsula and sea-surface temperature. Cryptogamie Algologie 33, 199-207.

Fraga, S., Rodriguez, F., Bravo, I., Zapata, M., Maranon, E., 2012. Review of the main ecological features affecting benthic dinoflagellate blooms. Cryptogamie Algologie 33, 171-179.

Furlan, M., Antonioli, M., Zingone, A., Sardo, A., Blason, C., Pallavicini, A., Umani, S.F., 2013. Molecular identification of *Ostreopsis* cf. *ovata* in filter feeders and putative predators. Harmful Algae 21-22, 20-29.

Garrabou, J., Coma, R., Bensoussan, N., Bally, M., ChevaldonnÉ, P., Cigliano, M., Diaz, D., Harmelin, J.G., Gambi, M.C., Kersting, D.K., Ledoux, J.B., Lejeusne, C., Linares, C., Marschal, C., PÉRez, T., Ribes, M., Romano, J.C., Serrano, E., Teixido, N., Torrents, *O.*, Zabala, M., Zuberer, F., Cerrano, C., 2009. Mass mortality in Northwestern Mediterranean rocky benthic communities: effects of the 2003 heat wave. Global Change Biology 15, 1090-1103.

Graneli, E., Vidyarathna, N.K., Funari, E., Cumaranatunga, P.R.T., Scenati, R., 2011. Can increases in temperature stimulate blooms of the toxic benthic dinoflagellate *Ostreopsis ovata*? Harmful Algae 10, 165-172.

Guerrini, F., Pezzolesi, L., Feller, A., Riccardi, M., Ciminiello, P., Dell'Aversano, C., Tartaglione, L., Dello Iacovo, E., Fattorusso, E., Forino, M., Pistocchi, R., 2010. Comparative growth and toxin profile of cultured *Ostreopsis ovata* from the Tyrrhenian and Adriatic Seas. Toxicon 55, 211-220.

Hallegraeff, G.M., 2010. Ocean Climate Change, Phytoplankton Community Responses, and Harmful Algal Blooms: a Formidable Predictive Challenge. Journal of Phycology 46, 220-235.

Hariganeya, N., Tanimoto, Y., Yamaguchi, H., Nishimura, T., Tawong, W., Sakanari, H., Yoshimatsu, T., Sato, S., Preston, C.M., Adachi, M., 2013. Quantitative PCR Method for Enumeration of Cells of Cryptic Species of the Toxic Marine Dinoflagellate *Ostreopsis* spp. in Coastal Waters of Japan. PLoS One 8.

Heisler, J., Glibert, P.M., Burkholder, J.M., Anderson, D.M., Cochlan, W., Dennison, W.C., Dortch, Q., Gobler, C.J., Heil, C.A., Humphries, E., Lewitus, A., Magnien, R., Marshall, H.G., Sellner, K., Stockwell, D.A., Stoecker, D.K., Suddleson, M., 2008. Eutrophication and harmful algal blooms: A scientific consensus. Harmful Algae 8, 3-13.

Jeffrey, S.W., Humphrey, G.F., 1975. New Spectrophotometric Equations for Determining Chlorophylls a, B, C1 and C2 in Higher-Plants, Algae and Natural Phytoplankton. Biochemie Und Physiologie Der Pflanzen 167, 191-194.

Kérouel, R., Aminot, A., 1997. Fluorometric determination of ammonia in sea and estuarine waters by direct segmented flow analysis. Marine Chemistry 57, 265-275.

Laza-Martinez, A., Orive, E., Miguel, I., 2011. Morphological and genetic characterization of benthic dinoflagellates of the genera Coolia, *Ostreopsis* and Prorocentrum from the south-eastern Bay of Biscay. European Journal of Phycology 46, 45-65.

Legrand, C., Rengefors, K., Fistarol, G.*O.*, Graneli, E., 2003. Allelopathy in phytoplankton - biochemical, ecological and evolutionary aspects. Phycologia 42, 406-419.

Mangialajo, L., Ganzin, N., Accoroni, S., Asnaghi, V., Blanfuné, A., Cabrini, M., Cattaneo-Vietti, R., Chavanon, F., Chiantore, M., Cohu, S., Costa, E., Fornasaro, D., Grossel, H., Marco-Miralles, F., Masó, M., Reñé, A., Rossi, A.M., Sala, M.M., Thibaut, T., Totti, C., Vila, M., Lemée, R., 2011. Trends in *Ostreopsis* proliferation along the Northern Mediterranean coasts. Toxicon 57, 408-420.

Mangialajo, L., Bertolotto, R., Cattaneo-Vietti, R., Chiantore, M., Grillo, C., Lemee, R., Melchiorre, N., Moretto, P., Povero, P., Ruggieri, N., 2008. The toxic benthic dinoflagellate *Ostreopsis ovata*: Quantification of proliferation along the coastline of Genoa, Italy. Marine Pollution Bulletin 56, 1209-1214.

Monti, M., Cecchin, E., 2012. Comparative growth of three strains of *Ostreopsis ovata* at different light intensities with focus on inter-specific allelopathic interactions. Cryptogamie Algologie 33, 113-119.

Mounir, B.B., Asma, H., Sana, B.I., Lotfi, M., Abderrahmen, B., Lotfi, A., 2013. What factors drive seasonal variation of phytoplankton, protozoans and metazoans on leaves of Posidonia oceanica and in the water column along the coast of the Kerkennah Islands, Tunisia? Marine Pollution Bulletin 71, 286-298.

Okolodkov, Y.B., del Carmen Merino-Virgilio, F., Antolin Ake-Castillo, J., Concepcion Aguilar-Trujillo, A., Espinosa-Matias, S., Alfredo Herrera-Silveira, J., 2014. Seasonal Changes in Epiphytic Dinoflagellate Assemblages near the Northern Coast of the Yucatan Peninsula, Gulf of Mexic*O.* Acta Botanica Mexicana 107, 121-151.

Parsons, M.L., Aligizaki, K., Bottein, M.-Y.D., Fraga, S., Morton, S.L., Penna, A., Rhodes, L., 2012. Gambierdiscus and *Ostreopsis*: Reassessment of the state of knowledge of their taxonomy, geography, ecophysiology, and toxicology. Harmful Algae 14, 107-129.

Penna, A., Luca, G., 2013. The quantitative real-time PCR applications in the monitoring of marine harmful algal bloom (HAB) species. Environmental Science and Pollution Research 20, 6851-6862.

Penna, A., Fraga, S., Battocchi, C., Casabianca, S., Giacobbe, M.G., Riobo, P., Vernesi, C., 2010. A phylogeographical study of the toxic benthic dinoflagellate genus *Ostreopsis* Schmidt. J. Biogeogr. 37, 830-841.

Penna, A., Vila, M., Fraga, S., Giacobbe, M.G., Andreoni, F., Riobo, P., Vernesi, C., 2005. Characterization of *Ostreopsis* and Coolia (Dinophyceae) isolates in the western Mediterranean Sea based on morphology, toxicity and internal transcribed spacer 5.8s rDNA sequences. Journal of Phycology 41, 212-225.

Perini, F., Casabianca, A., Battocchi, C., Accoroni, S., Totti, C., Penna, A., 2011. New Approach Using the Real-Time PCR Method for Estimation of the Toxic Marine Dinoflagellate *Ostreopsis* cf. *ovata* in Marine Environment. PLoS One 6.

Pezzolesi, L., Guerrini, F., Ciminiello, P., Dell'Aversano, C., Dello Iacovo, E., Fattorusso, E., Forino, M., Tartaglione, L., Pistocchi, R., 2012. Influence of temperature and salinity on *Ostreopsis* cf. *ovata* growth and evaluation of toxin content through HR LC-MS and biological assays. Water Research 46, 82-92.

Pfannkuchen, M., Godrijan, J., Pfannkuchen, D.M., Ivesa, L., Kruzic, P., Ciminiello, P., Dell'Aversano, C., Dello Iacovo, E., Fattorusso, E., Forino, M., Tartaglione, L., Godrijan, M., 2012. Toxin-Producing *Ostreopsis* cf. *ovata* are Likely to Bloom Undetected along Coastal Areas. Environmental Science & Technology 46, 5574-5582.

Pistocchi, R., Pezzolesi, L., Guerrini, F., Vanucci, S., Dell'Aversano, C., Fattorusso, E., 2011. A review on the effects of environmental conditions on growth and toxin production of *Ostreopsis ovata*. Toxicon 57, 421-428.

Reise, K., van Beusekom, J.E.E., 2008. Interactive effects of global and regional change on a coastal ecosystem. Helgoland Marine Research 62, 85-91.

Rekik, A., Maalej, S., Ayadi, H., Aleya, L., 2013. Restoration impact of an uncontrolled phosphogypsum dump site on the seasonal distribution of abiotic variables, phytoplankton and zooplankton along the near shore of the south-western Mediterranean coast. Environmental Science and Pollution Research 20, 3718-3734.

Rhodes, L., 2011. World-wide occurrence of the toxic dinoflagellate genus *Ostreopsis* Schmidt. Toxicon 57, 400-407.

Riobo, P., Paz, B., Franco, J.M., Vazquez, J.A., Murado, M.A., 2008. Proposal for a simple and sensitive haemolytic assay for palytoxin Toxicological dynamics, kinetics, ouabain inhibition and thermal stability. Harmful Algae 7, 415-429.

Romagnoli, T., Totti, C., Accoroni, S., De Stefano, M., Pennesi, C., 2014. SEM analysis of the epibenthic diatoms on Eudendrium racemosum (Hydrozoa) from the Mediterranean Sea. Turkish Journal of Botany 38, 566-594.

Sabanci, F.C., 2012. Taxonomic Survey of Benthic Diatoms on Natural Substrata From Coastal Lagoon (Aegean Sea, Turkey). Turkish Journal of Fisheries and Aquatic Sciences 12, 841-849.

Sahraoui, I., Bouchouicha, D., Mabrouk, H.H., Hlaili, A.S., 2013. Driving factors of the potentially toxic and harmful species of Prorocentrum Ehrenberg in a semi-enclosed Mediterranean lagoon (Tunisia, SW Mediterranean). Mediterranean Marine Science 14, 353-362.

Salat, J., Garcia, M.A., Cruzado, A., Palanques, A., Arin, L., Gomis, D., Guillen, J., de Leon, A., Puigdefabregas, J., Sospedra, J., Velasquez, Z.R., 2002. Seasonal changes of water mass structure and shelf slope exchanges at the Ebre shelf (NW Mediterranean). Continental Shelf Research 22, 327-348.

Scalco, E., Brunet, C., Marino, F., Rossi, R., Soprano, V., Zingone, A., Montresor, M., 2012. Growth and toxicity responses of Mediterranean *Ostreopsis* cf. *ovata* to seasonal irradiance and temperature conditions. Harmful Algae 17, 25-34.

Selina, M.S., Morozova, T.V., Vyshkvartsev, D.I., Orlova, T.Y., 2014. Seasonal dynamics and spatial distribution of epiphytic dinoflagellates in Peter the Great Bay (Sea of Japan) with special emphasis on *Ostreopsis* species. Harmful Algae 32, 1-10.

Selina, M.S., Orlova, T.Y., 2010. First occurrence of the genus *Ostreopsis* (Dinophyceae) in the Sea of Japan. Botanica Marina 53, 243-249.

Shears, N.T., Ross, P.M., 2009. Blooms of benthic dinoflagellates of the genus *Ostreopsis*; an increasing and ecologically important phenomenon on temperate reefs in New Zealand and worldwide. Harmful Algae 8, 916-925.

Simoni, F., Gaddi, A., Di Paolo, C., Lepri, L., 2003. Harmful epiphytic dinoflagellate on Tyrrhenian Sea reefs. Hamrful Algae News 24, 13–14.

Sullivan, M.J., Currin, C.A., 2000, Community structure and functional dynamics of benthic microalgae in salt marshes. Concepts and Controversies in Tidal Marsh Ecology, pp. 81-106.

Tanimoto, Y., Yamaguchi, H., Yoshimatsu, T., Sato, S., Adachi, M., 2013. Effects of temperature, salinity and their interaction on growth of toxic *Ostreopsis* sp 1 and *Ostreopsis* sp 6 (Dinophyceae) isolated from Japanese coastal waters. Fisheries Science 79, 285-291.

Tichadou, L., Glaizal, M., Armengaud, A., Grossel, H., Lemee, R., Kantin, R., Lasalle, J.L., Drouet, G., Rambaud, L., Malfait, P., de Haro, L., 2010. Health impact of

unicellular algae of the *Ostreopsis* genus blooms in the Mediterranean Sea: experience of the French Mediterranean coast surveillance network from 2006 to 2009. Clinical Toxicology 48, 839-844.

Tindall, D.R., Miller, D.M., Bomber, J.W., 1989. Culture and Toxicity of Dinoflagellates from Ciguatera Endemic Regions of the World. Toxicon 27, 83-83.

Totti, C., Accoroni, S., Cerino, F., Cucchiari, E., Romagnoli, T., 2010. *Ostreopsis ovata* bloom along the Conero Riviera (northern Adriatic Sea): Relationships with environmental conditions and substrata. Harmful Algae 9, 233-239.

Totti, Cucchiari, De, S., Pennesi, Romagnoli, Bavestrello, 2007. Seasonal variations of epilithic diatoms on different hard substrates, in the northern Adriatic Sea. Marine Biological Association of the United Kingdom. Journal of the Marine Biological Association of the United Kingdom 87, 649-658.

Tubaro, A., Durando, P., Del Favero, G., Ansaldi, F., Icardi, G., Deeds, J.R., Sosa, S., 2011. Case definitions for human poisonings postulated to palytoxins exposure. Toxicon 57, 478-495.

Utermöhl H., 1958. Zur Vervollkomnung der quantitativen Phytoplankton-Methodik. Mitt. int. Ver. ther. angew. Limnol 9, 1-38.

Vanucci, S., Guerrini, F., Pezzolesi, L., Dell'Aversano, C., Ciminiello, P., Pistocchi, R., 2012a. Cell growth and toxins' content of *Ostreopsis* cf. *ovata* in presence and absence of associated bacteria. Cryptogamie Algologie 33, 105-112.

Vanucci, S., Pezzolesi, L., Pistocchi, R., Ciminiello, P., Dell'Aversano, C., Dello Iacovo, E., Fattorusso, E., Tartaglione, L., Guerrini, F., 2012b. Nitrogen and phosphorus limitation effects on cell growth, biovolume, and toxin production in *Ostreopsis* cf. *ovata*. Harmful Algae 15, 78-90.

Vidyarathna, N.K., Graneli, E., 2013. Physiological responses of *Ostreopsis ovata* to changes in N and P availability and temperature increase. Harmful Algae 21-22, 54-63.

Vidyarathna, N.K., Granéli, E., 2011. Influence of temperature on growth, toxicity and carbohydrate production of a Japanese *Ostreopsis ovata* strain, a toxic-bloom-forming dinoflagellate. Aquatic Microbial Ecology 65, 261-270.

Vila, M., Garces, E., Maso, M., 2001a. Potentially toxic epiphytic dinoflagellate assemblages on macroalgae in the NW Mediterranean. Aquatic Microbial Ecology 26, 51-60.

Vila, M., Camp, J., Garces, E., Maso, M., Delgado, M., 2001b. High resolution spatio-temporal detection of potentially harmful dinoflagellates in confined waters of the NW Mediterranean. Journal of Plankton Research 23, 497-514.

Waycott, M., Duarte, C.M., Carruthers, T.J.B., Orth, R.J., Dennison, W.C., Olyarnik, S., Calladine, A., Fourqurean, J.W., Heck, K.L., Hughes, A.R., Kendrick, G.A., Kenworthy, W.J., Short, F.T., Williams, S.L., 2009. Accelerating loss of seagrasses across the globe threatens coastal ecosystems. Proceedings of the National Academy of Sciences of the United States of America 106, 12377-12381.

Yamaguchi, H., Yoshimatsu, T., Tanimoto, Y., Sato, S., Nishimura, T., Uehara, K., Adachi, M., 2012. Effects of temperature, salinity and their interaction on growth of the benthic dinoflagellate *Ostreopsis* cf. *ovata* (Dinophyceae) from Japanese coastal waters. Phycological Research 60, 297-304.

Zina, A., Elbahri, T., Souad, T., Naceur, B., Ezzeddine, M., 2012. Composition and dynamics of potentially toxic dinoflagellates in a shallow Mediterranean lagoon. Oceanological and Hydrobiological Studies 41, 25-35.

CHAPTER 5

General Discussion

5.1. Contribution to the genus *Ostreopsis*

Morphological features are very much alike among the nine *Ostreopsis* species identified until date. Contradictions in the characterization of certain species by different authors have resulted in an ambiguity when referring to them, and no solution in that matter has been proposed yet. This reflects the urgent need to revise and harmonise the strategy when approaching the taxonomy of the genus *Ostreopsis*. Recently, molecular biology methodologies have been implemented to provide additional information on the species description, as morphological characterization is definitively not sufficient. Taxonomists have to confront a crucial problem at this point since no genetic material from the initial species is available, which makes difficult the assignment of new generated sequences to a specific species. As a consequence, the two most studied species in the last decade, *O.* cf. *siamensis* and *O.* cf. *ovata* use the "cf." terminology in their assignation, waiting for a confirmation in the attribution to the original morphotype or, on the contrary, the description of a new species. In order to shed light on this issue, it has been suggested to re-isolate cells from sites where species were first described, such as Reunion Island, in order to obtain genetic and morphological material. With the exception of *O. heptagona*, all the species of the genus have been reported in the Mascarene Islands, in the Indian Ocean. Hence, the chances of finding the primary described morphotypes in that area are very high.

After an initial morphological overview of *Ostreopsis* spp cells, collected on macroalgae in the coral reef of the western coast of Reunion Island, two types of cell sizes were identified (two morphotypes). As a result of cells isolation from these samples, a total of thirty three strains were sequenced in our study. Subsequently, a phylogenetic analysis from the ITS-5.8S rDNA was performed, differentiating three distinct genotypes. The group of cells corresponding to the larger morphotype found in the microalgae community, were clustered into a same genetic clade. The sequences were closely related with *Ostreopsis* sp 5 identified in Sato *et al.,* 2011. Morphologically, our description was limited to light microscopy, so the characterization was incomplete to establish a correspondence, being essential further analysis with scanning electron microscope. However, cell dimensions average, dorsoventral and width diameters, fitted within the order of magnitude of *O. marinus* size described in Faust, 1999. From this result, there is a high probability that this stain could be *O. marinus*. However, we cannot conclude without more exhaustive morphological and genetic analysis.

As for the second morphotype, smaller than the other morphotype, found in isolated strains from field samples, the phylogenetic analysis reported two different genotypes. The major number of isolates were clustered together but not aligned with any other sequence from GenBank. Regarding cell sizes, as the average cell dimensions from field samples did not correspond to a single species, we could not confirm a specific size. Nevertheless, based on the cellular oblong shape and the

species previously reported in these waters, we can speculate that the unidentified species found in Reunion Island corresponded to *O. caribbeanus* or *O. belizeanus,* or eventually to a not previously identified species.

The second genotype belonging to the small sized group of cells was clustered in the *O.* cf. *ovata* from the Indo-Pacific clade. Comparing with cells isolated from our sampling sites in the NW Mediterranean Sea, *O.* cf. *ovata* was grouped within the Atlantic-Mediterranean clade. This sub-division reflects the geographical distance among both strains, possibly caused by the formation of the Isthmus of Panama, separating two different climate regions. However, considering the increasing number of studies focused on *Ostreopsis* spp., new insights appear on the knowledge of the genus. Interestingly, *O.* cf. *ovata* strains that belong to the Mediterranean-Atlantic clade have been detected in Japan. This result reflects a gene flow, probably due to anthropogenic activities. Taking into consideration the presence of resting cells in the life cycle of benthic dinoflagellates, cysts of *Ostreopsis* spp. could be encounterd especially as overwinter populations, and these may have the capacity to survive in ballast waters.

Some species of the genus *Ostreopsis* are producers of PLTX and PLTX analogs which constitute a risk to human health and marine ecosystems. For this reason, we analyzed the toxic potency of cell extracts of *Ostreopsis* strains through haemolytical assay. From the strains isolated in Reunion Island, we did not detect PLTX-like compounds in any of the three genotypes. Our results are in agreement with toxic analysis performed in *Ostreopsis* sp 5 and *O.* cf. *ovata,* belonging to the same genetic clade, isolated in Japanese waters, which proved to be non toxic. The description of toxin content supposes additional information in the species definition that may contribute to clarify taxonomical discrepancies. As far as the characterization of these species is concerned, the complementary genetic and toxicological description with other strains increases the probability that they may be the same species.

Contrarily, *O.* cf. *ovata* strains isolated in the Mediterranenan Sea were clustered in a different genetic clade separated from the Indo-Pacific population and resulted to be PLTX-like compounds producers. A deep study was performed regarding toxin profile by liquid chromatography coupled with mass spectrometry. Palytoxin analogs toxin profile was similar to the majority of Mediterranean strains studied until date, dominated by ovatoxin-a. However, particular toxin profiles have been detected in some strains of the Mediterranean Sea. This variation among isolates from the same population may come from specific nucleotides polymorphism related with toxin biosynthesis. Further investigation is needed to better understand differences in toxin profiles within the same species.

5.2. Cell enumeration and detection methodologies

Precise enumeration of benthic dinoflagellates, especially *Ostreopsis* spp, is a challenge since they produce mucilage that embeds cells, forming aggregates. This circumstance makes very difficult to homogenize samples in order to obtain

accurate cell abundance estimations. Different strategies have been attempted in order to reduce the error. The addition of chemicals, such as hydrocloridric acid or sodium-ethylenediaminetetraacetic acid to fixed samples for microscopy counting, has been the most used methods by several authors. It is hypothesized that, as the mucilage consist of polysaccharides, the contact with these solutions may minimize ionic interactions, disaggregating cells. We performed an experiment testing those two strategies evaluating sample and settling volumes. In order to perform an accurate growth curve, we recommend not treating samples during the exponential phase, and adding sodium-ethylenediaminetetraacetic acid the rest of growth phases. It is likewise suggested to take big sample ($\geq$ 10 mL) and settlement (3 mL) volumes.

Regarding cell enumeration in field samples, it is highly important to have simultaneously an accurate identification of the species and a toxicity evaluation of some of them, since they may represent a human threat. In that sense, in recent years, qPCR methodologies have gained importance in field research. This technique provides high reproducibility efficiency and sensibility, crucial for monitoring programs where a great number of samples have to be processed. The early detection of toxic *Ostreopsis* spp. present in field samples may prevent potential risks. Unfortunately, our qPCR methodology needs to evaluate more samples in order to achieve an accurate cell enumeration method. However, in our study, by the use of qPCR we could discard the presence of *O.* cf. *siamensis* in our blooms, dominated exclusively by *O.* cf. *ovata*. The support with molecular biology analisis is crucial since it is practically impossible to distinguish between these two species under light microscopy with such high cells concentrations in samples.

5.3. Effects of environmental factors on *O.* cf. *ovata* physiology

5.3.1. Temperature and salinity under controlled conditions

O. cf. *ovata*, which is distributed in different areas worldwide, is able to grow in a wide range of environmental conditions, both in tropical and temperate areas. Temperature seems to be the most important factor influencing growth. However, the interaction with other environmental parameters may represent the inflection point for a bloom development. In order to study the interaction with salinity, we performed a multi-factorial experiment with two strains acclimated for one year. We observed that, at 19°C and all salinities, the stationary phase was not achieved and aberrant cells were present since the first days of growth, indicating sub-optimal conditions. For higher temperatures, growth rates were above 0.3 div. day^{-1}. Average growth rate was higher at 24°C than at 28°C and significantly influenced by salinity in both temperatures. Interestingly, at 28°C, maximum values were found at 36 and decreasing in growth was detected at 32 and 38. We can thus hypothesize that for long periods of warm temperature and high salinity, predicted in the following years in the scenarios of climate change, *O.* cf. *ovata* growth may not be enhanced. However, although in these conditions blooms may not be intensified, the frequency

or duration of blooms may increase as warm temperatures will last longer. In any case, there are many other environmental factors involved in microalgae dynamics, and for that reason, results obtained in experimental studies cannot be directly extrapolated to environmental conditions, thus conclusions should be taklen with caution. In that sense, we conducted a field survey in order to evaluate these factors in natural conditions.

5.3.2. O. cf. ovata dynamics in the Ebre Delta area

Sampling sites were located in the rocky coast area, adjacent to the Ebre Delta, in the NW Mediterranean Sea. We observed a seasonal pattern in *O.* cf. *ovata* distribution, already reported in many studies performed in temperate waters, in accordance with water temperature variability during the year. No cells were detected for temperatures under 16°C. The average water temperature in sampling sites during blooms period (when epiphytic cells were higher than 5×10^4 cell.g fwm^{-1}) was 24.49±1.96°C, coinciding most blooms when temperatures started to decrease. This fact may indicate that it is the duration of warm water what drives the formation of blooms and not maximal temperatures. Meanwhile, salinity during this period was 37.32±1.69 and no blooms were observed for salinities under 30, also in agreement with the average conditions observed in other Mediterranean blooms.

A spatial pattern was also detected in our study area. Southern sites, apparently, were more influenced by freshwater inputs, resulting in lower salinities and higher concentration of silicates and nitrates, finding a slightly significant correlation between *O.* cf. *ovata* abundance and these factors. A higher number of blooms were registered in the north, which led to hypothesize that water conditions in the north could be more favorable than in the south. Nevertheless, some sites registered a higher number of blooms respect to other sites where water conditions were similar. This spatial heterogeneity in *O.* cf. *ovata* blooms has been reported in other studies showing that it may have preference for certain spots.

In our study, we registered wind speed during sampling, finding stronger values in the north, coinciding with higher number of blooms, than in the south. Though we cannot directly extrapolate blooms to wave motion, since other factors are involved, we may suggest that probably *O.* cf. *ovata* in temperate areas has preference for "moderate wave exposure" than for "quite waters", as found in other studies. The production of a mucilaginous mat providing attachment to the substrate may represent an adequate strategy for growth under conditions of "moderate wave exposure".

Regarding the epiphytic microalgal community, a similar assemblage was found in all samples dominated by small-sized diatoms, a group of generalists' species occuring in widely varying conditions. However, a spatial distribution was also reflected in the rest of microalgae epiphytic community. Higher amount of diatoms were observed in the south compared with the north, which may be due to higher

silicate concentrations that favored their growth. Nevertheless, though less frequent, intense blooms of *O.* cf. *ovata* also occurred in southern sites.

Ostreopsis cf. *ovata* ecological niche was more restricted than the rest of species or group of species studied, highlighting temperature as a determinant factor, together with a strong influence of salinity and wind speed on *O.* cf. *ovata* growth. Nevertheless, the effect of environmental factor interactions involved in microalgae dynamics is difficult to ascertain. As an example, indirect responses from grazers and macroalgae life cycle changes according to water conditions affect epiphytic communities. However, these factors are not always considered in *Ostreopsis* spp. studies. An effort has to be done in the knowledge of microalgae proliferations in benthic ecosystems as they undergo specific dynamics, different from planktonic communities. In this context, in order to develop future predictive models for the formation of blooms in this particular habitat, a high number of data is necessary. Nevertheless, quantification of some environmental factors is not an easy task, so the interpretation of results will have to be taken with caution.

5.3.3. Physiological responses to environmental factors

Cultured and field cells were measured in order to evaluate the morphological response in relation to different environmental factors. In the literature, variability in cell size within the same strain or population has been observed in cultured and natural cells, and this was also observed in other studies. Results derived from the multi-factorial experiment, showed that during the exponential phase, there were a higher amount of small cells. It has been hypothesized that these could represent vegetative cells that undergo an active division, contributing to increase the number of cells. In the same way, cells size in field populations increased after the exponential phase. Interestingly, populations of *O.* cf. *ovata* from the northern site had significantly smaller average cell size than in the south. This result could reflect the fact that environmental conditions in northern sites could be more favorable for growth of *O.* cf. *ovata* resulting in an active cell division.

As mentioned above, *O.* cf. *ovata* strains from the Mediterranean resulted to be PLTX analog producers. Similar results have been observed among Mediterranean strains with increasing toxin content during growth phases and the highest amounts at the end of the stationary phase. It is still unclear to what extent toxin production is linked with environmental conditions. Further investigation is necessary in order to better understand toxin synthesis. In our multi-factorial experiment, we did not find correlations between toxin content and growth rate, however, at 28°C, cell toxicity increased earlier within the growth phases than at 24°C. We can thus hypothesize that at higher temperatures toxin production may be accelerated by other routes not implicated in cell growth.

As far as toxin profile is concerned, *O.* cf. *ovata* from the Mediterranean Sea produce ovatoxins as the major component in similar percentages among the two studied strains. However, for some other strains coming from distinc areas of the

Mediterranean Sea, new analogs or different proportions of toxins have been described, constituting a strain-specific marker.

CHAPTER 6

Conclusions and Future work

6.2 Conclusions

Three genotypes of the genus *Ostreopsis* were described in Reunion Island. Isolates with a morphotype fitting *O. marinus* original description were clustered close to *Ostreopsis* sp 5 described by Sato *et al.,* (2011) genetic clade. The strains did not show palytoxin-like compounds production. *Ostreopsis* cf. *ovata* was present in the benthic microalgae population, corresponding to the Indo-Pacific clade, as concluded by phylogenetic analyses. Toxicity was discarded. An unidentified species, not previously sequenced could correspond to *O. carribeanus*, *O. belizeanus* or a new species. Non toxicity was found for this genotype.

For accurate cell estimation abundance in *Ostreopsis* spp. we obtained less variability in cell countings from big subsamples and settlement volumes (larger than 10 and 3 mL, respectively). The addition of Na-EDTA to samples after the exponential phase would contribute to disrupt aggregates and obtain a higher homogeneity.

O. cf. *ovata* from the NW Mediterranean Sea is able to grow in a wide range of temperatures (19-28°C) and salinities (32-38).
Highest average growth rates were found at 24°C. At 19°C, growth was reduced and aberrant cells were present during all growth phases.
Both at 24 and 28°C, growth rates showed significant differences according to salinities. At 28°C growth rates were significantly lower at salinities 32 and 38 in relation to salinity 36.
A positive correlation between small size cells and growth rate during the exponential phase was observed.
Toxin content increased with time in all salinities at 24 and 28°C. Toxicity of the cultures was higher at 28°C than at 24°C. Toxin profiles did not change with different conditions of temperature, or salinity, and it was similar to the majority found in the Mediterranean clade.
In the Ebre Delta surrounding areas, within the genus *Ostreopsis*, a single genotype, *O.* cf. *ovata,* was present, and *O.* cf. *siamensis* was absent.
Temperature was the most determinant factor influencing the presence of *O.* cf. *ovata*, reflected by a seasonal pattern, where the presence of cells was restricted to temperatures above 16°C which represents a restricted ecological niche.
The significant correlations of *O.* cf. *ovata* abundances with high salinities and low nitrate and silicate concentrations, constitued a more favorable growth conditions, reflected by a higher number of blooms in the area were those conditions were found.
In the more favorable conditions of growth for *O.* cf. *ovata*, where higher densities of cells were encountered, cell size resulted to be smaller.

6.3. Future work

Further morphological analysis is required to assign correctly the genotypes found in Reunion Island to original holotypes. This would contribute to reassess the controversial status of the taxonomy of the genus *Ostreopsis*.

As for the influence of biotic and abiotic factors on *Ostreopsis* spp. growth, the development of a predictive model adapted to benthic ecosystems is crucial for the coastal authorities. Collecting all available data is necessary in order to project future distributions and blooms proliferations derived from scenarios of global change, facilitating management actions to protect human health and the environment.

Implementing surveillance of epiphytic community in monitoring programs is recommended, and if possible, including qPCR analyses in order to identify potentially toxic species and prevent potential risks.

ANNEX

Additional scientific contribution
submitted to Analytical and
Bioanalytical Chemistry

Putative Palytoxin and the Novel Ovatoxin-g from *Ostreopsis* cf. *ovata* (NW Mediterranean Sea): Structural Insights by Liquid Chromatography-High Resolution Mass Spectrometry

María García-Altares,[1,#] Luciana Tartaglione,[2,#] Carmela Dell'Aversano,[2,*] Olga Carnicer,[1] Pablo de la Iglesia,[1] Martino Forino,[2] Jorge Diogène,[1] Patrizia Ciminiello[2]

[1] IRTA, Seguiment del Medi Marí. Carretera de Poble Nou, km 5.5, 43540 Sant Carles de la Ràpita, Spain.

[2] Dipartimento di Farmacia, Università degli Studi di Napoli Federico II, Via D. Montesano 49, 80131 Napoli, Italy.

*Correspondence to Carmela Dell'Aversano; e-mail dellaver@unina.it.

#These authors contributed equally to this work.

Running title: Putative palytoxin and ovatoxin-g by LC-HRMS

Abstract

Blooms of the benthic dinoflagellate *Ostreopsis* cf. *ovata* are a concern in the Mediterranean Sea, since this species produces a wide range of palytoxin-like compounds listed among the most potent marine toxins. This study focused on two analogs of palytoxin found in cultures of six strains of *Ostreopsis* cf. *ovata* isolated from the south of Catalonia (NW Mediterranean Sea). In addition to some already known ovatoxins, our strains produced two minor compounds, ovatoxin-g and an isomer of palytoxin (putative palytoxin), whose structures had not been elucidated before. Insufficient quantity of these compounds impeded a full NMR-based structural elucidation, thus we studied their structure through Liquid Chromatography Electro Spray Ionization High Resolution Mass Spectrometry[n] (LC-ESI-HRMS[n]) in positive ion mode. Under the used MS conditions, the molecules underwent fragmentation at many sites of their backbone and a large number of diagnostic fragment ions were identified. As a result, tentative structure was assigned to both ovatoxin-g and putative palytoxin.

Introduction

Ovatoxins (OVTXs) are complex macromolecules produced by the benthic dinoflagellate Ostreopsis cf. ovata (Figure 1) [1-3]. Structurally, they are closely related to palytoxin (PLTX, C129H223N3O54), one of the most toxic non-peptidic marine compound (LD50 by intra-venous administration of 0.15 µg/kg in mouse) [4] first isolated from soft corals of the genus Palythoa [5-7] (Figure 1).

Although little is known on their toxicity [8], ovatoxins have been frequently involved in several Ostreopsis-related toxic outbreaks following inhalation of marine aerosols in the Mediterranean basin [9-11]. The presence of ovatoxins and O. cf. ovata cells in the aerosols has been recently proved by chemical and biomolecular means [12, 13].

Within the complex pool of palytoxin-like compounds produced by Mediterranean O. cf. ovata, OVTX-a usually represents the major component of the toxin-profile, accounting for about 60% of the total toxin content [3]. In most of the analyzed strains, OVTX-a is followed by OVTX-b, OVTX-d and/or –e, OVTX-c, and a putative palytoxin (pPTLX), listed in decreasing order of abundance. Putative PLTX was the first analog of the toxin profile to be discovered [1] based on liquid chromatography tandem mass spectrometry (LC-MS/MS) evidences. The term "putative" was added since, due to the complex stereo-structure of palytoxin molecule (Figure 1), the possibility that the detected compound was a structural- and/or a stereo-isomer of palytoxin itself could not be excluded.
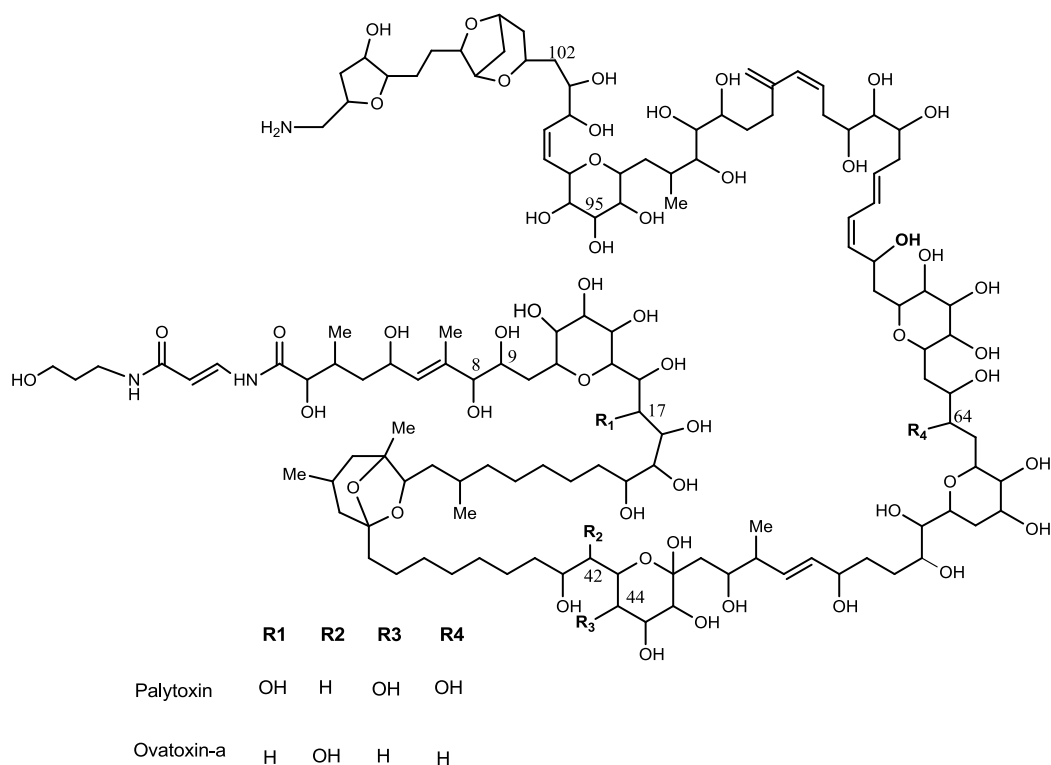
Fig. 1 Planar structure of palytoxin ($C_{129}H_{223}N_3O_{54}$) from the soft coral *Palythoa tuberculosa* [6, 18] and ovatoxin-a ($C_{129}H_{223}N_3O_{52}$) from the Mediterranean dinoflagellate *Ostreopsis* cf. *ovata* [6, 18].

O. cf. ovata toxin profiles have been proven to be strain-specific, since some strains lack some toxins and/or produce individual toxins with different relative abundances. For example, unlike most of the analyzed Italian O. cf. ovata strains presenting the typical toxin profile [2], some were found not to produce OVTX-b and –c [14]. In addition, OVTX-f was identified only in one strain, of which it also represented the major toxin [3]. Recently, a O. cf. ovata strain from the French Mediterranean coast has been reported to produce all the ovatoxins (OVTX-a to –f) and quite high levels of pPLTX (12% of the total toxin content) [15]. Toxins scenario becomes even more complicate considering toxin profiles of Ostreopsis spp. strains from Japan, that produce a number of different isomers of ovatoxins, namely ovatoxins AC [16] and ovatoxins IKA2 [17]. Such findings suggest that toxin profiles may be a valuable feature to characterize new strains of O. cf. ovata belonging to the same genetic clade.

Only ovatoxin-a has been isolated and stereo-structurally elucidated by NMR [14, 18]. For all the other ovatoxins, their quantity in O. cf. ovata extracts was not sufficient for a full NMR-based structural elucidation, and only high resolution (HR) LC-MS data have been provided [19]. They include (a) elution order of the toxins on reversed phase column, (b) molecular formulae of protonated and adduct ions of multiple charge states (1+, 2+ and 3+) which are contained in their full HRMS

spectra, and (c) preliminary structural information deriving from the favoured cleavage between C-8 and C-9 in fragmentation spectra (Figure 1).

More detailed insights into the chemical structures of ovatoxins can be obtained through LC-MS/MS methods, especially when low concentrations of toxins hamper any NMR-based investigation. In 2012, Ciminiello et al. developed a LC-HRMSn method on the LTQ-Orbitrap, highlighting that palytoxin-like compounds undergo characteristic fragmentations at several sites of their skeleton in positive ion mode [20]. The fragmentation behavior proved useful for gaining structural insights into ovatoxin-a in crude extract [20], that were all confirmed by an NMR-based study on pure compound [14] . The approach was successively used for a preliminary structural characterization of OVTX-f which turned out to differ from OVTX-a only in the C-95/C-102 region (Figure 1) [3]. In 2013, Uchida et al. [17] proposed a LC-QTOFMS method in both positive and negative ion modes for structural characterization of ovatoxins IKA2; it allowed to identify sites where such compounds are different from the Mediterranean OVTXs.

In this paper we report on the chemical analysis of O. cf. ovata strains from Spain where blooms of Ostreopsis spp. have been reported since 2001 [21]. O. cf. ovata was the dominant species but occasionally coexisted with O. cf. siamensis [10]. In some cases, blooms have caused respiratory distress in humans [10, 11, 22]. Although studies based on LC with fluorescence detection (LC-FLD) and LC-MS have highlighted the presence of palytoxin-like compounds in some Spanish strains [23], algal toxin profiles have not been detailed yet [10]

Since the summer of 2011, the presence of O. cf. ovata has been detected in the south of Catalonia at the Ebre River Delta (Carnicer et al., submitted). Several strains of O. cf. ovata were isolated from this area and included in the Mediterranean clade according to their genetic characterization.

We here report on LC-HRMSn quali-quantitative investigation of the toxin profile of six cultured O. cf. ovata strains from the Ebre River Delta. Besides identifying the most common ovatoxins in the algal extracts, we gained structural insights into putative PLTX and the novel ovatoxin-g.

Experimental

Chemicals and Materials

For extraction, methanol gradient grade for HPLC was purchased from Merck (Darmstadt, Germany) and ultrapure water was obtained though a Milli-Q purification system (resistivity >18 MW•cm) from Millipore (Bedford, MA). For LC-MS analyses, acetonitrile (HPLC grade) and water (HPLC grade) were purchased from Sigma Aldrich (Steinheim, Germany). Glacial acetic acid (laboratory grade) was purchased from Carlo Erba (Milan, Italy). Palytoxin standard (from Palythoa tuberculosa) was purchased from Wako Chemicals GmbH (Neuss, Germany). An

Adriatic O. cf. ovata extract previously characterized (strain OOAN0601) [23] was used as reference for the Mediterranean ovatoxins.

Collection, Identification and Culturing of Ostreopsis cf. ovata strains

Six strains of O. cf. ovata (IRTA-SMM-11-10 from August 2011; IRTA-SMM-12-38, IRTA-SMM-12-46, IRTA-SMM-12-51, IRTA-SMM-12-57 and IRTA-SMM-12-62 from August 2012) were isolated from macroalgae samples (Jania rubens) collected in south Catalonia rocky coasts. Cells were isolated by the capillary method [24] and identified under an inverted microscope (Leica DM-IL). Full detailed description of the isolation, morphological and genetic characterization of the O. cf. ovata strains is described in Carnicer et al. 2014 (submitted). Cultures were made in 500 mL with autoclaved natural filtered seawater and one of them (IRTA-SMM-11-10) was scaled-up to 4 L. Salinity was set at 36, temperature at 24oC, and illumination was set to 100 μmol photons m-2·s-1 under 12:12-h light:dark photoperiod. Extraction of DNA was performed according to Andree et al. [25] and polymerase chain reaction (PCR) conditions were set as in Sato et al. [26]. Resulted fragments of rRNA were sequenced bidirectionally by Sistemas Genómicos LLC (Valencia, Spain). Molecular analyses confirmed the identity of O. cf. ovata in all the strains.

Cell counting was performed in aliquots of each culture using the Utermöhl method [27] as described in Carnicer et al. 2014 (submitted). Cultures were collected in the late stationary phase. Cell densities where 3.6·106 cell/L in IRTA-SMM-11-10, 5.3·105 cell/L in IRTA-SMM-12-38, 9.0·105 cell/L in IRTA-SMM-12-46, 6.2·105 cell/L in IRTA-SMM-12-51, 7.1·105 cell/L in IRTA-SMM-12-57 and 5.2·105 cell/L in IRTA-SMM-12-62. The cultures were filtered under mild vacuum conditions thought 0.45 μm GF filters and stored at -80oC until extraction.

Extraction

Cell pellets on filters were extracted with 5 mL of methanol/water solution (80:20, v/v), vortex-mixed for 30 seconds by MS2 Minishaker (IKA Labortechnik, Staufen, Germany) and sonicated for 35 minutes in pulse mode at 37% amplitude with in an ultrasonic processor Vibra-CellTM (Sonics and Materials, Inc., Newton, CT, USA) while cooling in ice bath. The mixture was centrifuged at 2000 rpm for 10 minutes using Jouan MR 23i Centrifuge (Thermo Fisher Scientific Inc., Waltham, MA, USA) and the supernatant was decanted and then filtered by 0.45 μm nylon membrane syringe filters. This procedure was repeated thrice. The extracts were combined, evaporated and made up to a final volume of 10 mL with the extracting mixture. Extraction was slightly modified for strain IRTA-SMM-11-10 (scaled up culture); its filters were extracted thrice with 10 mL of methanol/water solution

(80:20, v/v) and made up to a final volume of 20 mL. The extracts were stored at -20ºC until analyses.

Liquid Chromatography-High Resolution Mass Spectrometry (LC-HRMS)

The analysis were performed on a hybrid linear ion trap LTQ Orbitrap XL™ Fourier transform mass spectrometer (FTMS) equipped with an ESI ION MAX™ source (Thermo Fisher, San José, USA) coupled to an Agilent 1100 LC binary system (Palo Alto, CA, USA). The following LC-HRMS method developed by Ciminiello et al (submitted) was used, slightly modifiying the gradient condition to achieve a complete chromatographic resolution of the new ovatoxins. A column of 2.7 μm Poroshell 120 EC-C18, 100 x 2.10 mm (Agilent), was kept at room temperature and eluted at 0.2 mL/min with water (eluent A) and 95% acetonitrile/water (eluent B), both containing 30 mM acetic acid. Gradient elution was 28-29% B in 10 min., 29-30% B in 10 min., 30-100% B in 1 min, and hold for 1 min. Re-equilibration time was 13 min. Injection volume was 5 μL.

High Resolution full MS experiments (positive ions) were acquired in the m/z 700-1600 range at a resolving power of 60,000. The following source settings were used: spray voltage = 4.8 kV; capillary temperature = 290 ºC; capillary voltage = 50 V; sheath gas flow = 32 and auxiliary gas flow = 4 (arbitrary units); tube lens voltage = 130 V.

High Resolution collision induced dissociation (CID) MS2 experiments were acquired at a resolving power of 60,000 (FWHM at m/z 400) using a collision energy (CE) = 35%, isolation width (IW) = 4.0 Da, activation Q = 0.250 and activation time (at) = 30 msec. The precursors were [M+H+Ca]3+ ions at m/z 906.8 (pPLTX and PLTX), m/z 896.1 (OVTX-a), m/z 910.8 (OVTX-b), m/z 916.1 (OVTX-c), m/z 901.4 (OVTX-d and -e) and m/z 890.8 (OVTX-g).

Calculation of elemental formulae was performed on the mono-isotopic peak of each ion cluster using Xcalibur software v2.0.7. with a mass tolerance of 3 to 5 ppm. The following constrains were used in assignment of molecular formulae: C 50 to 200; H 80 to 300; O 5 to 80; N 1 to 3; assorted cations (Ca, Mg, Na, K) 0 to 1. The isotopic pattern of each ion cluster was taken into consideration in assigning molecular formula.

An external standard calibration curve at four levels of concentration (25, 50, 100 and 1000 ng/mL) was prepared by serial dilution of the palytoxin standard 1000 ng/mL in methanol:water (1:1 v/v) and was used in quantitative analyses. The calibration curve was obtained from triplicate injections. Extracted ion chromatograms (XIC) for all palytoxin-like compounds were obtained by selecting the three most abundant ion peaks of both [M+H+Ca]3+ and [M+2H-H2O]2+ ion clusters [2, 20]. Concentration was quantified against the external standard

calibration curves by less squared adjustment of the linear regression (Area (cps) = 10147·[PLTX] (ng/mL) - 124714) using chromatographic peak area integrated manually. Instrumental limit of quantification was measured (ILQ= 6 ng/mL). Analytical standards for pPTLX and OVTXs are not available, thus quantification was performed assuming that these compounds would have the same molar response as PLTX.

Results and Discussion

Six batch-cultures of O. cf. ovata strains from the Ebre River Delta were extracted and their toxin profiles characterized by LC-HRMS experiments. A newly developed method for ovatoxins (Ciminiello et al., 2014 submitted) was used to analyze the crude extracts under very slow gradient elution. This allowed baseline chromatographic separation of all palytoxin-like compounds contained in the extracts (Figure 2). The analyses of the extracts were carried out in parallel with a palytoxin standard (from P. tuberculosa) and with an Adriatic O. cf. ovata extract previously characterized [23] that was used as reference for the Mediterranean ovatoxins. All the samples were analyzed under the same experimental conditions.

All of the six analyzed O. cf. ovata extracts contained OVTX-a, -b, -c, -d, -e and pPLTX, whose presence was ascertained by:

a) comparison of retention times of individual compounds with those of toxins contained in the Adriatic extract;

b) ion profile of PLTX-like compounds in full HRMS spectra (mass range m/z 700-1600), which represents the fingerprint of this class of molecules [2]. It consists of triply-charged ions in the region m/z 830-950 and doubly-charged ions in the region m/z 1250-1400 (Table 1, Figure 1S Supplementary Material). Among them, $[M+H+Ca]^{3+}$ and $[M+2H-H2O]^{2+}$ ions are the most intense;

c) elemental formula assigned to the mono-isotopic ion peak of each of the formed ions (mass tolerance <3ppm; Table 1);

d) consistency of the isotopic pattern of each ion with that simulated for the expected elemental formula;

e) fragmentation behavior of individual compounds in LC-HRMS2 spectra compared to that of ovatoxins contained in the Adriatic extract used as reference. Results were interpreted according to the previous work on PLTX and OVTX-a [20].

Table 1 HRMS data of putative palytoxin and ovatoxins acquired in full MS spectra in the mass range m/z 700-16[...] mass and elemental formulas assigned to the mono-isotopic ion peaks of triply charged and doubly charged ions, a[...] equivalent (RDB). Mass errors were below 3 ppm in all cases. n.d. = not detected.

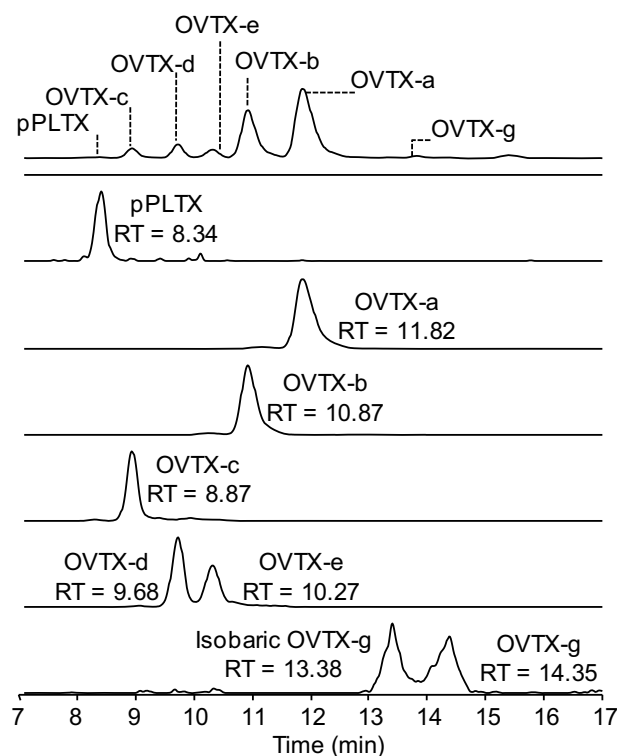|		Triply charged ions								D[...]
		Theoretical [M]	$[M+H+Ca]^{3+}$	$[M+H+Mg]^{3+}$	$[M+3H-H_2O]^{3+}$	$[M+3H-2H_2O]^{3+}$	$[M+3H-3H_2O]^{3+}$	$[M+H+K]^{2+}$	$[M+H+Na]^{2+}$	$[M+2$
pPLTX	m/z	2678.4790	906.4830	901.1579	887.8294	881.8268	875.8228	1359.2212	1351.2353	134[...]
	Formula	$C_{129}H_{223}O_{54}N_3$	$C_{129}H_{224}O_{54}N_3Ca$	$C_{129}H_{224}O_{54}N_3Mg$	$C_{129}H_{224}O_{53}N_3$	$C_{129}H_{222}O_{52}N_3$	$C_{129}H_{220}O_{51}N_3$	$C_{129}H_{224}O_{54}N_3K$	$C_{129}H_{224}O_{54}N_3Na$	$C_{129}H_{2}$
	(RDB)	20.0	19.5	19.5	19.5	20.5	21.5	19.0	19.0	
OVTX-a	m/z	2646.4892	895.8197	890.4941	877.1674	871.1640	865.1602	1343.2269	1335.2425	132[...]
	Formula	$C_{129}H_{223}O_{52}N_3$	$C_{129}H_{224}O_{52}N_3Ca$	$C_{129}H_{224}O_{52}N_3Mg$	$C_{129}H_{224}O_{51}N_3$	$C_{129}H_{222}O_{50}N_3$	$C_{129}H_{220}O_{49}N_3$	$C_{129}H_{224}O_{52}N_3K$	$C_{129}H_{224}O_{52}N_3Na$	$C_{129}H_{2}$
	(RDB)	20.0	19.5	19.5	19.5	20.5	21.5	19.0	19.0	
OVTX-b	m/z	2690.5154	910.4950	905.1696	891.8431	885.8393	879.8358	1365.2400	1357.2557	134[...]
	Formula	$C_{131}H_{227}O_{53}N_3$	$C_{131}H_{228}O_{53}N_3Ca$	$C_{131}H_{228}O_{53}N_3Mg$	$C_{131}H_{228}O_{52}N_3$	$C_{131}H_{226}O_{51}N_3$	$C_{131}H_{224}O_{50}N_3$	$C_{131}H_{228}O_{53}N_3K$	$C_{131}H_{228}O_{53}N_3Na$	$C_{131}H_{2}$
	(RDB)	20.0	19.5	19.5	19.5	20.5	21.5	19.0	19.0	
OVTX-c	m/z	2706.5103	915.8270	910.5015	897.1747	891.1713	885.1676	1373.2384	1365.2535	135[...]
	Formula	$C_{131}H_{227}O_{54}N_3$	$C_{131}H_{228}O_{54}N_3Ca$	$C_{131}H_{228}O_{54}N_3Mg$	$C_{131}H_{228}O_{53}N_3$	$C_{131}H_{226}O_{52}N_3$	$C_{131}H_{224}O_{51}N_3$	$C_{131}H_{228}O_{54}N_3K$	$C_{131}H_{228}O_{54}N_3Na$	$C_{131}H_{2}$
	(RDB)	20.0	19.5	19.5	19.5	20.5	21.5	19.0	19.0	
OVTX-d	m/z	2662.4841	901.1512	895.8257	882.4988	876.4952	870.4917	1351.2244	1343.2399	133[...]
	Formula	$C_{129}H_{223}O_{53}N_3$	$C_{129}H_{224}O_{53}N_3Ca$	$C_{129}H_{224}O_{53}N_3Mg$	$C_{129}H_{224}O_{52}N_3$	$C_{129}H_{222}O_{51}N_3$	$C_{129}H_{220}O_{50}N_3$	$C_{129}H_{224}O_{53}N_3K$	$C_{129}H_{224}O_{53}N_3Na$	$C_{129}H_{2}$
	(RDB)	20.0	19.5	19.5	19.5	20.5	21.5	19.0	19.0	
OVTX-e	m/z	2662.4841	901.1513	895.8259	882.4991	876.4953	870.4918	1351.2249	1343.2401	133[...]
	Formula	$C_{129}H_{223}O_{53}N_3$	$C_{129}H_{224}O_{53}N_3Ca$	$C_{129}H_{224}O_{53}N_3Mg$	$C_{129}H_{224}O_{52}N_3$	$C_{129}H_{222}O_{51}N_3$	$C_{129}H_{220}O_{50}N_3$	$C_{129}H_{224}O_{53}N_3K$	$C_{129}H_{224}O_{53}N_3Na$	$C_{129}H_{2}$
	(RDB)	20.0	19.5	19.5	19.5	20.5	21.5	19.0	19.0	
OVTX-g	m/z	2630.4943	890.4870	885.1611	871.8343	865.8303	859.8275	n.d.	1327.2432	131[...]
	Formula	$C_{129}H_{223}O_{51}N_3$	$C_{129}H_{224}O_{51}N_3Ca$	$C_{129}H_{224}O_{51}N_3Mg$	$C_{129}H_{224}O_{50}N_3$	$C_{129}H_{222}O_{49}N_3$	$C_{129}H_{220}O_{48}N_3$	--	$C_{129}H_{224}O_{51}N_3Na$	$C_{129}H_{2}$
	(RDB)	20.0	19.5	19.5	19.5	20.5	21.5	--	19.0	

Fig. 2 TIC of *O.* cf. *ovata* strain IRTA-SMM-11-10 (top trace) and XIC of the [M+H+Ca]$^{3+}$ ions of each toxin (mass tolerance 3 ppm). Analysis were carried out in full HRMS positive ion mode in the mass range *m/z* 700-1600. Under the same experimental conditions, PLTX standard eluted at 10.72 min

Figure 2 shows the total ion chromatogram (TIC) of one out of the six O. cf. ovata extracts (IRTA-SMM-11-10) and XIC of [M+H+Ca]3+ ions of individual palytoxin-like compounds. Relative abundance of each toxin was similar to that observed for most of the Mediterranean O. cf. ovata strains analyzed so far [2, 3, 28-30]. In particular, in this representative sample, OVTX-a accounted for 52% of the total toxin content, followed by OVTX -b (29%), OVTX -e (7%), OVTX -d (6%), OVTX -c (4%), and pPLTX (0.5%). However, total toxin contents among strains were quite different ranging from 50 to 250 pg/cell (Table 2). Toxin content on a per cell basis was in most cases higher than that reported for the other Mediterranean O. cf. ovata strains (7.5 to 75 pg/cell) [2, 3, 15, 28, 30, 31] and quite similar to that recently reported for a French Mediterranean strain (up to 300 pg/cell) [2, 3, 15, 28, 30, 31].

Strain name	Total toxin content (pg/cell)	Relative abundances (%)						
		pPLTX	OVTX-a	OVTX-b	OVTX-c	OVTX-d	OVTX-e	OVTX-g
IRTA-SMM-11-10	50	0.5	52	29	4	7	6	0.7
IRTA-SMM-12-38	143	0.3	58	25	3	6	6	0.7
IRTA-SMM-12-46	140	0.6	53	26	5	8	6	0.9
IRTA-SMM-12-51	102	0.6	55	21	6	8	8	0.6
IRTA-SMM-12-57	104	0.7	55	22	6	8	7	0.6
IRTA-SMM-12-62	250	0.4	59	20	4	7	7	0.9

Table 2 Total toxin content on a per cell basis (pg/cell) and relative abundance (%) of pPLTX and OVTXs in the 6 analysed *O.* cf. *ovata* strains from south Catalonia rocky coasts (NW Mediterranean Sea).

Under the used conditions, pPLTX eluted about 2 min earlier than palytoxin standard, which indicated that pPLTX was indeed an isomer (either structural or stereo-isomer) of PLTX itself. In addition, the analysis of full HRMS spectra associated to the region of TIC nearby OVTX-a revealed the presence in all the extracts of two new isobaric ovatoxins eluting at 13.38 min and 14.35 min respectively, each of them accounting for 0.7% of the total toxin content. We referred to these compounds as ovatoxin-g (OVTX-g) and isobaric OVTX-g. This prompted us to further analyze these molecules on the basis of their full HRMS and collision-induced dissociation (CID) MSn behavior. The obtained results were interpreted in the light of palytoxin and ovatoxin-a (17,44,64-trideoxy-42-hydroxypalytoxin) fragmentation behavior [20], whose structures had been confirmed by NMR [18]. The resulting structural hypotheses are reported below.

Putative palytoxin

Full HRMS spectra of pPLTX and PLTX appeared superimposable in terms of diagnostic ions and their relative intensities (Figure 3). Ion assignment (Table 1) indicated that pPLTX had the same molecular formula as palytoxin ($C_{129}H_{223}N_3O_{54}$; theoretical mass m/z 2678.4790, RBD 20.0) [5, 6].

Structural differences between PLTX and pPLTX have been assessed by interpretation of their full HRMSn spectra of the [M+H+Ca]3+ ion at m/z 906.8. Elemental formulae assigned to all the fragment ions are listed in Table 3. Figure 4 shows the structural hypotheses based on the observed cleavages.

| | Palytoxin | | Putative palytoxin | |
| | A-side | B-side | A-side | B-side |
#Clv	m/z (-nH_2O) Formula (RDB)	m/z (-nH_2O) Formula (RDB)	m/z (-nH_2O) Formula (RDB)	m/z (-nH_2O) Formula (RDB)
#4	327.1910 (1+) (-1H_2O) $C_{16}H_{27}O_5N_2$ (4.5)	1187.1212 (2+) (-6H_2O) $C_{113}H_{195}O_{48}NCa$ (17.0) 791.7500 (3+)(-4H_2O) $C_{113}H_{196}O_{48}NCa$ (16.5)	343.1863 (1+) $C_{16}H_{27}O_6N_2$ (4.5)	1179.1206 (2+) (-4H_2O) $C_{113}H_{195}O_{47}NCa$ (17.0) n.d.
#11	446.2212 (2+) (-2H_2O) $C_{40}H_{72}O_{17}N_2$ Ca (6.0)		446.2221 (2+) $C_{40}H_{72}O_{17}N_2Ca$ (6.0)	
#12	544.2943 (2+) (-2H_2O) $C_{52}H_{92}O_{19}N_2Ca$ (8.0)	807.8890 (2+) (-1H_2O) $C_{77}H_{125}O_{32}NCa$ (16.0)	544.2945 (2+) $C_{52}H_{92}O_{19}N_2Ca$ (8.0)	n.d.
#13	566.3074 (2+) (-2H_2O) $C_{54}H_{96}O_{20}N_2Ca$ (8.0)	803.8863 (2+) (-1H_2O) $C_{75}H_{123}O_{33}NCa$ (14.0)	574.3051(2+) $C_{54}H_{96}O_{21}N_2Ca$ (8.0)	n.d.
#14	572.3074 (2+) (-1H_2O) $C_{55}H_{96}O_{20}N_2Ca$ (9.0)	797.8860 (2+) (-2H_2O) $C_{74}H_{125}O_{33}NCa$ (13.0)		762.8721(2+) (–H_2O) $C_{74}H_{119}O_{29}NCa$ (14.0)
#15	596.3179 (2+) (-3H_2O) $C_{56}H_{100}O_{22}N_2Ca$ (8.0)	782.8808 (2+)(-3H_2O) $C_{73}H_{123}O_{32}NCa$ (13.0) 1526.8077 (1+)(-3H_2O) $C_{73}H_{124}O_{32}N$ (12.5)	604.3157 (2+) (-2H_2O) $C_{56}H_{100}O_{23}N_2Ca$ (8.0)	n.d. 1510.8142 (1+)(-3H_2O) $C_{73}H_{124}O_{31}N$(12.5)
#16	633.3363 (2+) (-3H_2O) $C_{59}H_{106}O_{24}N_2Ca$ (8.0)	745.8624 (2+)(-5H_2O) $C_{70}H_{117}O_{30}NCa$ (13.0) 1452.7713 (1+)(-5H_2O) $C_{70}H_{118}O_{30}N$ (12.5)	641.3340 (2+) (-2H_2O) $C_{59}H_{106}O_{25}N_2Ca$ (8.0)	737.8661 (2+)(-3H_2O) $C_{70}H_{117}O_{29}NCa$ (13.0) 1436.7777 (1+) (-3H_2O) $C_{70}H_{118}O_{29}N$ (12.5)
#17	647.3337 (2+) (-2H_2O) $C_{60}H_{106}O_{25}N_2Ca$ (9.0)	1406.7658 (1+) (-3H_2O) $C_{69}H_{116}O_{28}NCa$ (12.5)	655.3317 (2+) (-1H_2O) $C_{60}H_{106}O_{26}N_2Ca$ (9.0)	n.d.
#18		694.8289 (2+) (-3H_2O) $C_{65}H_{107}O_{28}NCa$ (13.0)		686.8316 (2+) $C_{65}H_{107}O_{27}NCa$ (13.0)
#19	948.4986(2+) $C_{90}H_{156}O_{37}N_2Ca$ (14.0)	804.4366 (1+) (-1H_2O) $C_{39}H_{66}O_{16}N$ (7.5)	948.5029 (2+) $C_{90}H_{156}O_{37}N_2Ca$ (14.0)	n.d.
#20	n.d.	n.d.	n.d.	n.d.
#21	1129.5955 (2+) (-4H_2O) $C_{107}H_{186}O_{45}N_2Ca$ (16.0)	406.2217 (1+) (-1H_2O) $C_{22}H_{32}O_6N$ (7.5)	1129.5965 (2+) $C_{107}H_{186}O_{45}N_2Ca$ (16.0)	n.d.
#22	1144.6011 (2+) (-2H_2O) $C_{108}H_{188}O_{46}N_2Ca$ (16.0)		n.d.	
#23	1174.6123 (2+) (-4H_2O) $C_{110}H_{192}O_{48}N_2$ Ca (16.0)		n.d.	
#24	1215.6323 (2+) (-1H_2O) $C_{115}H_{198}O_{49}N_2Ca$ (18.0)		n.d.	
#25	1222.6411 (2+) (-3H_2O) $C_{116}H_{200}O_{49}N_2Ca$ (18.0)		n.d.	
#26	1235.6480 (2+) (-4H_2O) $C_{118}H_{202}O_{49}N_2Ca$ (19.0)		n.d.	
#27	1236.6335 (2+) (-4H_2O) $C_{117}H_{200}O_{50}N_2Ca$ (19.0)		n.d.	
#28	1321.6819 (2+) (-3H_2O) $C_{117}H_{200}O_{53}N_2Ca$ (21.0)		n.d.	

| | Palytoxin Internal fragments | Putative palytoxin Internal fragments |
#Clv	m/z (-nH_2O) Formula (RDB)	m/z (-nH_2O) Formula (RDB)
#4+#12	372.1975 (2+) $C_{36}H_{64}O_{13}Ca$ (5.0) 743.3878 (1+) $C_{36}H_{63}O_{13}Ca$ (5.5)	n.d. n.d.
#4+#13	394.2105 (2+) $C_{38}H_{68}O_{14}Ca$ (5.0)	n.d.
#4+#15	424.2210 (2+) (-1H_2O) $C_{40}H_{72}O_{16}Ca$ (5.0)	n.d.
#4+#16	461.2389 (2+) (-2H_2O) $C_{43}H_{78}O_{18}Ca$ (5.0)	n.d.
#5+#12	657.3511(1+) $C_{32}H_{57}O_{11}Ca$ (4.5)	n.d.
#6+#12	n.d.	567.3244 (1+) (-1H_2O) $C_{29}H_{51}O_8Ca$ (4.5)
#7+#12	537.3088 (1+) (-1H_2O) $C_{28}H_{49}O_7Ca$ (4.5)	521.3145 (1+) $C_{28}H_{49}O_6Ca$ (4.5)
#8+#12	507.2982 (1+) $C_{27}H_{47}O_6Ca$ (4.5)	507.2983(1+) $C_{27}H_{47}O_6Ca$ (4.5)
#9+#12	477.2877(1+) $C_{26}H_{45}O_5Ca$ (4.5)	477.2888 (1+) $C_{26}H_{45}O_5Ca$ (4.5)
#10+#12	447.2771 (1+) (-1H_2O) $C_{25}H_{43}O_4Ca$ (4.5)	447.2770 (1+) $C_{25}H_{43}O_4Ca$ (4.5)

Table 3 Assignment of A-side, B-side and internal fragments contained in HRMS[2] spectra of palytoxin standard and putative palytoxin to relevant cleavages (#Clv) reported in Figure 4. Elemental formulae of the monoisotopic ion peaks (m/z) are reported together with number of water losses (-nH_2O) and relative double bonds (RDB). Mass errors were below 5 ppm in all cases. n.d. = not detected.
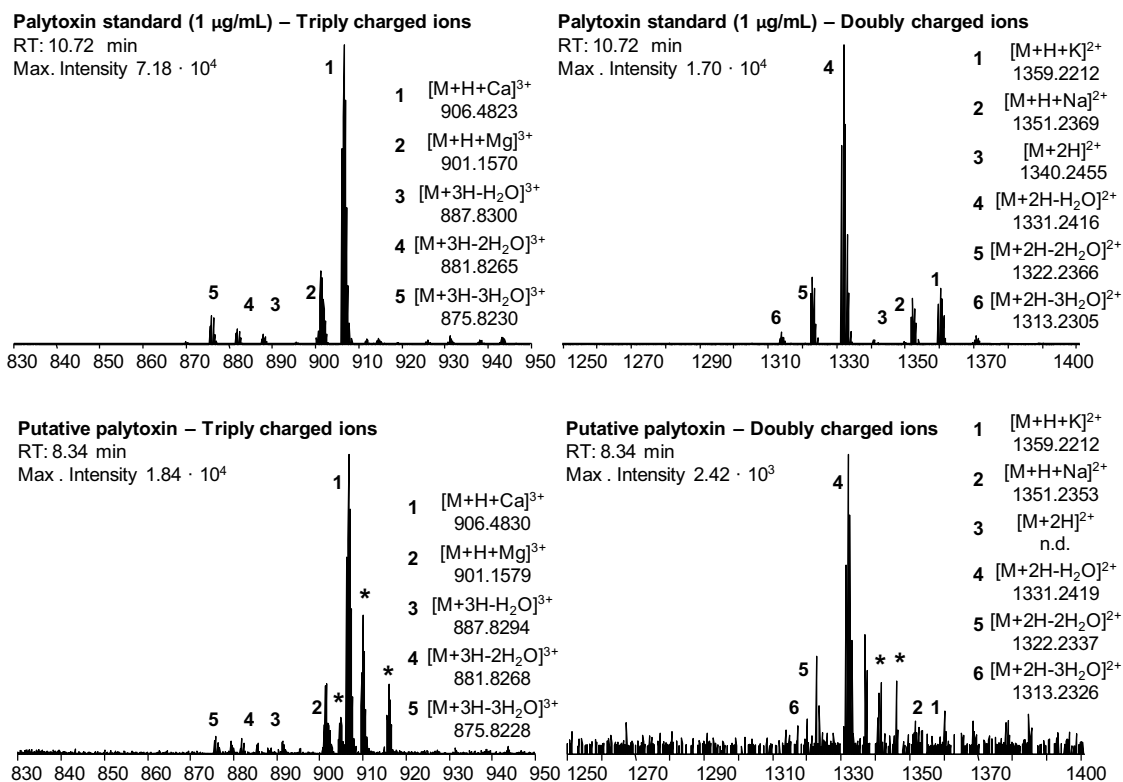
147

Fig. 3 Full HRMS spectra of palytoxin standard and putative palytoxin (*m/z* 700-1600) zoomed in *m/z* 830-950 and *m/z* 1250-1400 ranges. Elemental formula assignment of triply and doubly charged ions. n.d. = not detected. * = ions corresponding to co-eluting palytoxin-like compounds, still under investigation.
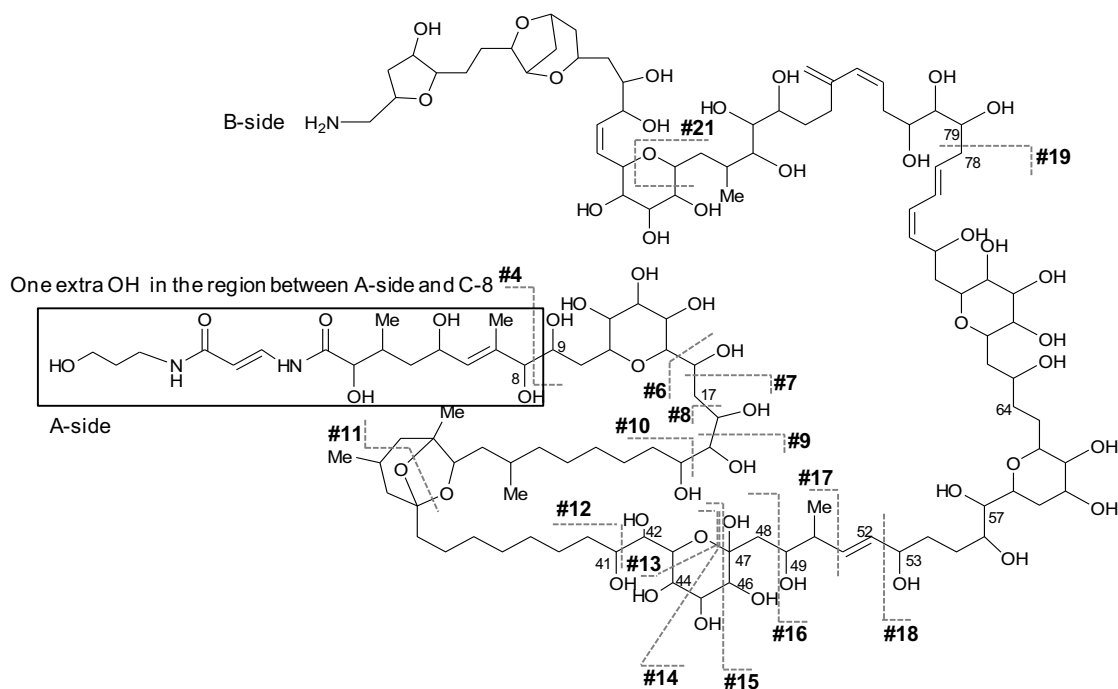

Fig. 4 Tentative planar structure of putative palytoxin ($C_{129}H_{223}N_3O_{54}$) including all the cleavages emerging from its HRMS[2] spectrum. Assignment of fragment ions is reported in Table 3.

148

The key cleavages highlighting the structural differences between the two analogs are discussed below. The first such cleavage was #4 that produced an A-side fragment at m/z 343.1863 (C16H27O6N2) in pPLTX as opposed to that of PLTX at m/z 327.1910 (C16H27O5N2). Therefore, pPLTX was deduced to possess one more oxygen than PLTX in the region stretching from the A-side terminal to C-8. Consistently, the B-side moiety due to cleavage #4 yielded a fragment containing one O less than the relevant fragment in PLTX.

Unlike #4, cleavages #11 and #12 produced doubly-charged A-side fragments (C40H72O17N2Ca and C52H92O19N2Ca) in pPLTX identical to the relevant fragments in PLTX. This suggested that pPLTX in comparison to PLTX lacked one O in the part structure stretching from C-9 to C-41. A cross interpretation of the internal fragments relevant to the part structures C-17 to C-41 (cleavage #7+#12) and C-18 to C-41 (cleavage #8+#12) provided insightful structural details. In fact, the fragment stretching from C-17 to C-41 possessed one oxygen less than PLTX, while the C-18 to C-41 fragment appeared identical to that of PLTX (Table 3). Hence, pPLTX turned out to lack the hydroxyl group at C-17, in analogy with OVTX-a.

Moving along the structural determination of pPLTX, cleavage #13 originated an A-side fragment featuring again an extra oxygen atom compared to PLTX. As cleavage #12 gave rise to an A-side fragment superimposable to that of PLTX, it was inferred that the additional oxygen was reasonably present at position 42. This was once again in accordance with the chemical structure of OVTX-a (Figure 1). Fragment ions deriving from cleavages #14 through #17 showed that the PLTX and pPLTX shared the same C-43 to C-50 part structure.

Further differences between the two toxins were deduced by a comparative analysis of the elemental formulae of fragments deriving from cleavages #18 (C-52/C53) and #19 (C-78/C-79). In particular, the pPLTX B-side fragment due to cleavage #18 lacked one oxygen with respect to PLTX, while the A-side fragment consequent to cleavage #19 matched again that of PLTX. Thus, one oxygen was missing in the region stretching from C-53 to C-78. As already observed for other palytoxin-like compounds further fragmentation does not occur in this region [20], thus preventing us to identify the exact position of the structural modification. However, by analogy with OVTX-a, it was reasonable to hypothesize that pPLTX was dehydroxylated at position 64. In order to more deeply investigate the C-53/C-78 segment, the Uchida et al. approach [17] was applied. This method is based on MS/MS analysis of conjugated polyenes produced from polyol structures through subsequent water losses. According to the authors, the serial loss of water molecules comes to an end when there are no more hydroxyl groups properly located to extend the conjugation process. Such a method was successfully applied to gain structural information on palytoxin analogs basing on the number of water losses observed in MS2 spectra [17].

We successfully applied the Ukida et al. method to OVTX-a, contained at a concentration level of 6 𝗴g/mL in the O. cf. ovata extract. In the part structure under investigation (C-53/C-78), the most favored cleavage #16 (C-48/C-49) was selected for this approach. The B-side fragment ion due to this cleavage in OVTX-a underwent six water losses, consistent with the dehydroxylation at C-64 of this molecule [18] (Figure 1).

On the contrary, in the case of pPLTX, cleavage #16 generated a B-side fragment ion accompanied by only three detectable water losses. Even if this apparently points to a dehydroxylation at C-57 for pPLTX, we don't feel like excluding that the low concentration of pPLTX in the extract (168 ng/mL) may have limited the detectable number of water losses

It should be noted that putative palytoxin contained in the O. cf. ovata reference extract from the Adriatic Sea eluted practically at the same retention time (8.33 min) as pPLTX in the strain IRTA-SMM-11-10. However, concentration of pPLTX in the Adriatic sample impeded the acquisition of HRMSn spectra needed to fully confirm that both pPLTXs were actually the same compound.

Ovatoxin-g

The full HRMS spectrum of ovatoxin-g (Rt = 14.35 min) showed, the most intense triply- and doubly-charged ion at m/z 890.4870 and m/z 1307.2486 (mono-isotopic peaks). According to the expected ionization behavior of palytoxin-like compounds [2, 3, 19], these ions were assigned to $[M+H+Ca]^{3+}$ and $[M+2H-H_2O]^{2+}$, respectively. A cross-check of elemental formulae of all the ions contained in the spectrum (Table 1) pointed to an elemental formula for ovatoxin-g of $C_{129}H_{223}N_3O_{51}$ (theoretical mass m/z 2630.4943, RBD 20.0) displaying one O less than OVTX-a ($C_{129}H_{223}N_3O_{52}$). Figure 5 shows the full HRMS spectrum of OVTX-g in comparison with that of OVTX-a.
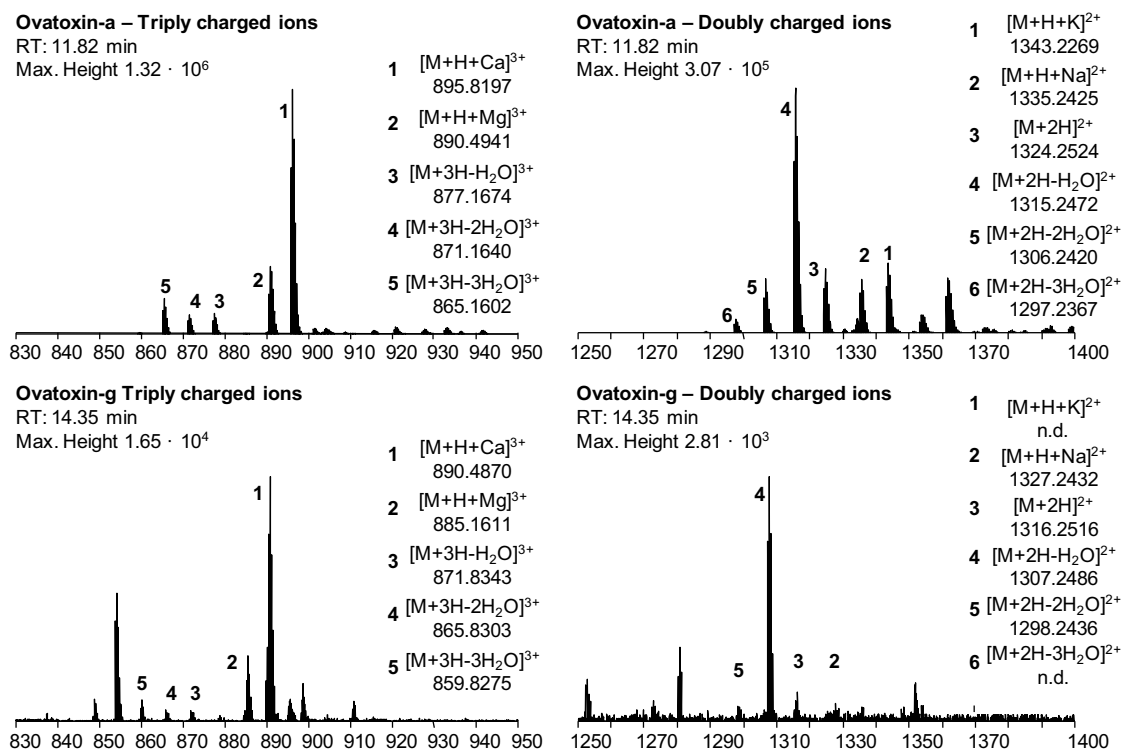
Fig. 5 Full HRMS spectra of ovatoxin-a and ovatoxin-g (*m/z* 700-1600) zoomed in *m/z* 830-950 and *m/z* 1250-1400 ranges. Elemental formula assignment of triply and doubly charged ions. n.d. = not detected

It is noteworthy that the [M+H+Ca]3+ ion of OVTX-g (m/z 890.4870) is only 6.7 mDa lower than the [M+H+Mg]3+ ion of OVTX-a (m/z 890.4937) and a resolving power of 150,000 (FWHM) would be needed to resolve ion peaks at 50% of peak width (Figure 2S, Supplementary Material). Thus, quantification of OVTX-g based on XICs of the calcium adduct might be biased if chromatographic separation between OVTX-a and OVTX-g is not achieved.

Positive HRMS2 spectrum of the m/z 890.8 was acquired to gain structural insights into ovatoxin-g and identify the specific site(s) of difference between OVTX-g and –a. Figure 6 shows the structural hypotheses for OVTX-g based on the observed fragmentations. Table 4 reports elemental formulae assigned to each fragment.

#Clv	Ovatoxin-a A-side m/z (-nH$_2$O) Formula (RDB)	Ovatoxin-a B-side m/z (-nH$_2$O) Formula (RDB)	Ovatoxin-g A-side m/z (-nH$_2$O) Formula (RDB)	Ovatoxin-g B-side m/z (-nH$_2$O) Formula (RDB)
#4	327.1906 (1+) (-1H$_2$O) $C_{16}H_{27}O_5N_2$ (4.5)	1171.1254 (2+)(-6H$_2$O) $C_{113}H_{195}O_{46}NCa$ (17.0) 781.0860 (3+)(-3H$_2$O) $C_{113}H_{196}O_{46}NCa$ (16.5)	327.1906 (1+) (-1H$_2$O) $C_{16}H_{27}O_5N_2$ (4.5)	1163.1261 (2+)(-5H$_2$O) $C_{113}H_{195}O_{45}NCa$ (17.0) 769.7508 (3+)(-1H$_2$O) $C_{113}H_{196}O_{46}NCa$ (17.5)
#11	438.2238 (2+) (-2H$_2$O) $C_{40}H_{72}O_{16}N_2$ Ca (6.0)		n.d.	
#12	536.2965 (2+) (-2H$_2$O) $C_{52}H_{92}O_{18}N_2Ca$ (8.0)	799.8905 (2+) (-1H$_2$O) $C_{77}H_{125}O_{31}NCa$ (16.0)	536.2958 (2+) (-1H$_2$O) $C_{52}H_{92}O_{18}N_2Ca$ (8.0)	n.d.
#13	566.3071(2+) (-2H$_2$O) $C_{54}H_{96}O_{20}N_2Ca$ (8.0)	778.8855 (2+) (-3H$_2$O) $C_{75}H_{123}O_{30}NCa$ (15.0)	n.d.	n.d.
#14		n.d.		n.d.
#15	588.3201 (2+) (-3H$_2$O) $C_{56}H_{100}O_{21}N_2Ca$ (8.0)	774.8829 (2+)(-3H$_2$O) $C_{73}H_{123}O_{31}NCa$ (13.0) 1510.8122 (1+)(-3H$_2$O) $C_{73}H_{124}O_{31}N$ (12.5)	588.3195 (2+) (-2H$_2$O) $C_{56}H_{100}O_{21}N_2Ca$ (8.0)	766.8841 (2+)(-2H$_2$O) $C_{73}H_{123}O_{30}NCa$ (13.0) 1494.8126 (1+)(-3H$_2$O) $C_{73}H_{124}O_{30}N$ (12.5)
#16	625.3385 (2+) (-3H$_2$O) $C_{59}H_{106}O_{23}N_2Ca$ (8.0)	737.8646 (2+)(-5H$_2$O) $C_{70}H_{117}O_{29}NCa$ (13.0) 1436.7757 (1+)(-6H$_2$O) $C_{70}H_{118}O_{29}N$ (12.5)	617.3406 (2+) (-2H$_2$O) $C_{59}H_{106}O_{22}N_2Ca$ (8.0)	737.8642 (2+)(-3H$_2$O) $C_{70}H_{117}O_{29}NCa$ (13.0) 1436.7749 (1+) (-3H$_2$O) $C_{70}H_{118}O_{29}N$ (12.5)
#17	639.3359 (2+) (-3H$_2$O) $C_{60}H_{106}O_{24}N_2Ca$ (9.0)	1390.7716 (1+) (-3H$_2$O) $C_{69}H_{116}O_{27}N$ (12.5)	631.3374 (2+) (-1H$_2$O) $C_{60}H_{106}O_{23}N_2Ca$ (9.0)	
#18		686.8308 (2+) (-2H$_2$O) $C_{65}H_{107}O_{27}NCa$ (13.0)		n.d.
#19	932.5032 (2+) $C_{90}H_{156}O_{35}N_2Ca$ (14.0)	804.4360 (1+) (-1H$_2$O) $C_{39}H_{66}O_{16}N$ (7.5)	924.50291 (2+) $C_{90}H_{156}O_{34}N_2Ca$ (14.0)	n.d.
#20	n.d.	n.d.	n.d.	n.d.
#21	1113.6005 (2+) (-3H$_2$O) $C_{107}H_{186}O_{43}N_2Ca$ (16.0)	406.2216 (1+) (-2H$_2$O) $C_{22}H_{32}O_6N$ (7.5)	1105.6007 (2+) (-2H$_2$O) $C_{107}H_{186}O_{42}N_2Ca$ (16.0)	n.d.
#22	1128.6053 (2+) (-2H$_2$O) $C_{108}H_{188}O_{44}N_2Ca$ (16.0)		n.d.	
#23	1158.6164 (2+) (-3H$_2$O) $C_{110}H_{192}O_{46}N_2Ca$ (16.0)		n.d.	
#24	1199.6367 (2+) (-1H$_2$O) $C_{115}H_{198}O_{47}N_2Ca$ (18.0)		n.d.	
#25	1206.6449 (2+) (-4H$_2$O) $C_{116}H_{200}O_{47}N_2Ca$ (18.0)		1190.1423 (2+) (-1H$_2$O) $C_{116}H_{200}O_{46}N_2Ca$ (18.0)	
#26	1219.6517 (2+) (-4H$_2$O) $C_{118}H_{202}O_{47}N_2Ca$ (19.0)		n.d.	
#27	1220.6386 (2+) (-5H$_2$O) $C_{117}H_{200}O_{48}N_2Ca$ (19.0)		n.d.	
#28	n.d.	n.d.	n.d.	n.d.

#Clv	Ovatoxin-a Internal fragments m/z (-nH$_2$O) Formula (RDB)	Ovatoxin-g Internal fragments m/z (-nH$_2$O) Formula (RDB)
#4+#12	364.1999 (2+) $C_{36}H_{64}O_{12}Ca$ (5.0) 727.3924 (1+) $C_{36}H_{63}O_{12}Ca$ (5.5)	n.d. 727.3920 (1+) $C_{36}H_{63}O_{12}Ca$ (5.5)
#4+#13	394.2104 (2+) $C_{38}H_{68}O_{14}Ca$ (5.0)	n.d.
#4+#15	416.2234 (2+) (-2H$_2$O) $C_{40}H_{72}O_{15}Ca$ (5.0)	416.2224 (2+) (-1H$_2$O) $C_{40}H_{72}O_{15}Ca$ (5.0)
#4+#16	453.2415 (2+) (-1H$_2$O) $C_{43}H_{78}O_{17}Ca$ (5.0)	n.d.
#5+#12	641.3557 (1+) $C_{32}H_{57}O_{10}Ca$ (4.5)	641.3554 (1+) $C_{32}H_{57}O_{10}Ca$ (4.5)
#6+#12	n.d.	n.d.
#7+#12	521.3136 (1+) (-1H$_2$O) $C_{28}H_{49}O_6Ca$ (4.5)	521.3134 (1+) $C_{28}H_{49}O_6Ca$ (4.5)
#8+#12	507.2979 (1+) $C_{27}H_{47}O_6Ca$ (4.5)	507.2975 (1+) $C_{27}H_{47}O_6Ca$ (4.5)
#9+#12	477.2875 (1+) $C_{26}H_{45}O_5Ca$ (4.5)	477.2866 (1+) $C_{26}H_{45}O_5Ca$ (4.5)
#10+#12	447.2771 (1+) (-1H$_2$O) $C_{25}H_{43}O_4Ca$ (4.5)	447.2760 (1+) (-1H$_2$O) $C_{25}H_{43}O_4Ca$ (4.5)

Table 4 Assignment of A-side, B-side and internal fragments contained in HRMS[2] spectra of ovatoxin-a and ovatoxin-g to relevant cleavages (#Clv) reported in Figure 6. Elemental formula of the monoisotopic ion peaks (m/z) are reported together with number of water losses observed in the spectra (-nH$_2$O) and relative double bonds (RDB). Mass errors were below 5 ppm in all cases. n.d. = not detected.

The first crucial information on OVTX-g was provided by cleavage #4 that originated an A-side fragment ion (m/z 327.1906; C16H27O5N2) identical to that of OVTX-a and a B-side fragment ion (C113H195O45NCa) with one O less than that observed for OVTX-a (C113H195O46NCa). So, the two molecules shared the same A-side terminal-C-8 part structure. The structural analogy between the two OVTXs was extended up to C-45 in the light of cleavage #15 that still generated identical A-side fragment ions for both OVTXs. This was confirmed by internal fragments due to double cleavages that were the same for both compounds (Table 4).

The first difference in the elemental formulae of the A-side fragment ions of the two toxins appeared with cleavage #16, which generated an A-side fragment in OVTX-g displaying one O less (C59H106O22N2Ca) than OVTX-a (C59H106O23N2Ca) and B-side fragments with the same elemental formulae. This clearly indicated that the structural difference between OVTX-g and OVTX-a lied in the region stretching from C-46 to C-48. Reasonably, the missing oxygen atom is that belonging to the alcoholic functionality at C-46, as the other O is involved in a hemiketal functionality.

All the A-side fragments generated by cleavages #17, #19, #21 and #25 in OVTX-g presented one O less than in OVTX-a (Table 4), which was consistent with the hypothesis that the only structural difference between the two toxins was the missing O at C-46. So, by analogy with OVTX-a, OVTX-g would be dehydroxylated at C-64. However, isomerism in this region cannot be discarded. The already mentioned approach proposed by Uchida et al. was applied [17] also to OVTX-g. The B-side fragment ion due to cleavage #16 underwent only three detectable water losses, so OVTX-g could lack the hydroxyl at C-57. However, such as for pPLTX, OVTX-g concentration in the crude extract (235 ng/mL) might be constraining the number of water losses detected.

Besides OVTX-g (Rt 14.35 min), XIC of [M+H+Ca]3+ ion at m/z 890.4870 displayed another peak eluting about one minute earlier (Figure 2). Its full HRMS spectrum showed a similar ion profile as OVTX-g, which suggested that it was an OVTX-g isomer. However, the fragmentation behavior in the HRMS2 spectrum of this compound was significantly different from that we have usually observed for palytoxins, thus preventing us from any reliable interpretation.

Conclusions

The LC-HRMS analyses of cultures of O. cf. ovata from the Ebre River Delta allowed to highlight the presence in the extracts of the novel ovatoxin-g. HRMS2 studies provided insights into the structure of this new ovatoxin in addition to disclosing that putative palytoxin is indeed a structural isomer of palytoxin itself. Compared to palytoxin, putative palytoxin from the analyzed O. cf. ovata strains is hydroxylated at C-42 and dehydroxylated at C-17 and most likely at C-64 (like OVTX-a). In addition, an-extra oxygen is contained in the segment stretching from

the A-side terminal to C-8. Compared to ovatoxin-a, ovatoxin-g is dehydroxylated at C-46.

The ever growing number of palytoxins being discovered makes even more urgent the need of evaluating the toxicity on humans of this class of compounds. The study of mechanisms of action and potency of individual palytoxin-like compounds should be performed to ensure a correct risk assessment of Ostreopsis-related syndromes.

Acknowledgments

Conflicts of Interest

The authors declare no conflict of interest.

References

1. Ciminiello, P.; Dell'Aversano, C.; Fattorusso, E.; Forino, M.; Tartaglione, L.; Grillo, C.; Melchiorre, N., Putative Palytoxin and Its New Analogue, Ovatoxin-a, in Ostreopsis Ovata Collected Along the Ligurian Coasts During the 2006 Toxic Outbreak. J. Am. Soc. Mass Spectrom. 2008, 19 (1), 111-120.

2. Ciminiello, P.; Dell'Aversano, C.; Iacovo, E. D.; Fattorusso, E.; Forino, M.; Grauso, L.; Tartaglione, L.; Guerrini, F.; Pistocchi, R., Complex Palytoxin-Like Profile of Ostreopsis Ovata. Identification of Four New Ovatoxins by High-Resolution Liquid Chromatography/Mass Spectrometry. Rapid Commun. Mass. Spec. 2010, 24 (18), 2735-2744.

3. Ciminiello, P.; Dellaversano, C.; Iacovo, E. D.; Fattorusso, E.; Forino, M.; Tartaglione, L.; Battocchi, C.; Crinelli, R.; Carloni, E.; Magnani, M.; Penna, A., Unique Toxin Profile of a Mediterranean Ostreopsis Cf. Ovata Strain: Hr Lc-Msn Characterization of Ovatoxin-F, a New Palytoxin Congener. Chem. Res. Toxicol. 2012, 25 (6), 1243-1252.

4. Munday, R., Palytoxin Toxicology: Animal Studies. Toxicon 2011, 57 (3), 470-477.

5. Moore, R. E.; Bartolini, G., Structure of Palytoxin. J. Am. Chem. Soc. 1981, 103 (9), 2491-2494.

6. Uemura, D.; Hirata, Y.; Iwashita, T.; Naoki, H., Studies on Palytoxins. Tetrahedron 1985, 41 (6), 1007-1017.

7. Uemura, D.; Ueda, K.; Hirata, Y.; Naoki, H.; Iwashita, T., Further Studies on Palytoxin. Ii. Structure of Palytoxin. Tetrahedron Lett. 1981, 22 (29), 2781-2784.

8. Crinelli, R.; Carloni, E.; Giacomini, E.; Penna, A.; Dominici, S.; Battocchi, C.; Ciminiello, P.; Dell'Aversano, C.; Fattorusso, E.; Forino, M., Palytoxin and an Ostreopsis Toxin Extract Increase the Levels of Mrnas Encoding Inflammation-Related Proteins in Human Macrophages Via P38 Mapk and Nf-Kb. PloS One 2012, 7 (6), e38139.

9. Durando, P.; Ansaldi, F.; Oreste, P.; Moscatelli, P.; Marensi, L.; Grillo, C.; Gasparini, R.; Icardi, G., Ostreopsis Ovata and Human Health: Epidemiological and Clinical Features of Respiratory Syndrome Outbreaks from a Two-Year Syndromic Surveillance, 2005-06, in North-West Italy. Euro surveillance 2007, 12 (23), http://www.eurosurveillance.org/ViewArticle.aspx?ArticleId=3212 (accessed June 10, 2014).

10. Mangialajo, L.; Ganzin, N.; Accoroni, S.; Asnaghi, V.; Blanfuné, A.; Cabrini, M.; Cattaneo-Vietti, R.; Chavanon, F.; Chiantore, M.; Cohu, S., Trends in Ostreopsis Proliferation Along the Northern Mediterranean Coasts. Toxicon 2011, 57 (3), 408-420.

11. Tubaro, A.; Durando, P.; Del Favero, G.; Ansaldi, F.; Icardi, G.; Deeds, J.; Sosa, S., Case Definitions for Human Poisonings Postulated to Palytoxins Exposure. Toxicon 2011, 57 (3), 478-495.

12.   Casabianca, S.; Casabianca, A.; Rioboó, P.; Franco, J. M.; Vila, M.; Penna, A., Quantification of the Toxic Dinoflagellate Ostreopsis Spp. By Qpcr Assay in Marine Aerosol. Environ. Sci. Technol. 2013, 47 (8), 3788-3795.

13.   Ciminiello, P.; Dell'Aversano, C.; Iacovo, E. D.; Fattorusso, E.; Forino, M.; Tartaglione, L.; Benedettini, G.; Onorari, M.; Serena, F.; Battocchi, C.; Casabianca, S.; Penna, A., First Finding of Ostreopsis Cf. Ovata Toxins in Marine Aerosols. Environ. Sci. Technol. 2014, 48 (6), 3532-3540.

14.   Ciminiello, P.; Dell'Aversano, C.; Dello Iacovo, E.; Fattorusso, E.; Forino, M.; Grauso, L.; Tartaglione, L.; Guerrini, F.; Pezzolesi, L.; Pistocchi, R.; Vanucci, S., Isolation and Structure Elucidation of Ovatoxin-a, the Major Toxin Produced by Ostreopsis Ovata. J. Am. Chem. Soc. 2012, 134 (3), 1869-1875.

15.   Brissard, C.; Herrenknecht, C.; Séchet, V.; Hervé, F.; Pisapia, F.; Harcouet, J.; Lémée, R.; Chomérat, N.; Hess, P.; Amzil, Z., Complex Toxin Profile of French Mediterranean Ostreopsis Cf. Ovata Strains, Seafood Accumulation and Ovatoxins Prepurification. Mar. Drugs 2014, 12 (5), 2851-2876.

16.   Suzuki, T.; Watanabe, R.; Uchida, H.; Matsushima, R.; Nagai, H.; Yasumoto, T.; Yoshimatsu, T.; Sato, S.; Adachi, M., Lc-Ms/Ms Analysis of Novel Ovatoxin Isomers in Several Ostreopsis Strains Collected in Japan. Harmful Algae 2012, 20, 81-91.

17.   Uchida, H.; Taira, Y.; Yasumoto, T., Structural Elucidation of Palytoxin Analogs Produced by the Dinoflagellate Ostreopsis Ovata Ik2 Strain by Complementary Use of Positive and Negative Ion Liquid Chromatography/Quadrupole Time of Flight Mass Spectrometry. Rapid Commun. Mass. Spec. 2013, 27 (17), 1999-2008.

18.   Ciminiello, P.; Dell'Aversano, C.; Dello Iacovo, E.; Fattorusso, E.; Forino, M.; Grauso, L.; Tartaglione, L., Stereochemical Studies on Ovatoxin-A. Chem. Eur. J. 2012, 18 (52), 16836-16843.

19.   Ciminiello, P.; Dell'Aversano, C.; Iacovo, E. D.; Fattorusso, E.; Forino, M.; Tartaglione, L., Lc-Ms of Palytoxin and Its Analogues: State of the Art and Future Perspectives. Toxicon 2011, 57 (3), 376-389.

20.   Ciminiello, P.; Dell'Aversano, C.; Iacovo, E. D.; Fattorusso, E.; Forino, M.; Grauso, L.; Tartaglione, L., High Resolution Lc-Msn Fragmentation Pattern of Palytoxin as Template to Gain New Insights into Ovatoxin-a Structure. The Key Role of Calcium in Ms Behavior of Palytoxins. J. Am. Soc. Mass Spectrom. 2012, 23 (5), 952-963.

21.   Vila, M.; Garcés, E.; Masó, M., Potentially Toxic Epiphytic Dinoflagellate Assemblages on Macroalgae in the Nw Mediterranean. Aquat. Microb. Ecol. 2001, 26 (1), 51-60.

22.   Barroso García, P.; de la Puerta, P. R.; Parrón Carreño, T.; Marín Martínez, P.; Guillén Enríquez, J., Brote Con Síntomas Respiratorios En La Provincia De Almería Por Una Posible Exposición a Microalgas Tóxicas. Gaceta sanitaria 2008, 22 (6), 578-584.

23. Pezzolesi, L.; Guerrini, F.; Ciminiello, P.; Dell'Aversano, C.; Iacovo, E. D.; Fattorusso, E.; Forino, M.; Tartaglione, L.; Pistocchi, R., Influence of Temperature and Salinity on Ostreopsis Cf. Ovata Growth and Evaluation of Toxin Content through Hr Lc-Ms and Biological Assays. Water Res. 2012, 46 (1), 82-92.

24. Hoshaw, R. W.; Rosowski, J. R., Methods for Microscopic Algae. In Handbook of Phycological Methods, Stein, J. R., Ed. CUP Archive: 1973; Vol. 1, pp 53-67.

25. Andree, K. B.; Fernández-Tejedor, M.; Elandaloussi, L. M.; Quijano-Scheggia, S.; Sampedro, N.; Garcés, E.; Camp, J.; Diogène, J., Quantitative Pcr Coupled with Melt Curve Analysis for Detection of Selected Pseudo-Nitzschia Spp.(Bacillariophyceae) from the Northwestern Mediterranean Sea. Appl. Environ. Microbiol. 2011, 77 (5), 1651-1659.

26. Sato, S.; Nishimura, T.; Uehara, K.; Sakanari, H.; Tawong, W.; Hariganeya, N.; Smith, K.; Rhodes, L.; Yasumoto, T.; Taira, Y., Phylogeography of Ostreopsis Along West Pacific Coast, with Special Reference to a Novel Clade from Japan. PloS One 2011, 6 (12), e27983.

27. Utermöhl, v. H., Neue Wege in Der Quantitativen Erfassung Des Planktons. Verh. int. Verein. theor. angew. Limnol 1931, 5, 567-596.

28. Accoroni, S.; Romagnoli, T.; Colombo, F.; Pennesi, C.; di Camillo, C. G.; Marini, M.; Battocchi, C.; Ciminiello, P.; Dell'Aversano, C.; Dello Iacovo, E.; Fattorusso, E.; Tartaglione, L.; Penna, A.; Totti, C., Ostreopsis Cf. Ovata Bloom in the Northern Adriatic Sea During Summer 2009: Ecology, Molecular Characterization and Toxin Profile. Mar. Pollut. Bull. 2011, 62 (11), 2512-2519.

29. Guerrini, F.; Pezzolesi, L.; Feller, A.; Riccardi, M.; Ciminiello, P.; Dell'Aversano, C.; Tartaglione, L.; Iacovo, E. D.; Fattorusso, E.; Forino, M., Comparative Growth and Toxin Profile of Cultured Ostreopsis Ovata from the Tyrrhenian and Adriatic Seas. Toxicon 2010, 55 (2), 211-220.

30. Honsell, G.; De Bortoli, M.; Boscolo, S.; Dell'Aversano, C.; Battocchi, C.; Fontanive, G.; Penna, A.; Berti, F.; Sosa, S.; Yasumoto, T., Harmful Dinoflagellate Ostreopsis Cf. Ovata Fukuyo: Detection of Ovatoxins in Field Samples and Cell Immunolocalization Using Antipalytoxin Antibodies. Environ. Sci. Technol. 2011, 45 (16), 7051-7059.

31. Rossi, R.; Castellano, V.; Scalco, E.; Serpe, L.; Zingone, A.; Soprano, V., New Palytoxin-Like Molecules in Mediterranean Ostreopsis Cf. Ovata (Dinoflagellates) and in Palythoa Tuberculosa Detected by Liquid Chromatography-Electrospray Ionization Time-of-Flight Mass Spectrometry. Toxicon 2010, 56 (8), 1381-1387.